Validation of Detailed Reaction Mechanisms for Detonation Simulation

E. Schultz, J. Shepherd

Graduate Aeronautical Laboratories
California Institute of Technology
Pasadena, CA 91125

Explosion Dynamics Laboratory Report FM99-5

February 8, 2000

Abstract

This report considers the adequacy of existing detailed reaction mechanisms for use in detonation simulation with chemical systems containing hydrogen, ethylene, and propane fuels. Shock tube induction time data are compiled from the literature and compared to detonation thermodynamic conditions to establish validation limits. Existing detailed reaction mechanisms are then used in constant-volume explosion simulations for validation against the shock tube data. A quantitative measure of mechanism accuracy is obtained from the validation study results, and deficiencies in the experimental data and reaction mechanisms are highlighted. Two mechanisms were identified which include the chemistry for all three fuels and simulated the experimental induction time data to within an average factor of three for temperatures above 1200 K. These mechanisms are incorporated into steady, one-dimensional detonation simulations to provide quantitative information on the reaction zone structure, characteristic reaction time/length scales, and activation and thermal energy parameters.

Table of Contents

List of Figures

List of Tables

Nomenclature

β	nitrogen to oxygen molar ratio
Δ	characteristic induction/reaction length
Δh^0	heat of reaction extrapolated to zero temperature
ϕ	equivalence ratio
γ	specific heat ratio
Ω	chemical production rate
ρ	density
σ	thermicity coefficient
τ	characteristic induction/reaction time
$\tau_{e,j}$	j-th experimental induction time
$\tau_{s,j}$	j-th simulated induction time
θ	non-dimensional activation energy parameter
0	pre-shock state
A	reaction rate multiplier constant
c	frozen acoustic speed
c_p	constant pressure specific heat capacity
c_v	constant volume specific heat capacity
c	acoustic speed
CJ	Chapman-Jouguet
e	specific internal energy
E	activation energy
i	species index
k	reaction rate
K	total number of species
M	Mach number
n	reaction rate temperature dependence power
P	pressure
q	energy release per unit mass
Q	non-dimensional energy release

R	mixture gas constant
t	time
T	temperature
t^*	induction time
v	specific volume
vN	von-Neumann (post-shock) state
w	fluid velocity (shock-frame)
y	mass fraction
[X]	concentration of constituent X

1 Introduction

Computational simulation is extensively used to study the gasdynamics and chemistry of gaseous detonations. The gasdynamics are given by the Euler equations and are coupled to the chemistry through a reaction mechanism which specifies how the chemical species evolve. One, two, or three step models of the global chemical behavior represent the most simplistic mechanisms. Detailed reaction mechanisms consisting of a comprehensive set of species and reaction rates are the most realistic, attempting to represent all chemical processes within a given system. In between are reduced reaction mechanisms derived systematically from detailed reaction mechanisms.

Simulations of steady, one-dimensional detonation models with detailed reaction mechanisms have been possible for many years. Unsteady, one-dimensional simulations are beginning to use the smallest detailed reaction mechanisms while most unsteady and all multi-dimensional simulations resort to the less complex mechanisms. Given significantly increased computational power over time, these higher fidelity simulations will also incorporate detailed reaction mechanisms. Confidence must be established in the accuracy of all computational simulations through validation with experimental data.

Here we consider the adequacy of existing detailed reaction mechanisms for use in detonation simulation with chemical systems containing hydrogen, ethylene, or propane fuels. Shock tube induction time data are compiled from the literature and compared to detonation thermodynamic conditions to establish validation limits. Existing detailed reaction mechanisms are then used in constant-volume explosion simulations for validation against the shock tube data. A quantitative measure of mechanism accuracy is obtained from the validation study results and deficiencies in the experimental data and reaction mechanisms are highlighted. Finally, the most accurate mechanisms are incorporated into calculations for steady, one-dimensional detonations to provide quantitative information on the reaction zone structure, characteristic reaction time/length scales, and activation and thermal energy parameters.

2 Detonation Thermodynamic Conditions

The chemical reactions associated with detonations are strongly dependent upon the thermodynamic conditions imposed by the shock wave(s). Therefore, consideration of the post-shock thermodynamic conditions provides a range of states over which reaction mechanisms must be validated. One-dimensional, steady detonation models typically use a normal shock velocity equal to the Chapman-Jouguet detonation velocity (V_{CJ}). Multi-dimensional and/or unsteady models are faced with varying shock velocities. Experimental measurements of shock decay in cellular detonations indicate that the shock velocity varies from approximately 60% to 140% of V_{CJ} (Voitsekhovskii et al. 1963, Edwards 1970, Takai et al. 1974, Dormal et al. 1979, Tarver 1982, Lee 1984, Lefebvre et al. 1993). This velocity range does not cover all possible situations in self-propagating cellular detonations and also neglects significantly overdriven states which might be achieved, for example, in direct initiation. Nevertheless, consideration of 60% - 140% V_{CJ} shock velocities is representative of the wide range of thermodynamic conditions existing within detonations.

Mixture compositions considered include hydrogen, ethylene, and propane fuels, oxygen as the oxidizer, and argon, carbon dioxide, helium, and nitrogen diluents. Fuel-oxygen and fuel-air mixtures are the most practical and commonly studied while the mixtures including diluents other than nitrogen are useful tools for elucidating the coupling between the detonation chemistry and gasdynamics. Calculations with varying equivalence ratio (ϕ) from 0.2 to 3.0 were performed for the fuel-oxygen ($\beta = 0.0$) and fuel-air ($\beta = 3.76$) mixtures:

$$\phi H_2 + 0.5(O_2 + \beta N_2) \qquad \phi C_2H_4 + 3(O_2 + \beta N_2) \qquad \phi C_3H_8 + 5(O_2 + \beta N_2)$$

The equivalence ratio remained fixed at 1.0 (stoichiometric) for calculations in which the diluent concentration was varied from 0% to 90% by volume.

The chemical equilibrium program, STANJAN, is used to calculate V_{CJ} for initial pressure and temperature conditions of 1 bar and 295 K, respectively (Reynolds, 1986). The detonation velocities, Mach numbers, and pre-shock ratio of specific heats (γ_1) for hydrogen, ethylene, and propane mixtures are presented in Figs. 1, 2, and 3, respectively. Note that the Mach numbers and specific heat ratios for argon and helium diluted mixtures are identical and therefore, these data curves overlap. The conditions immediately behind the shock front are calculated with STANJAN using frozen chemistry at shock velocities of $0.6V_{CJ}$, $1.0V_{CJ}$, and $1.4V_{CJ}$. Figures 4 - 5, 6 - 7, and 8 - 9 contain post-shock pressure and temperature data for hydrogen, ethylene, and propane mixtures, respectively. The first of each figure pair provides fuel-oxygen-nitrogen mixture information, and the second includes argon, carbon dioxide, and helium dilution data. In all cases, the $0.6V_{CJ}$ shock velocities give the minimum pressure and temperature conditions while those for $1.4V_{CJ}$ represent the maxima.

The post-shock pressures and temperatures are greater for fuel-oxygen relative to fuel-air mixtures at all equivalence ratios because of decreased energy per unit mass associated with nitrogen dilution. Maximum pressures and temperatures occur very close to the stoichiometric condition for fuel-air mixtures and are shifted to rich equivalence ratios for the fuel-oxygen cases

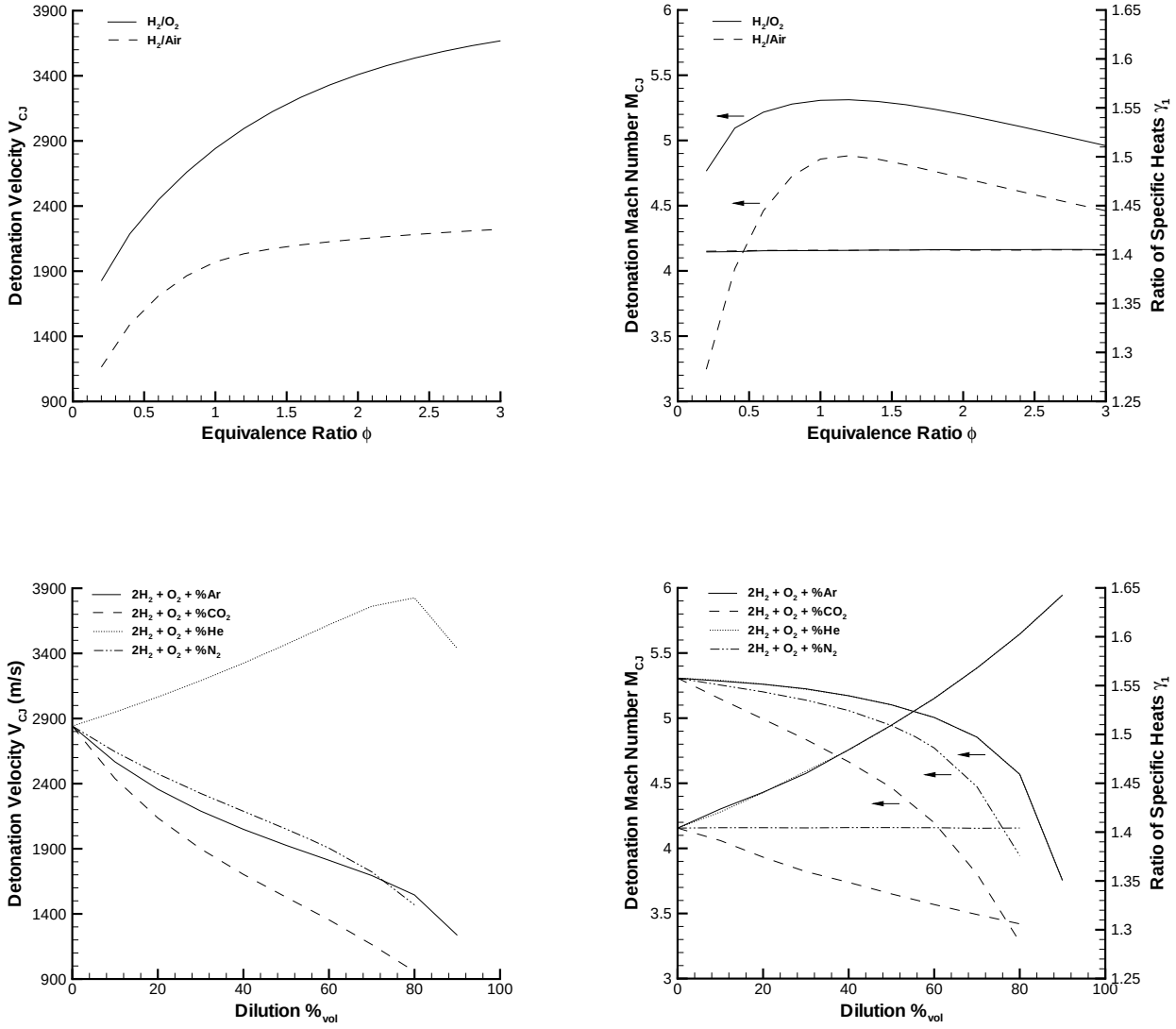

Fig. 1 Hydrogen detonation velocities, Mach numbers, and pre-shock ratio of specific heats with initial conditions of 295 K and 1 bar.

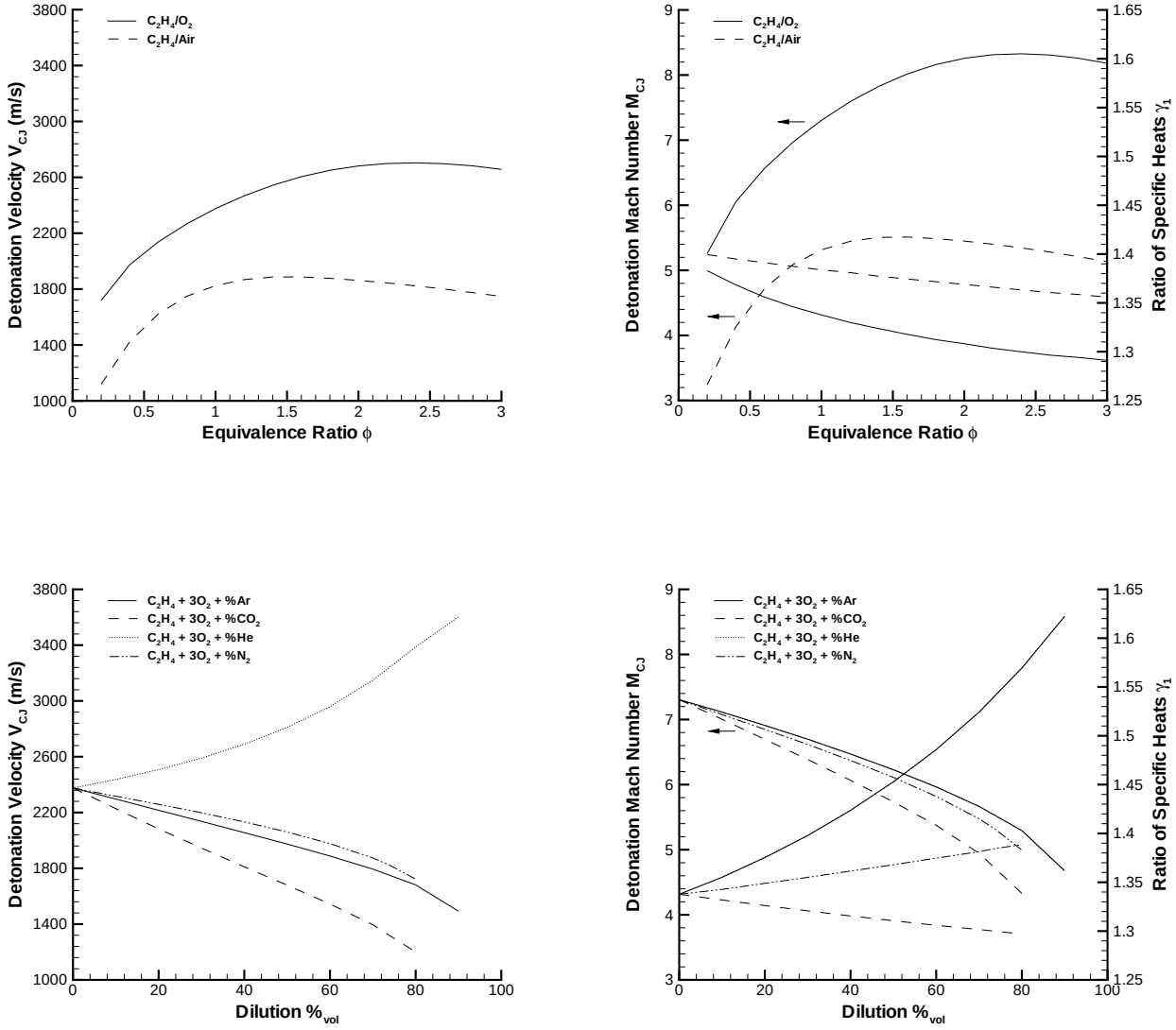

Fig. 2 Ethylene detonation velocities, Mach numbers, and pre-shock ratio of specific heats with initial conditions of 295 K and 1 bar.

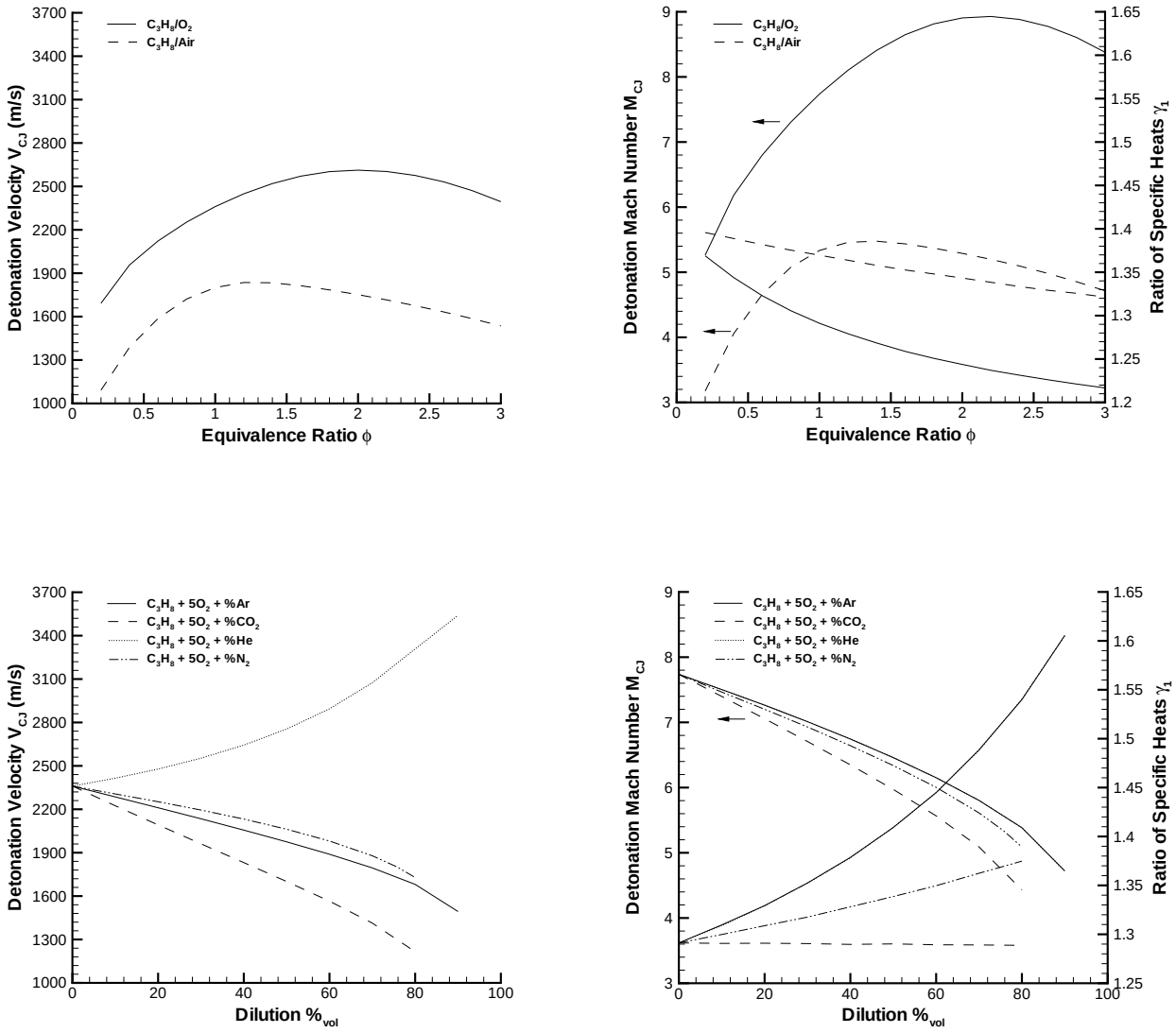

Fig. 3 Propane detonation velocities, Mach numbers, and pre-shock ratio of specific heats with initial conditions of 295 K and 1 bar.

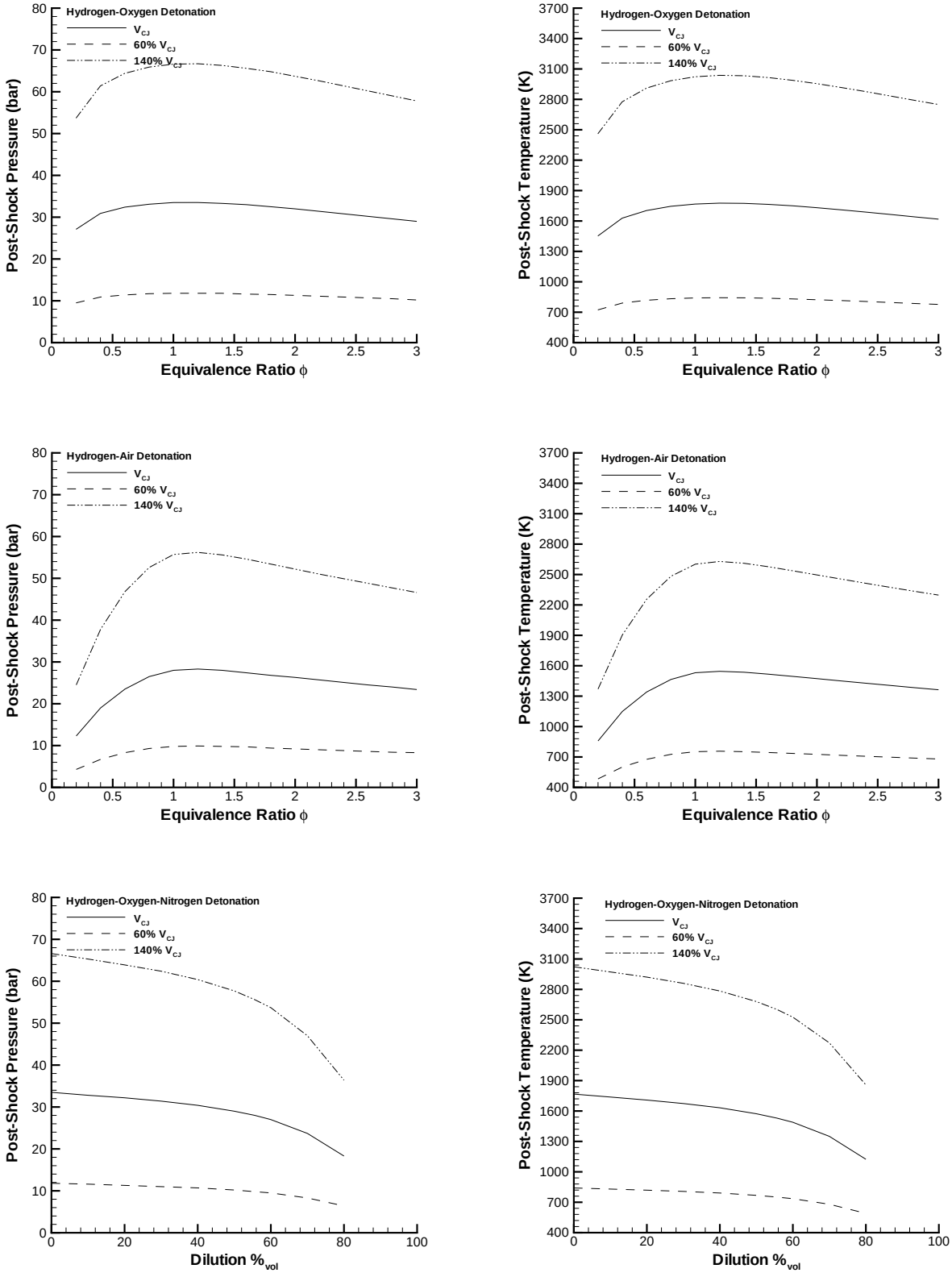

Fig. 4 $H_2/O_2/N_2$ detonation post-shock thermodynamic conditions (295 K, 1 bar).

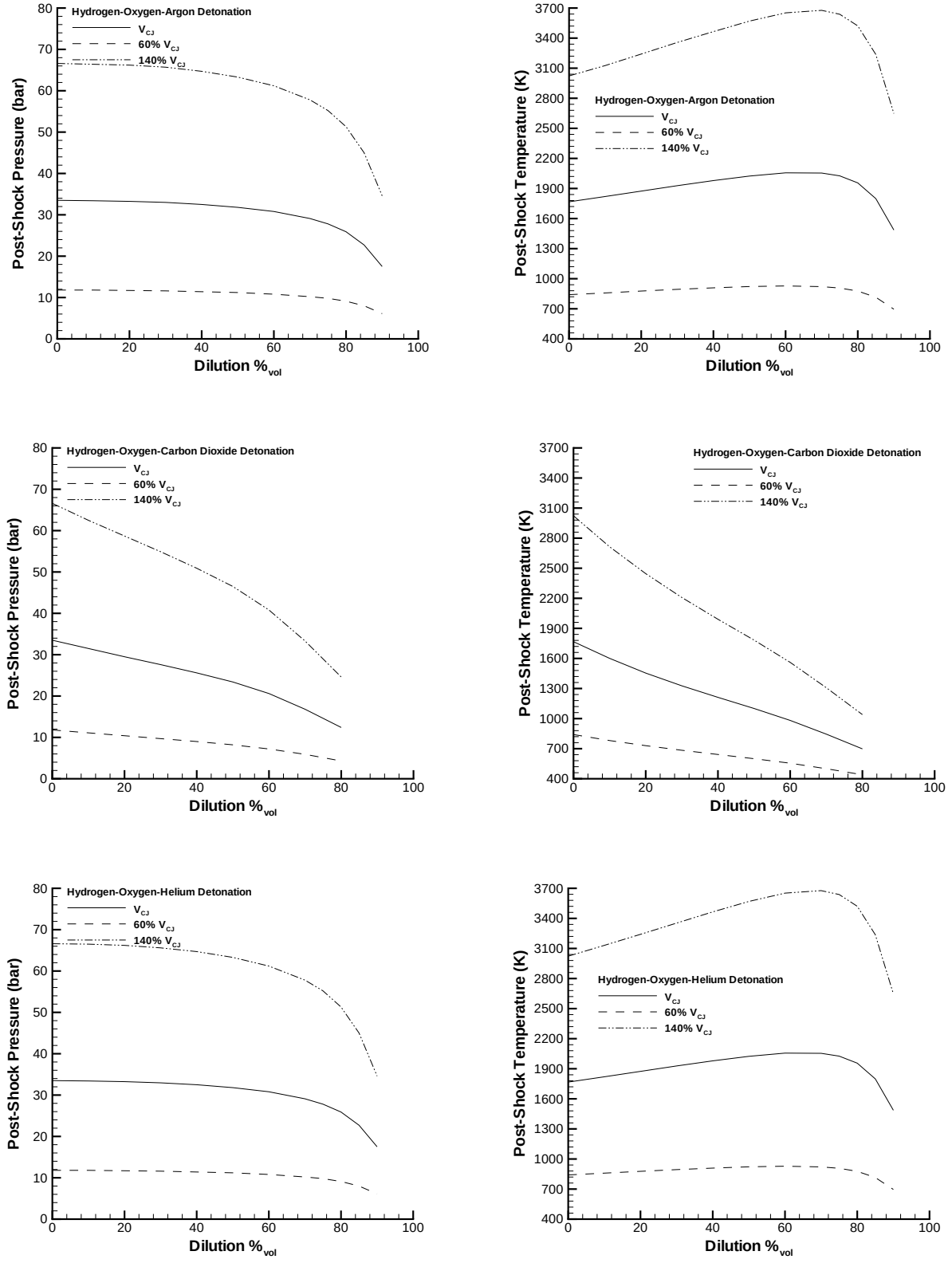

Fig. 5 $H_2/O_2/Ar/CO_2/He$ detonation post-shock thermodynamic conditions (295 K, 1 bar).

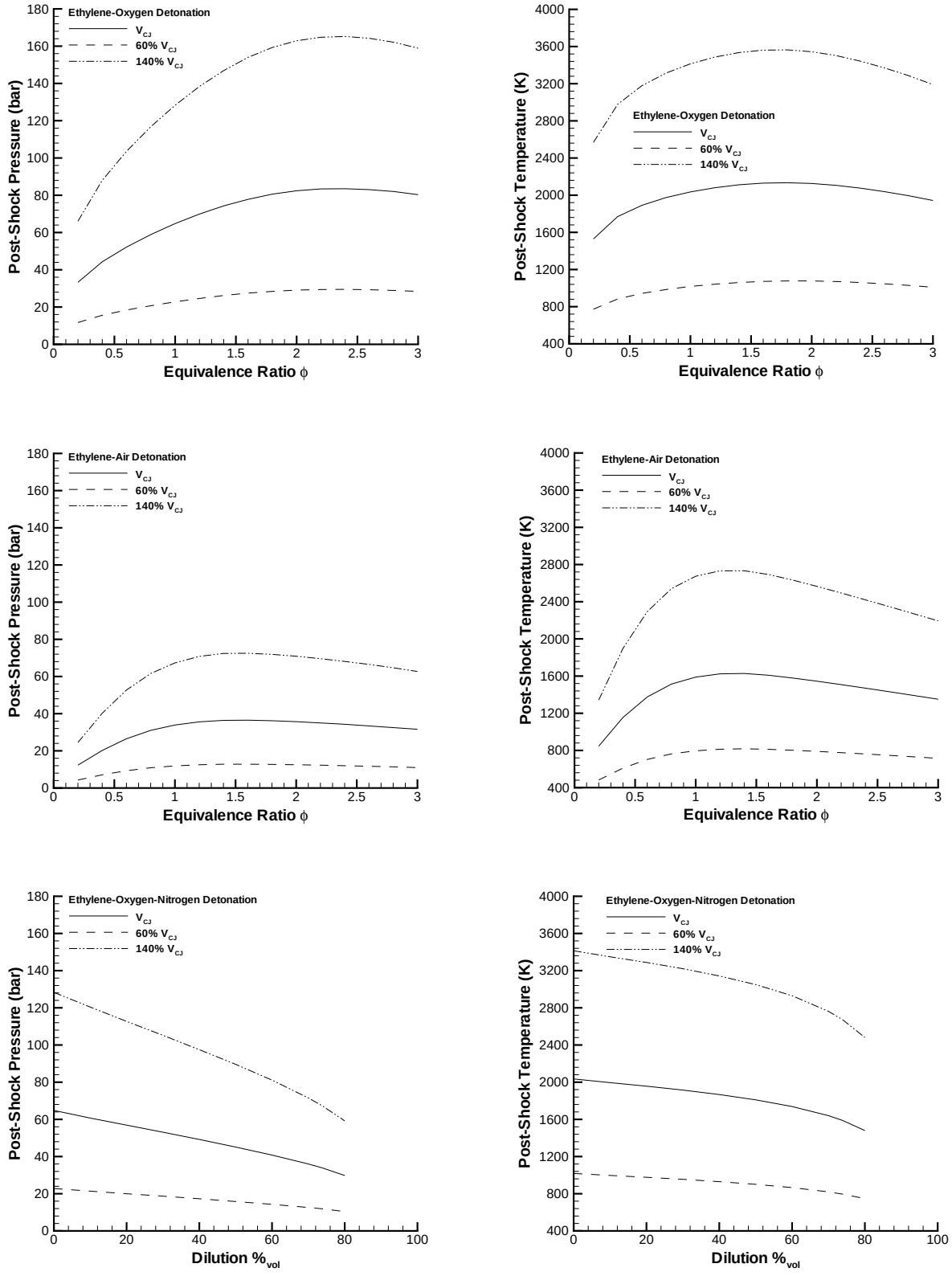

Fig. 6 $C_2H_4/O_2/N_2$ detonation post-shock thermodynamic conditions (295 K, 1 bar).

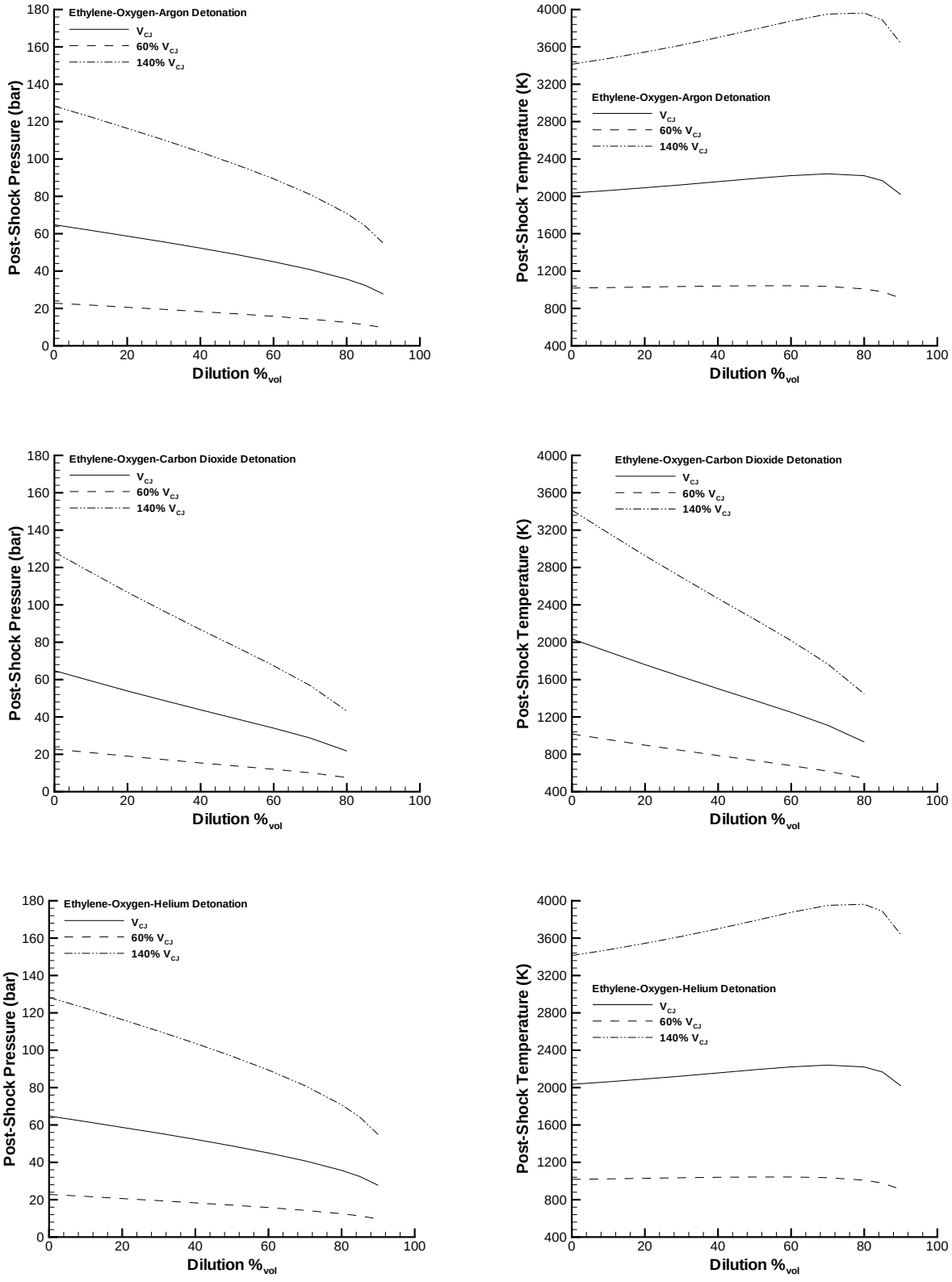

Fig. 7 $C_2H_4/O_2/Ar/CO_2/He$ detonation post-shock thermodynamic conditions (295 K, 1 bar).

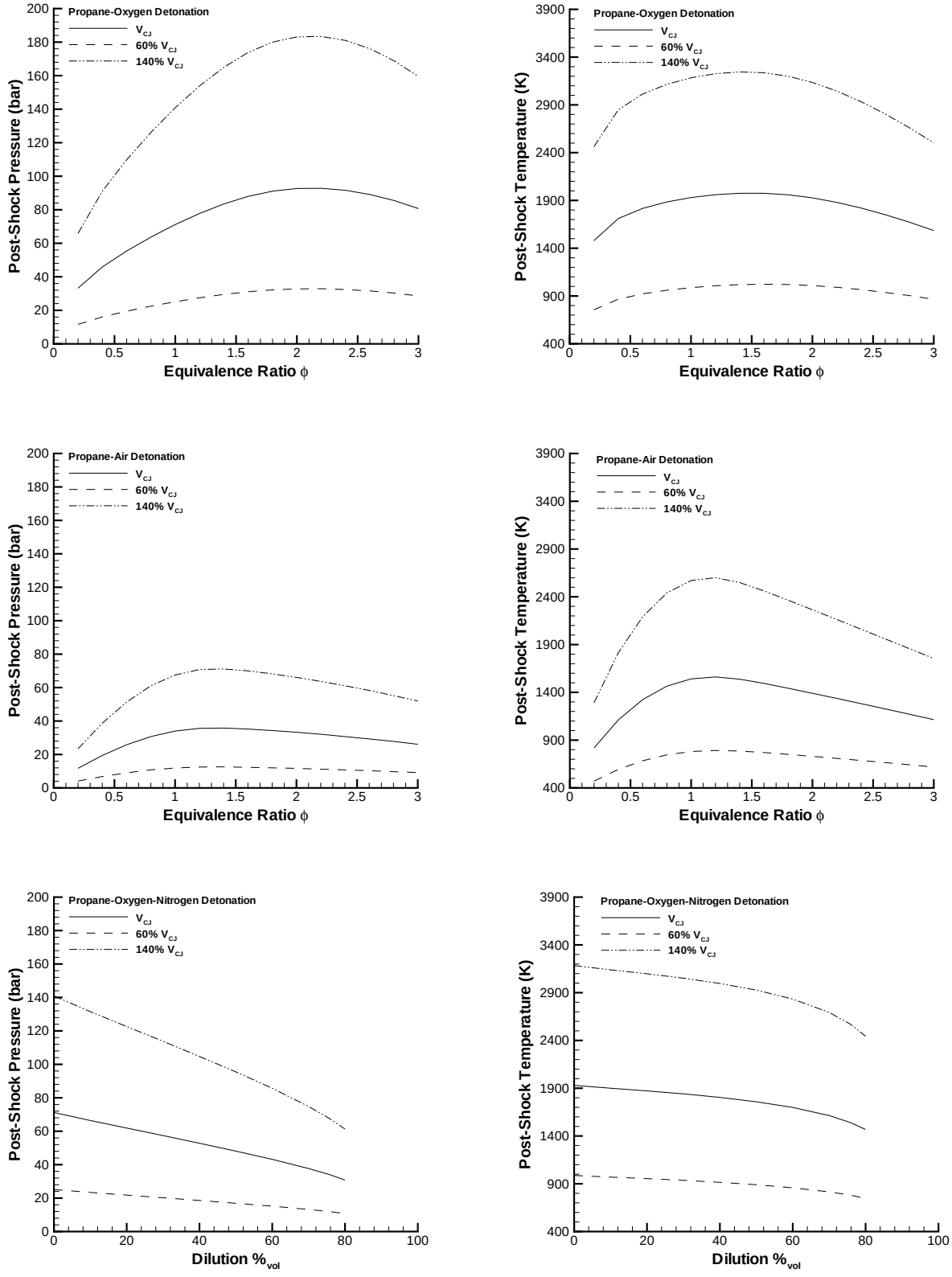

Fig. 8 $C_3H_8/O_2/N_2$ detonation post-shock thermodynamic conditions (295 K, 1 bar).

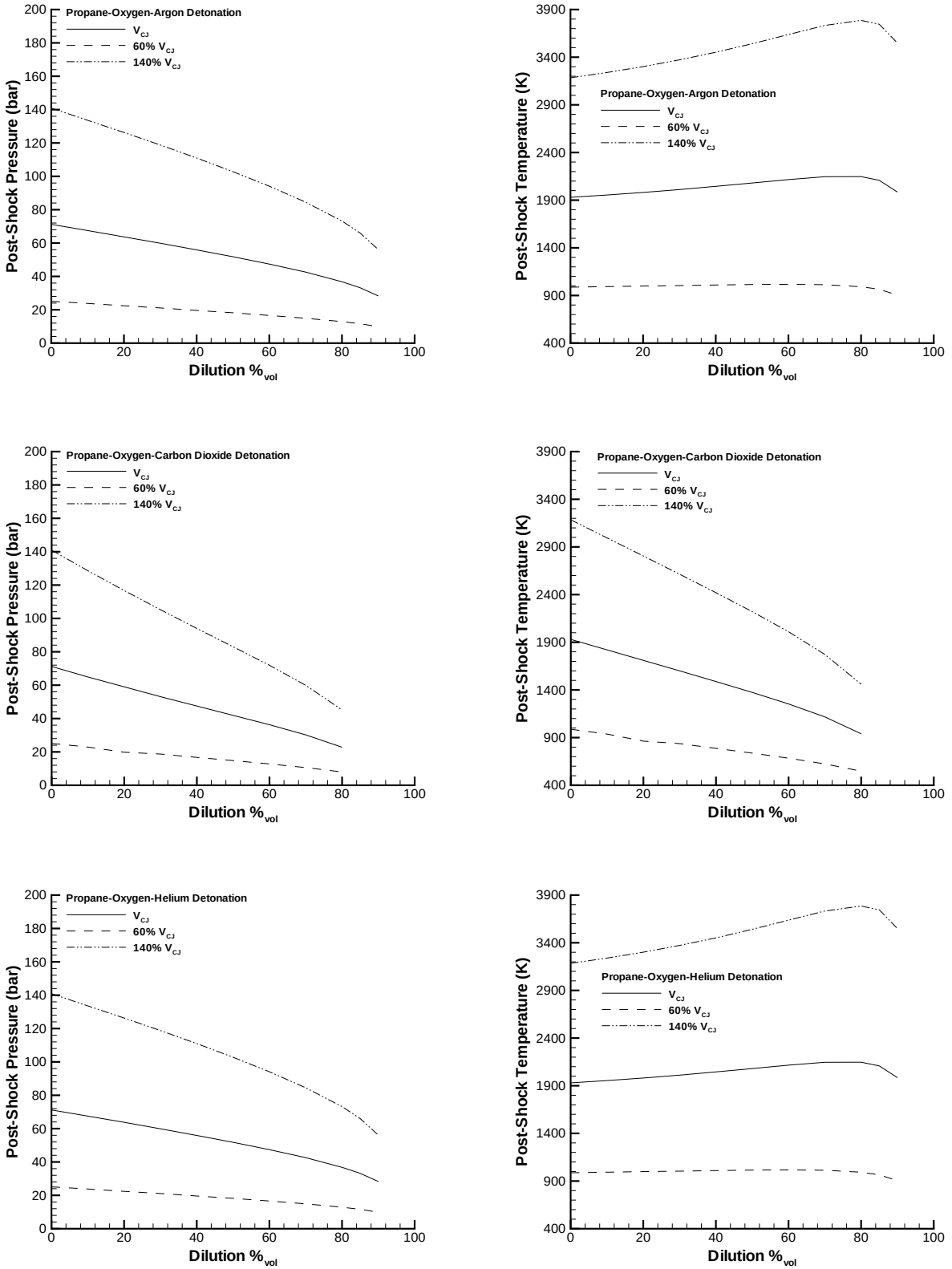

Fig. 9 $C_3H_8/O_2/Ar/CO_2/He$ detonation post-shock thermodynamic conditions (295 K, 1 bar).

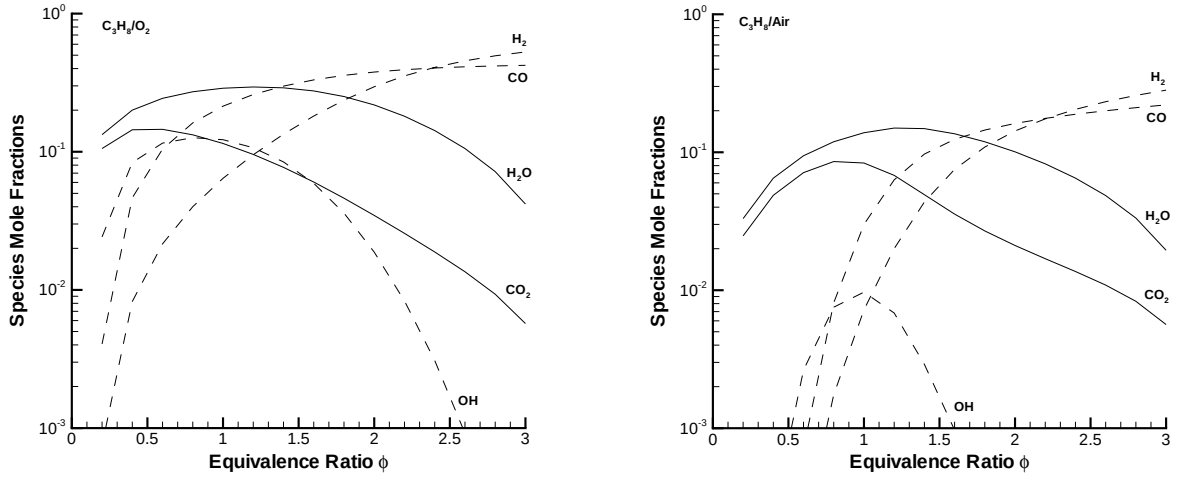

Fig. 10 Propane detonation equilibrium products.

because of dissociative competition between major and intermediate product species. Consider the example of propane mixtures of varying stoichiometry. The equilibrium product compositions for fuel-oxygen and fuel-air mixtures are shown in Fig. 10. Due to the higher temperatures of the fuel-oxygen mixture, there are greater concentrations of species H_2, CO, and OH in the fuel-oxygen mixture than the fuel-air mixture. This shift in the product composition results in the maximum energy release occurring at rich conditions for fuel-oxygen mixtures as compared to near-stoichiometric conditions for the fuel-air mixtures. As discussed in Section 6.3, the CJ Mach number is dependent upon the square root of the specific energy release and the post-shock pressure and temperature vary through the shock jump conditions with the square of the shock Mach number. Therefore, neglecting the effects of composition specific heat ratio, maxima exist in the shock Mach numbers (Figs. 1 - 3) and thermodynamic properties (Figs. 4, 6, 8) near the stoichiometric condition for propane-air mixtures and off-stoichiometric for propane-oxygen mixtures. This illustration applies to the hydrogen and ethylene mixtures as well although the fuel-oxygen maxima shift for hydrogen mixtures is somewhat smaller due to the lack of the CO_2 - CO dissociation step important for reducing the energy release in hydrocarbon mixtures.

Detonation Mach numbers decrease monotonically with increasing diluent concentration for all diluents. However, the effect of diluent addition on reactant molar mass results in an increase in detonation velocity with increasing helium dilution. Dilution by argon and helium also lower the mixture heat capacity resulting in slightly increasing post-shock temperatures up to approximately 80% volumetric dilution. For argon and helium concentrations greater than 80%, the decrease in energy release per unit mass offsets the decreasing heat capacity causing the post-shock temperature to decrease with increasing dilution. Post-shock pressures decrease montonically with increasing dilution for all diluents. This can be explained through consideration of the perfect gas shock jump condition for pressure,

$$\frac{P_{vN}}{P_0} = 1 + \frac{2\gamma}{\gamma + 1}(M_{CJ}^2 - 1)$$

which is insensitive to the specific heat ratio relative to the squared dependence on the detonation Mach number.

Table 1 contains a summary of the detonation post-shock thermodynamic conditions. Different fuel-based mixtures, fuel-oxygen-diluent mixtures, and shock velocities are grouped separately for ease of comparison and establishing the range of conditions over which a reaction mechanism must be validated depending upon the application. Note that particular ranges can be further restricted if limited equivalence ratios and/or diluent concentrations are desired. As shown in Table 1, shock velocities of 60% - 140% V_{CJ} significantly broaden the pressure and temperature range from that of the CJ case. For a given fuel, expanding the diluents considered from nitrogen to include argon, carbon dioxide, and helium has no effect on the pressure range and a modest effect (mostly in hydrogen-based mixtures) on the temperature range.

Table 1: Summary of detonation post-shock thermodynamic conditions with initial conditions of 295 K and 1 bar.

Composition	Shock Velocity	Pressure Range (bar)	Temperature Range (K)
$H_2/O_2/N_2$	V_{CJ}	12 - 34	850 - 1800
	60% - 140% V_{CJ}	4 - 67	450 - 3050
$H_2/O_2/Ar/CO_2/He/N_2$	V_{CJ}	12 - 34	700 - 2050
	60% - 140% V_{CJ}	4 - 67	400 - 3700
$C_2H_4/O_2/N_2$	V_{CJ}	12 - 84	850 - 2150
	60% - 140% V_{CJ}	4 - 165	450 - 3600
$C_2H_4/O_2/Ar/CO_2/He/N_2$	V_{CJ}	12 - 84	850 - 2250
	60% - 140% V_{CJ}	4 - 165	450 - 4000
$C_3H_8/O_2/N_2$	V_{CJ}	11 - 93	800 - 2000
	60% - 140% V_{CJ}	4 - 184	450 - 3250
$C_3H_8/O_2/Ar/CO_2/He/N_2$	V_{CJ}	11 - 93	800 - 2150
	60% - 140% V_{CJ}	4 - 184	450 - 3800

3 Shock Tube Experiments

Chemical reaction experiments in shock tubes most closely represent the type of initial and thermodynamic conditions associated with detonations. Data from such experiments often include a measurement of the chemical induction time of the shocked mixture. The induction time is qualitatively defined as the initial thermally neutral period of free radical species concentration growth, beginning with shock heating and compression of the fluid particle and ending with the onset of thermal explosion (Fig. 11). A variety of quantitative experimental induction time definitions exist, usually associated with an initial rise or maxima in signals including pressure, radiation absorption, or radiation emission from a chemical species. The onset of a signal is defined as the signal rise above some arbitrary level, which tends to complicate matters in analysis or when comparing to other data. Maximum values are typically well-defined, although measurements based on maxima extend the induction time into the thermal explosion process. This is often inconsequential because the induction time is usually much larger than the time for thermal explosion in shock tube experiments.

A shock tube experiment induction time measurement can be idealized as taking place in one-dimensional, inviscid flow behind either the incident (Fig. 12a) or reflected (Fig. 13a) shock. The incident shock case involves a correction for the fluid particle velocity past a stationary measurement device where the induction time (τ_i) is related via the mass conservation equation to the time measured (τ_m) and the shock density ratio (ρ_2/ρ_1) by

$$\tau_i = \left(\frac{\rho_2}{\rho_1}\right)\tau_m$$

The fluid velocity in the reflected shock case is zero and therefore, no frame of reference correction is necessary. The maximum test time is governed by the presence of the contact surface separating the driver and driven (test) gases and can be determined given the initial conditions.

Shock tube experiments depart from ideality due to viscous, heat transfer, and non-equilibrium effects which are manifested through non-uniform flow properties and reduced test time. The boundary layer along the wall behind the incident shock causes attenuation of the shock and acceleration of the contact surface as illustrated in Fig. 12b (Roshko 1960, Gaydon et al. 1963,

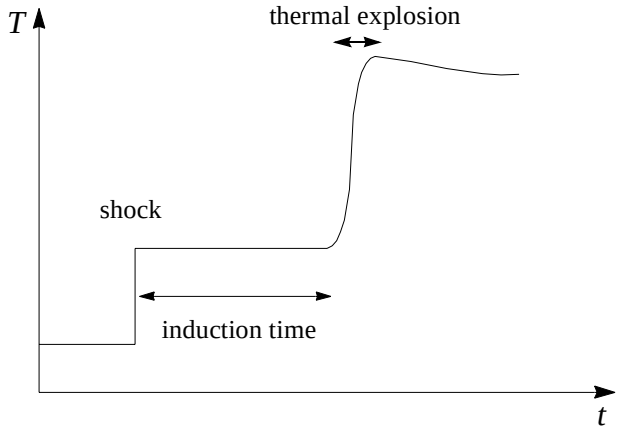

Fig. 11 Temperature evolution in a shock tube experiment.

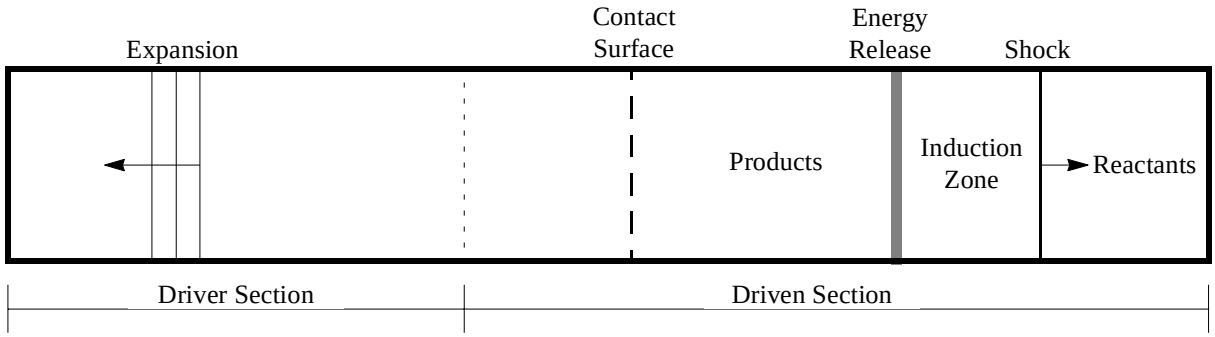

(a) Ideal conditions.

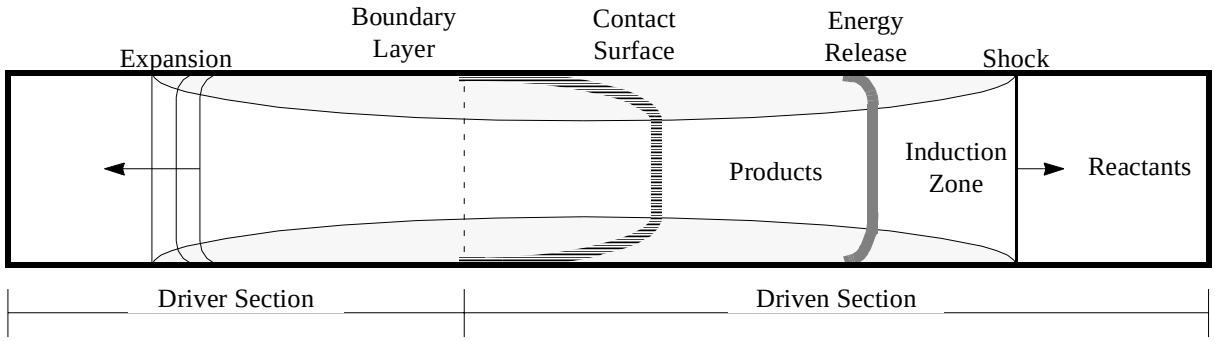

(b) Non-ideal conditions.

Fig. 12 Incident shock experiment schematic.

Mirels 1963, Belford et al. 1969, Sturtevant et al. 1969, Schott et al. 1973, Glass et al. 1994). Chemical energy release is also a source of departure from one-dimensional flow (Schott et al. 1973). Reflection of the incident shock from the end wall can cause separation of the boundary layer and transformation of the reflected shock into a bifurcated lambda configuration as illustrated in Fig. 13b (Mark 1958, Strehlow et al. 1959, Dyner 1966, Belford et al. 1969). The reflected shock may be propagating into a mixture different from the initial test mixture if chemical reactions have been initiated behind the incident shock. A thermal boundary layer forms due to the compressible nature of the flow and heat transfer from the shocked mixture to the relatively cool tube walls, including the end wall in a reflected shock experiment (Belford et al. 1969). Turbulence, wall roughness, and thermal explosion of the mixture can induce non-uniformities in the flow (Belford et al. 1969). Non-equilibrium processes, such as vibrational relaxation of the post-shock mixture, can also complicate the thermodynamic conditions and associated induction time measurements in shock tube experiments (Gaydon et al. 1963).

Mixtures are usually highly diluted to reduce the energy per unit mass and therefore decouple the fluid motion from the chemical reactions as much as possible. Argon is the primary choice among potential diluents because it is relatively inexpensive, increases the driven gas molecular mass (decreases the acoustic speed) and specific heat ratio relative to the driver gas for improved shock tube performance, and the increased specific heat ratio also inhibits reflected shock bifurcation and boundary layer separation. Use of a monatomic diluent bath gas also reduces the influ-

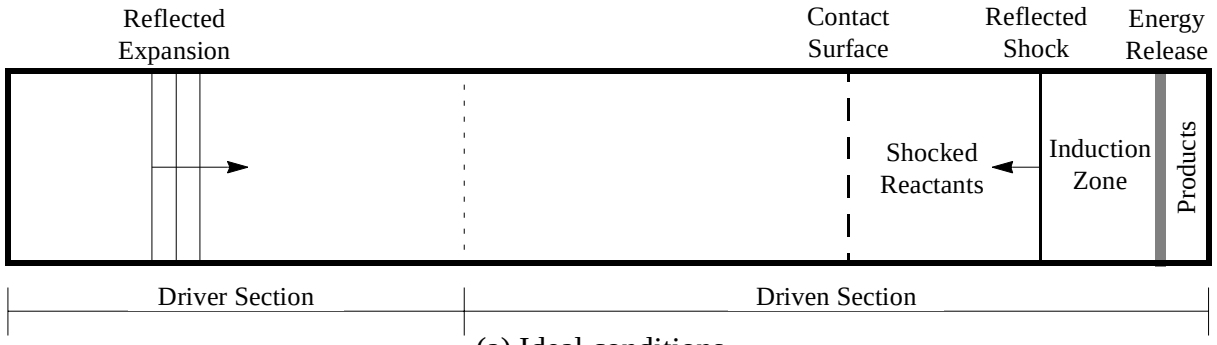

(a) Ideal conditions.

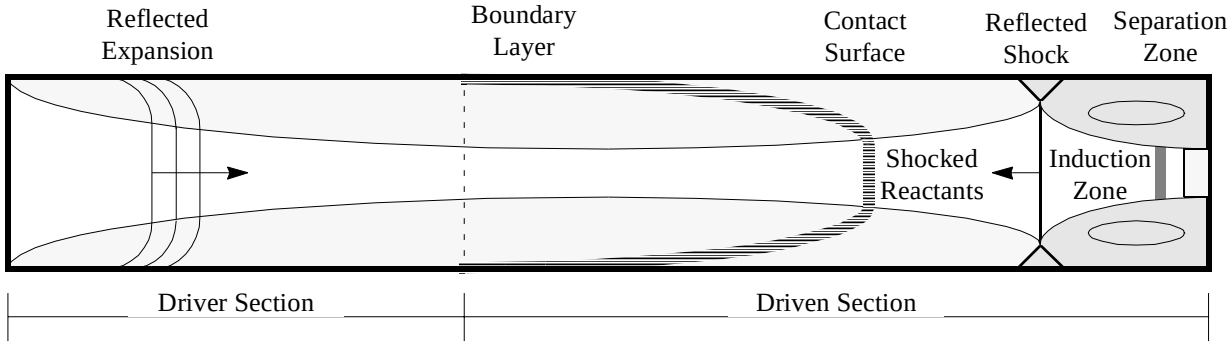

(b) Non-ideal conditions.

Fig. 13 Reflected shock experiment schematic.

ence of non-equilibrium relaxation processes.

The aforementioned complicating experimental aspects play a greater or lesser role in all experiments depending upon the particular shock tube conditions and diagnostic techniques. In addition, two distinct modes of ignition have been observed in shock tube experiments by Meyer et al. (1971). The weak ignition mode occurs at relatively low temperatures and is characterized by a non-uniform distribution of local reaction centers, introducing large variability in induction time measurements. High temperature conditions typically result in the so-called strong ignition mode involving the instantaneous formation of a planar reaction wave which is much more conducive to line-of-sight induction time measurements and one-dimensional modeling techniques.

A database of shock tube induction time measurements has been compiled for hydrogen, ethylene, and propane oxidation. Data taken from the literature and provided via personal communication for inclusion in the database met the following criteria: the induction time definition and two thermodynamic state variables corresponding to each induction time data point are provided. The conditions spanned by the experimental data are summarized in Table 2 and presented graphically in Figs. 14 - 46. In general, the data are sparse to non-existent at detonation thermodynamic conditions for all three fuels considered (Table 1). Most of the data were presented in the original reports in tabulated form or plotted versus inverse post-shock temperature. The values for the plotted data were derived by digitizing and computationally analyzing the plots. Data pro-

cessing requirements particular to individual data sets are outlined where applicable.

There were a number of induction time data sets that were not included in the database because complete information was not available. Additional thermodynamic data are required for the shock tube induction time data of Blumenthal (1996a), Brossard (1979), Miyama (1964), White (1965), White (1967), and Zaitsev (1958). An induction time definition and complete thermodynamic data are not available for the work of Voevodsky (1965), Strehlow (1962) does not provide accurate mixture information, and the induction time data are not provided for the shock tube ignition studies of Blumenthal (1996b). The shock tube data of Brown (1999) and Hidaka (1999) is useful but was received too late for consideration in the present investigation.

The data available in the literature often does not provide a direct indication of the variability in the post-shock thermodynamic conditions and induction time due to any of these effects. The use of the experimental data for validation of induction time data obtained through numerical simulation must proceed under the recognition of these experimental uncertainties. Following the presentation of the experimental data, a simple analysis of the experimental error is included based on the data itself.

Table 2: Shock tube data summary.

Mixture	# Sets	# Points	ϕ	% Diluent	P (atm)	T (K)
$H_2/O_2/Ar/N_2$	14	940	0.06 - 9.0	0.0 - 99.9	0.15 - 87.0	775 - 2650
$C_2H_4/O_2/Ar$	7	530	0.12 - 4.0	70 - 99	0.2 - 12.0	900 - 2350
$C_3H_8/O_2/Ar/N_2$	6	370	0.06 - 2.0	76 - 99	0.6 - 21.8	1000 - 1700

3.1 Hydrogen Shock Tube Data

The hydrogen oxidation shock tube data sets are summarized in Table 3. The raw data are listed in Appendix A and an induction time versus temperature plot for all of the data is shown in Fig. 14. The same data points are plotted in pressure versus temperature format in Fig. 15 along with delineated regions indicating the post-shock thermodynamic conditions for atmospheric initial condition hydrogen detonations (Table 1). Note that the data contained in Figs. 14 - 15 span a range of equivalence ratios and diluent concentrations and this presentation is intended to indicate the range of pressures, temperatures, and induction times for which data is available. Relative to all of the shock tube data collected, the hydrogen data are most numerous and cover the widest range of pressure, temperature, equivalence ratio, and dilution conditions. In general, the data are sparse at detonation thermodynamic conditions. Figures 16 - 29 contain the induction time data grouped according to data set in the order given by Table 3.

Table 3: Summary of hydrogen oxidation shock tube data sets.

Data Set	Technique	Mixture	ϕ	% Diluent	P (atm)	T (K)	Induction Period End
Asaba (1965)	Incident	$H_2/O_2/Ar$	0.085 - 1.5	96 - 99	0.2 - 0.5	1400 - 2400	OH absorption & emission onset
Belles (1965)	Incident	$H_2/O_2/N_2$	0.125 - 0.595	63 - 75	0.2 - 0.5	1100 - 1900	OH emission maximum
Bhaskaran (1973)	Reflected	$H_2/O_2/N_2$	1.0	55.6	2.5	800 - 1400	Pressure rise and light emission onset
Cheng (1977)	Reflected	$H_2/O_2/Ar$	0.5 - 1.0	90	1.0 - 3.0	1000 - 1800	Pressure rise onset
Cohen (1967)	Reflected	$H_2/O_2/Ar$	1.0 - 2.0	0 - 94	0.25 - 8.3	900 - 1650	UV emission and pressure maximum, UV absorption
Craig (1966)	Reflected	$H_2/O_2/N_2$	1.0	55.6	1 - 2	875 - 1000	OH emission onset
Fujimoto (1963)	Reflected	$H_2/O_2/Ar$	1.0	70	0.88 - 2.7	800 - 1400	Pressure rise and light emission onset
Jachimowski (1971)	Incident	$H_2/O_2/Ar$	0.063 - 2.0	91 - 95	0.2 - 0.75	1200 - 1800	OH absorption at 5% of maximum
Just (1968)	Reflected	$H_2/O_2/N_2$	0.1 - 1.0	55 - 76	0.4 - 1.4	900 - 1250	Luminosity onset
Petersen (1996)	Reflected	$H_2/O_2/Ar$	1.0	97 - 99.9	33 - 87	1100 - 1900	OH absorption maximum rate of change
Schott (1958)	Incident & Reflected	$H_2/O_2/Ar$	0.125 - 9.0	75.3 - 98.9	0.15 - 9.5	1050 - 2650	OH absorption onset
Skinner (1966)	Reflected	$H_2/O_2/Ar$	2.0	90	5	900 - 1100	OH emission maximum
Snyder (1965)	Reflected	$H_2/O_2/N_2$	0.5 - 1.0	55.6 - 65.3	1.0 - 9.0	800 - 1100	Pressure rise and UV emission onset
Steinberg (1955)	Reflected	H_2/O_2	1.0	0	4.5 - 9.0	700 - 1000	Luminosity onset

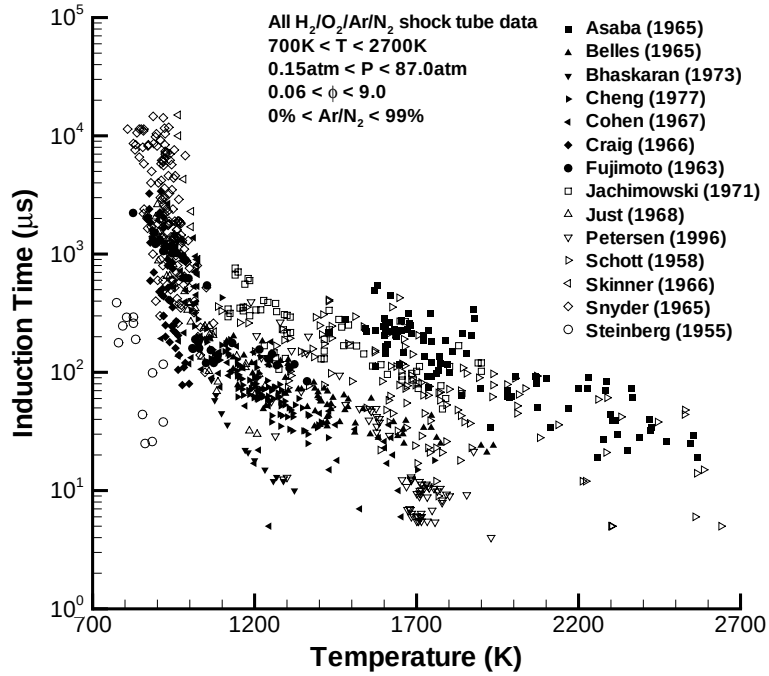

Fig. 14 Hydrogen induction time versus temperature data from shock tube experiments.

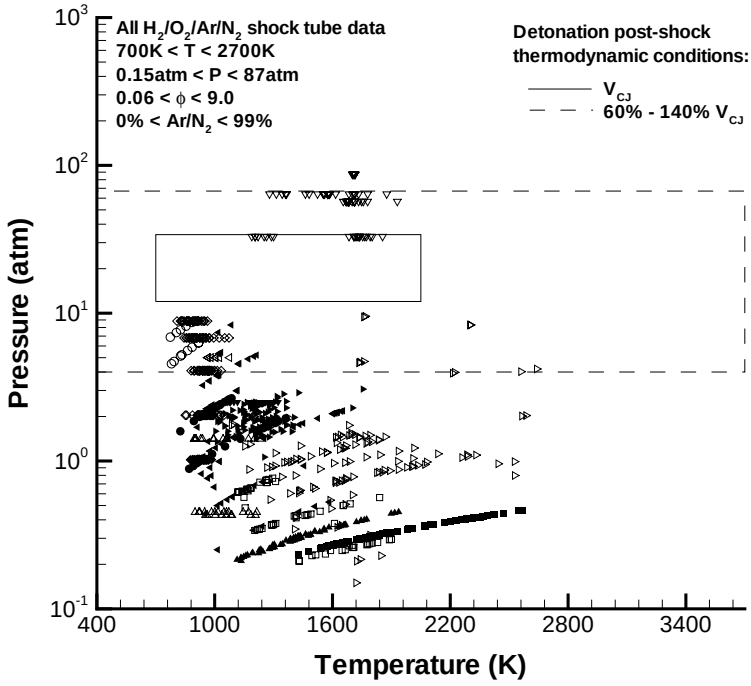

Fig. 15 Hydrogen pressure versus temperature data from shock tube experiments.

The Asaba (1965) post-shock pressures were not given and some of the data were presented in $\tau[O_2]$ form, where τ is the induction time and $[O_2]$ the post-shock oxygen concentration. The incident shock velocity was calculated assuming a frozen shock jump from 295 K to the post-shock temperature which then provided the post-shock pressure from the shock velocity and given initial pressures. The post-shock oxygen concentration followed from the mixture composition and post-shock pressure and temperature. The same procedure was used to determine the post-shock pressure for the Belles (1965) data set. Frozen incident and reflected shock calculations were performed for the Cohen (1967) data set to determine the post-shock pressure and oxygen concentration, given the initial pressure, mixture composition, and assuming an initial temperature of 295 K. The post-shock pressures for Jachimowski (1971) were calculated from the given mixture composition and post-shock concentration and temperature. Data from Cheng (1977), Cohen (1967), Petersen (1996), and Schott (1958) were supplemented by information obtained through personal communication with Cheng (1999), Cohen (1999), Petersen (1999), and Schott (1999), respectively.

.

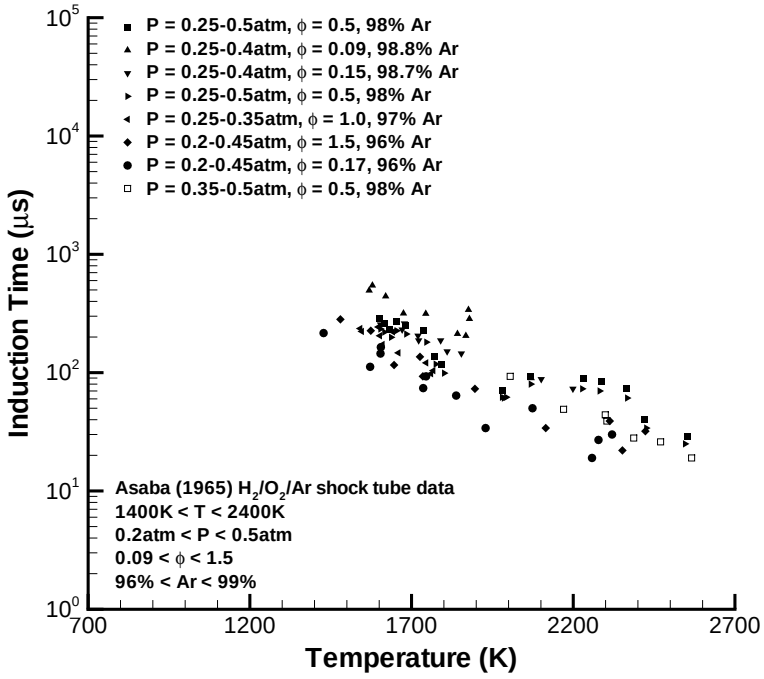

Fig. 16 Asaba (1965) hydrogen oxidation induction time data.

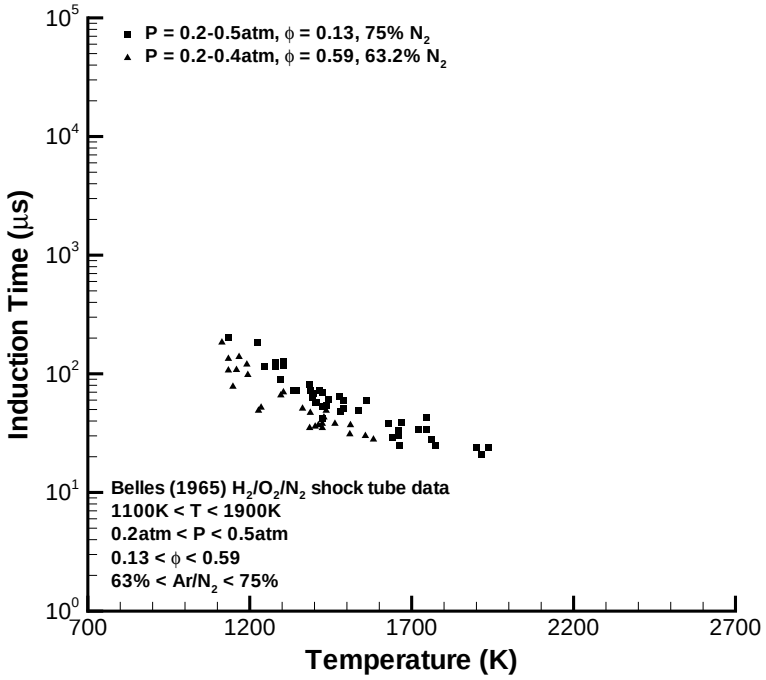

Fig. 17 Belles (1965) hydrogen oxidation induction time data.

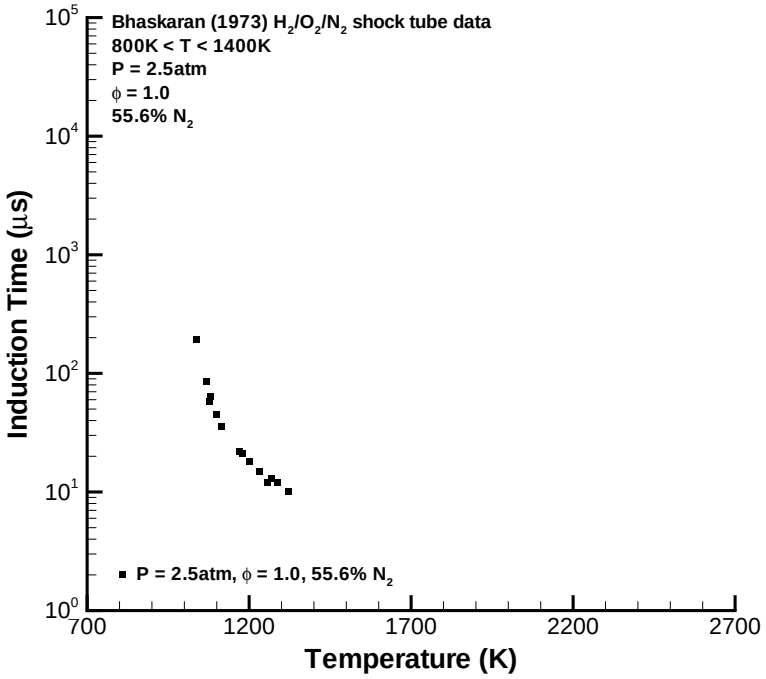

Fig. 18 Bhaskaran (1973) hydrogen oxidation induction time data.

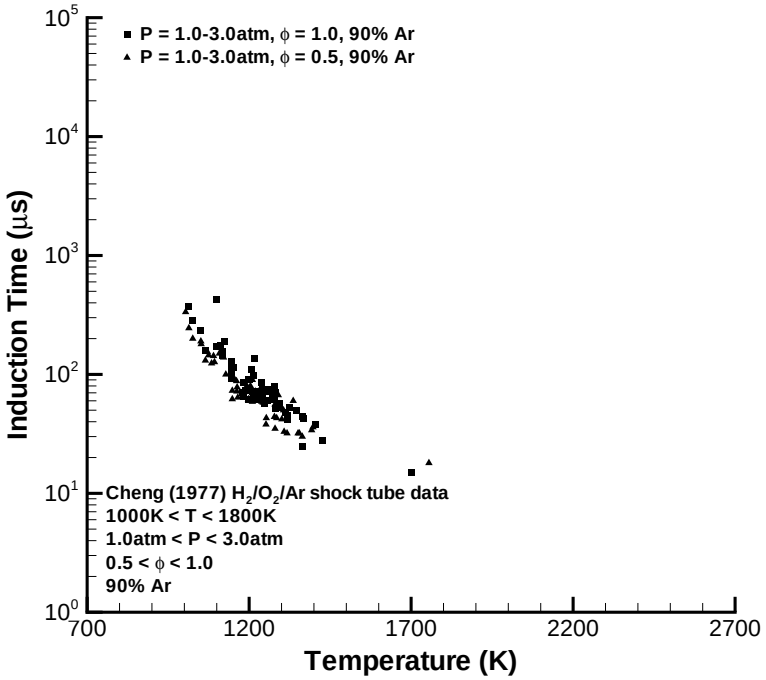

Fig. 19 Cheng (1977) hydrogen oxidation induction time data.

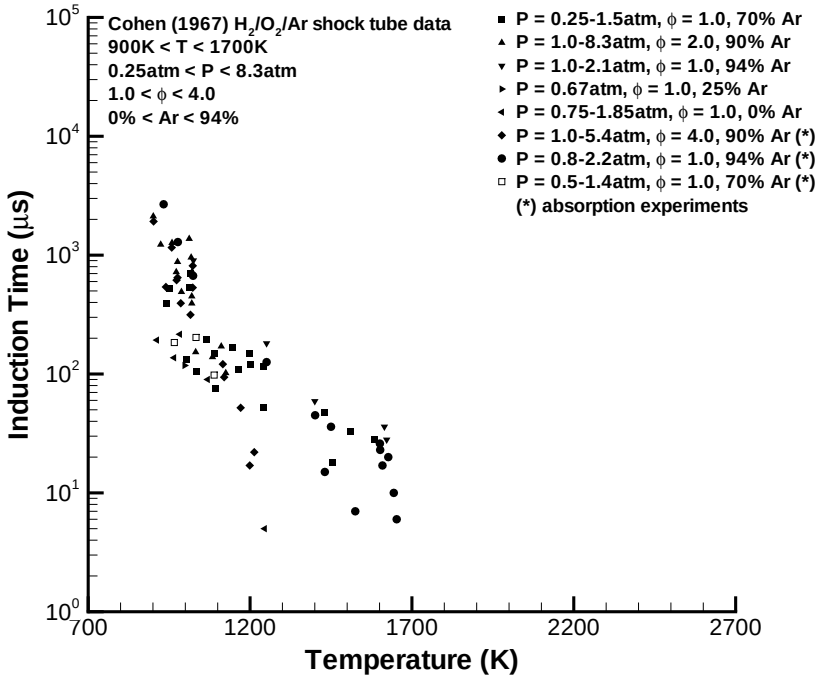

Fig. 20 Cohen (1967) hydrogen oxidation induction time data.

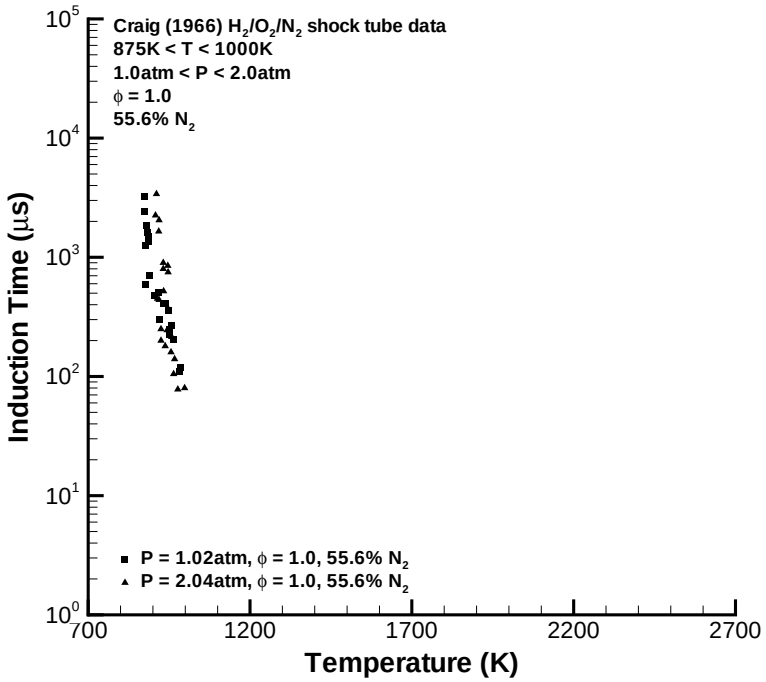

Fig. 21 Craig (1966) hydrogen oxidation induction time data.

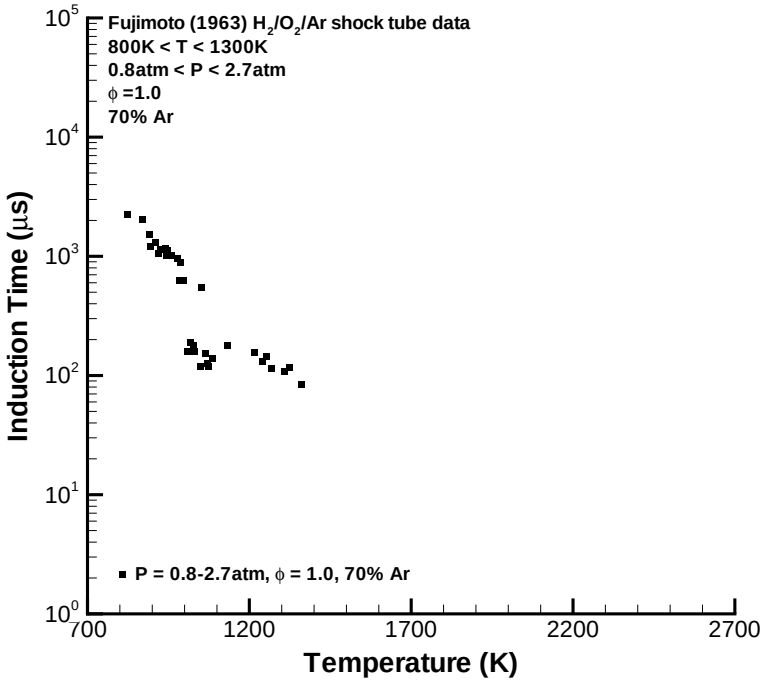

Fig. 22 Fujimoto (1963) hydrogen oxidation induction time data.

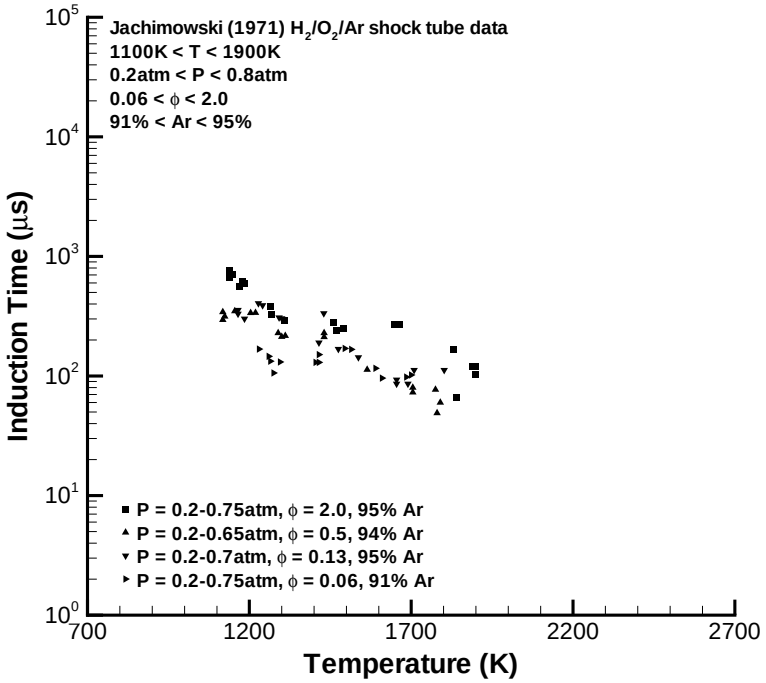

Fig. 23 Jachimowski (1971) hydrogen oxidation induction time data.

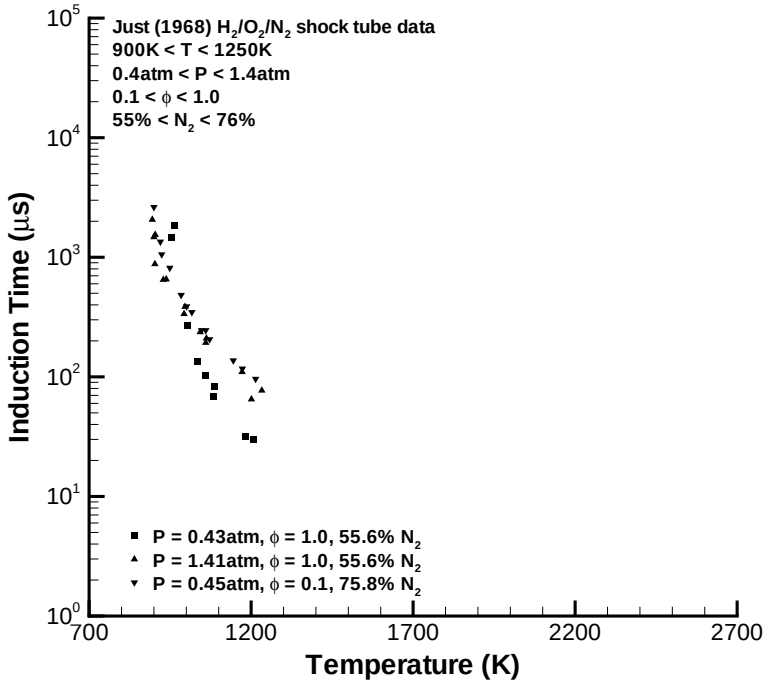

Fig. 24 Just (1968) hydrogen oxidation induction time data.

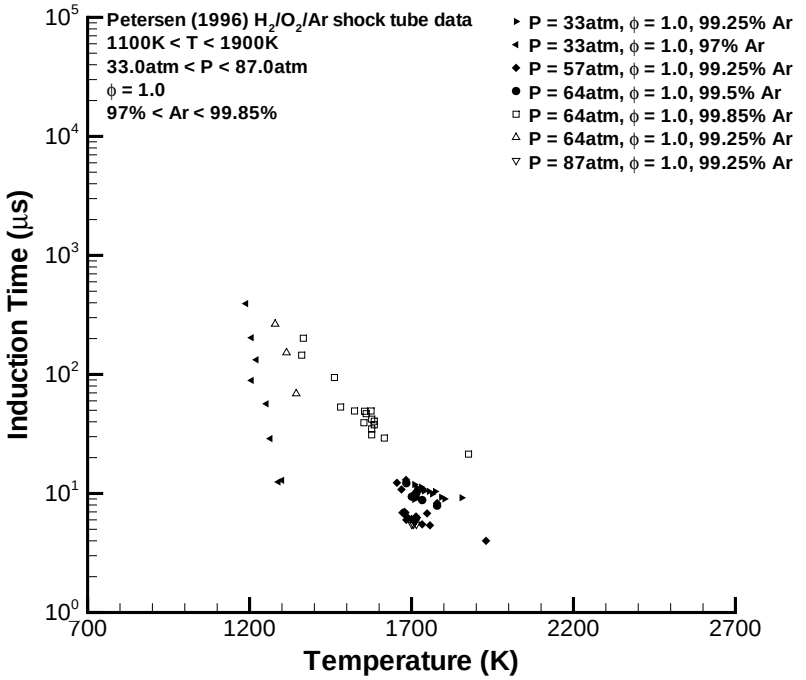

Fig. 25 Petersen (1996) hydrogen oxidation induction time data.

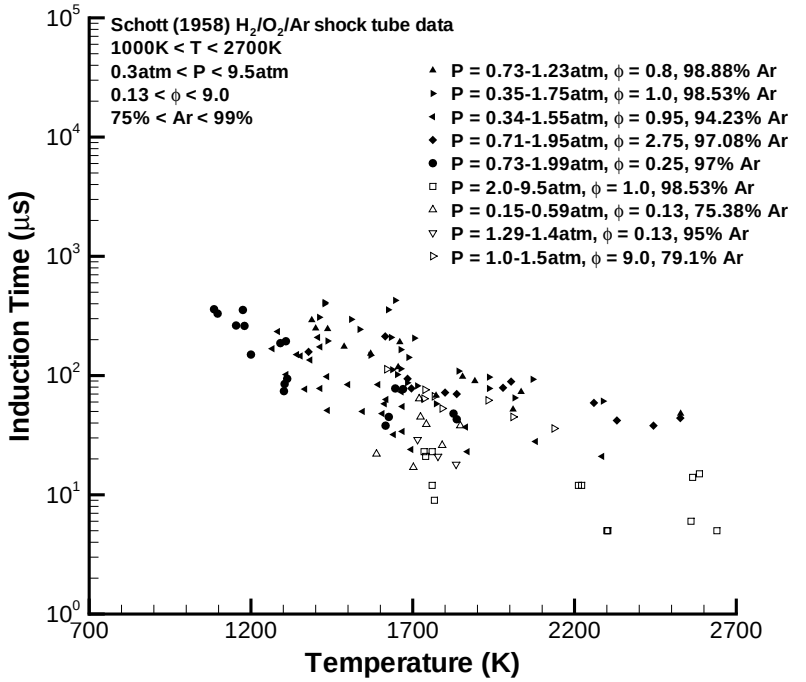

Fig. 26 Schott (1958) hydrogen oxidation induction time data.

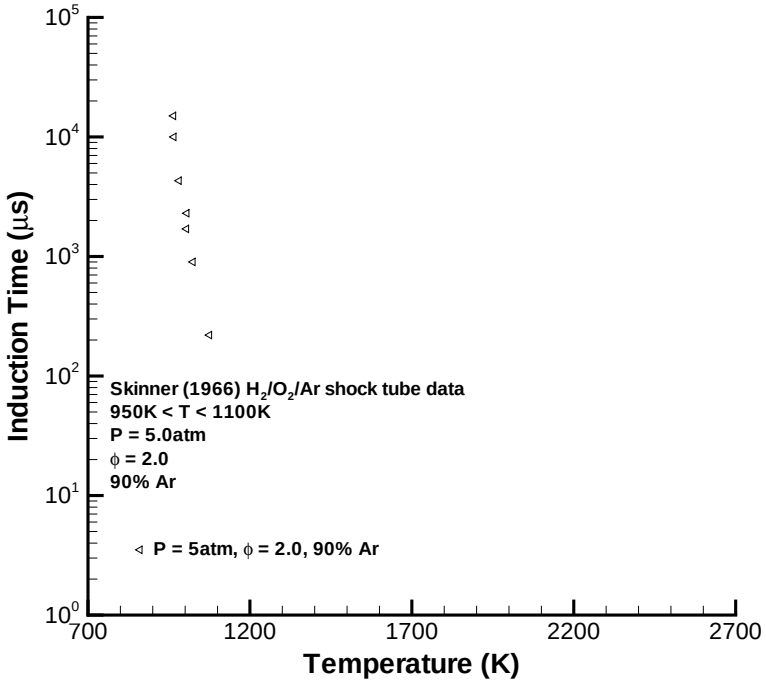

Fig. 27 Skinner (1966) hydrogen oxidation induction time data.

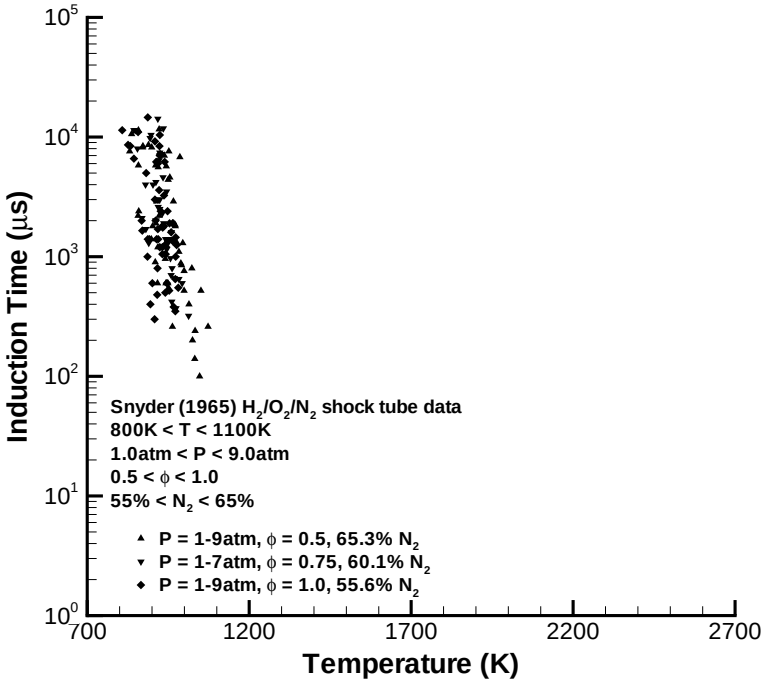

Fig. 28 Snyder (1965) hydrogen oxidation induction time data.

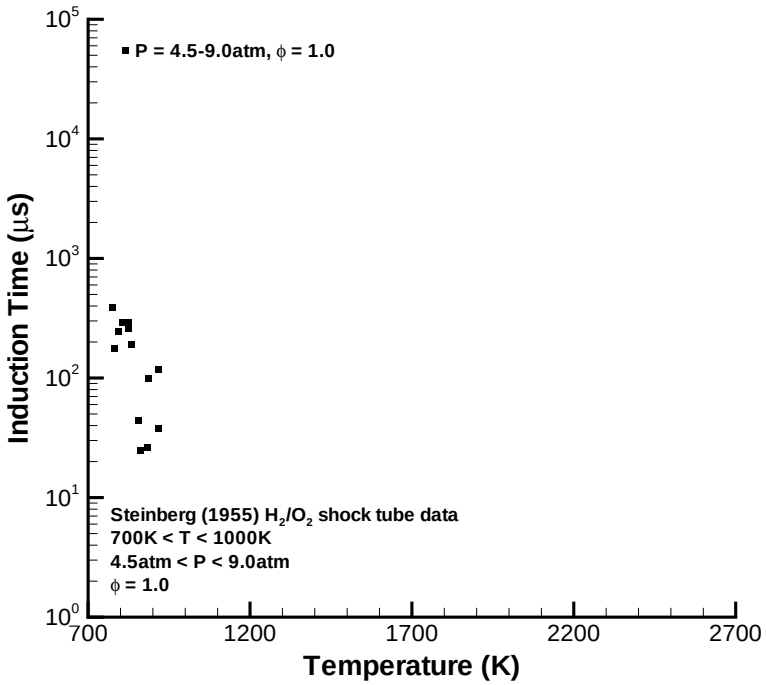

Fig. 29 Steinberg (1955) hydrogen oxidation induction time data.

3.2 Ethylene Shock Tube Data

The ethylene oxidation shock tube data sets are summarized in Table 4. The raw data are listed in Appendix B and an induction time versus temperature plot for all of the data is shown in Fig. 30. The same data points are plotted in pressure versus temperature format in Fig. 31 along with delineated regions indicating the post-shock thermodynamic conditions for atmospheric initial condition ethylene detonations (Table 1). Note that the data contained in Figs. 30 - 31 span a range of equivalence ratios and diluent concentrations and this presentation is intended to indicate the range of pressures, temperatures, and induction times for which data is available. All experiments utilized relatively high concentrations of argon diluent and the equivalence ratio was varied over a broad range. In general, the data are non-existent at detonation thermodynamic conditions. Figures 32 - 38 contain the induction time data grouped according to data set in the order given by Table 4.

Frozen incident and reflected shock calculations were performed for the Drummond (1968) data set to determine the post-shock pressure and oxygen concentration, given the initial pressure, mixture composition, and assuming an initial temperature of 295 K. These values were then used to derive the induction time from the plotted format product of induction time, post-shock pressure, and oxygen concentration. The post-shock pressures for Gay (1967) and Homer (1967) were calculated from the given mixture composition and post-shock concentration and temperature. Note that Gay (1967) is unclear as to whether or not the post-incident-shock fluid velocity was accounted for in the induction time measurements; we have assumed the correction was made. Data from Baker (1972) and Suzuki (1971) were supplemented by information obtained through personal communication with Skinner (1999) and Tanzawa (1998), respectively.

Table 4: Summary of ethylene oxidation shock tube data sets.

Data Set	Technique	Mixture	ϕ	% Diluent	P (atm)	T (K)	Induction Period End
Baker (1972)	Reflected	$C_2H_4/O_2/Ar$	0.125 - 2.0	93 - 99	3 - 12	1000 - 1900	OH emission maximum
Drummond (1968)	Reflected	$C_2H_4/O_2/Ar$	1.0 - 2.0	84 - 95	1.0 - 2.2	1000 - 1700	OH emission maximum
Gay (1967)	Incident	$C_2H_4/O_2/Ar$	0.214 - 4.0	96 - 99	0.2 - 0.4	1400 - 2300	CH* emission onset
Hidaka (1974)	Reflected	$C_2H_4/O_2/Ar$	1.0 - 3.0	96 - 98	1.0 - 5.0	1400 - 2100	CH* emission onset
Homer (1967)	Reflected	$C_2H_4/O_2/Ar$	0.5 - 1.5	96.5 - 98.5	0.3 - 0.8	1500 - 2300	$CO + CO_2$ emission 10% of maximum
Jachimowski (1977)	Incident	$C_2H_4/O_2/Ar$	0.5 - 1.5	91 - 93	1.1 - 1.7	1800 - 2400	$CO + CO_2$ emission for [O][CO] maximum
Suzuki (1971)	Reflected	$C_2H_4/O_2/Ar$	0.462 - 2.625	70	1 - 3.2	800 - 1400	OH absorption maximum rate of change

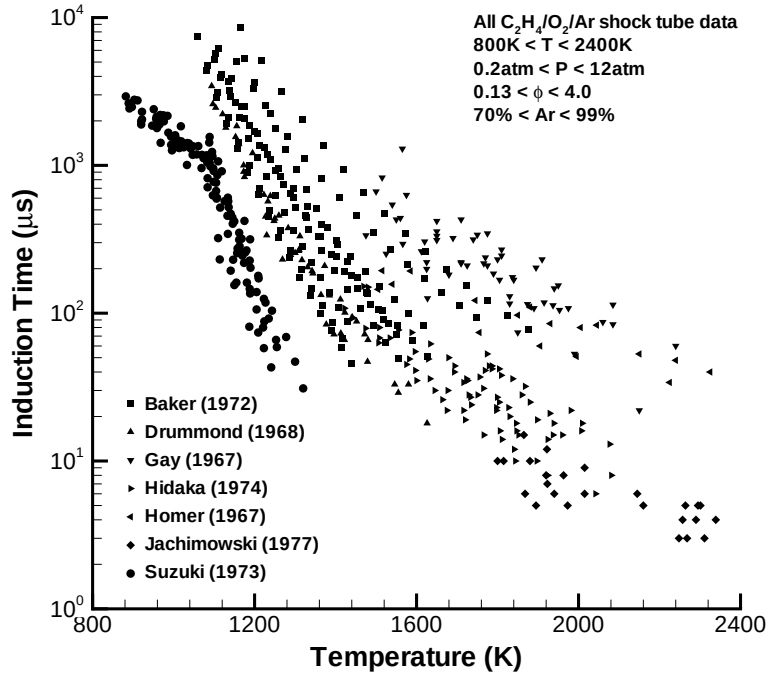

Fig. 30 Ethylene induction time versus temperature data from shock tube experiments.

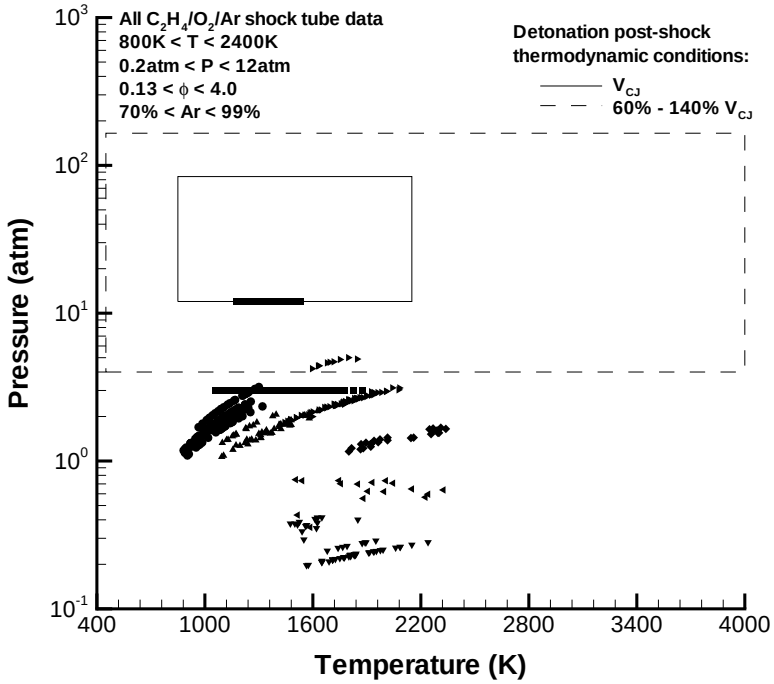

Fig. 31 Ethylene pressure versus temperature data from shock tube experiments.

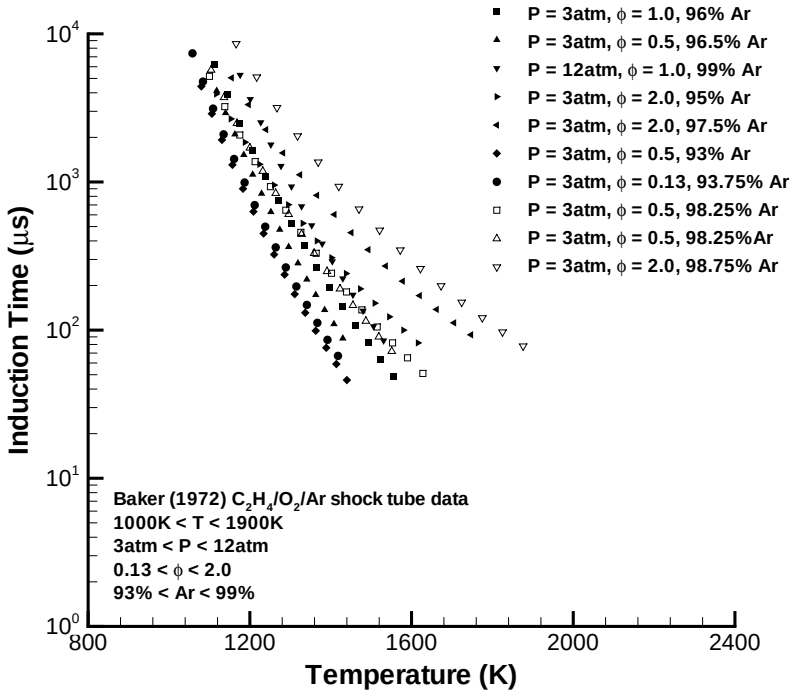

Fig. 32 Baker (1972) ethylene oxidation induction time data.

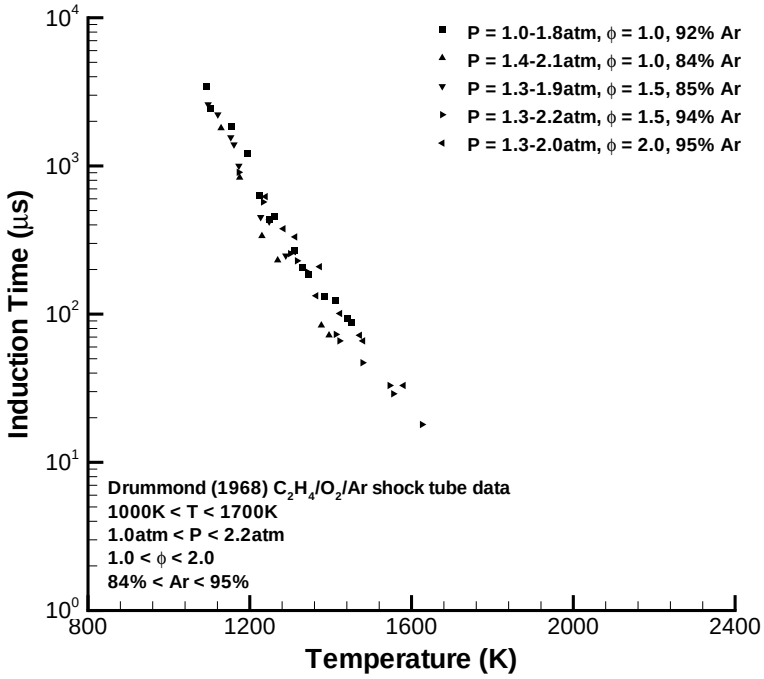

Fig. 33 Drummond (1968) ethylene oxidation induction time data.

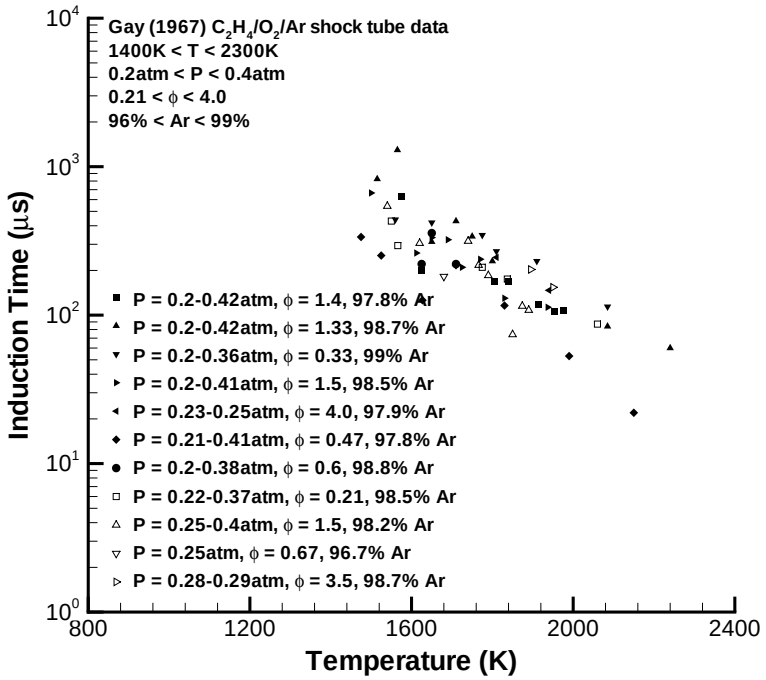

Fig. 34 Gay (1967) ethylene oxidation induction time data.

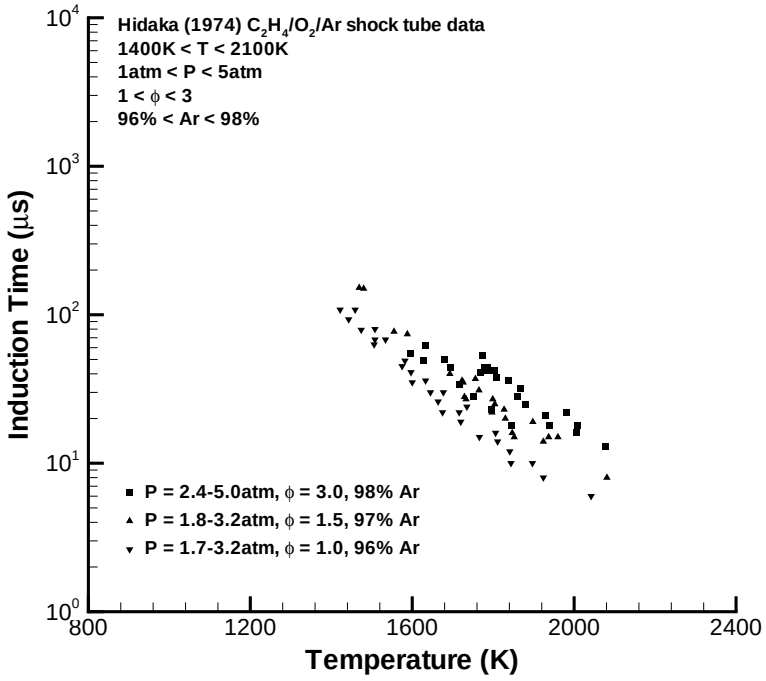

Fig. 35 Hidaka (1974) ethylene oxidation induction time data.

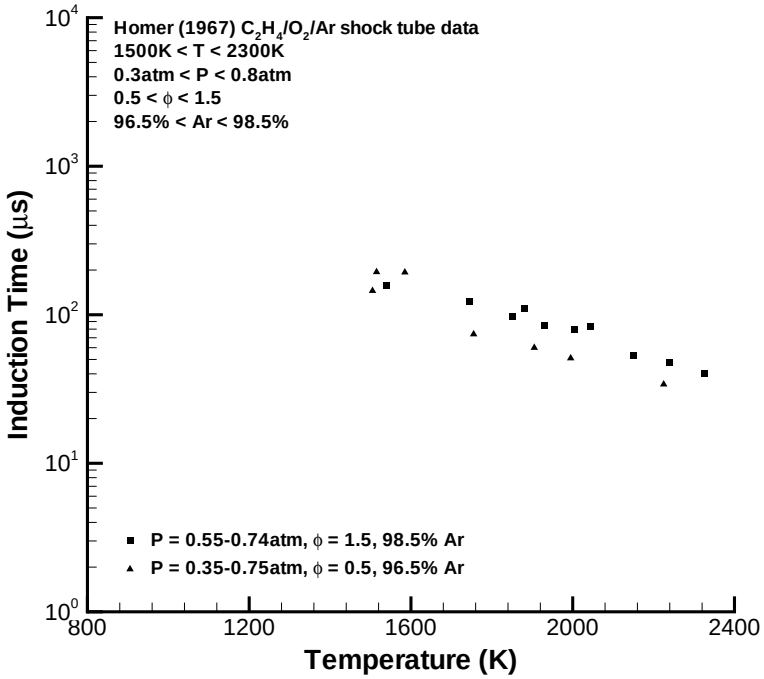

Fig. 36 Homer (1967) ethylene oxidation induction time data.

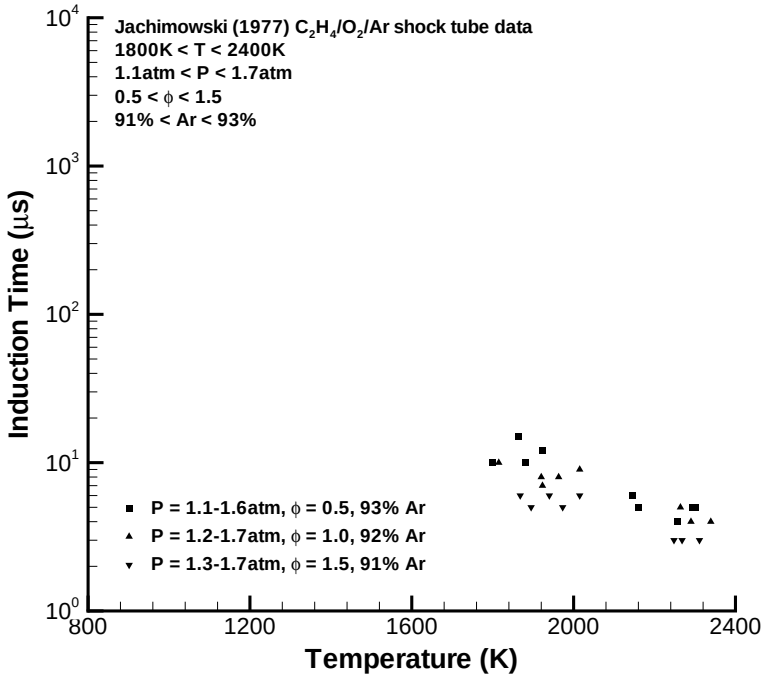

Fig. 37 Jachimowski (1977) ethylene oxidation induction time data.

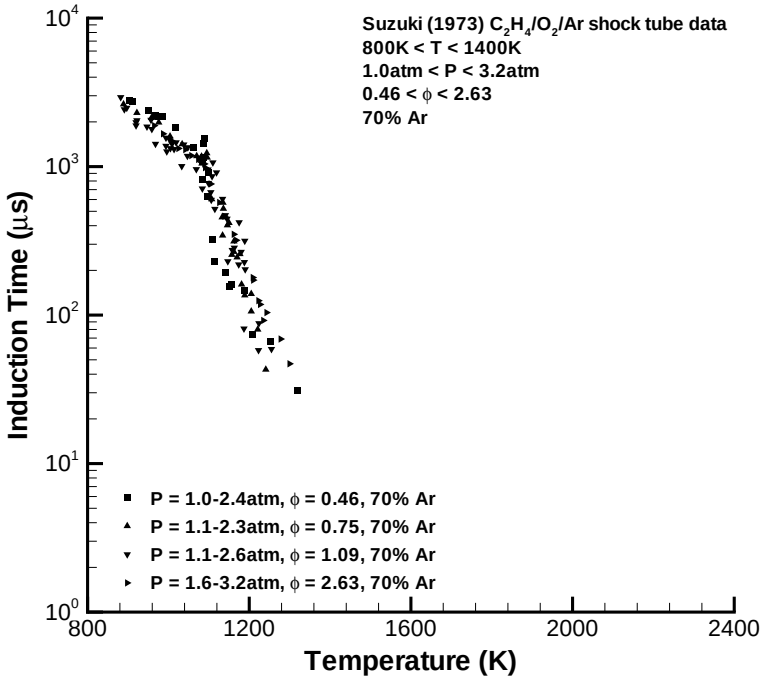

Fig. 38 Suzuki (1973) ethylene oxidation induction time data.

3.3 Propane Shock Tube Data

The propane oxidation shock tube data sets are summarized in Table 5. The raw data are listed in Appendix C and an induction time versus temperature plot for all of the data is shown in Fig. 39. The same data points are plotted in pressure versus temperature format in Fig. 40 along with delineated regions indicating the post-shock thermodynamic conditions for atmospheric initial condition ethylene detonations (Table 1). Note that the data contained in Figs. 39 - 40 span a range of equivalence ratios and diluent concentrations and this presentation is intended to indicate the range of pressures, temperatures, and induction times for which data is available. All experiments utilized relatively high concentrations of argon or nitrogen diluent and the upper equivalence ratio was limited to 2.0. In general, the data are sparse at detonation thermodynamic conditions. Figures 41 - 46 contain the induction time data grouped according to data set in the order given by Table 5.

Frozen incident and reflected shock calculations were performed for the Burcat (1970, 1971) data sets to determine the post-shock pressure, given the initial pressure, mixture composition, and assuming an initial temperature of 295 K. Note that Hawthorn (1966) is unclear as to whether or not the post-incident-shock fluid velocity was accounted for in the induction time measurements; we have assumed the correction was made. Also note that the time for the second rise in hydroxyl emission was taken as the induction time for Myers (1969) stated by the author as occurring very close to the OH maximum. Data from Burcat (1970, 1971) and Gray (1994) were supplemented by information obtained through personal communication with Burcat (1998) and Gray (1998), respectively.

Table 5: Summary of propane oxidation shock tube data sets.

Data Set	Technique	Mixture	ϕ	% Diluent	P (atm)	T (K)	Induction Period End
Burcat (1970)	Reflected	$C_3H_8/O_2/Ar$	0.125 - 2.0	76 - 98	2 - 14.1	1100 - 1600	Pressure and heat flux rise onset
Burcat (1971)	Reflected	$C_3H_8/O_2/Ar$	1.0	80.7	8.0 - 14.2	1200 - 1700	Pressure and heat flux rise onset
Gray (1994)	Incident	$C_3H_8/O_2/Ar$	1.0	98.8	1.4 - 1.7	1400 - 1800	CH* emission maximum
Hawthorn (1966)	Incident	$C_3H_8/O_2/Ar$	0.063 - 2.0	95 - 99	0.61 - 1.7	1100 - 1500	Luminosity emission onset
Myers (1969)	Incident	$C_3H_8/O_2/Ar$	0.2	95	1	1000 - 1500	OH emission maximum
Steinberg (1954)	Reflected	$C_3H_8/O_2/N_2$	1.0	75.8	7.1 - 21.8	1100 - 1600	Luminosity emission onset

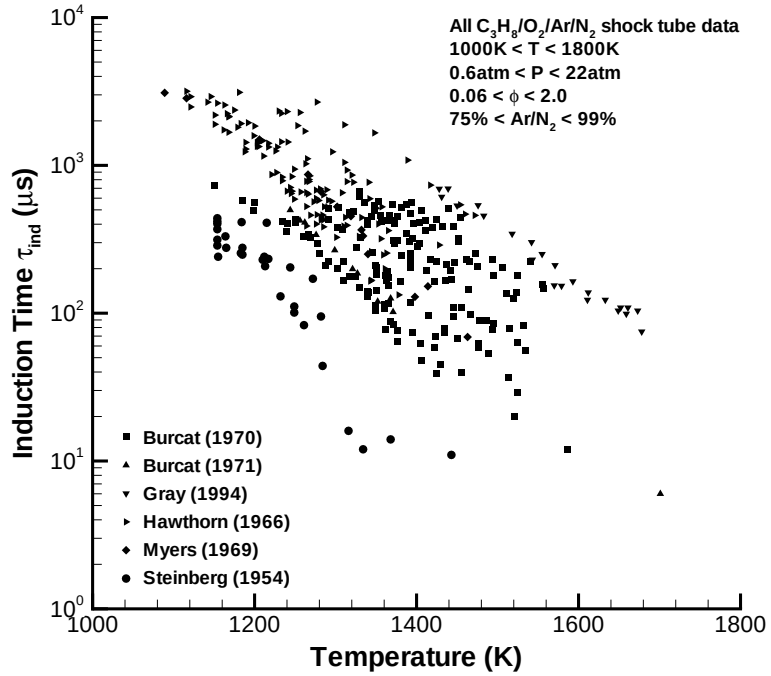

Fig. 39 Propane induction time versus temperature data from shock tube experiments.

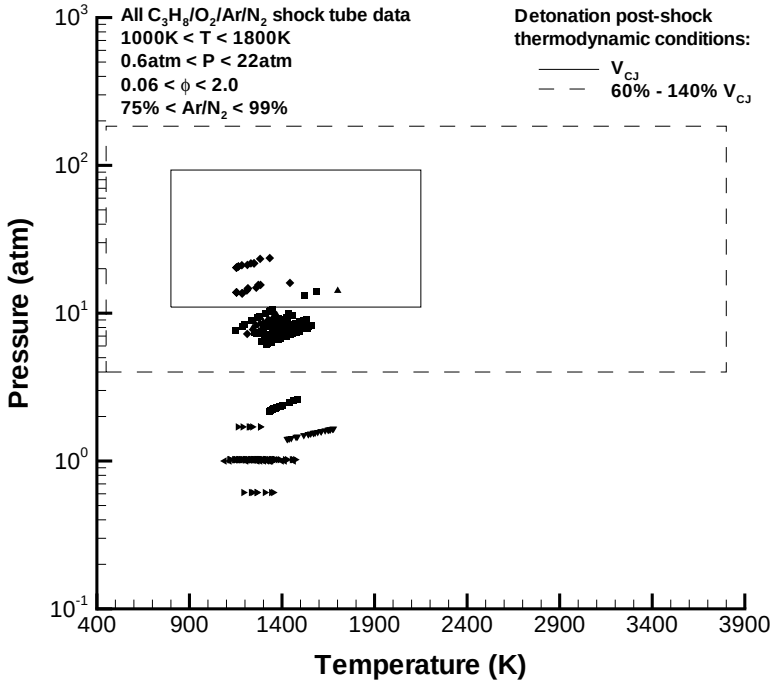

Fig. 40 Propane pressure versus temperature data from shock tube experiments.

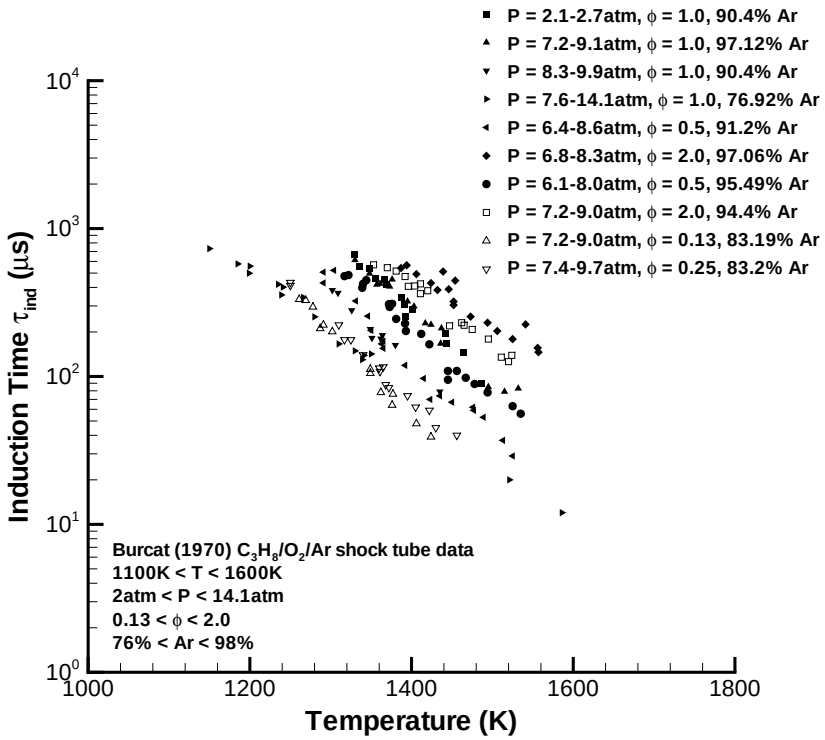

Fig. 41 Burcat (1970) propane oxidation induction time data.

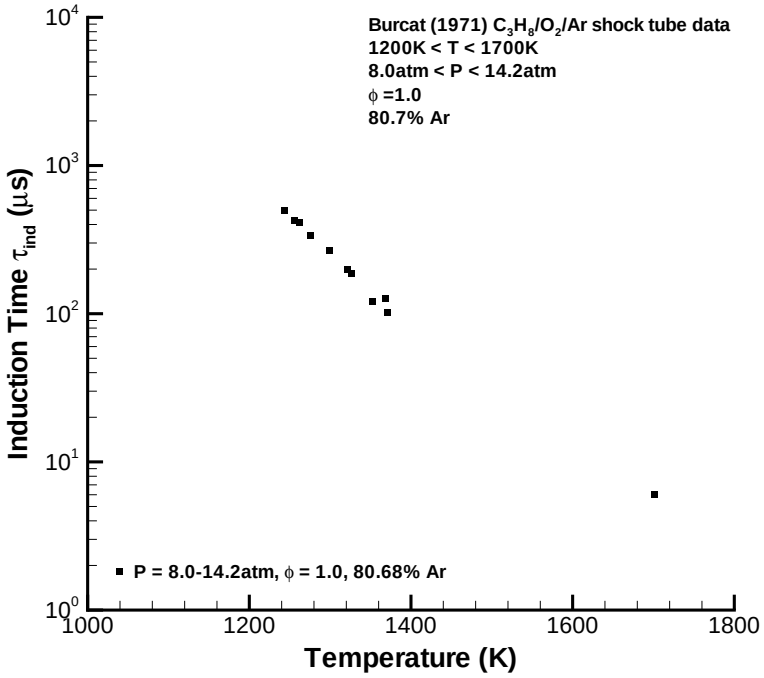

Fig. 42 Burcat (1971) propane oxidation induction time data.

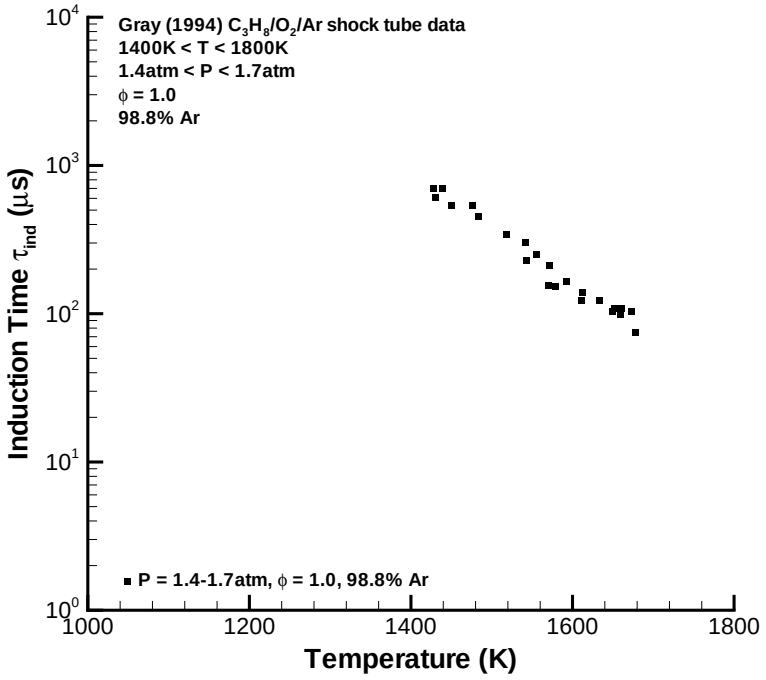

Fig. 43 Gray (1994) propane oxidation induction time data.

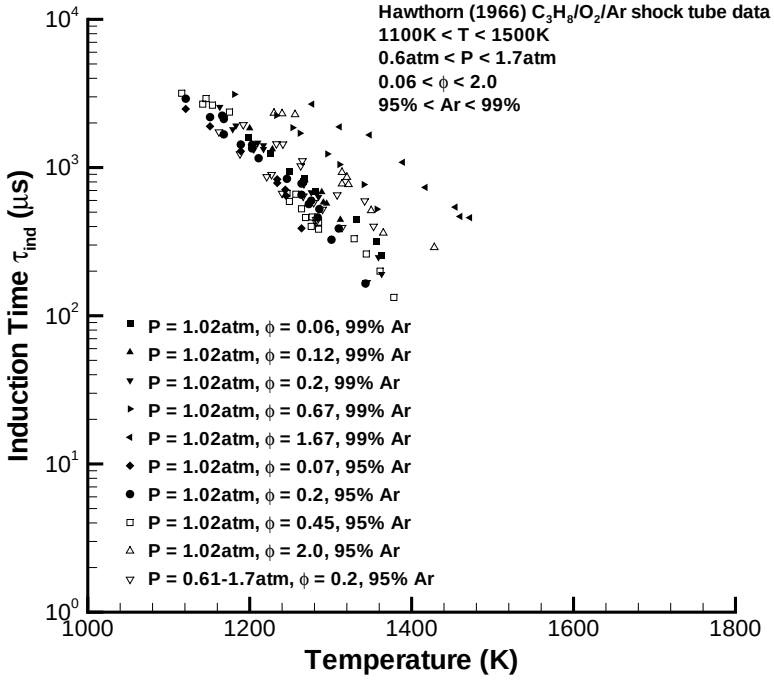

Fig. 44 Hawthorn (1966) propane oxidation induction time data.

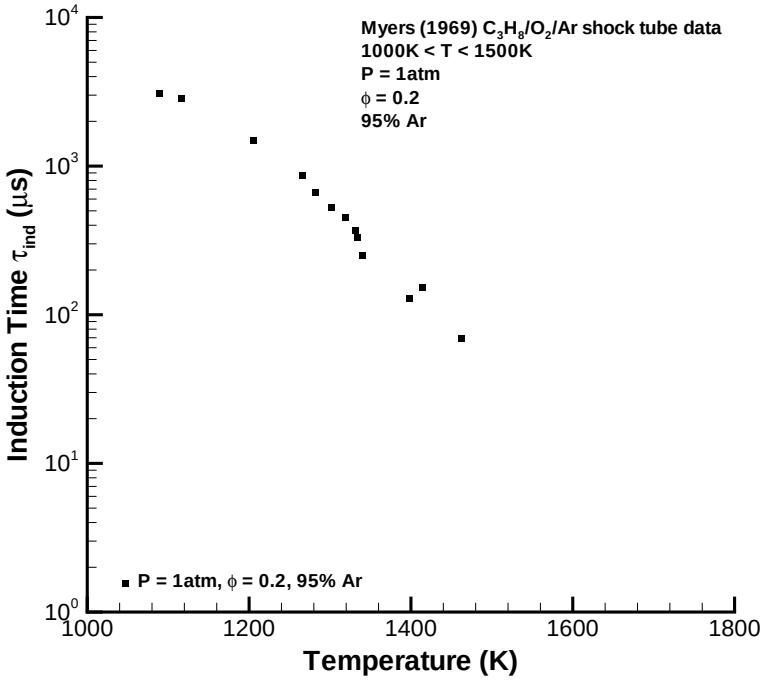

Fig. 45 Myers (1969) propane oxidation induction time data.

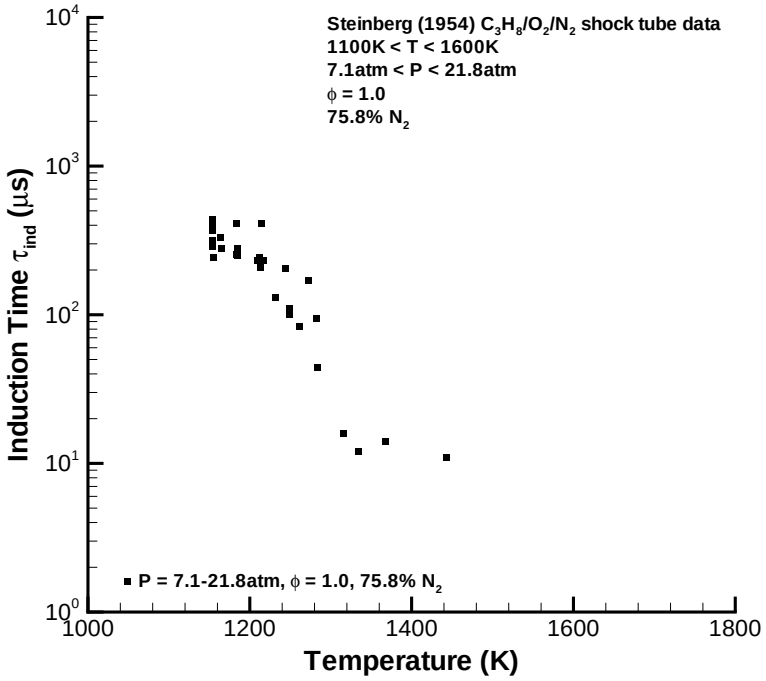

Fig. 46 Steinberg (1954) propane oxidation induction time data.

3.4 Experimental Uncertainty

Some quantitative measure of uncertainty associated with the experimental data must be established prior to comparison with computational results. Difficulties with ascertaining the experimental uncertainty include a general lack of error analysis accompanying the shock tube data and the fact that the data originates from many different sources utilizing an equally diverse array of techniques and diagnostics. The approach followed here is one of considering the "scatter" between induction time data points conforming to a specific criterion within a particular shock tube data set. The scatter between two data points, also used in comparison with the experimental versus simulation statistical error data of Chap. 5, is defined as:

$$Scatter = \left| \log\left(\frac{\tau_1}{\tau_2}\right) \right|$$

By this definition, a scatter value of 1.0 indicates that the two induction time data points (τ_1, τ_2) differ by an order of magnitude. For calculation of a scatter value, two data points are associated with the same mixture at pressures within 10% of one another and at temperatures within 5 K of one another. The arbitrary 10% pressure and 5 K temperature differences are intended to permit comparison of data points which have small differences in pressure and temperature due to experimental uncertainty or as a result of the data processing imposed by the present investigation.

Assuming that the induction time varies with some power (n) of pressure, the ratio of two induction time data points for which the thermodynamic conditions vary only by pressure (P_1, P_2) is given by

$$\frac{\tau_1}{\tau_2} = \left(\frac{P_1}{P_2}\right)^n$$

Taking the typical power of n = -1, a scatter value of approximately 0.1 is expected when imposing a 10% pressure difference.

The 5 K temperature difference criteria is within the temperature uncertainty estimates of tens of degrees from the literature (Skinner 1959, Belford et al. 1969). Assuming the induction time behavior of each mixture can be described by the Arrhenius expression

$$\tau = A\exp\left(\frac{E}{RT}\right)$$

the ratio of two induction time data points is given as

$$\frac{\tau_1}{\tau_2} = \exp\left[\frac{E}{R}\left(\frac{1}{T_1} - \frac{1}{T_2}\right)\right]$$

The greatest departure of induction time τ_1 from τ_2 occurs at low temperatures (T_1, T_2) and high activation temperatures (E/R). The worst-case corresponds to temperatures around 1000 K and activation temperatures near 40000 K estimated from the low temperature hydrogen induction time data (Fig. 14). In this case, a temperature variation of 5 K results in an induction time scatter of approximately 0.09. More prevalent combinations of temperature and activation temperature

existing in the shock tube data result in much smaller scatter values.

Figures 47, 48, and 49 are plots of the induction time scatter versus temperature for the hydrogen, ethylene, and propane shock tube data, respectively. Shock tube data sets for which no scatter data are plotted did not contain data which met the criteria for comparing induction time data points. As illustrated by Fig. 47 - 49 and statistically demonstrated in Fig. 50, most induction time scatter at temperatures above 1000 K falls below the 0.2 level for all fuels. This is just above the scatter expected from comparing induction time data points with pressure and temperature differences up to 10% and 5 K, respectively. The level of scatter for the hydrogen data at temperatures below 1000 K approaches the order of magnitude level. This corresponds to the regime in which the induction time is most sensitive to temperature, the weak mode of ignition dominates, and long induction times exacerbate the experimental non-idealities previously mentioned. Scatter values for the ethylene and propane fuels are non-existent at these temperatures. Insufficient data exists with which to address the issues of determining whether inherently more or less scatter can be associated with different mixture conditions, shock tube techniques, and measurement diagnostics.

The experimental uncertainty analysis of induction time data between different shock tube data sets was limited due to the lack of appropriate data. Some hydrogen-air data points from Craig (1966) and Snyder (1965) in the 900 - 980 K temperature range were comparable and found to exhibit scatter primarily below 0.3 with a few results up to 0.5. No ethylene induction time data met the comparison criteria across different shock tube data sets. Some atmospheric pressure propane data from Hawthorn (1966) and Myers (1969) at an equivalence ratio of 0.2 were comparable; half (5) of the scatter analysis results were below 0.1 while the remainder were less than 0.3.

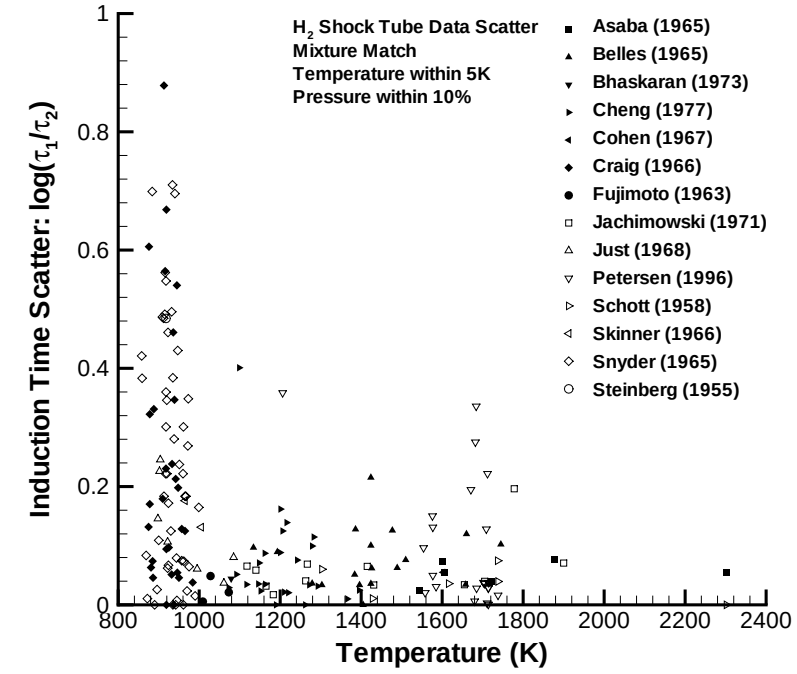

Fig. 47 Hydrogen shock tube induction time data scatter.

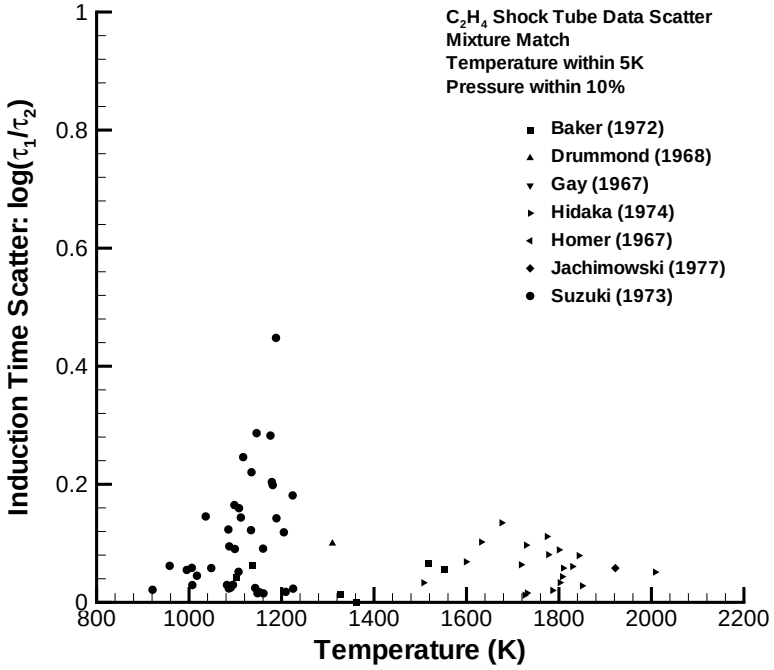

Fig. 48 Ethylene shock tube induction time data scatter.

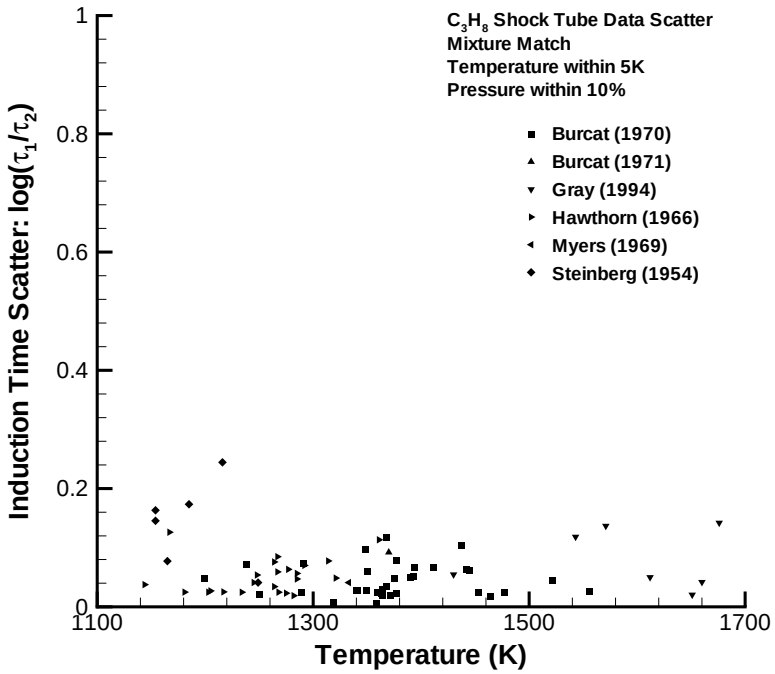

Fig. 49 Propane shock tube induction time data scatter.

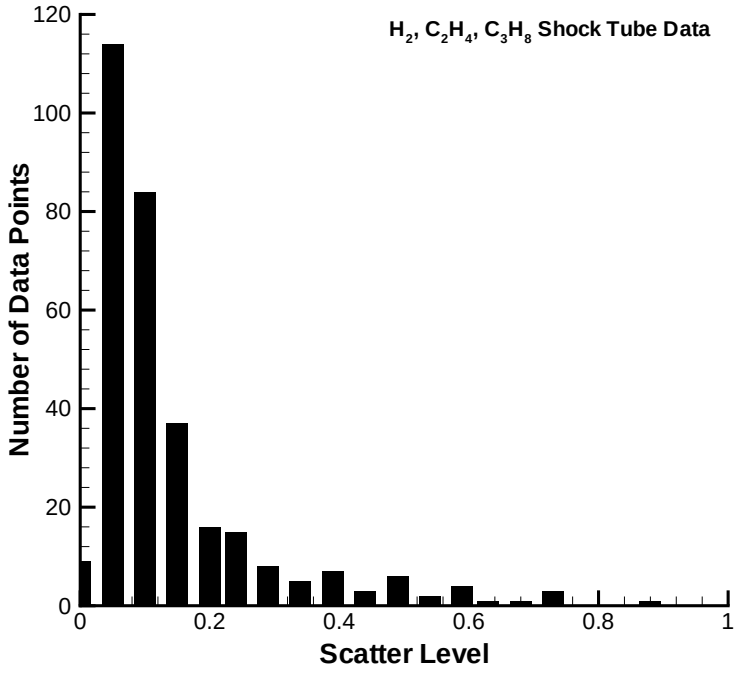

Fig. 50 Shock tube induction time data scatter histogram.

4 Detailed Reaction Mechanisms

The detailed reaction mechanisms considered along with the associated number of species, number of reactions, and fuel applicability are summarized in Table 6. Fuel applicability does not necessarily imply that the mechanism was originally intended for use in simulations with a particular fuel but only that the mechanism contains that fuel as a species. The present investigation does not evaluate simulation execution times with these mechanisms.

Table 6: Detailed reaction mechanisms.

Mechanism	Species	Reactions	H_2	C_2H_4	C_3H_8
Battin-Leclerc (1997)	63	439	Yes	Yes	Yes
Baulch (1994)	42	167	Yes	No	No
Bowman (1995)	49	279	Yes	Yes	No
Dagaut (1998)	112	688	Yes	Yes	Yes
Frenklach (1994, 1995)	32	177	Yes	Yes	No
Glassman (1996)	83	516	Yes	Yes	Yes
Konnov (1998)	121	1027	Yes	Yes	Yes
Lutz (1988)	39	154	Yes	Yes	No
Maas (1988)	10	37	Yes	No	No
Miller (1989)	53	235	Yes	Yes	No
Pilling (1996a)	37	190	Yes	Yes	No
Pilling (1996b)	10	46	Yes	No	No
Pilling (1998)	56	353	Yes	Yes	No
Tan (1994)	82	508	Yes	Yes	Yes
Wang (1997)	34	192	Yes	Yes	No
Wang (1999)	385	1896	Yes	Yes	Yes
Warnatz (1997)	34	164	Yes	Yes	No
Westbrook (1982)	29	93	Yes	Yes	No
Westbrook (1984)	36	168	Yes	Yes	Yes

The Frenklach (1994, 1995) mechanism is the Gas Research Institute (GRI) v1.2 mechanism and the Bowman (1995) mechanism is the GRI v2.11 mechanism; both are optimized for methane combustion, and GRI v2.11 includes some nitrogen chemistry. The Wang (1997) mechanism is the GRI v2.11 mechanism modified for improved ethylene performance. The Dagaut (1998) mechanism is the Tan (1994) mechanism with nitrogen chemistry included. The Pilling (1996b) and Pilling (1998) mechanisms are the Pilling (1996a) mechanism stripped to handle hydrogen fuel only and including nitrogen chemistry, respectively.

5 Shock Tube Simulations

Numerical simulations of the shock tube experiments are used to assess the accuracy of the detailed reaction mechanisms. Shock tube experiments designed to investigate the chemical kinetics of combustion usually attempt to minimize various non-ideal effects in the flow so that the data can be simply analyzed. These issues were mentioned previously and include (Belford 1969):

- The chemical energy release increases the temperature which accelerates the reactions. The ideal shock tube experiment would be carried out at infinite dilution to minimize the effects of energy release. Although many experiments are carried out at relatively high levels of dilution, some are not and the resulting data is subject to interpretation as discussed below.
- A non-uniform flowfield is associated with the boundary layer behind incident shock waves. This can be accounted for by using models of the boundary layer growth to predict the variations in properties along a streamtube behind the shock front.
- A non-uniform flowfield develops in the reflected shock region due to boundary layer separation and bifurcation of the shock wave. There is no simple way to account for this and it is important to recognize when this occurs so that the data is treated with caution. Model-based criteria can be used to predict when separation of the boundary layer will occur. The use of mixtures with large specific heat ratios obtained through high levels of monatomic gas dilution mitigates this problem.
- Test time is limited due to boundary layer growth, a short driver, and/or non-tailored interface conditions. Shock tube experimenters are responsible for avoiding test time limitations so that the driver gas does not contaminate the test mixture.

Suppose that the known non-ideal behavior has either been corrected for in the experimental data sets or can be neglected. Beyond these considerations, there is a further complication in interpreting the results of shock tube experiments since the pressure, volume, and temperature of a reacting fluid parcel will evolve with time as the state within the parcel changes and the surrounding fluid also reacts. The parcels of fluid are neither at constant volume or pressure because the only constraint is the surrounding fluid elements. Since adjacent fluid elements in the shocked gas have different extents of reaction, there will be spatial gradients in the post-shock fluid properties. The coupling between chemistry, thermodynamics, and fluid motion in the gas implies that these gradients may have a significant effect on the explosion processes.

A consequence of the existence of gradients is that, in general, an accurate simulation of a shock-tube induction time experiment requires modeling both the spatial and temporal evolution of the flowfield behind the shock wave. This may be particularly important in mixtures with a modest amount of dilution and significant temperature increases associated with chemical reaction. Volume changes in adjacent fluid elements will produce compression waves that propagate through the gas, coupling thermodynamic and chemical processes and producing cooperative effects such as pressure wave amplification and detonation initiation. However, numerical simulations of these phenomena are much too computationally intensive for parametric studies on even the simplest reaction mechanism. In the special case of a highly-diluted mixture, the chemical and physical processes are essentially uncoupled and a single fluid element can be considered

in isolation. Single fluid element simulations for less dilute mixtures are subject to modeling errors and must be considered with caution.

5.1 Modeling Considerations

There are several choices available for modeling the explosion process, all of which are approximate as discussed previously, and in the limit of high dilution these models yield equivalent results. In the present study, a constant-volume explosion process has been used for all shock tube experiment modeling. The constant-volume explosion model assumes that the adiabatic compression of the incident or reflected shock wave produces an instantaneous jump in temperature that initiates the chemical reactions. The reactions then proceed to completion in an adiabatic, homogeneous fluid parcel of fixed volume, independent of adjacent parcels. The only time dependence in the problem is that produced by the chemical reactions.

Alternatives to the constant-volume explosion model include constant-pressure or steady flow processes. A simple physical meaning can be ascribed to each model by considering how volume changes are produced in a reacting gas. Consider an element of fluid with a characteristic spatial dimension L and energy release time T. The motion created in the fluid will depend on the relative size of the acoustic speed c to the ratio L/T. For $c << L/T$, the explosion occurs so rapidly compared to motion in the fluid that the process is effectively occurring at constant volume. For $c >> L/T$, the energy release is so slow compared to the fluid motion that the explosion occurs at constant pressure. A steady-flow process might be relevant to ignition behind shock waves when there is sufficient test time available compared to the energy release time for steady-flow to be established in the shock-fixed reference frame.

The temperature ultimately increases in all cases for net exothermic explosions. Combining this fact with the ideal gas law $Pv = RT$ and unsteady constraints, as well as the Rayleigh line for the steady-flow case, all of these processes can be visualized as trajectories in the pressure-volume plane illustrated in Fig. 51. The pressure either increases (constant-volume), remains constant (constant-pressure), or decreases (steady flow) depending on the constraints. In most situations of interest, the energy release occurs after the radical chemistry, and the radical steps

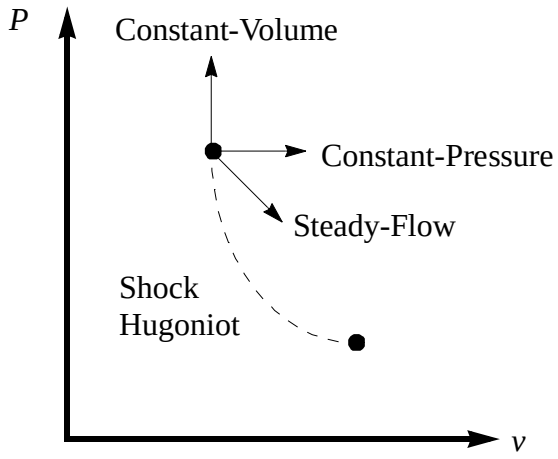

Fig. 51 Pressure-volume plane diagram of exothermic explosion model processes.

are of greatest importance in determining the induction time. When the energy release does occur in a highly-diluted mixture, the resulting temperature and pressure changes are very small and have a negligible effect on the induction time. This means that for highly-diluted mixtures, the entire explosion event occurs close to the post-shock point in the pressure-volume plane and the path that the transient follows is unimportant for analyzing the induction time.

5.1.1 Energy Release

In the limit of infinite dilution, the pressure, volume, and temperature are constant and the simulation of the chemical reactions need only consider the evolution of the species without energy release. The constant-volume explosion model approaches this limit with increasing diluent concentration. Since all experiments are carried out with finite dilution, the magnitude of uncertainty in the constant-volume model associated with energy release effects caused by varying dilution is of interest.

The primary effect of dilution at fixed post-shock temperature and pressure is to increase the induction time. Careful evaluation of Fig. 52 indicates that the adiabatic induction time is approximately inversely proportional to the reactant fraction, i.e., one minus the diluent fraction. This dependence reflects the concentration dependence of the rate-limiting reactions. These reactions, such as $H + O_2 \rightarrow OH + O$, are first order in the concentration of one reactant. The reactant concentration dependence of the reaction rate for this example is

$$\frac{d}{dt}[H] = k[H][O_2] \qquad k = AT^n \exp\left(\frac{-E}{RT}\right)$$

These expressions imply the inverse dependence of the induction time on the concentration of O_2 and underlies the frequently used representation $\tau[O_2] = f(T)$ of induction time data. While this format is compact and enables results from many different experiments to be plotted together, the dependence on pressure is sometimes obscured.

Simulations and experiments indicate that even in a simple case, the pressure dependence of the adiabatic induction time is not precisely inverse; for example, the data of Fig. 52 vary as $[O_2]^{-0.944}$, $[O_2]^{-0.666}$, and $[O_2]^{-0.749}$ for the hydrogen, ethylene, and propane mixtures, respectively. Three-body effects and pressure-dependent reaction rates (the so-called fall-off effect) introduce additional pressure dependencies that are not accounted for with the $\tau[O_2]$ representation. For this reason, just the induction time is used in the present investigation, computed at the same conditions (temperature, pressure, and mixture composition) as used in the experiment. This often requires additional computation since the exact pressure is usually not reported when the product of induction time and reactant concentration are given rather than just the induction time. The lack of such information was the reason for not including several shock tube data sets, as mentioned in Chapter 3.

Explosions involve very rapid growth in radical or intermediate species and can also result in rapid increases in gas temperature and/or pressure depending on the level of dilution. The two features are coupled together since the reaction rates depend exponentially on temperature and linearly on each species concentration (which are proportional to pressure). However, this coupling is moderated by the large number of chemical steps needed to transform reactants into prod-

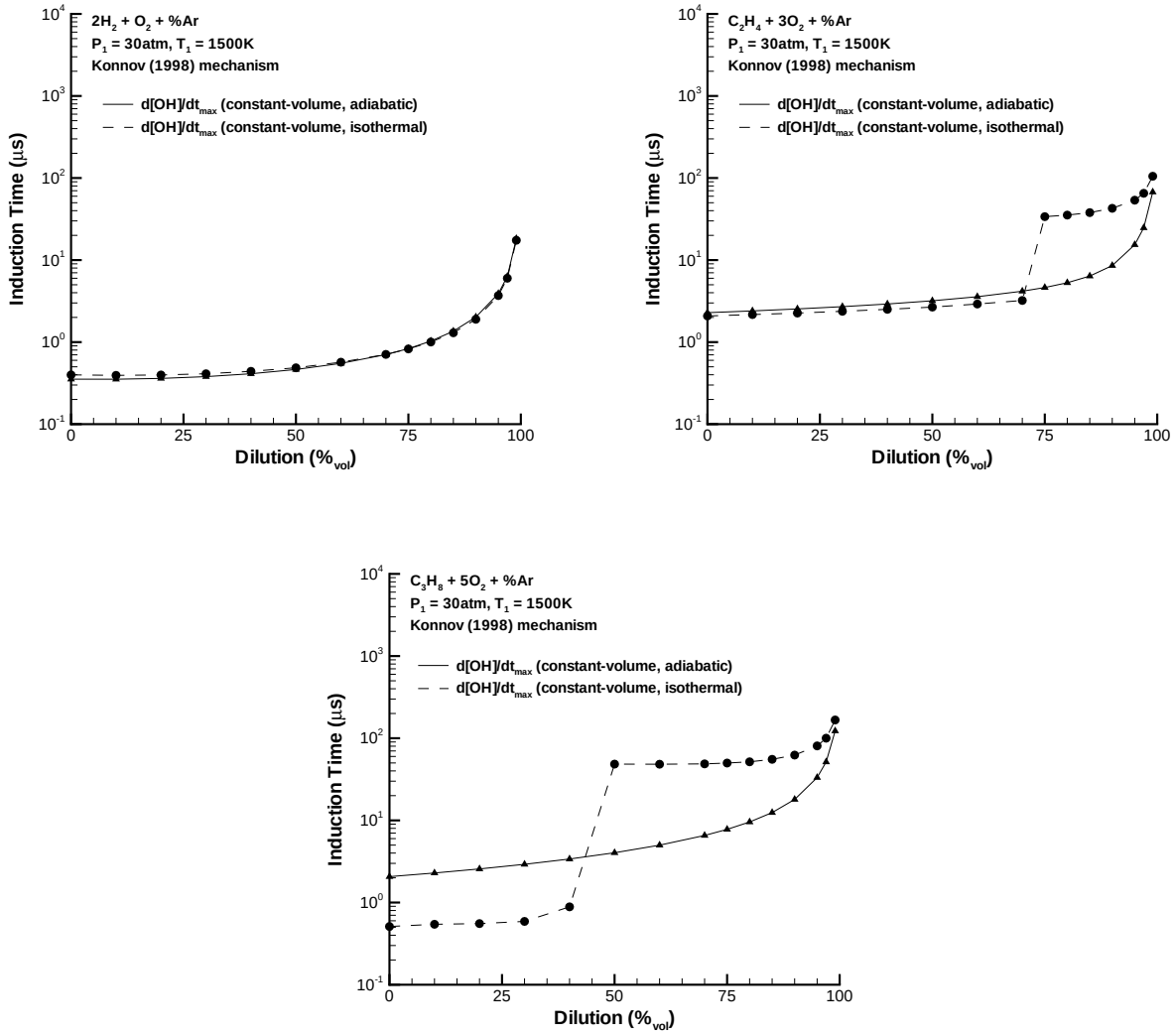

Fig. 52 Induction times calculated for varying dilution, with and without energy release.

ucts. Many of the initial decomposition and radical reaction steps are either endothermic or thermally neutral while the final recombination steps are the principal exothermic reactions that increase temperature.

In theoretical terms, this means that the explosions which occur in shock tube experiments have both a chain-branching and thermal character. In a chain-branching explosion, the active species (H, O, and OH in the hydrogen-oxygen system) increase exponentially with time. The characteristic e-folding time depends only on the initial mixture composition and temperature in the system. In a thermal explosion, energy release causes the temperature to increase in a singular fashion following an induction period known as the thermal explosion time. The characteristic thermal explosion time depends not only on the initial reaction rate but also on the amount of energy release relative to the initial energy content of the system. For a constant volume system, this is characterized by the parameter $q/c_v T$, which decreases towards zero as the amount of diluent increases to 100% since the energy released per unit mass is in direct proportion to the amount

of fuel. The adiabatic explosion process of fuel-oxygen mixtures is complicated by the fact that energy-releasing reactions such as $H + O_2 \rightarrow H_2O$, $CO + OH \rightarrow CO_2 + H$, and $CO + O \rightarrow CO_2$ will occur due to the reaction mechanism alone and the role of thermal explosion is indirect. Although theoretical notions about thermal explosions are often used in combustion simulations and in analyzing the results of experiments, actual chemical reaction mechanisms are not so simply characterized.

Several numerical calculations were performed to investigate the effect of energy release on induction time. Figure 52 illustrates the observations with stoichiometric argon-diluted hydrogen, ethylene, and propane mixtures at post-shock pressure and temperature of 30 atm and 1500 K, respectively. Adiabatic and isothermal constant-volume explosion times, defined by the maximum rate of OH production, are presented. Within the context of the constant-volume model, the effect of energy release for these hydrogen mixtures is minimal. The isothermal induction time at 0% dilution is within 10% of the adiabatic time, converging as the dilution increases. The hydrocarbon mixtures demonstrate more complex radical behavior within the isothermal reaction zone causing dilution-dependent multiple local maxima in OH production rate. This causes the apparent jump in isothermal induction times in Fig. 52 for ethylene and propane. Isothermal induction times are slightly less than adiabatic times for the ethylene mixtures up to 70% dilution at which point an OH production rate local maximum occurring later in the reaction zone becomes the absolute maximum. The isothermal induction times at low dilution for the propane mixtures are well below the adiabatic times with an abrupt change to a new maximum at a later time occurring around 40% dilution. Endothermic induction zones for the hydrocarbon mixtures are responsible for longer adiabatic induction times at low dilution. The time shift in maximum OH production rate for high dilution, which was also observed for an induction time definition based on maximum CH concentration, indicates an ill-defined induction time for isothermal reaction zones. However, for all mixtures considered, the isothermal and adiabatic induction times converge in the limit of high dilution.

These explosion simulations with and without thermal feedback affecting the rate of reaction indicate that hydrogen-oxygen mixtures have relatively weak coupling between late-time energy release and the earlier radical chemistry with increased coupling exhibited by the hydrocarbon mixtures. This should not be construed as validation of the constant-volume model for simulating undiluted mixture explosions. Because of the large temperature change, substantial volume changes can be induced in adjacent fluid elements when the energy release time is comparable to or greater than the acoustic relief time. However, the convergence of adiabatic and isothermal induction times at high dilution does mean that the effect of the thermodynamic constraints are relatively unimportant in highly-diluted mixtures characteristic of many shock tube induction time experiments. Many of the experiments analyzed were performed with greater than 90% argon dilution (Tables 3 - 5). For these cases, the chemistry and energy are effectively decoupled and the method of simulation introduces a minimal amount of uncertainty. In some cases, either no dilution or rather modest amounts of diluent were used by the experimenters. Caution should be exercised in interpreting these results with the constant-volume explosion model.

5.1.2 Induction Time Definition

Various numerical induction time definitions are possible, just as many different criteria exist

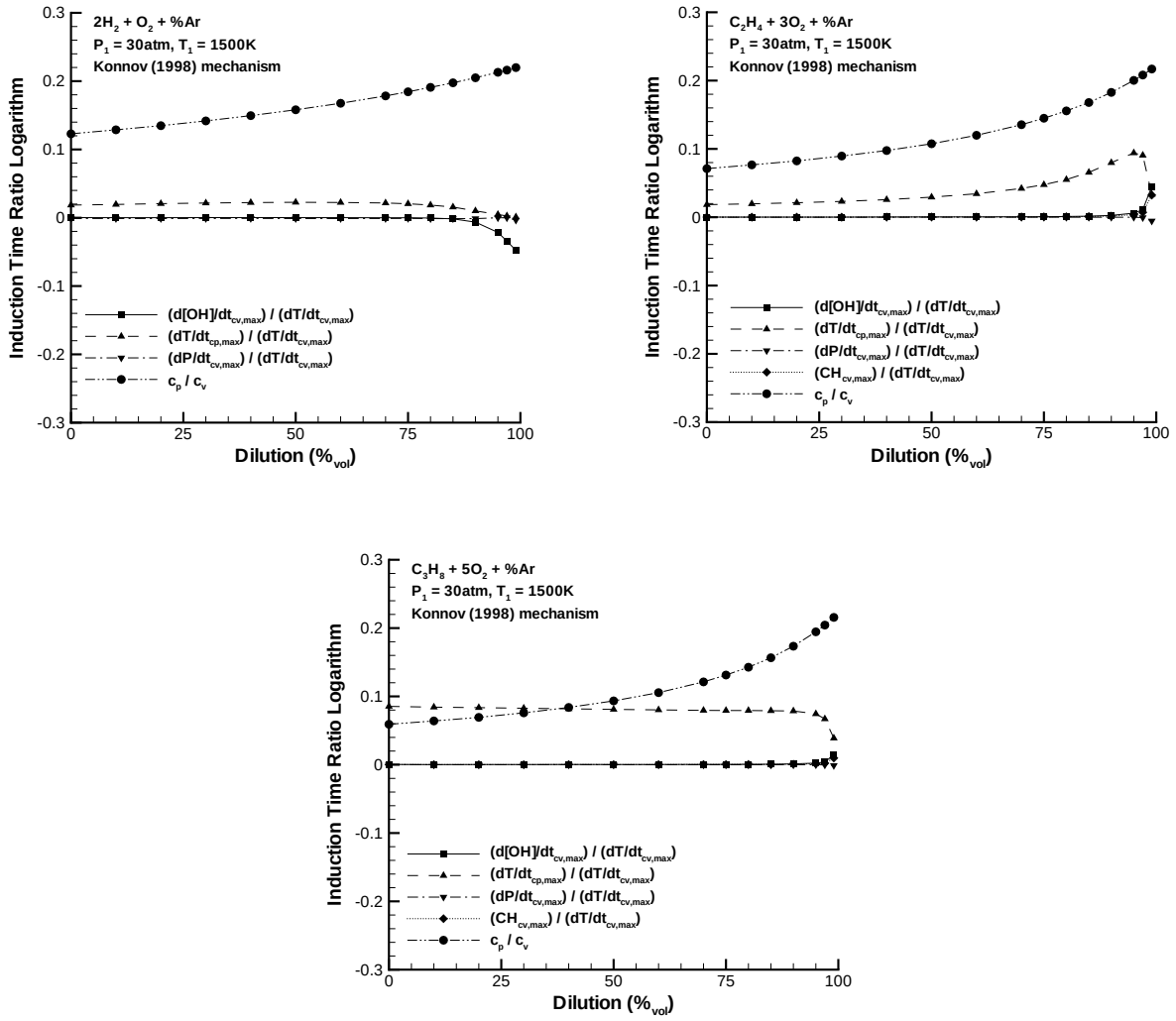

Fig. 53 Logarithmic induction time ratios calculated for varying dilution with different induction time definitions.

for the experimental data (Tables 3 - 5). The experimental data sets which use maxima as an induction time definition are well-defined, while using the onset of some signal is complicated by the fact that the signal is rising above some arbitrary level which is often not reported. Induction time calculations with the Konnov (1998) reaction mechanism were performed for hydrogen, ethylene, and propane mixtures with varying dilution in order to quantitatively assess the effect of different induction time definitions (Fig. 53). The data plots provide the logarithm of induction times determined for the same mixture, initial pressure (30 atm), and initial temperature (1500 K). Agreement between any two induction times improves as the logarithmic ratio approaches zero. Induction time definitions of the maximum rate of OH production in a constant-volume explosion, maximum temperature rate of change in a constant-pressure explosion, and maximum pressure rate of change in a constant-volume explosion are compared to the maximum temperature rate of change in a constant-volume explosion for the three fuel mixtures. In addition, the maximum CH concentration in a constant-volume explosion is compared to the maximum temperature

rate of change in a constant-volume explosion for the hydrocarbon mixtures. Calculations were also performed with an induction time definition of maximum OH concentration, but the relatively broad plateau in OH concentration results in poor numerical maximum identification (i.e., a very small change in OH concentration introduced by the numerical scheme near the maximum results in a very large change in the induction time).

The induction time definition based on maximum rate of pressure change and maximum rate of OH production definition agree very well with the maximum rate of temperature change across the entire dilution range. At high diluent concentration levels, the maximum rate of OH production diverges slightly from the maximum rate of temperature change due to the OH concentration going through two distinct high rate-of-change growth periods within the reaction zone. Myers (1969) observed this feature in shock tube induction time measurements of OH emission. At high dilution, the second OH growth period closely corresponds to the maximum temperature rate of change.

Agreement at low dilution between induction times for the maximum rate of temperature change for constant-pressure and constant-volume explosions is better for hydrogen and ethylene mixtures than for the propane mixtures. In the limit of high dilution, the constant-pressure and constant-volume induction time results converge. For a given energy release, the temperature rise is larger and therefore, the induction time is shorter in constant-volume explosions than in constant-pressure events. All of the energy released goes into increasing the gas temperature in the constant volume case, while a portion of the energy must be used to do work in displacing the surrounding fluid in the constant-pressure case. Note that the ratio of these two times is not what would be expected on the basis of a purely thermal explosion model. Classical thermal explosion theory (Strehlow 1984) predicts that the ratio of these times is proportional to the ratio of specific heats (c_p / c_v). The logarithm of the ratio of specific heats is also plotted in Fig. 53 and these values depart significantly from the constant-pressure to constant-volume logarithmic ratio as the dilution increases. This is further confirmation of the dominating radical chemistry nature within the explosion induction zone.

The CH concentration maximum definition agrees with the maximum rate of temperature change for the hydrocarbon mixture induction times until very high dilution levels. At high diluent concentration, the time corresponding to the maximum in CH concentration shifts to slightly later times relative to the maximum rate of temperature change point. This results in an increase in this particular logarithmic ratio above 98% dilution for the ethylene and propane mixtures.

The maximum rate of temperature change definition results in induction times close to those calculated with other definitions in most cases, with logarithmic induction time ratios (less than 0.1) within the uncertainty of the experimental data (approximately 0.2). This induction time definition always has a single, well-defined maximum within the reaction zone which is not always the case with species-related definitions. The calculations leading to these observations were repeated at 1 atm and 30 atm for a relatively low initial temperature of 1100 K with similar results. For these reasons and to provide a consistent definition for comparison of values calculated in this manner, all further shock tube simulations use the maximum rate of temperature change to define the induction time.

5.2 Constant Volume Explosion Simulations

The constant volume explosion model is used to simulate all of the shock tube experimental conditions (Chap. 3) with all applicable reaction mechanisms (Chap. 4). The numerical and experimental induction times are compared to evaluate reaction mechanism performance. Consideration is given to uncertainties associated with the experimental data, numerical integration, and constant-volume approximation. The simulations were carried out with a computer program incorporating the thermodynamic data and detailed reaction mechanisms through the Chemkin II chemical kinetics package (Kee 1989), and the *ddebdf* integrator (Shampine 1979) for systems of stiff ordinary differential equations. The program evolves the energy and species equations through time for an adiabatic, fixed-volume fluid particle:

$$\frac{de}{dt} = 0$$

$$\frac{dy_i}{dt} = \Omega_i$$

The internal energy for an ideal gas is related to the temperature and species through a caloric equation of state

$$e = e(T,\hat{y}) = \sum_{i=1}^{K} y_i e_i(T)$$

The internal energy of each species as a function of temperature is calculated with NASA polynomial functions from the thermodynamic database supplied with CHEMKIN (Kee 1989). Taking the differential of this expression gives

$$de = \sum_{i=1}^{K} dy_i e_i + dT \sum_{i=1}^{K} y_i \frac{de_i}{dT} = \sum_{i=1}^{K} dy_i e_i + dT \sum_{i=1}^{K} y_i c_{v,i} = \sum_{i=1}^{K} dy_i e_i + c_v dT$$

where c_v is the average constant-volume heat capacity for the mixture. Substituting into the original energy equation for the internal energy differential, the energy equation is re-formulated in terms of temperature

$$c_v \frac{dT}{dt} = -\sum_{i=1}^{K} \frac{dy_i}{dt} e_i = -\sum_{i=1}^{K} \Omega_i e_i$$

The species mass fraction production rate is calculated through Chemkin subroutines with the reaction mechanism providing the reaction rate constants in the standard form of

$$k_i = A_i T^{n_i} \exp\left(-\frac{E_i}{RT}\right)$$

Detailed discussion on the various forms of reaction rate expressions is provided by Kee (1989). The initial conditions for each simulation consisted of the gas mixture composition, post-shock pressure, and post-shock temperature.

The evolution of temperature, temperature rate of change, and some species for a representative constant-volume explosion simulation are presented in Fig. 54. Hydrogen and oxygen are consumed through the reaction zone while hydroxyl is the intermediate radical species and formation of the water product is the primary exothermic reaction. Note that the high level of dilution limits the pressure and temperature rise to within 1.5% of the initial values. The end of the induction period is defined as the time corresponding to the maximum rate of temperature change which is very close to the maximum rate of OH production time as discussed in the previous section.

Absolute and relative numerical tolerance constraints of $1x10^{-9}$ and $1x10^{-10}$, respectively, were imposed on the integrator for all simulations. These tolerances were varied to check the effect of numerical integration error on the computed induction time. For induction times less than 100 μs, tolerance variations from $1x10^{-8}$ to $1x10^{-11}$ made less than a 1% difference. The same tolerance variations applied to simulations with induction times up to 1000 μs resulted in changes of ±3%. Induction time differences of up to ±10% were observed for these tolerance variations in simulations with induction times up to 10000 μs.

The induction times computed from approximately 30,000 constant-volume explosion simulations were compared to the experimental shock tube data. The individual results are too voluminous to present here and so a statistical approach is taken. Figures 55 - 73 are the result of statistically comparing the simulation data to the experimental data for each reaction mechanism; this data is presented in tabulated form in Appendix D. Each figure includes the average deviation between the simulated and experimental induction times versus temperature range and fuel type for one reaction mechanism. The average deviation provides a quantitative assessment of the accuracy of the mechanism in simulating the chemistry and is defined by

$$Deviation = \frac{1}{N}\sum_{j=1}^{N}\log\left(\frac{\tau_{s,j}}{\tau_{e,j}}\right)$$

The average deviation is calculated for a group of data corresponding to a particular subset of temperature range (increments of 100 K except at the highest and lowest temperatures) and fuel type (hydrogen, ethylene, propane), where N is the total number of simulations/experiments in the group. Zero represents perfect correspondence between simulation and experiment whereas average deviations of 1.0 and -1.0 indicate that the simulated induction times in that group were an order of magnitude greater than and less than the experimental induction times, respectively. The vertical bars attached to each plotted data point indicate one statistical standard deviation of the average and therefore, indicate the range in which approximately 70% of the deviation lies on a point-by-point basis. The hydrogen data spans the temperatures from 775 - 2650 K while ethylene and propane data only cover 900 - 2350 K and 1100 - 1700 K, respectively.

Simulations with all mechanisms (Figs. 55 - 73) clearly indicate a general tendency for the

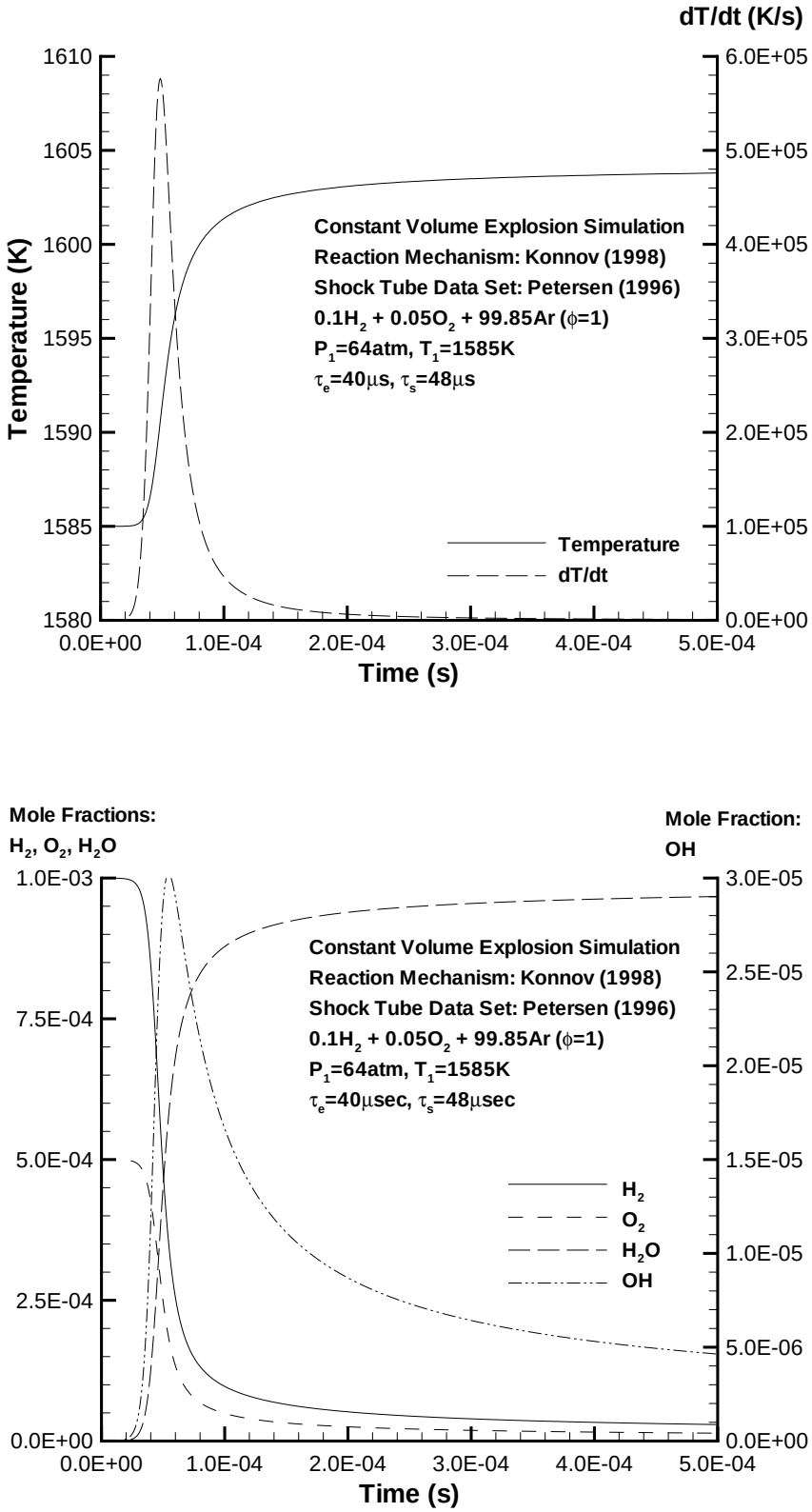

Fig. 54 Representative constant-volume explosion simulation results.

simulations to overpredict the experimental induction times and a decreasing deviation trend as the temperature increases. High temperatures also correspond to the regime of short induction times, less experimental uncertainty, improved applicability of the constant-volume explosion model, and smaller numerical integration errors. For this large parametric simulation study to remain viable, a maximum integration time of one second was imposed. This artificially lowers the average deviation of some low temperature simulations but these already overpredicted the experimental induction time by orders of magnitude.

Note that all shock tube data were used for this statistical analysis. Therefore, constant-volume explosion simulations were performed for low-dilution mixtures in which there is greater coupling between energy release and fluid motion, and nitrogen-diluted reflected shock experiments in which the boundary layer probably separated. The results were checked to see if high deviations between simulated and experimental induction times could be systematically attributed to low dilution levels or nitrogen-diluted reflected shock conditions for which the constant-volume approximation is expected to be less applicable.

The deviations for all hydrogen mixtures decrease with increasing dilution below 900 K but the deviation trend varies between reaction mechanisms above 900 K and at all temperatures for hydrogen mixtures without the nitrogen-diluted reflected shock data. Ethylene mixtures, for which no nitrogen-diluted reflected shock data exists, exhibited decreasing deviations with increasing dilution at all temperatures. Deviations for propane mixtures with and without nitrogen-diluted reflected shock data decrease with decreasing dilution below 1400 K and trends vary between mechanisms above 1400 K. These trends of deviation versus dilution with and without the nitrogen-diluted reflected shock data revealed no systematic dependence on fuel types, temperature ranges, or reaction mechanisms.

Soot formation in hydrocarbon mixtures is known to occur at relatively high equivalence ratios and is not accounted for by any of the reaction mechanisms considered here. Strehlow (1984) provides a carbon-to-oxygen atom ratio of 0.5 as a rule-of-thumb for the onset of soot formation in pre-mixed flames. This atomic ratio corresponds to equivalence ratios of 1.5 and 1.7 for ethylene and propane mixtures, respectively. Glassman (1996) gives corresponding equivalence ratios ranging from 1.6 to 2.0, discusses the strong temperature dependence in the soot formation process, and notes that soot production in shock tube experiments is low relative to flame-based studies due to the instantaneous jump in reactant temperature. It is not clear how the presence of soot would effect induction time measurements and calculations. The effect of equivalence ratio on induction time deviation was investigated but no systematic dependence was identified.

The reaction mechanisms of Tan (1994) and Dagaut (1998), Frenklach (1994, 1995) and Bowman (1995), and Pilling (1996a) and Pilling (1998) are identical with the exception that one mechanism of each pair treats nitrogen as an active chemical species. The deviation values for these reaction mechanisms are almost the same, indicating that nitrogen has primarily a thermal, rather than kinetic, effect in the post-shock reaction chemistry. This is due to the very high dissociation energy of the triply-bonded diatomic nitrogen species.

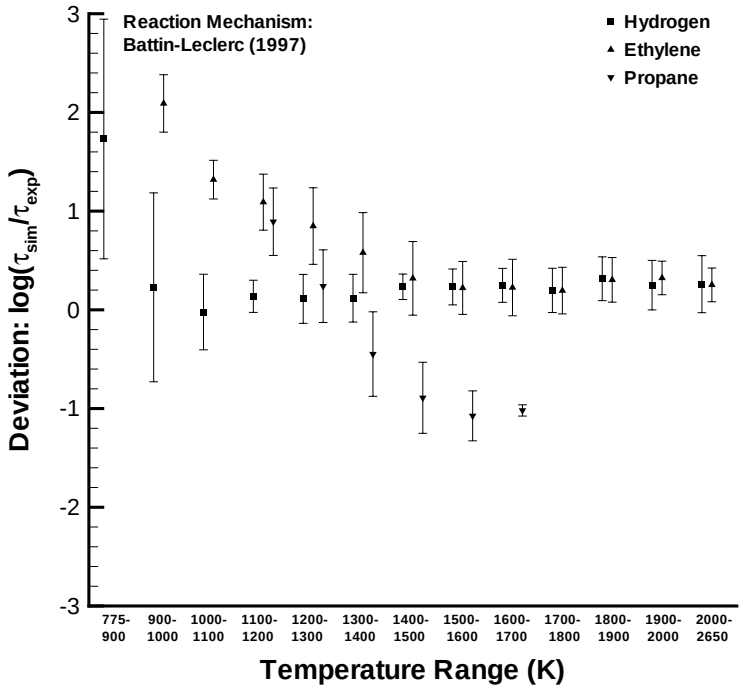

Fig. 55 Simulation-to-experiment induction time deviation for Battin-Leclerc (1997) reaction mechanism.

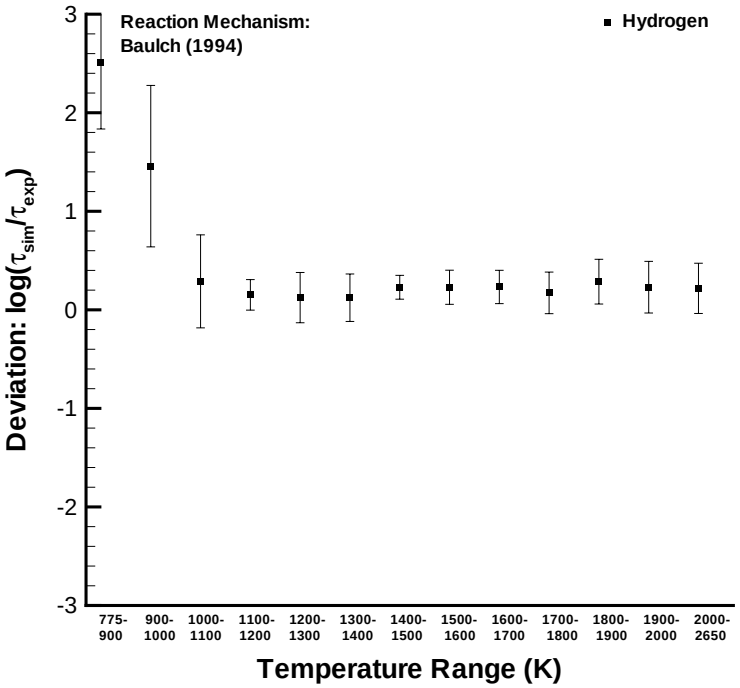

Fig. 56 Simulation-to-experiment induction time deviation for Baulch (1994) reaction mechanism.

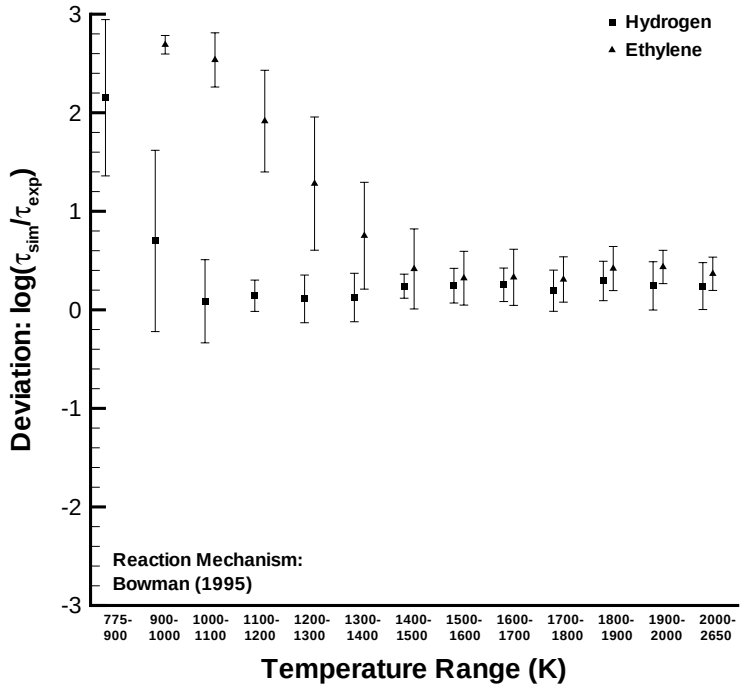

Fig. 57 Simulation-to-experiment induction time deviation for Bowman (1995) reaction mechanism.

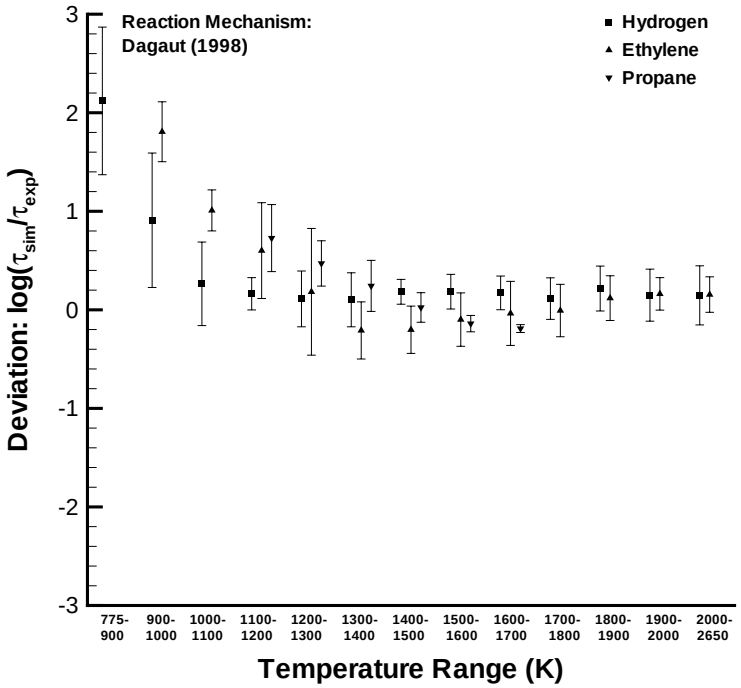

Fig. 58 Simulation-to-experiment induction time deviation for Dagaut (1998) reaction mechanism.

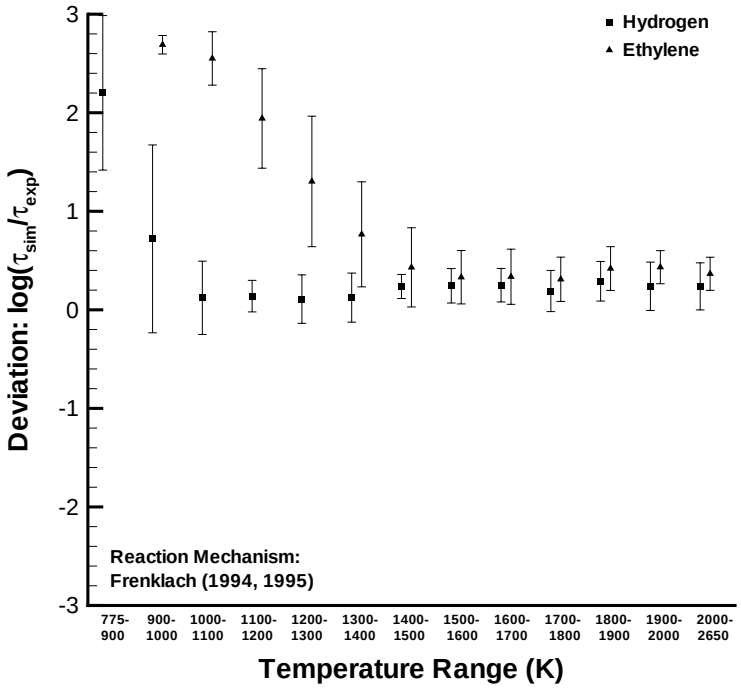

Fig. 59 Simulation-to-experiment induction time deviation for Frenklach (1994,1995) reaction mechanism.

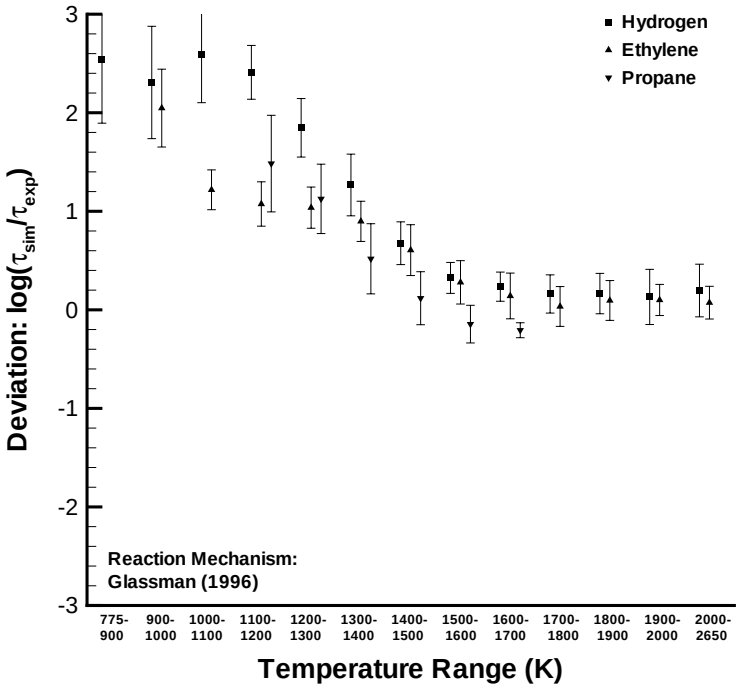

Fig. 60 Simulation-to-experiment induction time deviation for Glassman (1996) reaction mechanism.

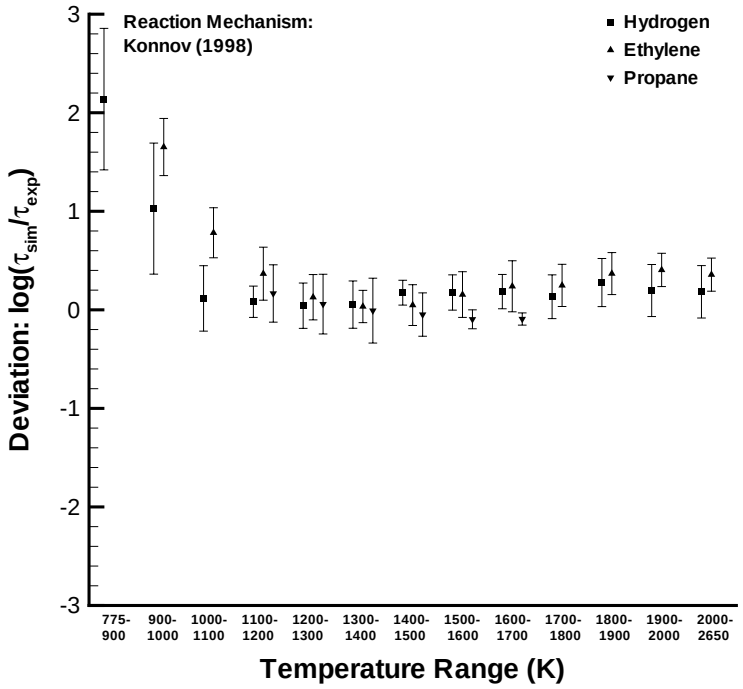

Fig. 61 Simulation-to-experiment induction time deviation for Konnov (1998) reaction mechanism.

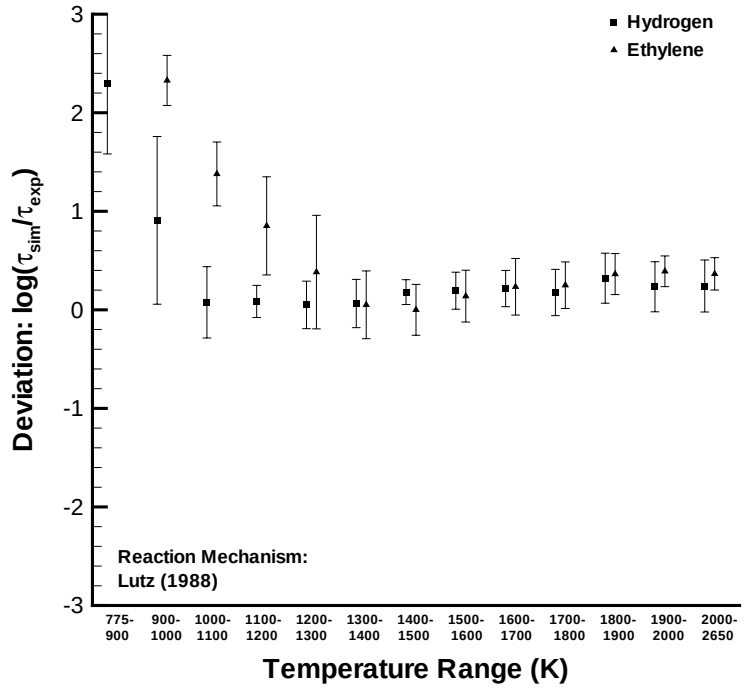

Fig. 62 Simulation-to-experiment induction time deviation for Lutz (1988) reaction mechanism.

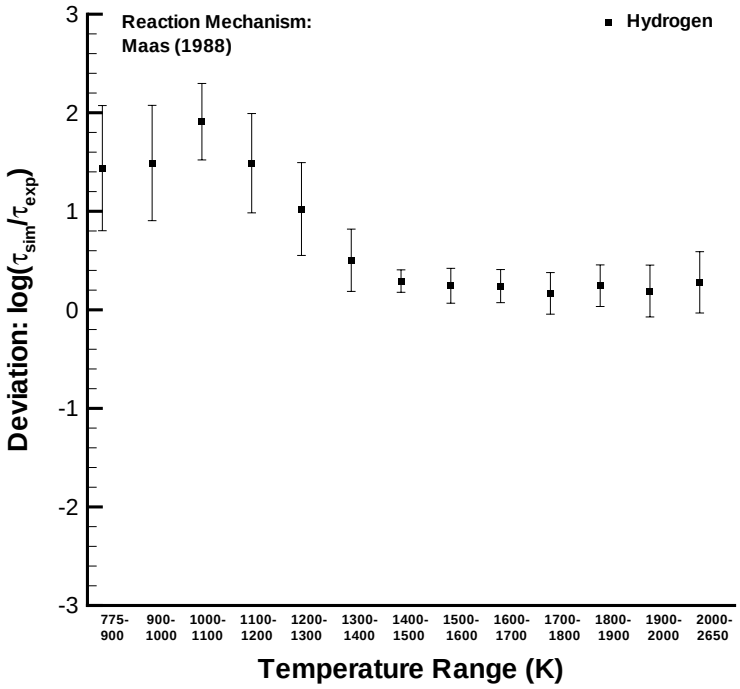

Fig. 63 Simulation-to-experiment induction time deviation for Maas (1988) reaction mechanism.

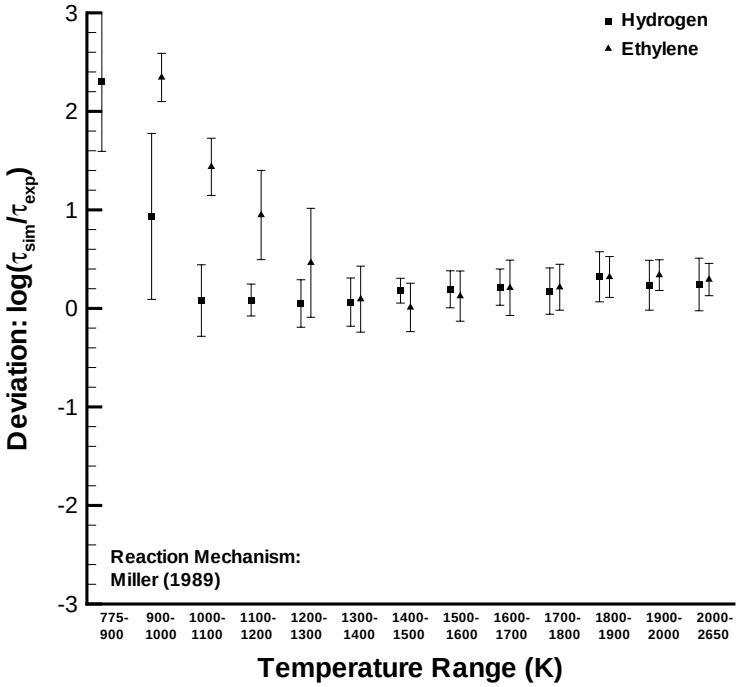

Fig. 64 Simulation-to-experiment induction time deviation for Miller (1989) reaction mechanism.

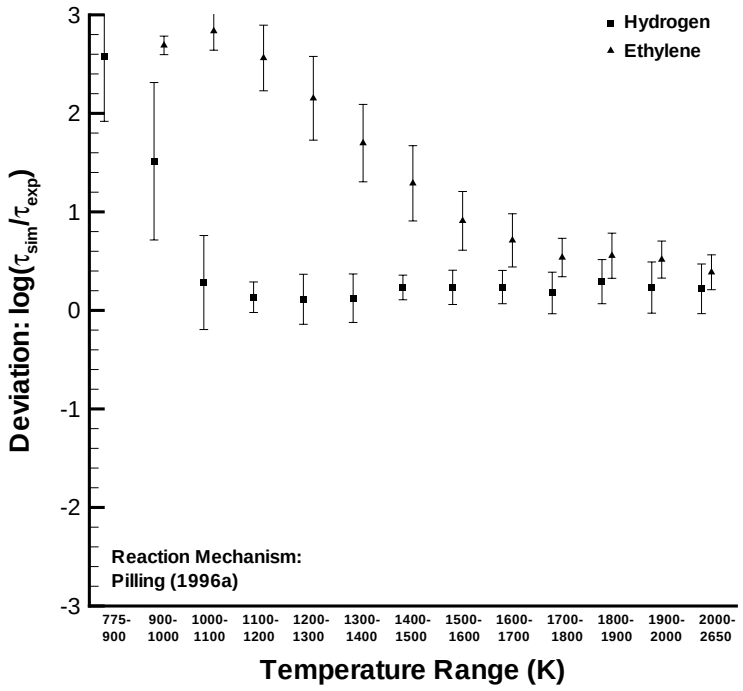

Fig. 65 Simulation-to-experiment induction time deviation for Pilling (1996a) reaction mechanism.

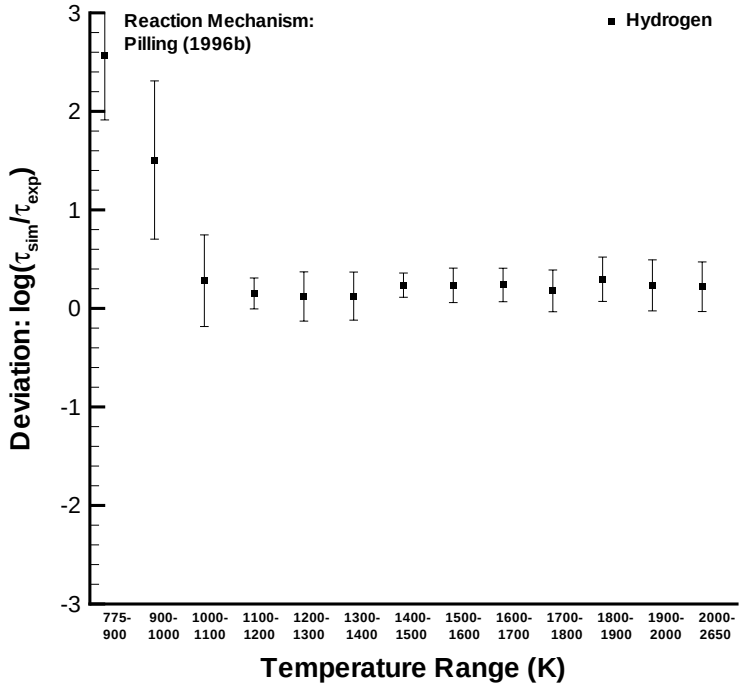

Fig. 66 Simulation-to-experiment induction time deviation for Pilling (1996b) reaction mechanism.

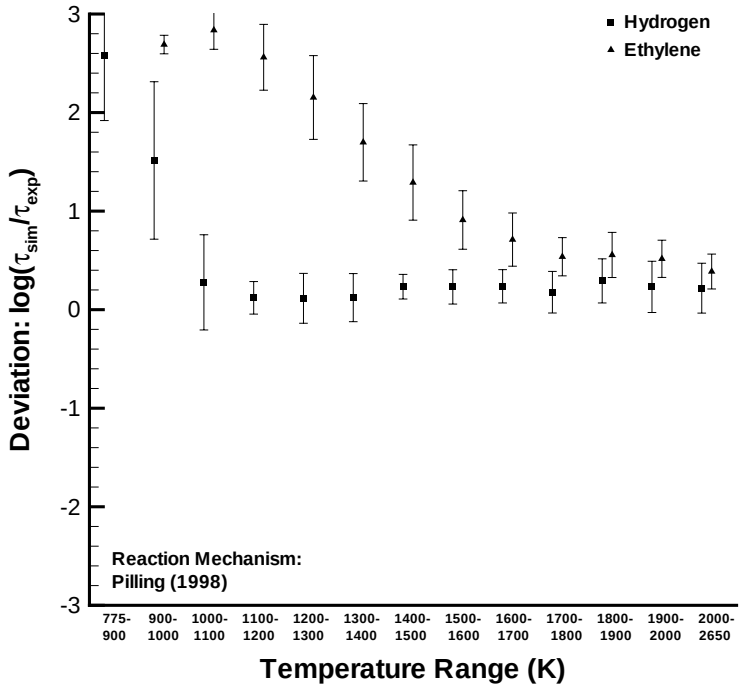

Fig. 67 Simulation-to-experiment induction time deviation for Pilling (1998) reaction mechanism.

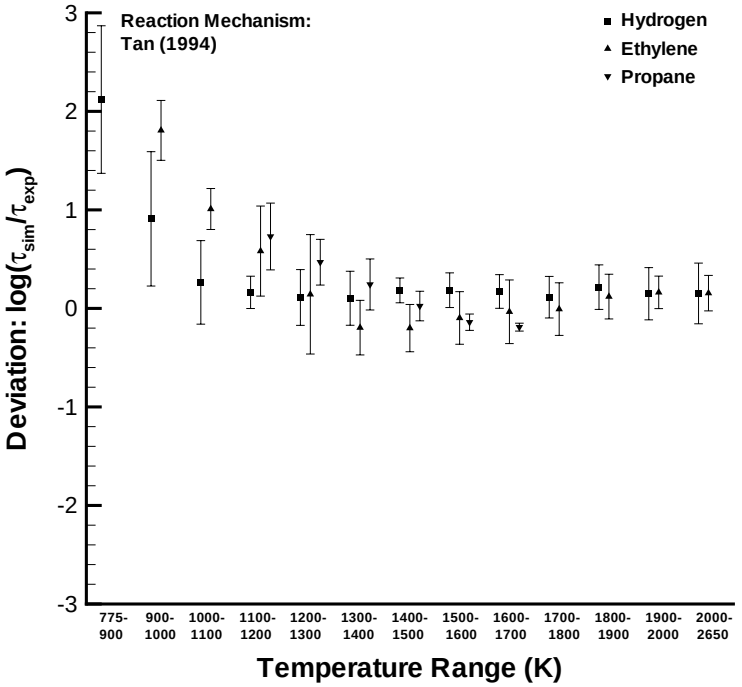

Fig. 68 Simulation-to-experiment induction time deviation for Tan (1994) reaction mechanism.

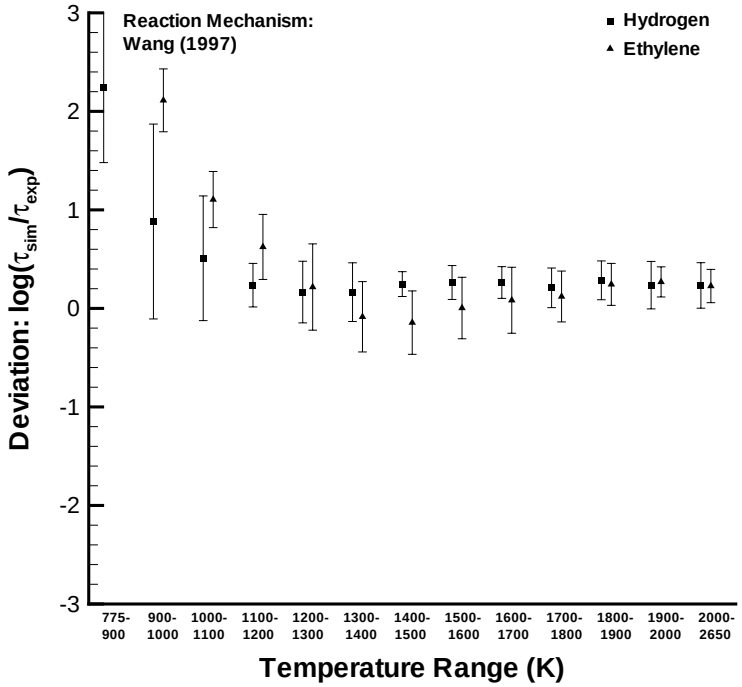

Fig. 69 Simulation-to-experiment induction time deviation for Wang (1997) reaction mechanism.

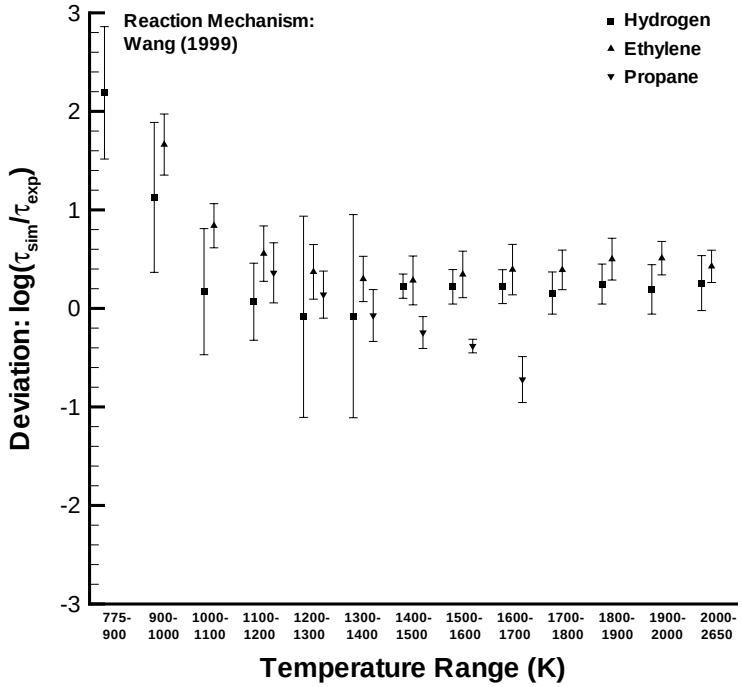

Fig. 70 Simulation-to-experiment induction time deviation for Wang (1999) reaction mechanism.

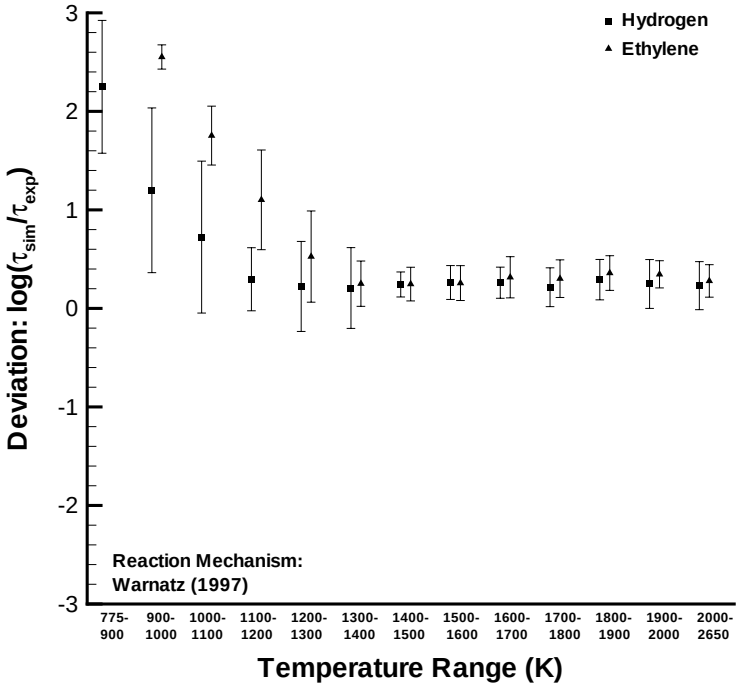

Fig. 71 Simulation-to-experiment induction time deviation for Warnatz (1997) reaction mechanism.

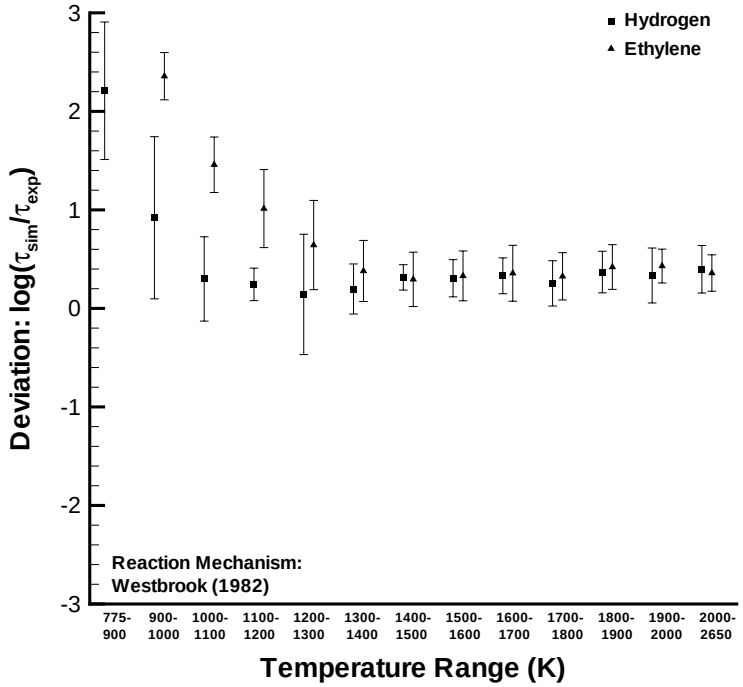

Fig. 72 Simulation-to-experiment induction time deviation for Westbrook (1982) reaction mechanism.

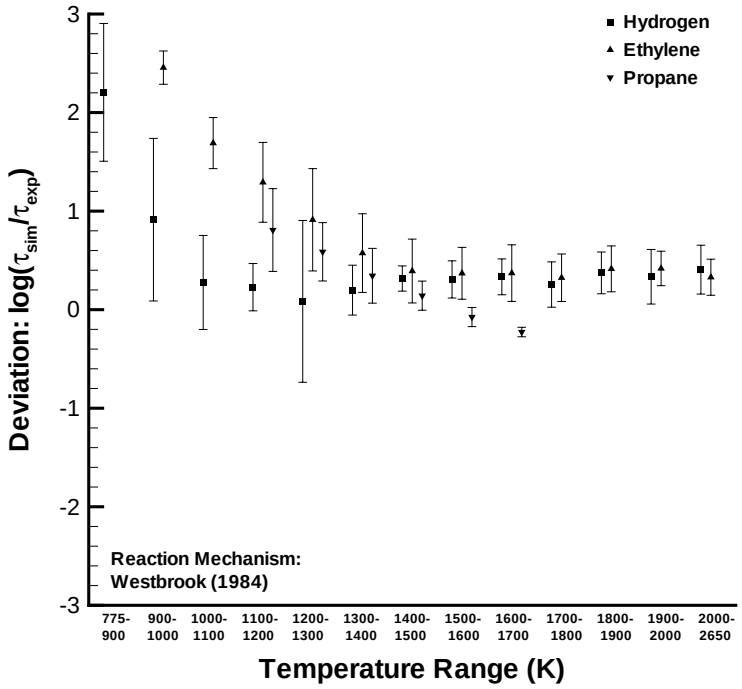

Fig. 73 Simulation-to-experiment induction time deviation for Westbrook (1984) reaction mechanism.

5.3 Discussion

The issue of how accurately a reaction mechanism reproduces the behavior of a chemical system under a given set of conditions must be addressed with consideration given to the uncertainty associated with experiments, the simulation model, and numerical integration. All of these uncertainties combined with reaction mechanism deficiencies are manifested within the comparison of experimental and simulation induction times to a greater or lesser degree and often difficult to distinguish. The present effort has sought to quantify all sources of uncertainty to some extent which can be summarized as follows.

Experimental uncertainties arise from a variety of non-ideal effects which occur in shock tube experiments and the different techniques employed from one research group to another. As shown in Chapter 3, the experimental scatter within individual shock tube data sets above 1000 K is typically less than 0.2 for all fuels. No scatter data exists for the hydrocarbon fuels below 1000 K but scatter in the hydrogen shock tube data at these temperatures reaches the 0.9 level. Note that the scatter analysis presented is limited by insufficient induction time data available for statistically significant comparison between different data sets and is intended to substitute for a general lack of error analysis accompanying data presented in the literature.

Modeling uncertainties arise from approximations made in simulating the shock tube experiment so that the problem becomes computationally tractable; in this case, the imposition of the constant-volume explosion model. The coupling of energy release with fluid motion in the experiments is neglected by the constant-volume model but is increasingly decoupled at high levels of dilution. The constant-volume model also does not account for non-uniform fluid properties behind the shock, significant for reflected shock experiments with low specific heat capacity mixtures in which the boundary layer separates. No systematic dependence was found for dilution or the use of nitrogen-diluted reflected shock data on simulated induction time deviation from experimental values. The effect of various induction time definitions was considered, including species, pressure, and temperature based criteria but was shown to have only a modest effect on calculated induction time values. Maximum logarithmic ratios of 0.05 resulted between induction times calculated with different criteria. Induction times calculated with a constant-pressure model agreed with constant-volume times to within a logarithmic ratio of 0.1. In terms of the relevant characteristic reaction and gasdynamic rates, low temperatures correspond to relatively long induction times and therefore, exacerbate the uncertainty associated with the constant-volume model. However, this would cause the constant-volume model to underpredict the induction time and so can not possibly account for the general overpredictive trend in the deviation results.

Numerical integration errors are controlled by the integrator convergence tolerances and were found to be no greater than 10% for the longest induction times considered. This error source was reduced to a maximum of 1% at the shorter induction times corresponding to higher temperatures. Both of these values are much smaller than the uncertainties associated with the experimental data and gasdynamic model.

The modeling and numerical integration uncertainties taken together are on the order of the experimental scatter at relatively high temperatures and somewhat less than the scatter at low temperatures. Cumulatively these three sources of uncertainty amount to maximum logarithmic

ratios of approximately 0.4 at relatively high temperatures and 1.0 at low temperatures. An estimate of the inaccuracy associated with a particular reaction mechanism can be made by comparing these values with the deviations indicated in Figs. 55 - 73. At high temperatures, the mechanism and other sources of uncertainty are of the same order while the mechanisms generally appear to be responsible for substantial deviation between simulated and experimental induction times at low temperatures. This statement is made with the caveat that the experimental uncertainty analysis is inadequate to make this statement conclusive.

Simulations of detonation phenomena involving relatively low temperatures such as deflagration to detonation transition (DDT), cellular structure, and off-stoichiometric and high dilution one-dimensional detonations will be significantly influenced by large reaction mechanism errors at these temperatures. Determination of which reaction mechanism performs “best” for any type of detonation simulation can only be made within the context of a particular application. Identification of the appropriate mechanism is illustrated by application considerations in the following chapter.

6 Computed Detonation Properties

Characteristic reaction time/length scales, activation energies, and thermal energies were calculated for one-dimensional detonations propagating at V_{CJ}. Parameters varied include fuel type (hydrogen, ethylene, propane), equivalence ratio (0.2 - 3.0), diluent (argon, carbon dioxide, helium, nitrogen), diluent concentration (0% - 90%), and initial pressure (0.2 - 2.0 bar). Many properties of these detonations are tabulated in Appendices E, F, and G for the hydrogen, ethylene, and propane mixtures, respectively. Note that some degree of soot formation is likely to occur at equivalence ratios above 2.0 and the effect on calculations incurred by reaction mechanisms not accounting for soot is unknown (Chap. 5).

The reaction mechanisms of Konnov (1998) and Tan (1994) were used for all simulations because they are associated with the lowest overall errors (Figs. 61,68) of the mechanisms which are capable of handling all three fuels of interest. All but a few simulations involved post-shock temperatures within the validation range above 1200 K (see Appendices E, F, G) for which the ratio of average simulated to experimental induction times of Konnov (1998) and Tan (1994) were no greater than a factor of 2.5 and 3.0, respectively (see Appendix D). These mechanisms are large relative to the other mechanisms of Chapter 4 in terms of number of species and reactions but execution speed is not a concern here. Two mechanisms were chosen to provide a point of comparison between the results.

6.1 Reaction Time/Length

Simulations of steady, one-dimensional detonations were performed by a program developed by Shepherd (1986) which utilized the same chemical kinetics package and stiff ordinary differential equation solver as the constant-volume explosion program. The code is based on the one-dimensional, steady reactive Euler equations known as the Zeldovich-von Neumann-Doring (ZND) detonation model (Fickett and Davis 1979):

$$\frac{Dw}{Dt} = \frac{w\dot{\sigma}}{1-M^2}$$

$$\frac{D\rho}{Dt} = \frac{-\rho\dot{\sigma}}{1-M^2}$$

$$\frac{DP}{Dt} = \frac{-\rho w^2\dot{\sigma}}{1-M^2}$$

$$\frac{Dy_i}{Dt} = \Omega_i$$

$$\dot{\sigma} = \sum_{i=1}^{K} \sigma_i \Omega_i \qquad \sigma_i = \frac{1}{\rho c^2}\frac{\partial P}{\partial y_i}\bigg|_{P,\,\rho,\,y_{j\neq i}}$$

where the species production rates are calculated with the Konnov (1998) and Tan (1994) reaction mechanisms. The initial conditions consist of the mixture composition, initial pressure, initial

temperature, and V_{CJ} shock velocity. As in Chapter 2, the detonation velocity was calculated by STANJAN and the post-shock conditions were determined through the shock jump conditions using frozen chemistry. The number of species used in STANJAN calculations is significantly smaller than those in the detonation simulations but this has no appreciable effect because of the negligible role minor species play in equilibrium calculations for the shock velocity. Output from the program includes the spatial evolution of chemical species, velocity, and thermodynamic variables behind the shock wave. Absolute and relative numerical tolerance constraints of $1x10^{-9}$ and $1x10^{-10}$, respectively, were imposed on the integrator for all simulations.

The reaction zone structure from a representative ZND simulation in stoichiometric propane-oxygen at initial conditions of 295 K and 1 atm is presented in Fig. 74. The pressure and temperature rise discontinuously from the initial values to the post-shock (vN) state. The shock is followed by an induction zone through which the thermodynamic state remains relatively constant while free radical (such as OH) concentrations increase. Significant energy release is indicated by the rapid rise in temperature, decrease in pressure, and formation of the major products in the recombination zone. The reaction zone thickness and the associated reaction time is defined as the distance from the shock to the maximum temperature gradient location. The reaction time or length is dominated by the post-shock temperature (Chap. 2) and radical chemistry reaction rates within the endothermic or thermally neutral induction zone. Significant energy release occurs late in the reaction zone and so does not directly affect the reaction time with the maximum temperature gradient definition. Exothermicity indirectly affects the reaction time by influencing the detonation shock velocity and therefore, the post-shock temperature.

The reaction lengths and times are plotted versus equivalence ratio for fuel-oxygen and fuel-air mixtures at atmospheric initial conditions in Figs. 75 - 77. The reaction time/length scales are always greater for the fuel-air mixtures relative to the corresponding fuel-oxygen mixtures. Reaction scales for the fuel-air mixtures exhibit a minimum near stoichiometric, sharply increase towards the lean side, and gradually rise for rich conditions. Fuel-oxygen mixture curves are relatively flat with all reaction lengths and times less than 1 mm and 1μs, respectively, except for some of the most lean and rich conditions considered. All of these trends are due to the post-shock temperature variation with equivalence ratio among fuel-oxygen and fuel-air mixtures discussed in Chapter 2. There is a clear hierarchy of reaction time/length scales in the fuel-air mixtures, increasing from hydrogen to ethylene and finally, propane. The post-shock temperatures for these fuel-air mixtures are comparable (Chap. 2) and therefore, the radical chemistry reaction rates determine this hierarchy.

The reaction length and time scales versus percent diluent data for stoichiometric mixtures at atmospheric initial conditions are presented in Figs. 78 - 80. Hydrogen is the most sensitive fuel to diluent addition. The argon and helium diluents are chemically inert and therefore, have a strictly thermal inhibiting effect. Addition of these monatomic gases to a fuel-oxygen mixture decreases the heat capacity, decreases the energy release, and raises the post-shock temperature over a wide range of dilution as discussed in Chapter 2 (Figs. 5,7,9) maintaining relatively constant reaction length/time scales over the same range. Argon and helium are quantitatively identical in their effect on the reaction time and the reaction lengths for helium are longer due to increased shock velocities relative to argon-diluted mixtures. Carbon dioxide increases the reac-

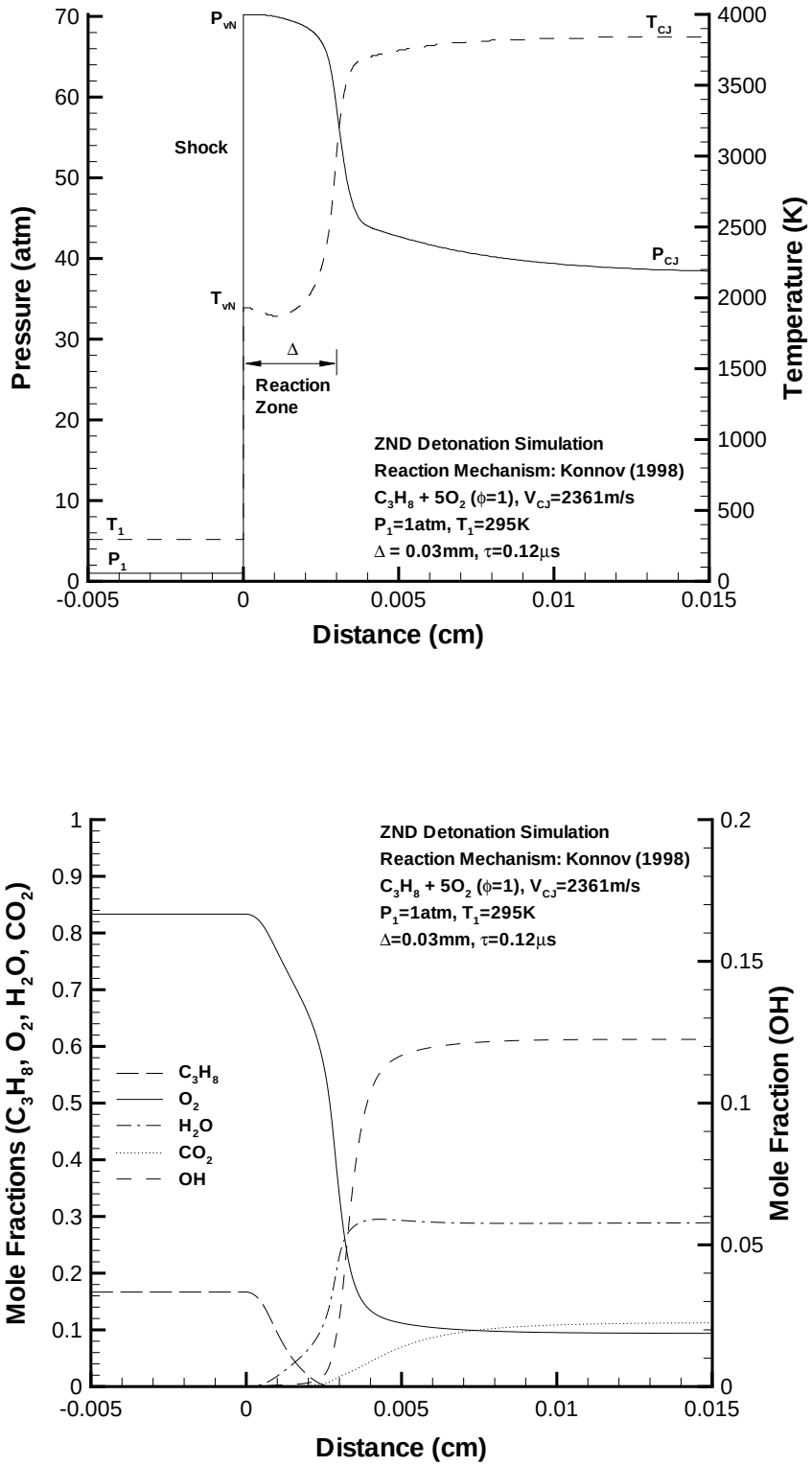

Fig. 74 Representative steady, one-dimensional detonation simulation.

tion time most significantly for all fuels, followed by nitrogen; this order is given by the effect of these diluents on the post-shock temperature (Chap. 2). The effect of carbon dioxide is primarily thermal for hydrogen mixtures as shown by Shepherd (1986) in which the thermal and kinetic effects of this diluent were investigated. The excellent agreement between constant-volume explosion induction times for mechanisms with and without nitrogen as a chemically active species indicates that nitrogen also has primarily a thermal effect for all of the fuel-oxygen mixtures (Chap. 5).

Reaction length and time scales for stoichiometric fuel-oxygen and fuel-air mixtures at atmospheric initial temperature with varying initial pressure are presented in Figs. 81 - 83. Increasing initial pressure results in decreasing reaction length/time scales varying approximately as $\tau, \Delta \sim P^{-1.0}$ for the fuel-oxygen mixtures. This variation is expected from the pressure dependence of rate-limiting reactions as discussed in Chapter 5. The fuel-air mixture pressure dependence is somewhat less relative to the fuel-oxygen dependence due to the prevalence of three-body effects in the nitrogen-diluted mixtures. Fuel-air mixture reaction scales are always greater than the corresponding fuel-oxygen mixture scales as expected from post-shock temperature considerations.

Variations in equivalence ratio, dilution, and initial pressure for all mixtures resulted in qualitatively similar trends no matter which mechanism was used. The Tan (1994) mechanism consistently resulted in greater reaction length/time scales than those calculated with the Konnov (1998) mechanism for all propane mixtures and the reaction scales were greater with the Konnov (1998) mechanism for all hydrogen mixtures. No such trend exists for the ethylene mixtures. The reaction length/time scales calculated with both mechanisms typically agree within a factor of two.

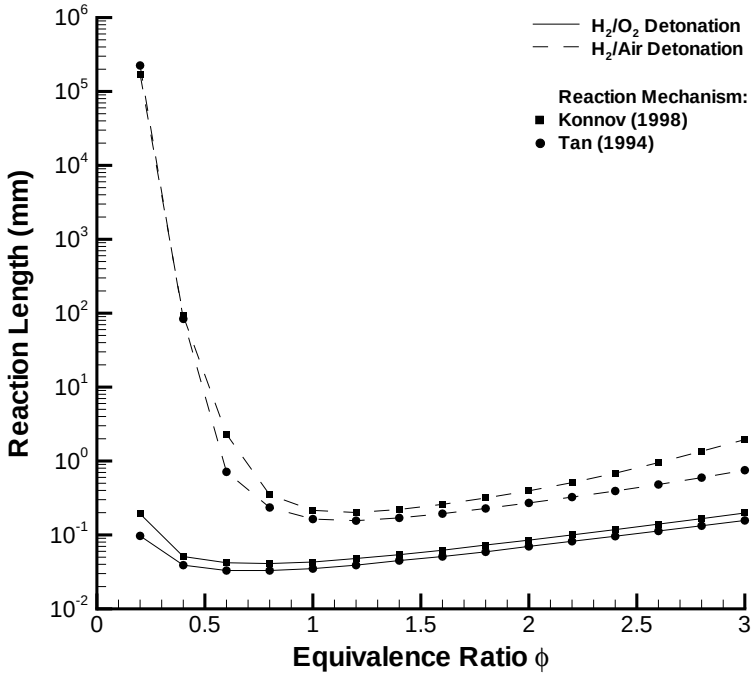

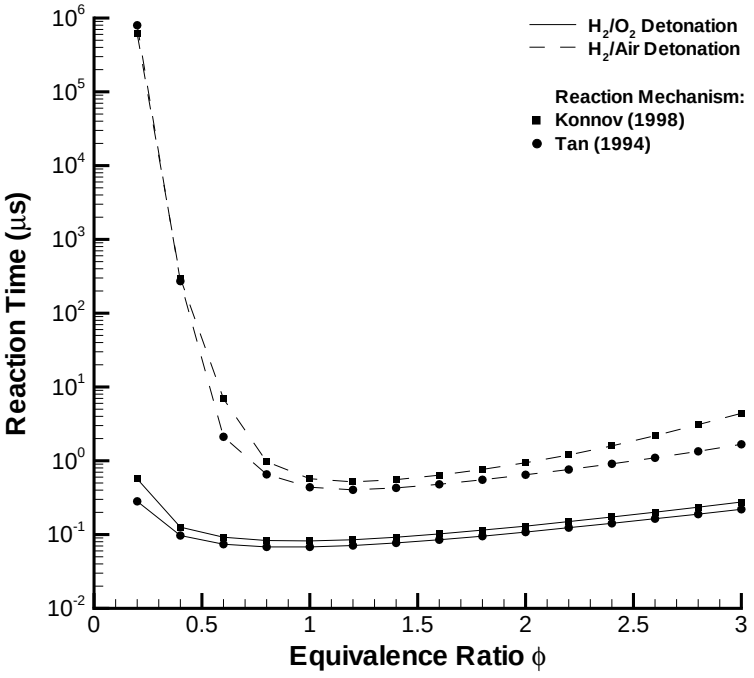

Fig. 75 Hydrogen detonation characteristic reaction scales versus equivalence ratio with initial conditions of 295 K and 1 bar.

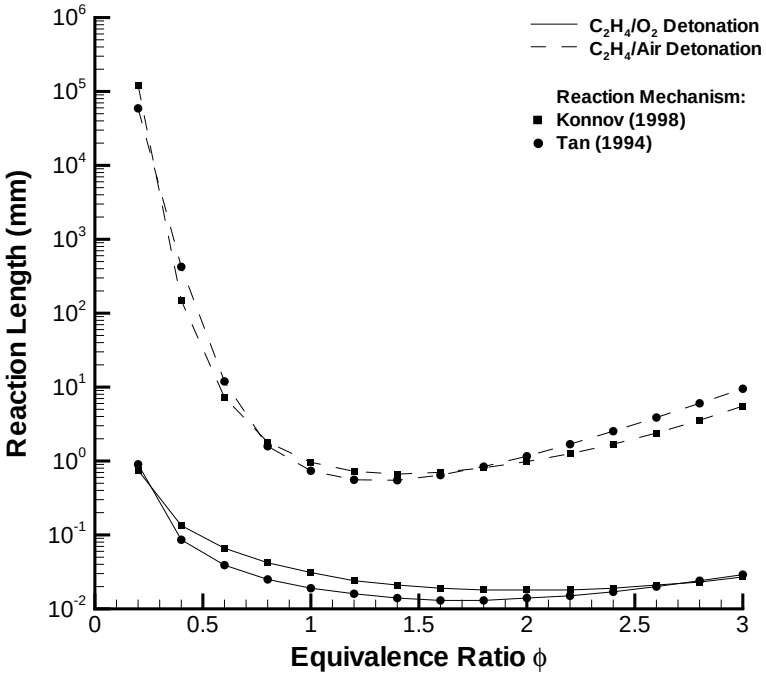

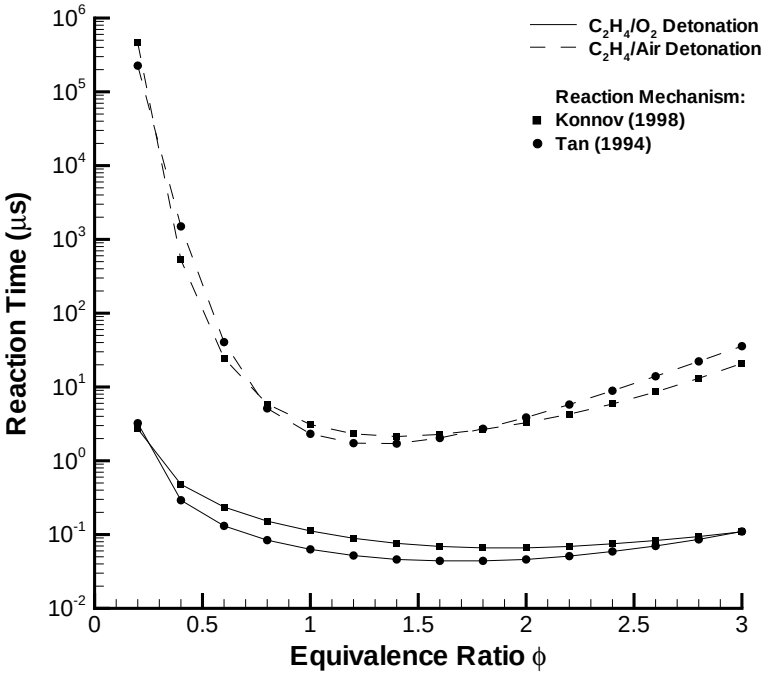

Fig. 76 Ethylene detonation characteristic reaction scales versus equivalence ratio with initial conditions of 295 K and 1 bar.

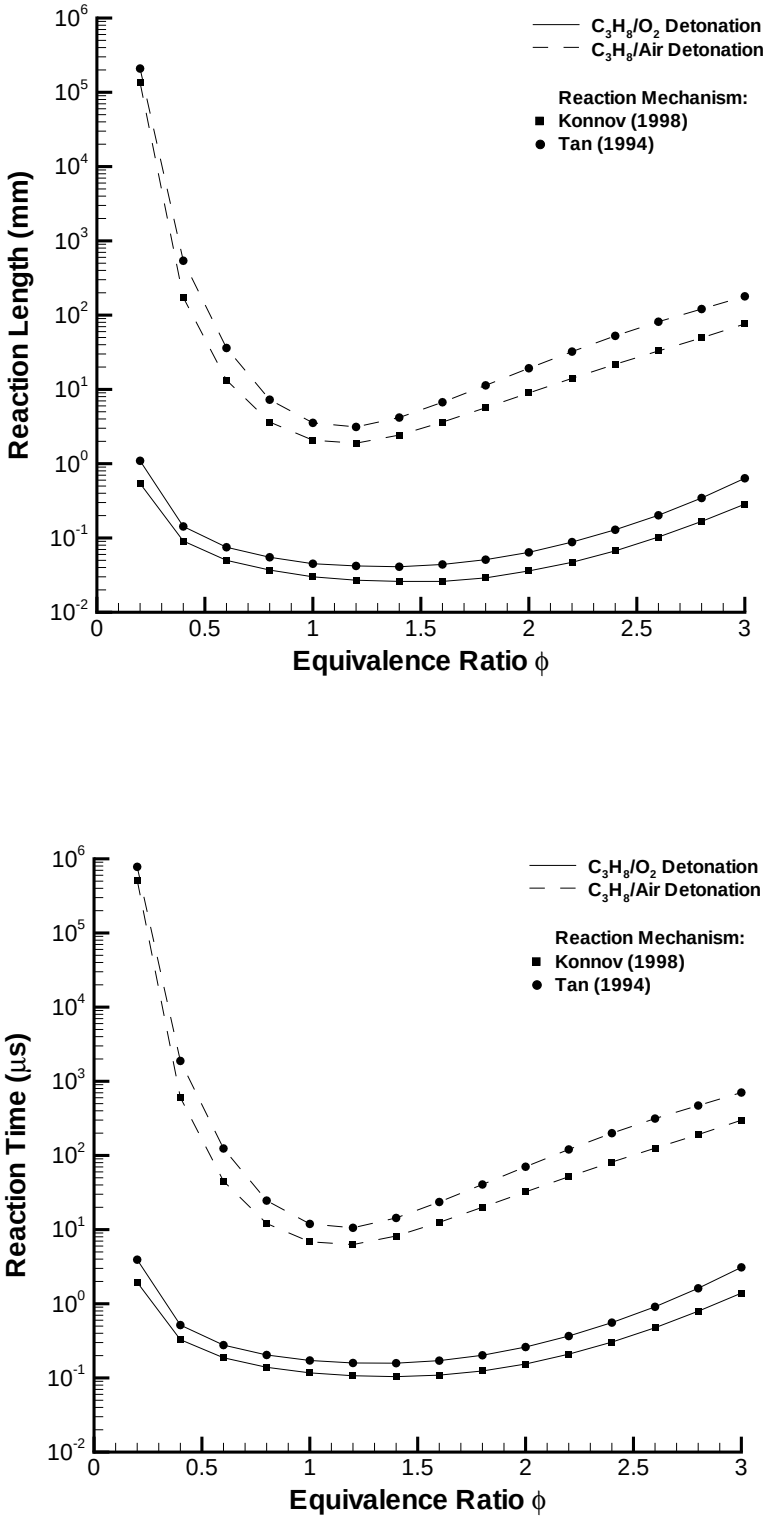

Fig. 77 Propane detonation characteristic reaction scales versus equivalence ratio with initial conditions of 295 K and 1 bar.

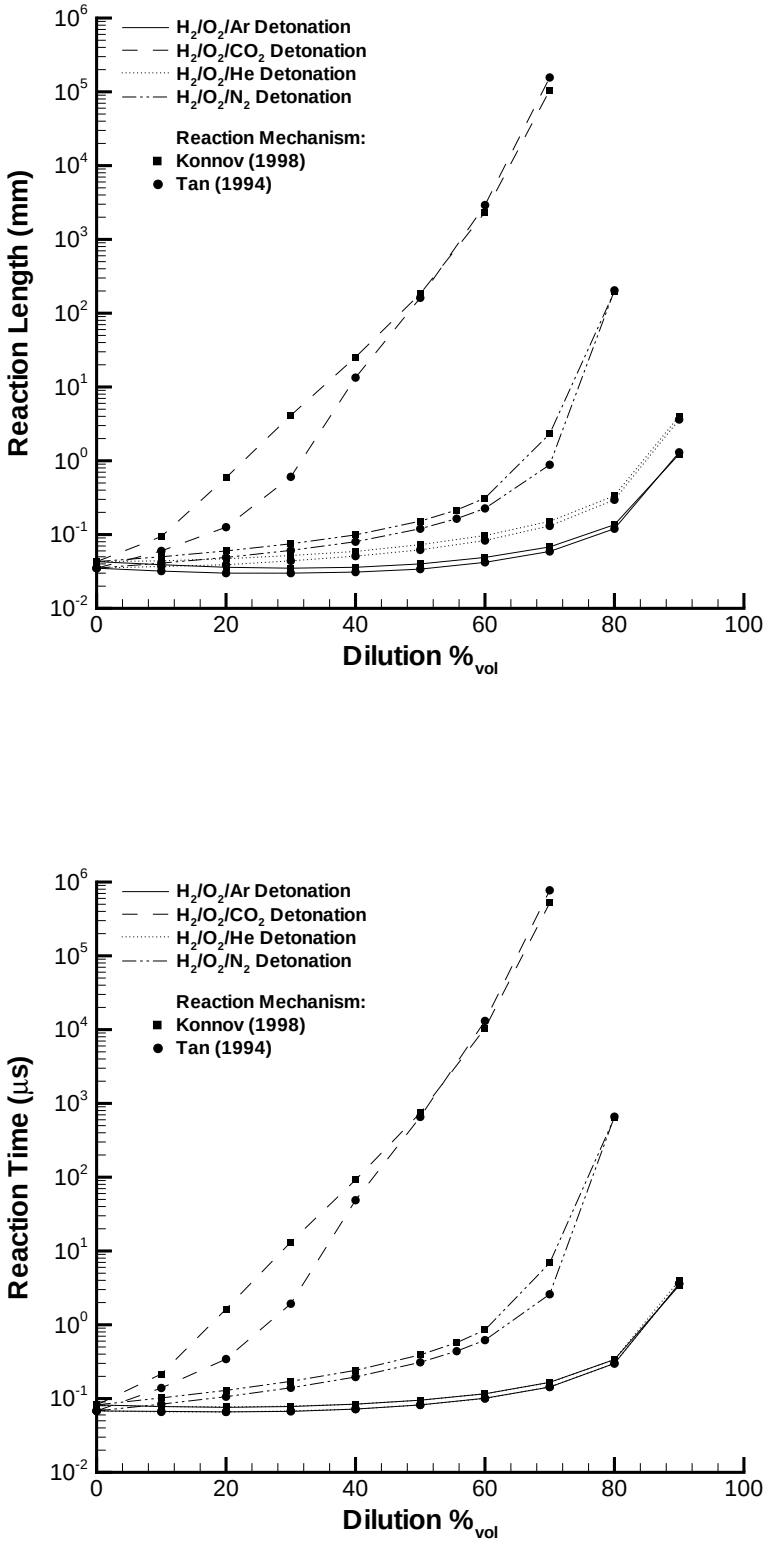

Fig. 78 Stoichiometric hydrogen detonation characteristic reaction scales versus dilution with initials conditions of 295 K and 1 bar.

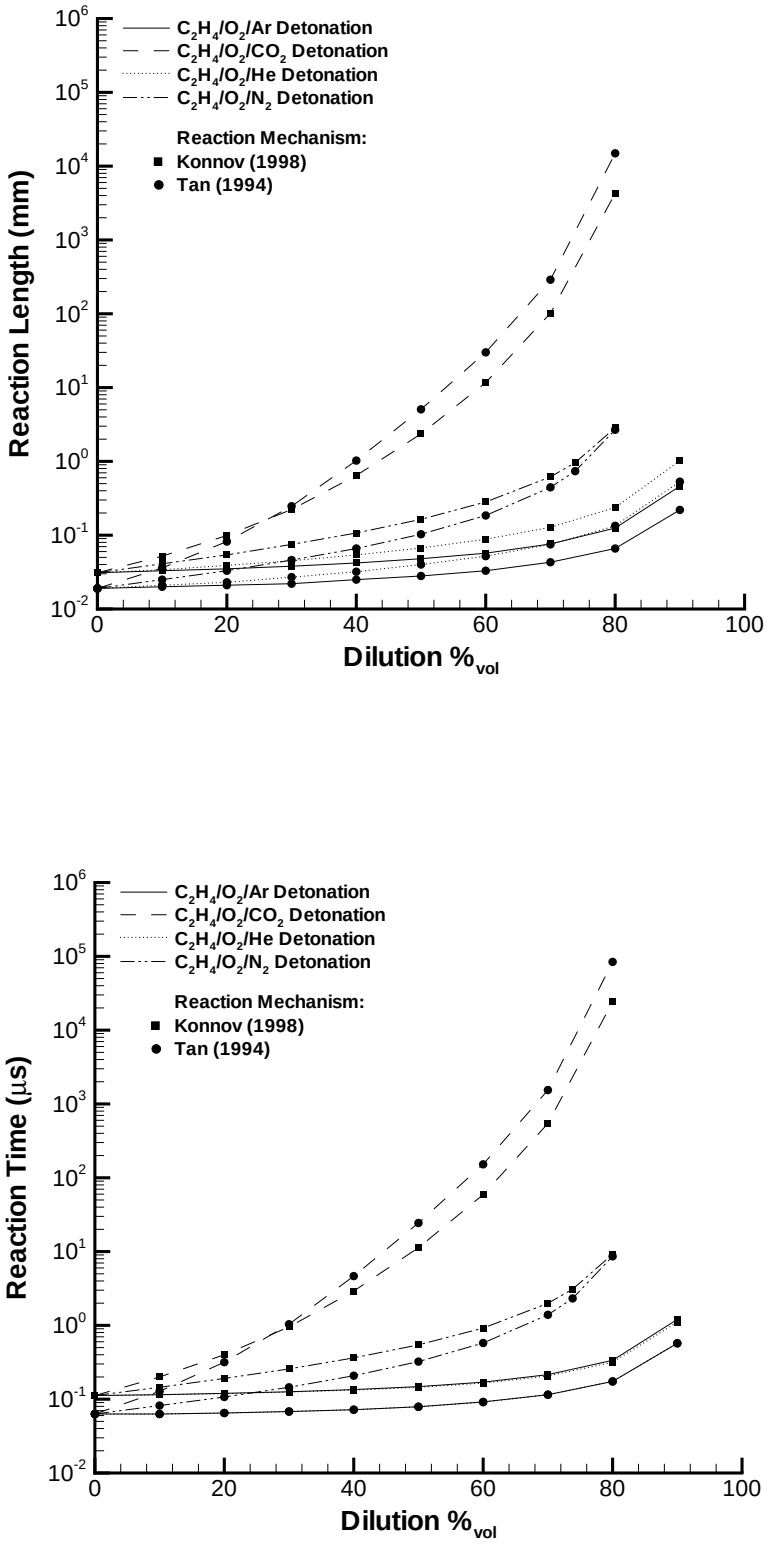

Fig. 79 Stoichiometric ethylene detonation characteristic reaction scales versus dilution with initial conditions of 295 K and 1 bar.

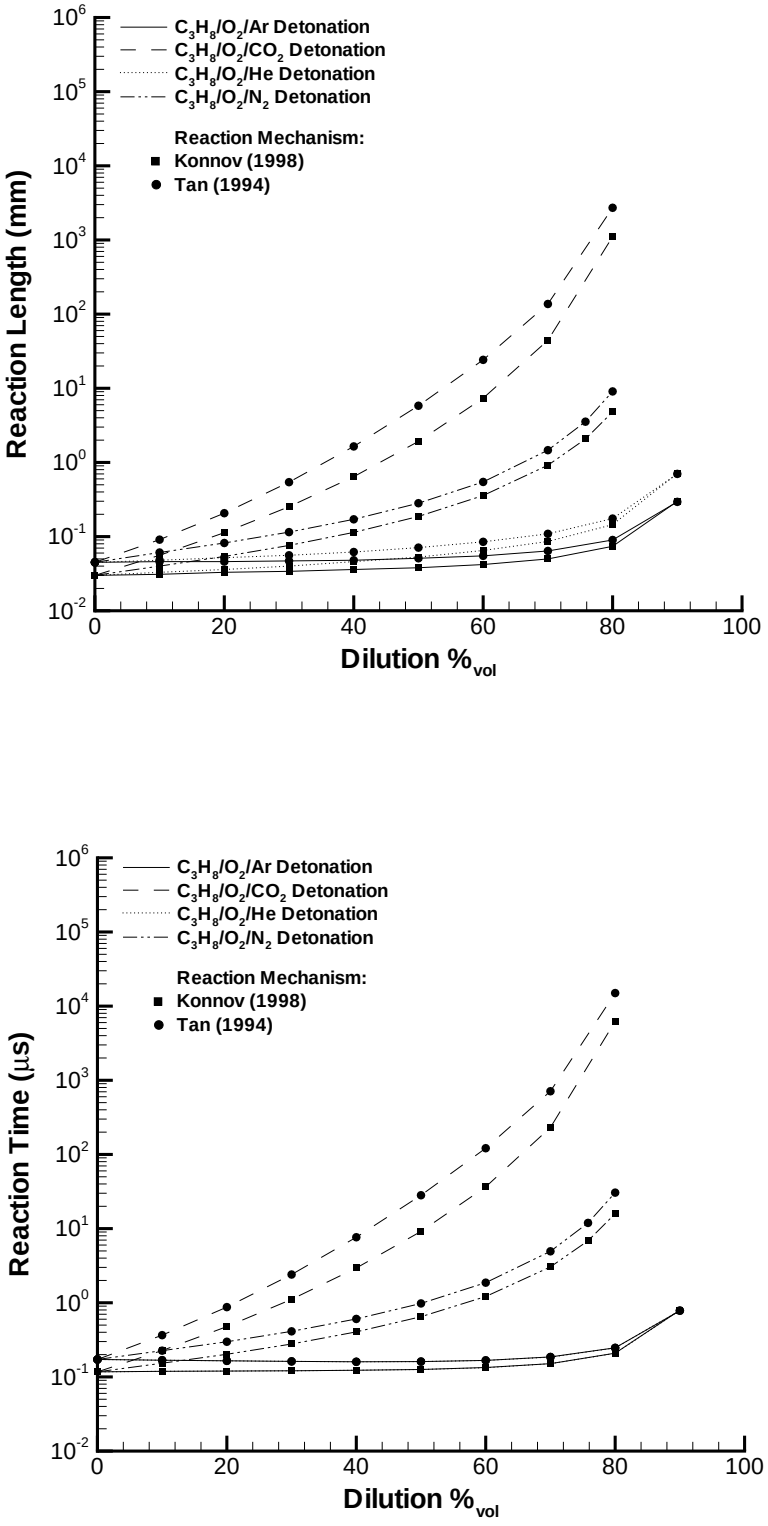

Fig. 80 Stoichiometric propane detonation characteristic reaction scales versus dilution with initial conditions of 295 K and 1 bar.

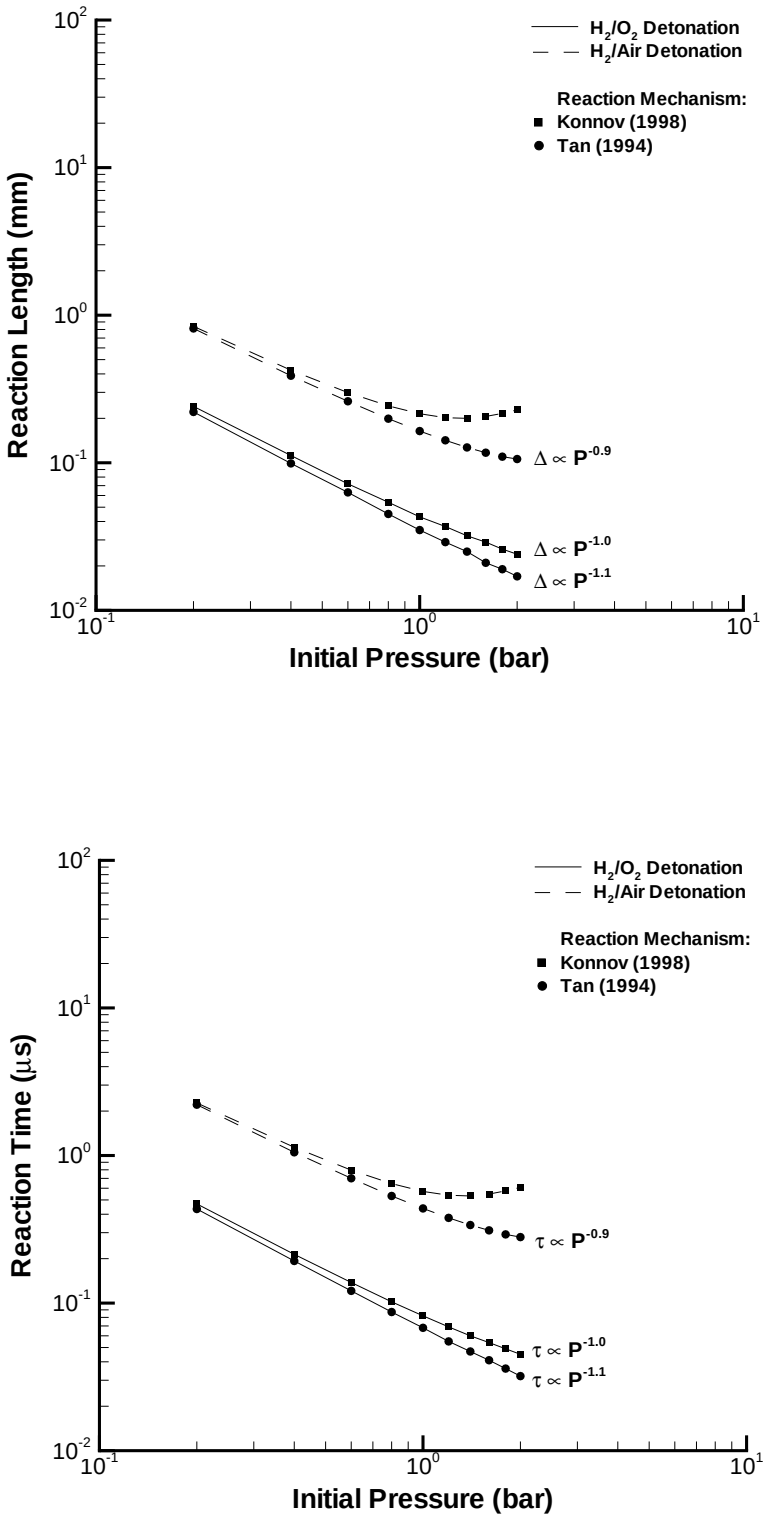

Fig. 81 Stoichiometric hydrogen detonation characteristic reaction scales versus initial pressure with initial temperature of 295 K.

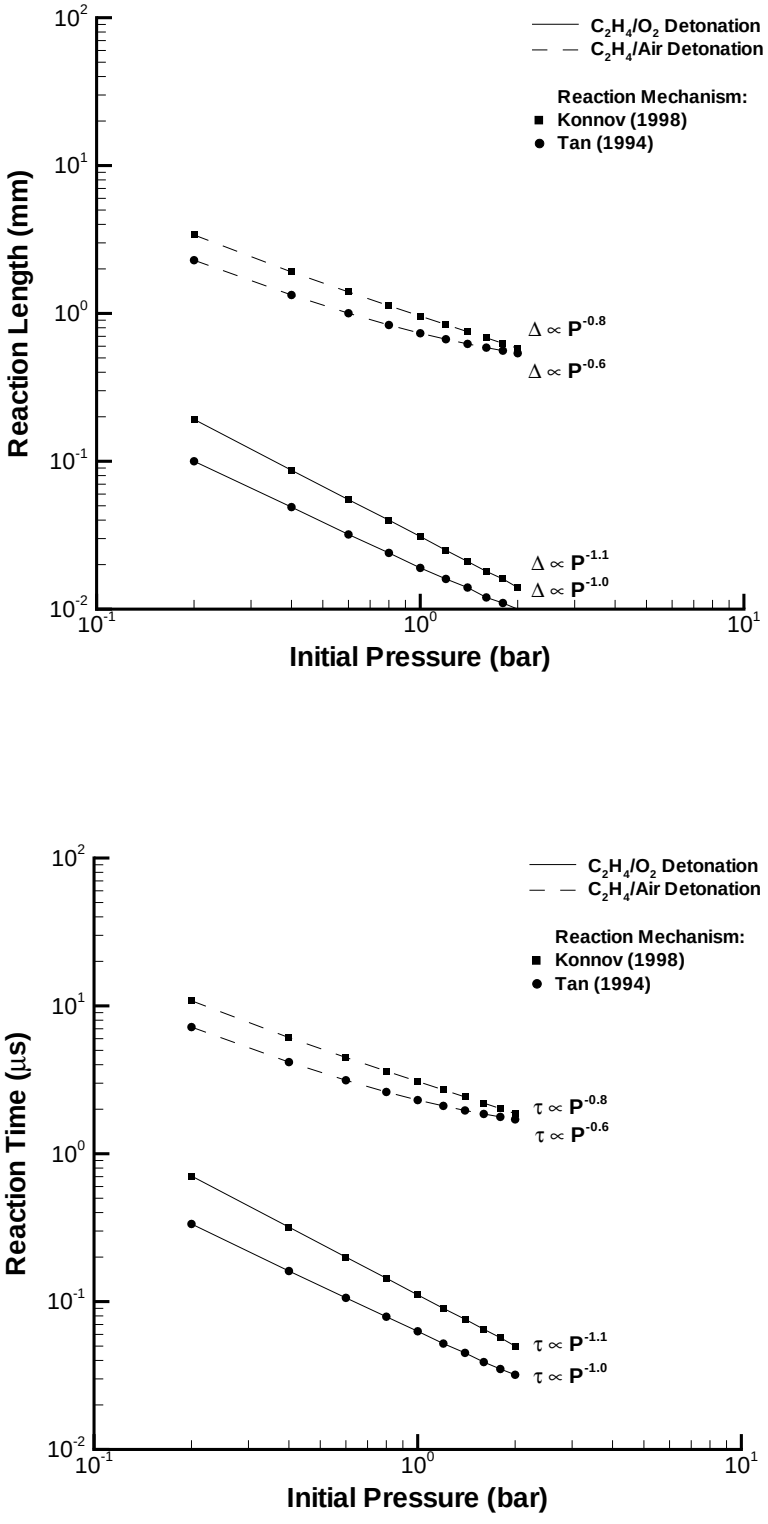

Fig. 82 Stoichiometric ethylene detonation characteristic reaction scales versus initial pressure with initial temperature of 295 K.

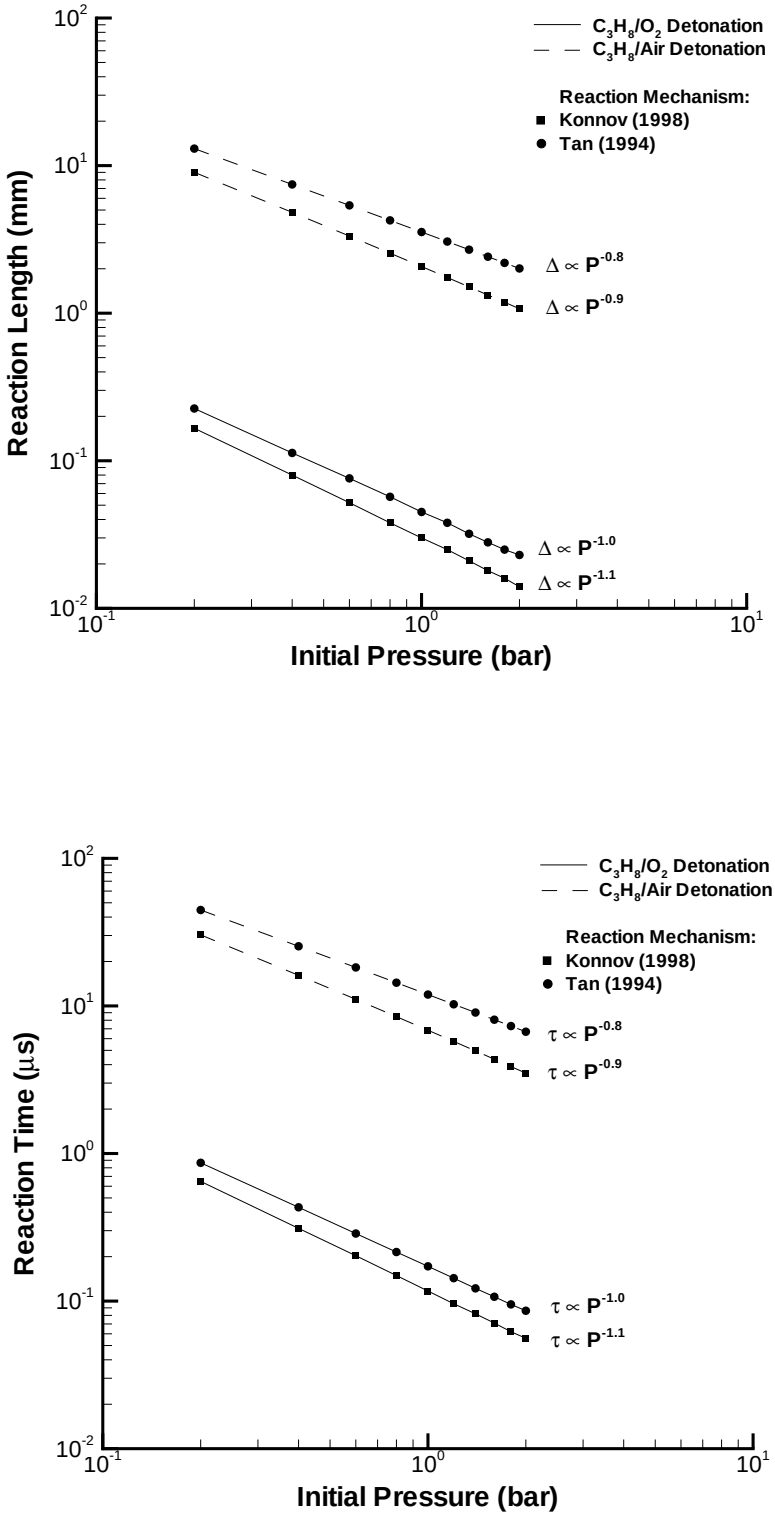

Fig. 83 Stoichiometric propane detonation characteristic reaction scales versus initial pressure with initial temperature of 295 K.

6.2 Activation Energy

Constant-volume explosion simulations can be used to estimate effective activation energies which are indicative of the reaction zone sensitivity to thermodynamic perturbations. Assume that the global chemical behavior can be represented by an Arrhenius induction time (τ) of

$$\tau = \frac{A}{\rho_{vN}} \exp\left(\frac{E}{RT_{vN}}\right)$$

The perfect gas shock jump expression for density is given by

$$\frac{\rho_{vN}}{\rho_0} = \frac{(\gamma+1)M_{CJ}^2}{(\gamma-1)M_{CJ}^2+2}$$

In the strong-shock limit appropriate for detonation Mach numbers (Chap. 2), this reduces to

$$\left.\frac{\rho_{vN}}{\rho_0}\right|_{M_{CJ}\to\infty} = \frac{\gamma+1}{\gamma-1}$$

The perfect gas shock jump expression for temperature is given by

$$\frac{T_{vN}}{T_0} = \left[1+\frac{2\gamma}{\gamma+1}(M_{CJ}^2-1)\right]\left[\frac{(\gamma-1)M_{CJ}^2+2}{(\gamma+1)M_{CJ}^2}\right]$$

which retains a squared dependence on the detonation Mach number in the strong-shock limit. Therefore the post-shock density is nearly a constant when varying the shock velocity relative to the significant temperature variation due to the squared Mach number and exponential induction time dependence on the post-shock temperature. Therefore, consideration is only given to the temperature dependence of the reaction time when considering how the thermodynamic state affects the explosion time. The effective activation energy parameter is defined by

$$\theta = \frac{E}{RT_{vN}} = \frac{1}{T_{vN}}\left(\frac{\ln\tau_2-\ln\tau_1}{\frac{1}{T_2}-\frac{1}{T_1}}\right)$$

where two constant-volume explosion simulations corresponding to (T_1,τ_1) and (T_2,τ_2) are run for each activation energy data point. Initial conditions for states one and two are generated by varying the shock velocity by ±1% V_{CJ}. The jump conditions were solved with these perturbed velocities to obtain the post-shock conditions used as initial conditions in the constant-volume explosion simulations.

The sensitivity of the calculated activation energy parameters to the choice of shock velocity perturbation was investigated by running all cases with shock velocities differing from V_{CJ} by factors of 10^{-2}, 10^{-3}, 10^{-4}, and 10^{-5}. Simulations performed with the 10^{-4} and 10^{-5} factors produced very erratic activation energy parameters. In some cases, the values converged to those obtained

with 10^{-2} and 10^{-3} factors but in many other cases, the values were abnormally high, low, or even negative. The reason for these observations is the very small shock velocity perturbation which produces variations in induction time on the order of the numerical accuracy of the constant-volume explosion simulations. Consequently, activation energy parameters obtained with the 10^{-2} (±1%) variation factor are presented here.

All propane activation energy parameters obtained with 10^{-2} and 10^{-3} variation factors agree to within 3% (most within 1%) with the exception of the two greatest argon dilution mixtures simulated with the Konnov (1998) mechanism. For these two cases, the 10^{-2} results matched the corresponding helium dilution activation energy parameters as expected, whereas the 10^{-3} results did not (providing confidence in the 10^{-2} values). All ethylene activation energy parameters obtained with 10^{-2} and 10^{-3} variation factors agree to within 4% (most within 1%) with the exception of the greatest argon diluted mixture simulated with the Tan (1994) mechanism for which the discrepancy between values was 7%. Significantly greater changes in the activation energy parameter with different shock velocity variation factors were observed for the hydrogen mixtures with both reaction mechanisms. Most of the hydrogen activation energy parameters obtained with 10^{-2} and 10^{-3} variation factors agree to within 5%, although one quarter of the cases have discrepancies of up to 20% between the values.

The activation energy parameters are plotted versus equivalence ratio for fuel-oxygen and fuel-air mixtures at atmospheric initial pressure and temperature in Figs. 84 - 86. Activation parameters are generally greater for fuel-air mixtures relative to the corresponding fuel-oxygen mixture indicating greater reaction zone sensitivity to temperature perturbations for fuel-air mixtures. Hydrogen mixtures exhibit minimum activation parameters near the stoichiometric condition which increase in the lean and rich directions while the minimum activation parameters for the hydrocarbon mixtures are on the rich side. The hydrogen-air activation parameters are in good agreement with the activation energy data presented by Shepherd (1986).

The activation energy parameter versus percent diluent data for stoichiometric fuel-oxygen mixtures at atmospheric initial pressure and temperature are presented in Figs. 87 - 89. Dilution of these mixtures with argon or helium has quantitatively the same effect and results in a slight decrease of the activation parameter, up to a maximum of 10% relative to the undiluted cases for the Konnov (1998) mechanism and 20% for the Tan (1994) mechanism. Carbon dioxide and nitrogen diluents significantly increase the activation parameter of all mixtures primarily due to post-shock temperature variations with diluent type and amount. The concentration of diluent required to raise the activation parameter and the magnitude by which it is increased varies greatly between the three fuels. Note that these two diluents result in complex variations in activation parameter behavior and do not always monotonously increase the activation parameter.

Activation energy parameters for stoichiometric fuel-oxygen and fuel-air mixtures at atmospheric initial temperature with varying initial pressure are presented in Figs. 90 - 92. Increasing the initial pressure increases the activation parameter for hydrogen and ethylene mixtures but decreases the parameter for propane mixtures. Activation parameters for the fuel-air mixtures are always greater than those for the corresponding fuel-oxygen mixtures.

Qualitatively different behavior was observed between activation parameters calculated with the Konnov (1998) and Tan (1994) mechanisms around 0.4 equivalence ratio for all fuel-air cases. Otherwise, the activation parameters calculated with the two mechanisms qualitatively follow the same trends except for some variations in the carbon dioxide and nitrogen dilution series. There is generally better quantitative agreement between the activation parameters calculated with the mechanisms for the fuel-oxygen mixtures versus the corresponding fuel-air mixtures. The quantitative discrepancy between results from the two mechanisms is worse for carbon dioxide and nitrogen dilution than for argon and helium dilution. Activation parameters calculated with the two mechanisms differed by a maximum factor of 1.5 with all but a few exceptions.

All of the calculated values are in good agreement with activation energies corresponding to the shock tube induction time data. Hydrogen mixtures typically have calculated activation energies of 20 - 25 kcal/mol with the exception of extreme stoichiometries and dilution levels. Similarly, the calculated activation energies are 30 - 35 kcal/mol for ethylene mixtures and 35 - 40 kcal/mol for propane mixtures. Activation energies derived from shock tube experiments of approximately 18 kcal/mol, 30 kcal/mol, and 42 kcal/mol are provided for hydrogen, ethylene, and propane mixtures by Schott (1973), Drummond (1968), and Burcat (1971), respectively. Others researchers present comparable shock tube activation energy results.

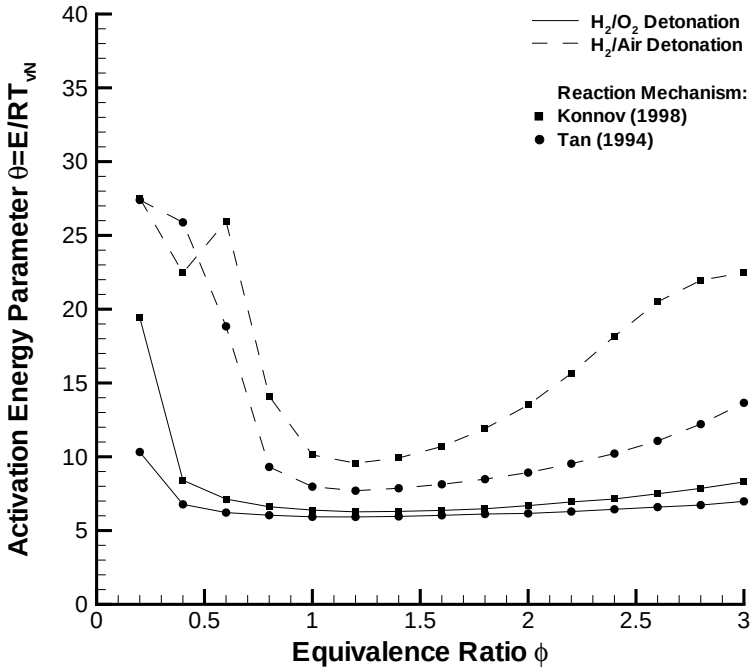

Fig. 84 Hydrogen detonation activation energy parameter versus equivalence ratio with initial conditions of 295 K and 1 bar.

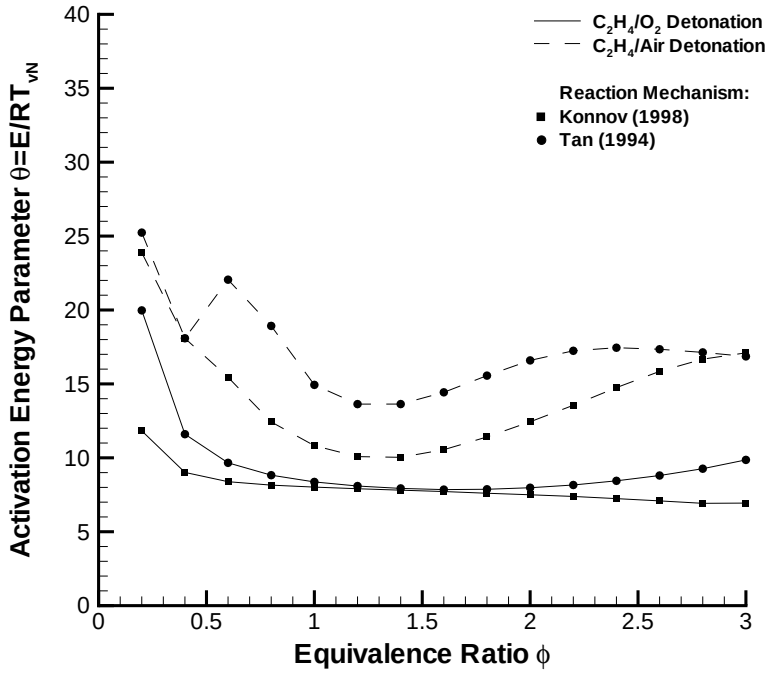

Fig. 85 Ethylene detonation activation energy parameter versus equivalence ratio with initial conditions of 295 K and 1 bar.

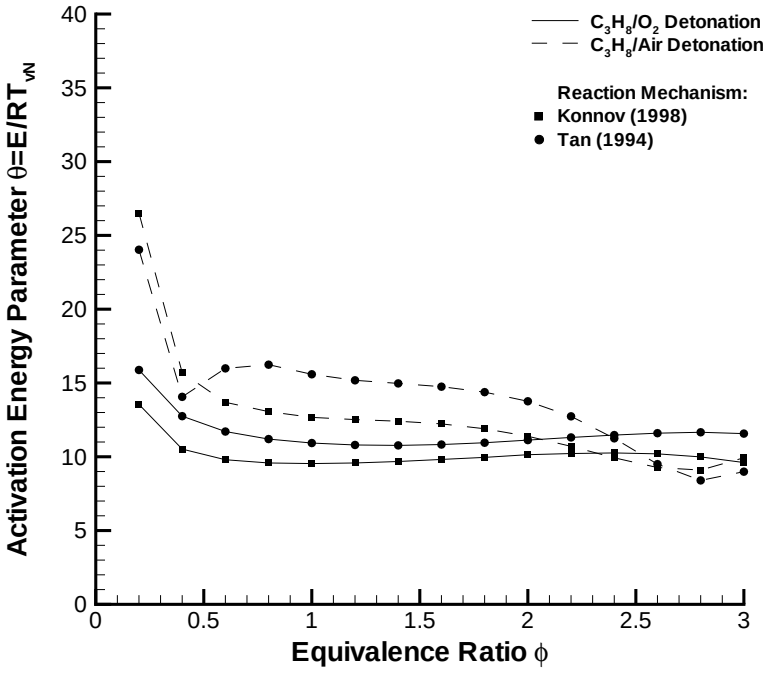

Fig. 86 Propane detonation activation energy parameter versus equivalence ratio with initial conditions of 295 K and 1 bar.

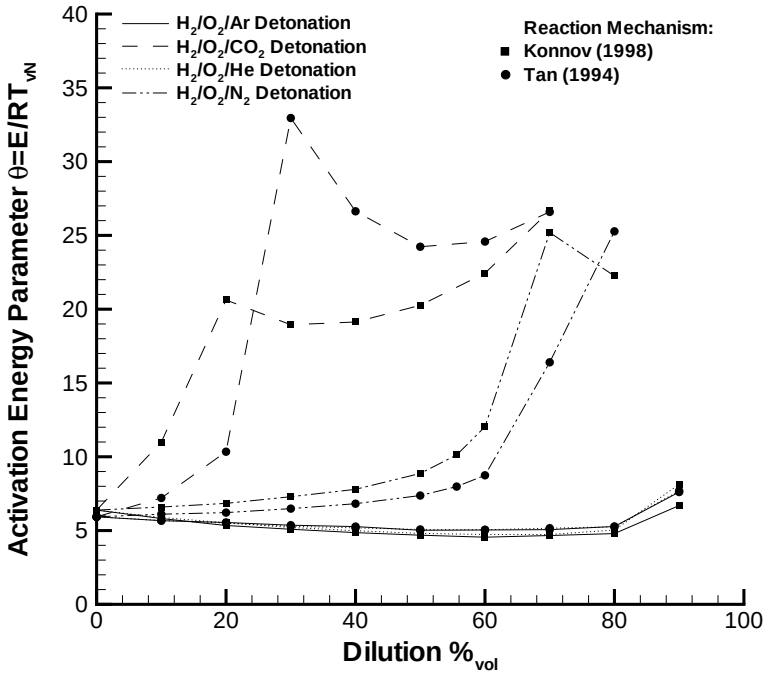

Fig. 87 Stoichiometric hydrogen detonation activation energy parameter versus dilution with initial conditions of 295 K and 1 bar.

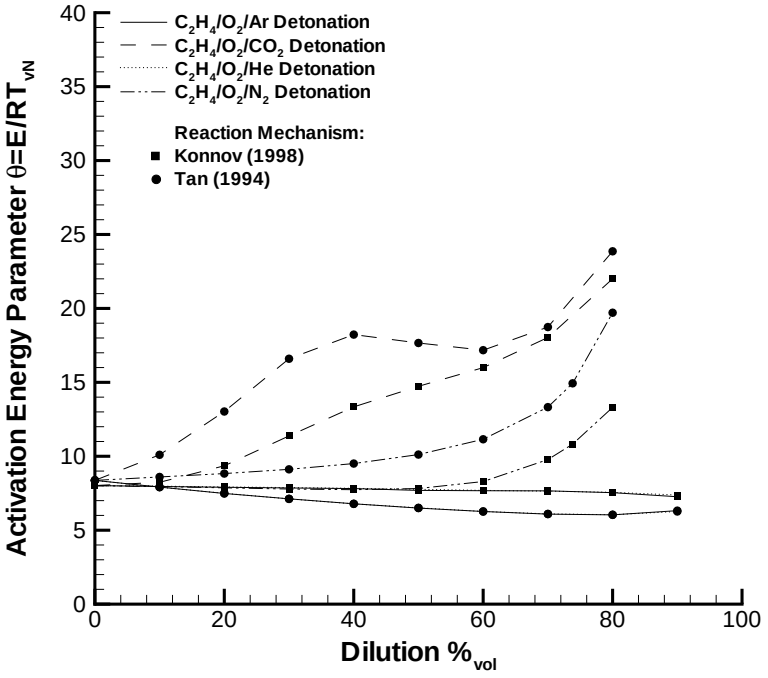

Fig. 88 Stoichiometric ethylene detonation activation energy parameter versus dilution with initial conditions of 295 K and 1 bar.

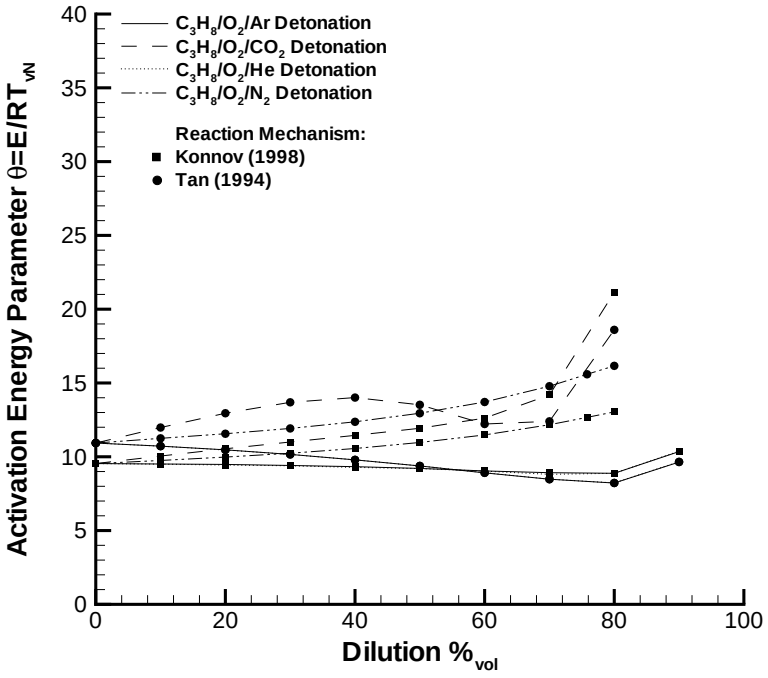

Fig. 89 Stoichiometric propane detonation activation energy parameter versus dilution with initial conditions of 295 K and 1 bar.

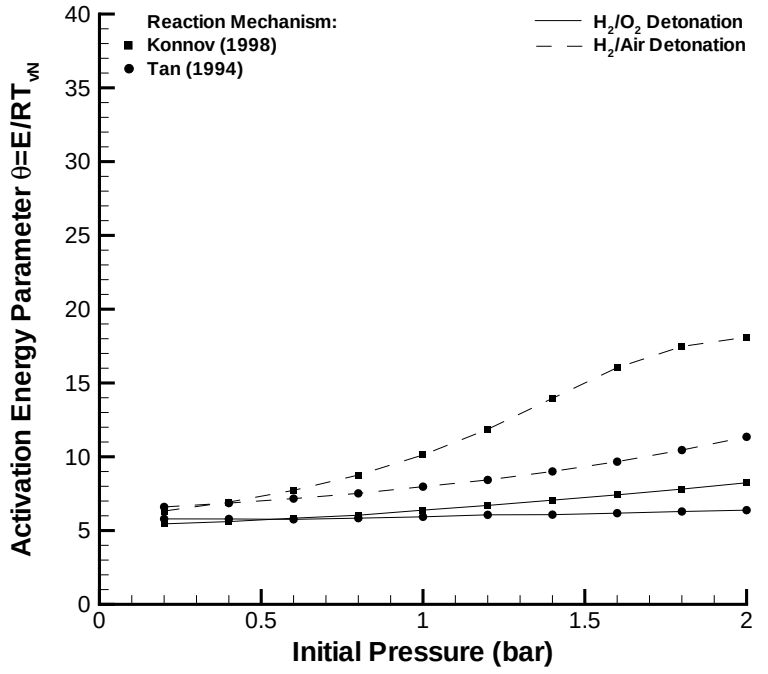

Fig. 90 Stoichiometric hydrogen detonation activation energy parameter versus initial pressure with initial temperature of 295 K.

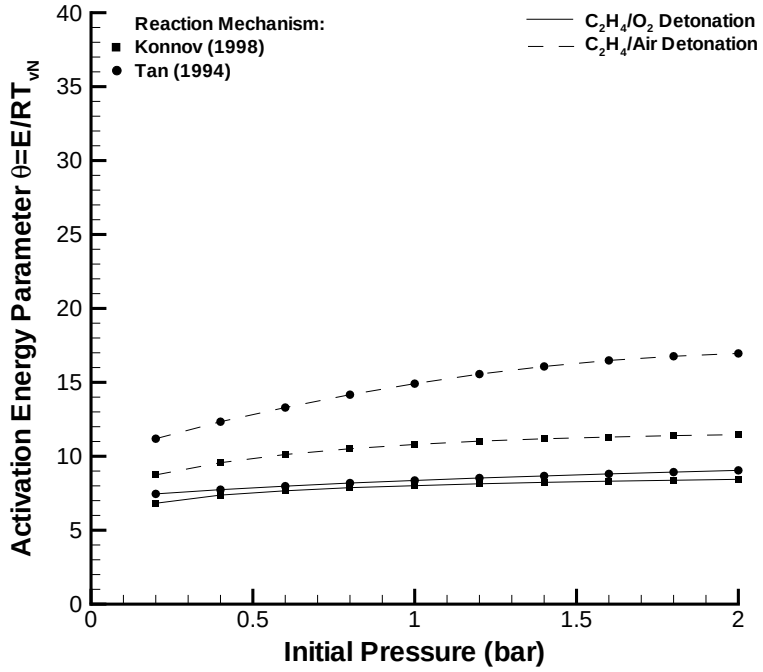

Fig. 91 Stoichiometric ethylene detonation activation energy parameter versus initial pressure with initial temperature of 295 K.

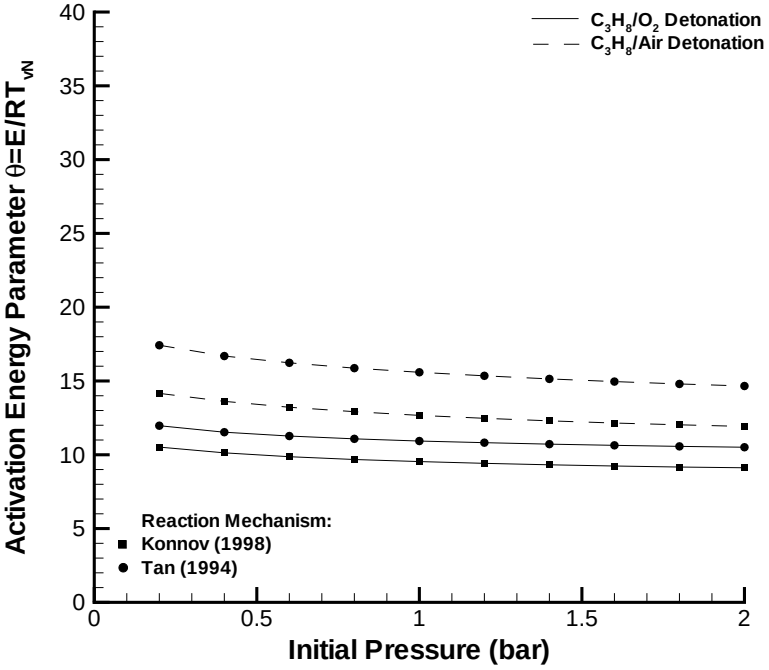

Fig. 92 Stoichiometric propane detonation activation energy parameter versus initial pressure with initial temperature of 295 K.

6.3 Thermal Energy

The STANJAN chemical equilibrium program was used to calculate a thermal energy parameter (Q) which is a measure of the chemical energy release in a detonation. Following the perfect gas 2-γ Chapman-Jouguet detonation model from Thompson (1988), the heat of reaction extrapolated to zero temperature (Δh^0) is given by

$$\Delta h^0 = R_{CJ} T_{CJ} \left(\frac{\gamma_{CJ}}{\gamma_{CJ} - 1} \right) \left(1 + \frac{\gamma_{CJ} - 1}{2} \right) - R_0 T_0 \left(\frac{\gamma_0}{\gamma_0 - 1} \right) \left(1 + \frac{\gamma_0 - 1}{2} M_{CJ}^2 \right)$$

STANJAN performs the equilibrium calculations which provide the detonation Mach number and gas mixture constant, temperature, and specific heat ratio at the Chapman-Jouguet state. The thermochemical database used in the STANJAN calculations does not include the entire species set used in the detailed reaction mechanisms but rather a subset including all reactants, primary products, and several intermediate species which may have non-negligible equilibrium concentrations. The non-dimensional thermal energy parameter is defined as

$$Q = \frac{\Delta h^0}{R_0 T_0}$$

Using this parameter and two specific heat ratios, the detonation Mach number can be calculated from

$$M_{CJ}^2 = \sqrt{\frac{(\gamma_{CJ} - 1)(\gamma_{CJ} + 1) Q}{2\gamma_0} + \frac{(\gamma_0 + \gamma_{CJ})(\gamma_{CJ} - 1)}{2\gamma_0(\gamma_0 - 1)}} + \sqrt{\frac{(\gamma_{CJ} - 1)(\gamma_{CJ} + 1) Q}{2\gamma_0} + \frac{(\gamma_{CJ} - \gamma_0)(\gamma_{CJ} + 1)}{2\gamma_0(\gamma_0 - 1)}}$$

The pressure, density, and temperature at the Chapman-Jouguet state then follow as

$$\frac{P_{CJ}}{P_0} = \frac{\gamma_0 M_{CJ}^2 + 1}{\gamma_{CJ} + 1}$$

$$\frac{\rho_{CJ}}{\rho_0} = \frac{\gamma_0 (\gamma_{CJ} + 1) M_{CJ}^2}{\gamma_{CJ} (1 + \gamma_0 M_{CJ}^2)}$$

$$\frac{T_{CJ}}{T_0} = \left(\frac{\gamma_0 M_{CJ}^2 + 1}{\gamma_{CJ} + 1} \right) \left(\frac{\gamma_{CJ} (1 + \gamma_0 M_{CJ}^2)}{\gamma_0 (\gamma_{CJ} + 1) M_{CJ}^2} \right) \left(\frac{R_0}{R_{CJ}} \right)$$

The non-dimensional thermal energy parameter is plotted versus equivalence ratio for fuel-oxygen and fuel-air mixtures at atmospheric initial pressure and temperature in Figs. 93 - 95. The parameter Q is always greater for the fuel-oxygen mixtures relative to the corresponding fuel-air mixture because the nitrogen dilution in the fuel-air case decreases the energy per unit mass of the

mixture. The exception occurs for hydrogen mixtures near the stoichiometric condition where significant product dissociation takes place in the fuel-oxygen case (Chap. 2). All of the fuel-air mixture thermal parameters range from approximately 10 to 50, exhibit a maximum thermal parameter near the stoichiometric condition, and monotonously decrease towards lean and rich conditions. The fuel-oxygen mixtures demonstrate more complex behavior with maxima at significantly rich conditions due to high temperatures for near-stoichiometric conditions resulting in significant product dissociation (Chap. 2). Thermal parameters for propane-oxygen mixtures are the greatest at a given equivalence ratio followed in decreasing order by ethylene-oxygen and hydrogen-oxygen mixtures.

Thermal energy parameters for stoichiometric fuel-oxygen mixtures at atmospheric initial pressure and temperature with varying dilution are presented in Figs. 96 - 98. All diluents have qualitatively the same effect on a given fuel/oxygen system as they reduce the energy per unit mass of the mixture. Argon and helium dilution has a quantitatively identical effect on the thermal parameter causing the data curves for these diluents to overlap. Diluting hydrogen-oxygen mixtures tends to increase the thermal parameter up to 40% dilution and decreases the thermal parameter thereafter. At low dilution levels, the energy per unit mass reduction results in less product dissociation causing the thermal parameter to rise (Chap. 2). The net effect of a decreasing thermal parameter occurs for high dilution levels because the primary products are stable but the mixture energy continues to decrease. Ethylene-oxygen mixtures maintain relatively constant thermal parameters up to 40% dilution and propane-oxygen mixture thermal parameters continuously decrease with increasing dilution. Decreasing mixture energy is again competing with product dissociation at low dilution for these stoichiometric mixtures (Chap. 2).

The thermal energy parameter versus initial pressure data for stoichiometric fuel-oxygen and fuel-air mixtures at atmospheric initial temperature are presented in Figs. 99 - 101. Increasing the initial pressure slightly increases the thermal parameter for fuel-oxygen mixtures (product dissociation is reduced) and decreases the thermal parameter for fuel-air mixtures. Fuel-oxygen mixture thermal parameters are greater than the corresponding fuel-air mixture thermal parameters for ethylene and propane and vice versa for hydrogen. The thermal parameters vary little over the 20 - 200 kPa initial pressure range because the energy per unit mass of the mixture is not changing, the detonation Mach number increases modestly as the initial pressure increases, and the thermodynamic equilibrium CJ state shifts only slightly for this small range of initial pressures.

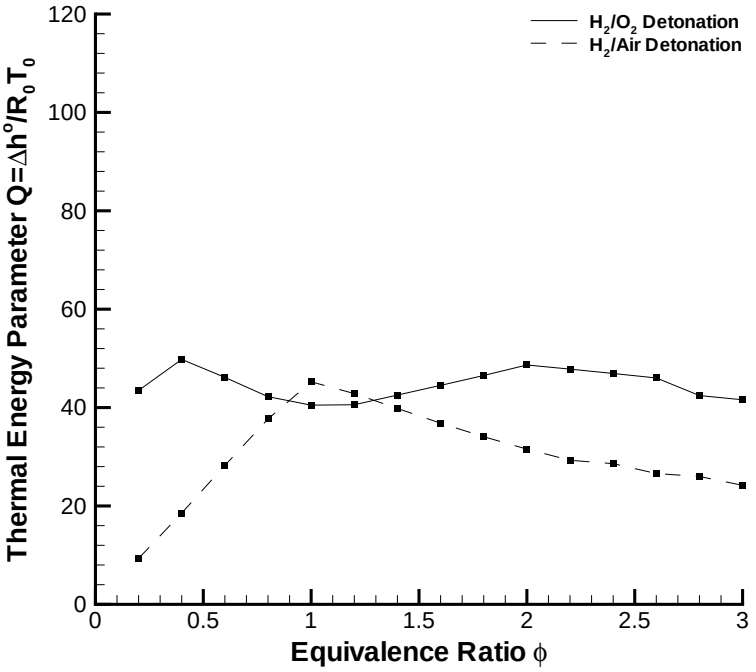

Fig. 93 Hydrogen detonation thermal energy parameter versus equivalence ratio with initial conditions of 295 K and 1 bar.

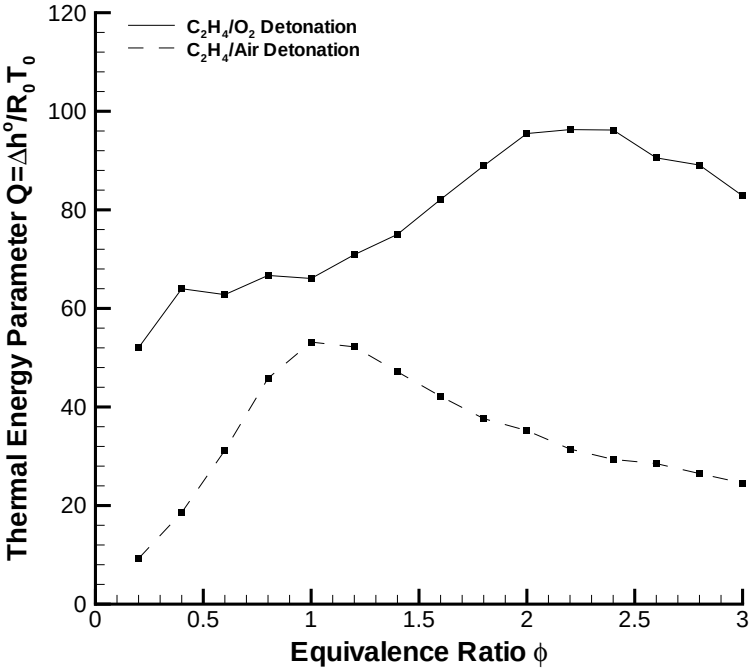

Fig. 94 Ethylene detonation thermal energy parameter versus equivalence ratio with initial conditions of 295 K and 1 bar.

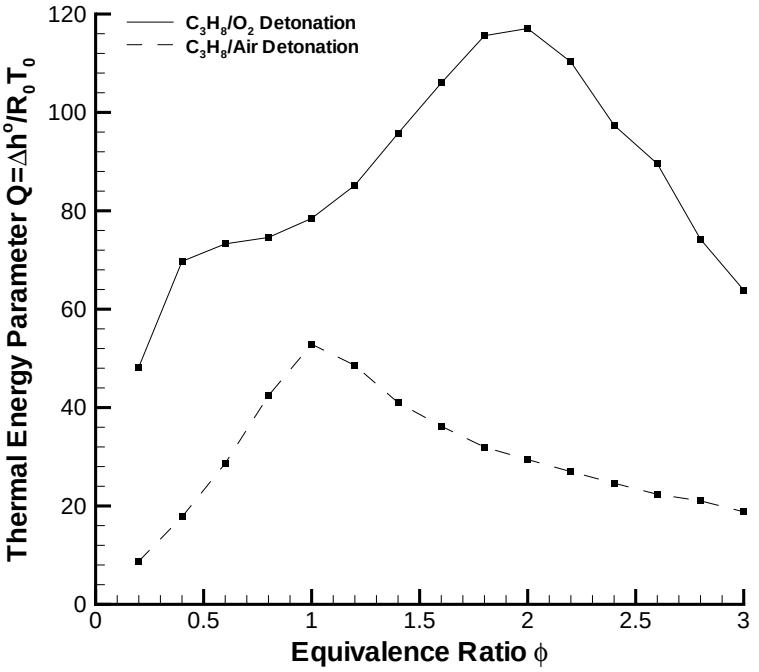

Fig. 95 Propane detonation thermal energy parameter versus equivalence ratio with initial conditions of 295 K and 1 bar.

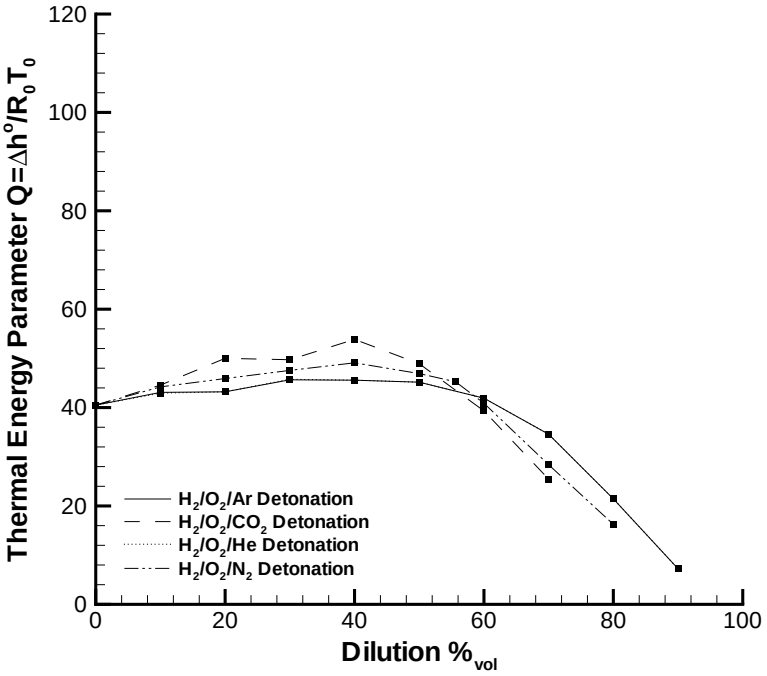

Fig. 96 Stoichiometric hydrogen detonation thermal energy parameter versus dilution with initial conditions of 295 K and 1 bar.

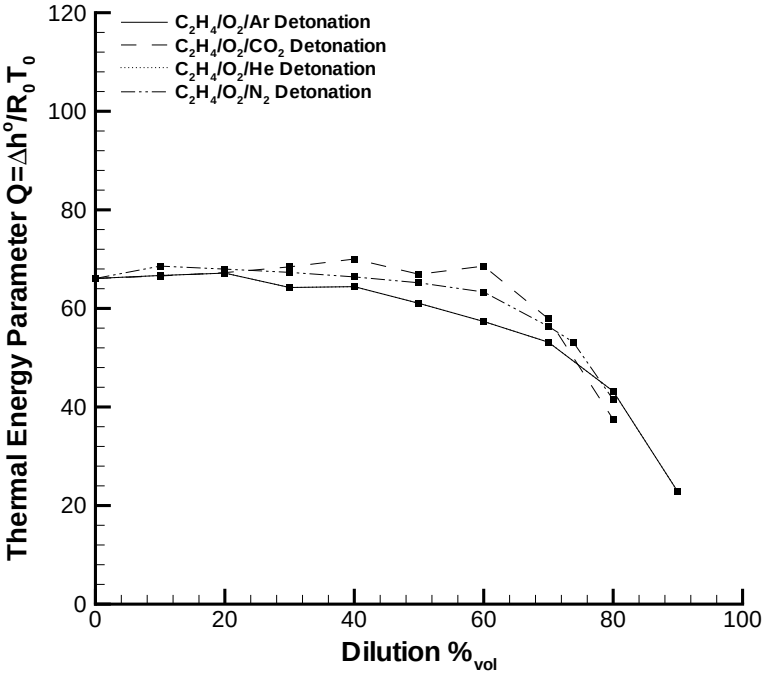

Fig. 97 Stoichiometric ethylene detonation thermal energy parameter versus dilution with initial conditions of 295 K and 1 bar.

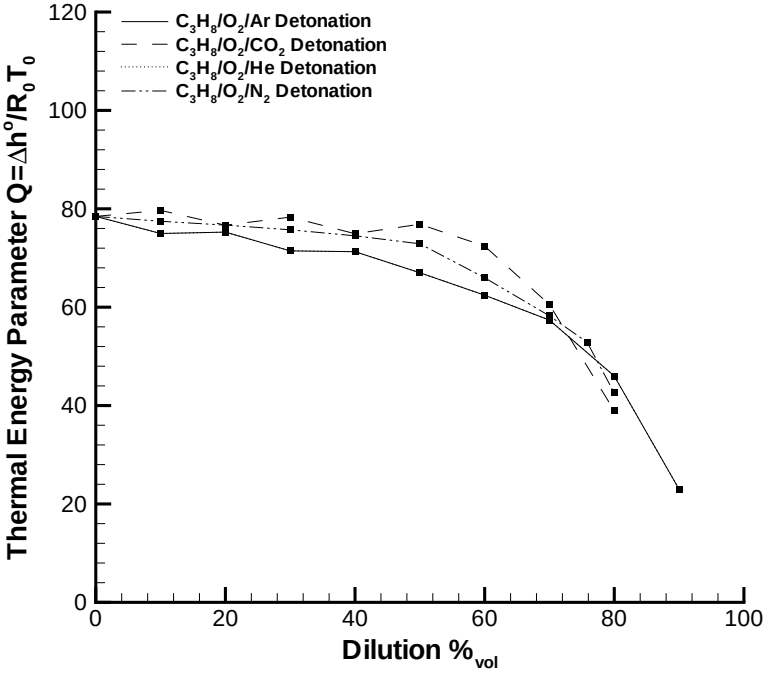

Fig. 98 Stoichiometric propane detonation thermal energy parameter versus dilution with initial conditions of 295 K and 1 bar.

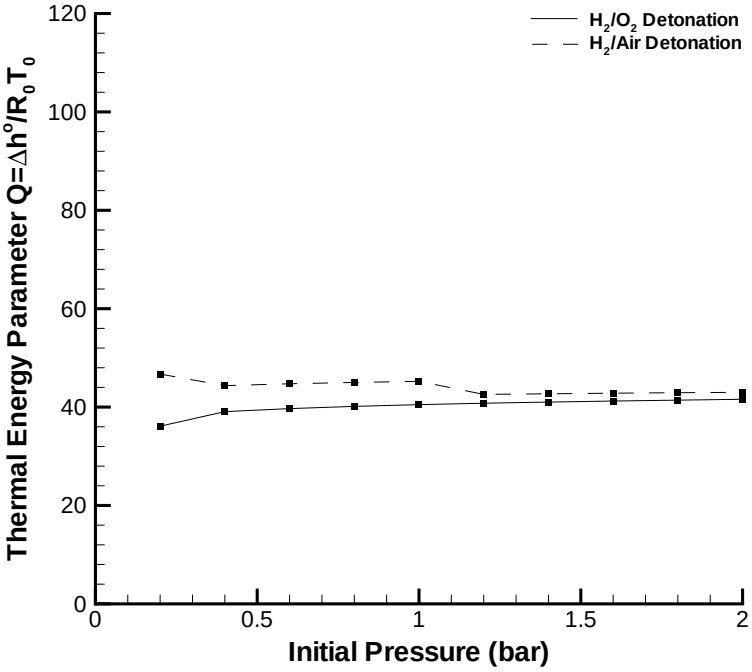

Fig. 99 Stoichiometric hydrogen detonation thermal energy parameter versus initial pressure with initial temperature of 295 K.

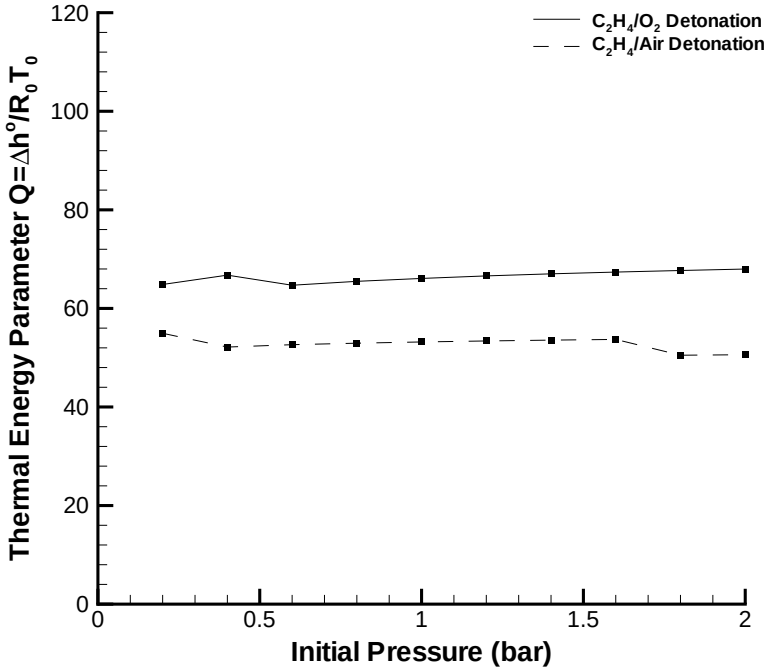

Fig. 100 Stoichiometric ethylene detonation thermal energy parameter versus initial pressure with initial temperature of 295 K.

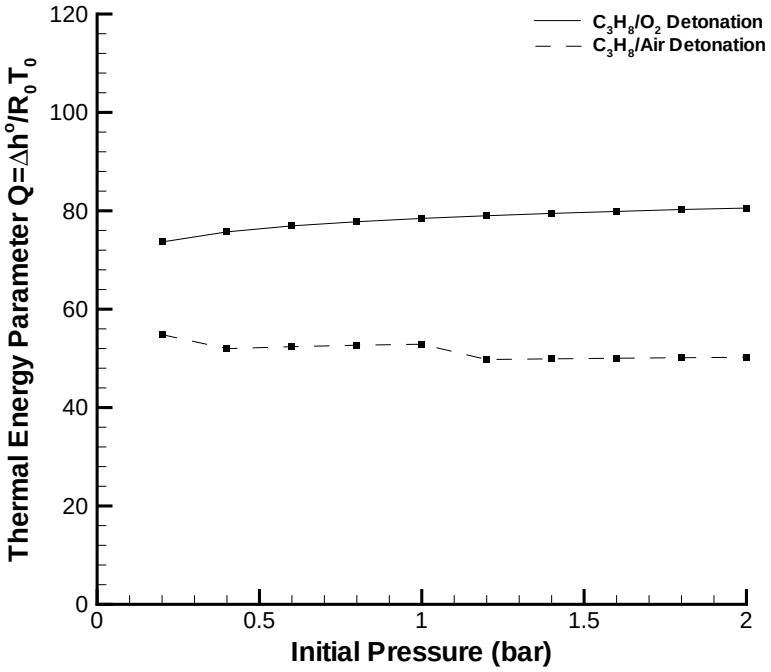

Fig. 101 Stoichiometric propane detonation thermal energy parameter versus initial pressure with initial temperature of 295 K.

7 Conclusions

A database of induction time measurements from shock tube experiments for hydrogen, ethylene, and propane fuel oxidation has been compiled from the literature. Detailed reaction mechanisms from the literature were validated through the comparison of constant-volume explosion simulation results with the experimental shock tube induction time data. Uncertainties associated with the experimental data, numerical integration, constant-volume approximation, and reaction mechanism chemistry have been examined. All mechanisms performed better at relatively high temperatures and are responsible for substantial simulation error at low temperatures. The Konnov (1998) and Tan (1994) mechanisms include the chemistry for all three fuels and simulated the experimental induction time data to within an average factor of 2.5 and 3.0, respectively, for temperatures above 1200 K.

Thermodynamic equilibrium calculations and steady, one-dimensional detonation simulations with the Konnov (1998) and Tan (1994) validated detailed reaction mechanisms were performed under conditions of varying stoichiometry, dilution, and initial pressure for hydrogen, ethylene, and propane fuel mixtures. The information obtained for these mixtures includes the detonation reaction zone structure, reaction time/length scale, effective activation energy, and thermal energy. Trends observed when varying the aforementioned conditions are discussed and nitrogen was shown to have primarily a thermal effect as a diluent. Future simulations will include a detailed investigation of the one-dimensional detonation properties variation with shock velocity.

The present study establishes a foundation for future experimental, analytical, and computational investigations. Reaction mechanism validation with the existing database of shock tube data has treated all data sets equally. A critical examination of each data set may reveal deficiencies which could then be used to establish confidence levels among the different data sets. This would permit a more targeted reaction mechanism validation effort which could narrow the error range of computational results.

Further potential analysis with the existing data includes investigation of reaction mechanism accuracy dependence on pressure and equivalence ratio. Experimental induction time definitions and measurement techniques, as well as systematic effects due to equivalence ratio, and diluent type and concentration, could also be evaluated relative to the simulated versus experimental data comparison. The consistently high error levels at relatively low temperatures should be explored, providing new directions for efforts on the acquisition of chemical kinetic data, development of more accurate detailed reaction mechanisms, and improvement of experimental techniques to acquire low temperature induction time data.

Additional shock tube data is required throughout the range of thermodynamic conditions existing in detonations and the availability of data throughout the equivalence ratio range of interest should be checked. Future work in the area of detailed reaction mechanism validation will also include the addition of new reaction mechanisms and extension to other hydrocarbon fuels; a significant body of data for acetylene and methane exists in the literature. Finally, unsteady one-dimensional simulations with detailed reaction mechanisms represent the next level of fidelity to achieve for more accurate validation studies.

8 References

Asaba T, Gardiner WC, Stubbeman RF (1965) Shock-tube study of the hydrogen-oxygen reaction. 10th Symp (Int'l) on Combustion, 295-302.

Baker JA, Skinner GB (1972) Shock-tube studies on the ignition of ethylene-oxygen-argon mixtures. Combustion and Flame, 19:347-350

Battin-Leclerc F, Barbe P (1997) A reactions database for $C_xH_yO_z$ species with 0, 1, or 2 carbon atmos in the molecule. http://www.ensic.u-nancy.fr/ENSIC/DCPR/chiminfo/textes/chiminfo.htm

Baulch D, Cobos C, Cox R, Esser C, Frank P, Hayman G, Just T, Kerr J, Murrells T, Pilling M, Troe J, Walker R, Warnatz J (1994) Evaluated kinetic data for combustion modeling: Supplement I. J Phys Chem Ref Data 23(6):847-1033.

Belford RL, Strehlow RA (1969) Shock tube technique in chemical kinetics. Annual Review of Physical Chemistry, 20:247-272.

Belles FE, Lauver MR (1964) Origin of OH chemiluminescence during the induction period of the H_2-O_2 reaction behind shock waves. J Chem Phys, 40:415-422.

Belles FE, Lauver MR (1965) Effects of concentration and of vibrational relaxation on the induction period of the H_2-O_2 reaction. 10th Symp (Int'l) on Combustion, 285-293.

Bhaskaran KA, Gupta MC, Just TH (1973) Shock tube study of the effect of unsymmetric dimethyl hydrazine on the ignition characteristics of hydrogen-air mixtures. Combustion and Flame, 21:45-48.

Blumenthal R, Fieweger K, Komp KH, Adomeit G, Gelfand BE (1996a) Self-ignition of H_2-air mixtures at high pressure and low temperature. 20th Int'l Symp on Shock Waves.

Blumenthal R, Fieweger K, Komp KH, Adomeit G (1996b) Gas dynamic features of self ignition of non diluted fuel/air mixtures at high pressure. Comb Sci Tech, 113-114:137-166.

Bowman CT, Hanson RK, Davidson DF, Gardiner WC, Lissianski V, Smith GP, Golden DM, Frenklach M, Goldenberg M (1995) GRI Mechanism v2.11. http://www.me.berkeley.edu/gri_mech/

Burcat A, Lifshitz A, Scheller K, Skinner GB (1970) Shock-tube investigation of ignition in propane-oxygen-argon mixtures. 13th Symp (Int'l) on Combustion, 745-755.

Brossard J, Fomin NA, Soloukhin RI (1979) Shock tube ignition and detonation studies by resonance absorption in propane. Acta Astronautica, 6:861-874.

Brown CJ, Thomas GO (1999) Experimental studies of shock-induced ignition and transition to detonation in ethylene and propane mixtures. Combustion and Flame, 117:861-870.

Burcat A, Scheller K, Lifshitz A (1971) Shock-tube investigation of comparative ignition delay times for C_1 - C_5 alkanes. Combustion and Flame, 16:29-33.

Burcat A (1998) Personal communication.

Cheng RK, Oppenheim AK (1984) Autoignition in methane-hydrogen mixtures. Combustion and Flame, 58:125-139.

Cheng RK (1977) Induction times and strong ignition limits for mixtures of methane with hydrogen. Ph.D. Dissertation, University of California, Berkeley.

Cheng RK (1999) Personal communication.

Cohen A, Larsen J (1967) Explosive mechanism of the H_2-O_2 reaction near the second ignition limit. Report BRL 1386.

Cohen A (1999) Personal communication.

Craig RR (1966) A shock tube study of the ignition delay of hydrogen-air mixtures near the second explosion limit. Report AFAPL-TR-66-74.

Curran HJ (1999) Personal communication.

Dagaut P (1998) Personal communication.

Dormal M, Libouton JC, Van Tiggelen PJ (1979) Evolution of induction time in detonation cells. Acta Astronautica, 6:875-884.

Drummond LJ (1968) Shock-initiated exothermic reactions: The oxidation of ethylene. Aust J Chem, 21:2641-2648.

Dyner HB (1966) Density variation due to reflected shock-boundary layer interaction. Physics of Fluids, 9(5):879-892.

Edwards DH, Hooper G, Job EM, Parry DJ (1970) The behavior of the frontal and transverse shocks in gaseous detonation waves. Astronautica Acta, 15:323-333.

Fickett W, Davis WC (1979) Detonation. University of California Press.

Frenklach M, Wang H, Yu CL, Goldenberg M, Bowman CT, Hanson RK, Davidson DF, Chang EJ, Smith GP, Golden DM, Gardiner WC, Lissianski V (1994) GRI Mechanism v1.2. http://www.me.berkeley.edu/gri_mech/

Frenklach M, Wang H, Goldenberg M, Smith GP, Golden DM, Bowman CT, Hanson RK, Gardiner WC, Lissianski V (1995) GRI-Mech---An optimized detailed chemical reaction mechanism for methane combustion. Gas Research Insititute Topical Report No. GRI-95/0058.

Fujimoto S (1963) Chemical reaction in a shock wave I: The ignition delay of a hydrogen-oxygen mixture in a shock tube. Bull Chem Soc Japan, 36:1233-1236.

Gay ID, Glass GP, Kern RD, Kistiakowsky GB (1967) Ethylene-oxygen reaction in shock waves. J Chemical Physics 47:313-320.

Gaydon AG, Hurle IR (1963) The Shock Tube in High-Temperature Chemical Physics. Reinhold Publishing Corporation, New York.

Glass II, Sislian JP (1994) Nonstationary Flows and Shock Waves. Oxford University Press, New York, 137-177.

Glassman I (1996) Combustion, 3rd ed. Academic Press.

Gray JA, Westbrook CK (1994) High-temperature ignition of propane with MTBE as an additive: Shock tube experiments and modeling. J Chem Kinet, 26:757-770.

Gray JA (1998) Personal communication.

Hawthorn RD, Nixon AC (1966) Shock tube ignition delay studies of endothermic fuels. AIAA J, 4:513-520.

Hidaka Y, Kataoka T, Suga M (1974) A shock-tube investigation of ignition in ethylene-oxygen-argon mixtures. Bull Chemical Society Japan 47:2166-2170.

Hidaka Y, Nishimori T, Sato K, Henmi Y, Okuda R, Inami K (1999) Shock-tube and modeling study of ethylene pyrolysis and oxidation. Combustion and Flame, 117:755-776.

Homer JB, Kistiakowsky GB (1967) Oxidation and pyrolysis of ethylene in shock waves. J Chemical Physics 47:5290-5295

Jachimowski CJ, Houghton WM (1971) Shock-tube study of the initiation process in the hydrogen-oxygen reaction. Combustion and Flame, 17:25-30.

Jachimowksi CJ (1977) An experimental and analytical study of acetylene and ethylene oxidation behind shock waves. Combustion and Flame 29:55-66.

Just T, Schmalz F (1968) Measurements of ignition delays of hydrogen-air mixtures under simulated conditions of supersonic combustion chambers. AGARD CP No 34, Part 2, Paper 19.

Kee R, Rupley F, Miller J (1989) Chemkin II: A fortran chemical kinetics package for the analysis of gas-phase chemical kinetics. Sandia National Laboratory Technical Report SAND89-8009.

Konnov AA (1998) Detailed reaction mechanism for small hydrocarbons combustion. Release 0.4. http://homepages.vub.ac.be/~akonnov/

Lee JHS (1984) Dynamic parameters of gaseous detonations. Ann Rev Fluid Mechanics, 16:311-336.

Lefebvre MH, Oran ES, Kailasanath K, Van Tiggelen PJ (1993) Simulation of cellular structure in a detonation wave. AIAA Prog Astro Aero, 153:64-77.

Lutz AE, Kee RJ, Miller JA, Dwyer HA, Oppenheim AK (1988) Dynamic effects of autoignition centers for hydrogen and C1,2-hydrocarbon fuels. 22nd Symp (Int'l) on Combustion, 1683-1693.

Maas U, Warnatz J (1988) Ignition processes in hydrogen-oxygen mixtures. Combustion and Flame, 74:53-69.

Mark H (1958) NACA TM-1418.

Meyer JW, Oppenheim AK (1971) On the shock-induced ignition of explosive gases. 13th Symp (Int'l) on Combustion: 1153-1164.

Miller JA, Bowman CT (1989) Mechanism and modeling of nitrogen chemistry in combustion. Prog Energy Combustion Sci, 15:287-338.

Mirels H (1963) Test time in low-pressure shock tubes. Phys Fluids, 6(9):1201-1214.

Miyama H, Takeyama T (1964) Kinetics of hydrogen-oxygen reaction in shock waves. J Chem Phys, 41(8):2287-2290.

Myers BF, Bartle ER (1969) Reaction and ignition delay times in the oxidation of propane. AIAA J, 7:1862-1869.

Petersen EL, Davidson DF, Rohrig M, Hanson RK (1996) High-pressure shock-tube measurements of ignition times in stoichiometric H_2/O_2/Ar mixtures. 20th Intl Symp on Shock Waves, 941-946.

Petersen EL (1999) Personal communication.

Pilling MJ, Turanyi T, Hughes KJ, Clague AR (1996a) Leeds methane oxidation mechanism v1.3. http://chem.leeds.ac.uk/Combustion/Combustion.html

Pilling MJ, Turanyi T, Hughes KJ, Clague AR (1996b) Hydrogen combustion mechanism; subset of the Leeds methane oxidation mechanism v1.3. http://chem.leeds.ac.uk/Combustion/Combustion.html

Pilling MJ, Turanyi T, Hughes KJ, Clague AR (1998) Leeds methane oxidation mechanism v1.3 including nitrogen chemistry. http://chem.leeds.ac.uk/Combustion/Combustion.html

Roshko A (1960) On flow duration in low-pressure shock tubes. Phys Fluids, 3(6):835-842.

Reynolds WC (1986) The element potential method for chemical equilibrium analysis: implementation in the interactive program STANJAN (3rd ed.). Mechanical Engineering Department, Stanford University.

Schott GL, Kinsey JL (1958) Kinetic studies of hydroxyl radicals in shock waves II: Induction times in the hydrogen-oxygen reaction. J Chem Phys, 29:1177-1182.

Schott GL, Getzinger RW (1973) Shock tube studies of the hydrogen-oxygen reaction system. Physical Chemistry of Fast Reactions vol. 1, 2:81-160. Levitt BP (ed), Plenum Publishing.

Schott GL (1999) Personal communication.

Shampine LF, Watts HA (1979) DEPAC - Design of a user oriented package of ODE solvers. Sandia National Laboratory Technical Report SAND79-2374.

Shepherd JE (1986) Chemical kinetics of hydrogen-air-diluent detonations. Progress in Astronautics and Aeronautics, 106:263-293.

Skinner GB (1959) Limitations of the reflected shock technique for studying fast chemical reactions. J. Chem Phys, 31:268-269.

Skinner GB, Ringrose GH (1965) Ignition delays of a hydrogen-oxygen-argon mixture at relatively low temperature. J Chem Phys, 42:2190-2192.

Skinner GB (1998) Personal communication.

Snyder AD, Robertson J, Zanders DL, Skinner GB (1965) Shock tube studies of fuel-air ignition characteristics. Report AFAPL-TR-65-93.

Steinberg M, Kaskan WE (1955) The ignition of combustible mixtures by shock waves. 5th Symp (Int'l) on Combustion, 664-672.

Strehlow RA, Cohen A (1959) Limitations of the reflected shock technique for studying fast chemical reactions and its application to the observation of relaxation in nitrogen and oxygen. Journal of Chemical Physics, 30(1):257-265.

Strehlow RA, Cohen A (1962) Initiation of detonation. Phys Fluids, 5(1):97-101.

Strehlow RA (1984) Combustion Fundamentals. McGraw-Hill.

Sturtevant B, Okamura TT (1969) Dependence of shock-tube boundary layers on shock strength. Phys Fluids, 12(8):1723-1725.

Suzuki M, Moriwaki T, Okazaki S, Okuda T, Tanzawa T (1971) Oxidation of ethylene in shock tube. Astronautica Acta, 18:359-365.

Takai R, Yoneda K, Hikita T (1974) Study of detonation wave structure. 15th Symp (Int'l) on Combustion, 69-78.

Tan Y, Dagaut P, Cathonnet M, Boettner JC, Bachman JS, Carlier P (1994) Natural gas and blends oxidation and ignition: experiments and modeling. 25th Symp (Int'l) on Combustion, 1563-1569.

Tanzawa T (1998) Personal communication.

Tarver CM (1982) Chemical energy release in the cellular structure of gaseous detonation waves. Combustion and Flame, 46:135-156.

Thompson PA (1988) Compressible-Fluid Dynamics. McGraw-Hill, New York. pp. 347-358.

Voevodsky VV, Soloukhin RI (1965) On the mechanism and explosion limits of hydrogen-oxygen chain self-ignition in shock waves. 10th Symp (Int'l) on Combustion, 279-283.

Voitsekhovskii BV, Mitrofanov VV, Topchian ME (1963) Front structure of detonation in gases. Izv SO Akad Nauk SSSR, Novosibirsk.

Wang H, Frenklach M (1997) Detailed kinetic modeling study of aromatics formation in laminar premixed acetylene and ethylene flames. Combustion and Flame 110:173-221.

Wang S, Miller DL, Cernansky NP, Curran HJ, Pitz WJ, Westbrook CK (1999) A flow reactor study of neopentane oxidation at 8 atm: experiments and modeling. Combustion and Flame, undergoing editorial review process.

Warnatz J, Karbach V (1997) C2 mechanism for methane-air combustion. http://www.ca.sandia.gov/tdf/3rdWorkshop/ch4mech.html

Westbrook CK, Dryer FL, Schug KP (1982) A comprehensive mechanism for the pyrolysis and oxidation of ethylene. 19th Symp (Int'l) on Combustion, 153-166.

Westbrook CK, Pitz WJ (1984) A comprehensive chemical kinetic mechanism for oxidation and pyrolysis of propane and propene. Comb Sci Tech, 37:117-152.

Westbrook (1998, 1999) Personal communication.

White DR, Moore GE (1965) Structure of gaseous detonation IV: induction zone studies in H_2-O_2 and CO-O_2 mixtures. 10th Symp (Int'l) on Combustion, 785-795.

White DR (1967) Density induction times in very lean mixtures of D_2, H_2, C_2H_2, and C_2H_4, with O_2. 11th Symp (Int'l) on Combustion, 147-154.

Zaitsev SG, Soloukhin RI (1958) Combustion in an adiabatically heated gaseous mixture. Doklady Akad Nauk SSSR, 122, 1039:745-747.

Appendix A: Hydrogen Shock Tube Data

Source:Asaba (1965) **Technique: Incident**
Mixture: $H_2/O_2/Ar$ **Equivalence Ratio (ϕ): 0.085 - 1.5**
% Diluent: 96 - 99 **Pressure (P): 0.2 - 0.5 atm**
Temperature (T): 1400 - 2400 K
Induction Period (τ_{ind}) End: OH absorption & emission onset

Fuel (mol)	Oxygen (mol)	Diluent (mol)	ϕ	% Diluent	P (atm)	T (K)	τ_{ind} (μsec)
1	1	98	0.50	98	0.460	2554	29
1	1	98	0.50	98	0.433	2420	40
1	1	98	0.50	98	0.422	2364	73
1	1	98	0.50	98	0.407	2287	84
1	1	98	0.50	98	0.396	2231	90
1	1	98	0.50	98	0.363	2067	93
1	1	98	0.50	98	0.346	1981	70
1	1	98	0.50	98	0.308	1794	117
1	1	98	0.50	98	0.303	1770	136
1	1	98	0.50	98	0.297	1738	225
1	1	98	0.50	98	0.286	1681	250
1	1	98	0.50	98	0.280	1653	273
1	1	98	0.50	98	0.276	1633	230
1	1	98	0.50	98	0.272	1615	262
1	1	98	0.50	98	0.270	1602	287
0.17	1	98.83	0.09	98.83	0.365	2070	90
0.17	1	98.83	0.09	98.83	0.324	1868	205
0.17	1	98.83	0.09	98.83	0.319	1842	213
0.17	1	98.83	0.09	98.83	0.327	1879	285
0.17	1	98.83	0.09	98.83	0.326	1876	340
0.17	1	98.83	0.09	98.83	0.300	1744	315
0.17	1	98.83	0.09	98.83	0.286	1675	317
0.17	1	98.83	0.09	98.83	0.275	1620	442
0.17	1	98.83	0.09	98.83	0.267	1579	546
0.17	1	98.83	0.09	98.83	0.265	1569	495
0.29	1	98.71	0.15	98.71	0.390	2199	73
0.29	1	98.71	0.15	98.71	0.371	2101	88
0.29	1	98.71	0.15	98.71	0.321	1854	145

Fuel (mol)	Oxygen (mol)	Diluent (mol)	ϕ	% Diluent	P (atm)	T (K)	τ_{ind} (μsec)
0.29	1	98.71	0.15	98.71	0.313	1810	151
0.29	1	98.71	0.15	98.71	0.309	1790	187
0.29	1	98.71	0.15	98.71	0.295	1722	187
0.29	1	98.71	0.15	98.71	0.295	1720	205
0.29	1	98.71	0.15	98.71	0.285	1671	231
0.29	1	98.71	0.15	98.71	0.286	1678	260
0.29	1	98.71	0.15	98.71	0.271	1604	255
1	1	98	0.50	98	0.459	2546	25
1	1	98	0.50	98	0.435	2426	34
1	1	98	0.50	98	0.423	2367	61
1	1	98	0.50	98	0.406	2282	70
1	1	98	0.50	98	0.395	2228	73
1	1	98	0.50	98	0.363	2069	80
1	1	98	0.50	98	0.348	1993	62
1	1	98	0.50	98	0.347	1986	61
1	1	98	0.50	98	0.345	1980	62
1	1	98	0.50	98	0.310	1801	99
1	1	98	0.50	98	0.304	1775	118
1	1	98	0.50	98	0.299	1746	181
1	1	98	0.50	98	0.286	1684	212
1	1	98	0.50	98	0.280	1654	226
1	1	98	0.50	98	0.277	1637	199
1	1	98	0.50	98	0.273	1616	220
1	1	98	0.50	98	0.270	1604	234
2	1	97	1.00	97	0.301	1760	98
2	1	97	1.00	97	0.302	1767	104
2	1	97	1.00	97	0.298	1745	121
2	1	97	1.00	97	0.281	1659	147
2	1	97	1.00	97	0.271	1610	173
2	1	97	1.00	97	0.277	1642	221
2	1	97	1.00	97	0.269	1602	205
2	1	97	1.00	97	0.268	1597	243
2	1	97	1.00	97	0.258	1546	223
2	1	97	1.00	97	0.257	1541	236

Fuel (mol)	Oxygen (mol)	Diluent (mol)	ϕ	% Diluent	P (atm)	T (K)	τ_{ind} (μsec)
3	1	96	1.50	96	0.418	2352	22
3	1	96	1.50	96	0.432	2423	32
3	1	96	1.50	96	0.410	2313	39
3	1	96	1.50	96	0.371	2115	34
3	1	96	1.50	96	0.327	1896	73
3	1	96	1.50	96	0.295	1735	93
3	1	96	1.50	96	0.293	1726	136
3	1	96	1.50	96	0.277	1646	116
3	1	96	1.50	96	0.262	1574	226
3	1	96	1.50	96	0.243	1480	282
1	3	96	0.17	96	0.399	2258	19
1	3	96	0.17	96	0.403	2278	27
1	3	96	0.17	96	0.412	2320	30
1	3	96	0.17	96	0.362	2074	50
1	3	96	0.17	96	0.334	1929	34
1	3	96	0.17	96	0.315	1838	64
1	3	96	0.17	96	0.295	1736	74
1	3	96	0.17	96	0.297	1745	93
1	3	96	0.17	96	0.262	1572	112
1	3	96	0.17	96	0.269	1604	145
1	3	96	0.17	96	0.269	1605	164
1	3	96	0.17	96	0.233	1428	216
1	1	98	0.50	98	0.463	2566	19
1	1	98	0.50	98	0.443	2470	26
1	1	98	0.50	98	0.427	2387	28
1	1	98	0.50	98	0.410	2304	39
1	1	98	0.50	98	0.409	2299	44
1	1	98	0.50	98	0.383	2170	49
1	1	98	0.50	98	0.350	2005	93

Source: Belles (1965) **Technique: Incident**
Mixture: $H_2/O_2/N_2$ **Equivalence Ratio (ϕ):0.125 - 0.6**
% Diluent:63 - 75 **Pressure (P): 0.2 - 0.5 atm**
Temperature (T): 1100 - 1900 K
Induction Period (τ_{ind}) End: OH emission maximum

Fuel (mol)	Oxygen (mol)	Diluent (mol)	ϕ	% Diluent	P (atm)	T (K)	τ_{ind} (μsec)
5	19.96	75.04	0.13	75.04	0.446	1917	21
5	19.96	75.04	0.13	75.04	0.452	1937	24
5	19.96	75.04	0.13	75.04	0.441	1899	24
5	19.96	75.04	0.13	75.04	0.403	1774	25
5	19.96	75.04	0.13	75.04	0.369	1661	25
5	19.96	75.04	0.13	75.04	0.399	1762	28
5	19.96	75.04	0.13	75.04	0.363	1642	29
5	19.96	75.04	0.13	75.04	0.368	1658	30
5	19.96	75.04	0.13	75.04	0.368	1659	33
5	19.96	75.04	0.13	75.04	0.387	1722	34
5	19.96	75.04	0.13	75.04	0.394	1745	34
5	19.96	75.04	0.13	75.04	0.371	1667	39
5	19.96	75.04	0.13	75.04	0.359	1629	38
5	19.96	75.04	0.13	75.04	0.395	1746	43
5	19.96	75.04	0.13	75.04	0.298	1424	42
5	19.96	75.04	0.13	75.04	0.314	1479	48
5	19.96	75.04	0.13	75.04	0.331	1535	49
5	19.96	75.04	0.13	75.04	0.317	1488	51
5	19.96	75.04	0.13	75.04	0.298	1424	53
5	19.96	75.04	0.13	75.04	0.302	1436	54
5	19.96	75.04	0.13	75.04	0.292	1406	57
5	19.96	75.04	0.13	75.04	0.318	1489	59
5	19.96	75.04	0.13	75.04	0.339	1560	60
5	19.96	75.04	0.13	75.04	0.292	1404	57
5	19.96	75.04	0.13	75.04	0.303	1442	61
5	19.96	75.04	0.13	75.04	0.313	1476	64
5	19.96	75.04	0.13	75.04	0.289	1395	63
5	19.96	75.04	0.13	75.04	0.290	1396	68
5	19.96	75.04	0.13	75.04	0.298	1425	69
5	19.96	75.04	0.13	75.04	0.295	1415	73

Fuel (mol)	Oxygen (mol)	Diluent (mol)	ϕ	% Diluent	P (atm)	T (K)	τ_{ind} (μsec)
5	19.96	75.04	0.13	75.04	0.286	1386	73
5	19.96	75.04	0.13	75.04	0.274	1345	72
5	19.96	75.04	0.13	75.04	0.271	1335	72
5	19.96	75.04	0.13	75.04	0.286	1383	82
5	19.96	75.04	0.13	75.04	0.259	1295	90
5	19.96	75.04	0.13	75.04	0.244	1245	115
5	19.96	75.04	0.13	75.04	0.254	1278	115
5	19.96	75.04	0.13	75.04	0.262	1303	118
5	19.96	75.04	0.13	75.04	0.262	1304	128
5	19.96	75.04	0.13	75.04	0.255	1280	125
5	19.96	75.04	0.13	75.04	0.238	1224	183
5	19.96	75.04	0.13	75.04	0.211	1135	202
20	16.81	63.19	0.59	63.19	0.356	1582	28
20	16.81	63.19	0.59	63.19	0.348	1557	30
20	16.81	63.19	0.59	63.19	0.334	1509	31
20	16.81	63.19	0.59	63.19	0.334	1511	37
20	16.81	63.19	0.59	63.19	0.308	1424	35
20	16.81	63.19	0.59	63.19	0.297	1385	35
20	16.81	63.19	0.59	63.19	0.302	1402	36
20	16.81	63.19	0.59	63.19	0.305	1412	37
20	16.81	63.19	0.59	63.19	0.308	1424	38
20	16.81	63.19	0.59	63.19	0.320	1463	38
20	16.81	63.19	0.59	63.19	0.310	1429	43
20	16.81	63.19	0.59	63.19	0.312	1436	49
20	16.81	63.19	0.59	63.19	0.297	1387	47
20	16.81	63.19	0.59	63.19	0.290	1363	51
20	16.81	63.19	0.59	63.19	0.249	1227	49
20	16.81	63.19	0.59	63.19	0.252	1235	52
20	16.81	63.19	0.59	63.19	0.270	1296	66
20	16.81	63.19	0.59	63.19	0.272	1304	70
20	16.81	63.19	0.59	63.19	0.225	1148	78
20	16.81	63.19	0.59	63.19	0.239	1194	98
20	16.81	63.19	0.59	63.19	0.221	1134	107
20	16.81	63.19	0.59	63.19	0.229	1159	108

Fuel (mol)	Oxygen (mol)	Diluent (mol)	ϕ	% Diluent	P (atm)	T (K)	τ_{ind} (μsec)
20	16.81	63.19	0.59	63.19	0.238	1191	120
20	16.81	63.19	0.59	63.19	0.221	1134	134
20	16.81	63.19	0.59	63.19	0.231	1167	139
20	16.81	63.19	0.59	63.19	0.215	1114	184

Source: Bhaskaran (1973) **Technique: Reflected**
Mixture: $H_2/O_2/N_2$ **Equivalence Ratio (ϕ): 1.0**
% Diluent: 55.6 **Pressure (P): 2.5 atm**
Temperature (T): 800 - 1400 K
Induction Period (τ_{ind}) End: Pressure rise and luminosity onset

Fuel (mol)	Oxygen (mol)	Diluent (mol)	ϕ	% Diluent	P (atm)	T (K)	τ_{ind} (μsec)
2	1	3.76	1.00	55.62	2.5	1323	10
2	1	3.76	1.00	55.62	2.5	1289	12
2	1	3.76	1.00	55.62	2.5	1268	13
2	1	3.76	1.00	55.62	2.5	1258	12
2	1	3.76	1.00	55.62	2.5	1232	15
2	1	3.76	1.00	55.62	2.5	1200	18
2	1	3.76	1.00	55.62	2.5	1180	21
2	1	3.76	1.00	55.62	2.5	1171	22
2	1	3.76	1.00	55.62	2.5	1116	36
2	1	3.76	1.00	55.62	2.5	1098	45
2	1	3.76	1.00	55.62	2.5	1081	64
2	1	3.76	1.00	55.62	2.5	1077	58
2	1	3.76	1.00	55.62	2.5	1067	86
2	1	3.76	1.00	55.62	2.5	1038	192

Source: Cheng (1977) **Technique: Reflected**
Mixture: $H_2/O_2/Ar$ **Equivalence Ratio (ϕ): 0.5 - 1.0**
% Diluent: 90 **Pressure (P): 1 - 3 atm**
Temperature (T): 1000 - 1800 K
Induction Period (τ_{ind}) End: Pressure rise onset

Fuel (mol)	Oxygen (mol)	Diluent (mol)	ϕ	% Diluent	P (atm)	T (K)	τ_{ind} (μsec)
6.67	3.33	90	1.0	90	2.393	1281	52
6.67	3.33	90	1.0	90	2.896	1427	28
6.67	3.33	90	1.0	90	2.395	1277	62
6.67	3.33	90	1.0	90	2.159	1202	90
6.67	3.33	90	1.0	90	1.729	1051	233
6.67	3.33	90	1.0	90	2.007	1184	65
6.67	3.33	90	1.0	90	2.139	1228	72
6.67	3.33	90	1.0	90	2.078	1209	72
6.67	3.33	90	1.0	90	2.531	1364	25
6.67	3.33	90	1.0	90	1.723	1117	157
6.67	3.33	90	1.0	90	2.101	1257	60
6.67	3.33	90	1.0	90	1.59	1066	158
6.67	3.33	90	1.0	90	2.145	1271	62
6.67	3.33	90	1.0	90	1.807	1146	118
6.67	3.33	90	1.0	90	1.631	1117	145
6.67	3.33	90	1.0	90	1.701	1146	128
6.67	3.33	90	1.0	90	1.961	1242	75
6.67	3.33	90	1.0	90	2.162	1318	45
6.67	3.33	90	1.0	90	1.618	1152	115
6.67	3.33	90	1.0	90	1.864	1252	72
6.67	3.33	90	1.0	90	1.966	1293	57
6.67	3.33	90	1.0	90	1.92	1272	67
6.67	3.33	90	1.0	90	1.785	1264	75
6.67	3.33	90	1.0	90	1.435	1111	175
6.67	3.33	90	1.0	90	1.636	1199	90
6.67	3.33	90	1.0	90	1.596	1184	86
6.67	3.33	90	1.0	90	1.701	1227	62
6.67	3.33	90	1.0	90	1.834	1293	53
6.67	3.33	90	1.0	90	1.93	1325	53
6.67	3.33	90	1.0	90	1.527	1218	135

Fuel (mol)	Oxygen (mol)	Diluent (mol)	ϕ	% Diluent	P (atm)	T (K)	τ_{ind} (μsec)
6.67	3.33	90	1.0	90	1.689	1282	71
6.67	3.33	90	1.0	90	1.534	1206	110
6.67	3.33	90	1.0	90	1.647	1260	75
6.67	3.33	90	1.0	90	1.973	1405	38
6.67	3.33	90	1.0	90	1.439	1213	98
6.67	3.33	90	1.0	90	1.754	1368	43
6.67	3.33	90	1.0	90	1.491	1239	85
6.67	3.33	90	1.0	90	1.453	1277	79
6.67	3.33	90	1.0	90	1.585	1347	50
6.67	3.33	90	1.0	90	2.668	1318	42
6.67	3.33	90	1.0	90	2.347	1220	65
6.67	3.33	90	1.0	90	2.436	1247	57
6.67	3.33	90	1.0	90	2.263	1189	73
6.67	3.33	90	1.0	90	2.131	1146	93
6.67	3.33	90	1.0	90	1.982	1099	428
6.67	3.33	90	1.0	90	1.834	1025	282
6.67	3.33	90	1.0	90	2.227	1145	103
6.67	3.33	90	1.0	90	2.381	1190	73
6.67	3.33	90	1.0	90	2.482	1220	62
6.67	3.33	90	1.0	90	2.35	1181	70
6.67	3.33	90	1.0	90	2.391	1199	62
6.67	3.33	90	1.0	90	1.959	1098	170
6.67	3.33	90	1.0	90	1.892	1242	63
6.67	3.33	90	1.0	90	1.35	1012	375
6.67	3.33	90	1.0	90	2.008	1312	48
6.67	3.33	90	1.0	90	1.544	1125	189
6.67	3.33	90	1.0	90	1.746	1364	44
6.67	3.33	90	1.0	90	2.286	1702	15
5	5	90	0.5	90	2.039	1071	155
5	5	90	0.5	90	2.473	1198	61
5	5	90	0.5	90	2.506	1207	60
5	5	90	0.5	90	1.896	1026	200
5	5	90	0.5	90	1.957	1084	124
5	5	90	0.5	90	2.167	1148	73

Fuel (mol)	Oxygen (mol)	Diluent (mol)	ϕ	% Diluent	P (atm)	T (K)	τ_{ind} (μsec)
5	5	90	0.5	90	2.735	1317	32
5	5	90	0.5	90	2.84	1351	32
5	5	90	0.5	90	2.503	1308	33
5	5	90	0.5	90	2.057	1163	78
5	5	90	0.5	90	2.048	1161	88
5	5	90	0.5	90	2.41	1278	44
5	5	90	0.5	90	1.723	1051	190
5	5	90	0.5	90	1.87	1151	95
5	5	90	0.5	90	1.902	1162	72
5	5	90	0.5	90	2.238	1280	35
5	5	90	0.5	90	2.288	1364	30
5	5	90	0.5	90	1.951	1239	59
5	5	90	0.5	90	1.876	1210	67
5	5	90	0.5	90	1.901	1219	72
5	5	90	0.5	90	1.856	1202	76
5	5	90	0.5	90	1.504	1065	131
5	5	90	0.5	90	1.5	1121	139
5	5	90	0.5	90	1.469	1108	150
5	5	90	0.5	90	1.896	1285	43
5	5	90	0.5	90	1.674	1193	80
5	5	90	0.5	90	1.62	1243	58
5	5	90	0.5	90	1.856	1355	32
5	5	90	0.5	90	1.592	1230	72
5	5	90	0.5	90	2.206	1090	143
5	5	90	0.5	90	2.495	1165	64
5	5	90	0.5	90	2.421	1148	62
5	5	90	0.5	90	1.063	1253	43
5	5	90	0.5	90	2.02	1075	145
5	5	90	0.5	90	2.477	1210	59
5	5	90	0.5	90	2.197	1128	100
5	5	90	0.5	90	2.433	1252	38
5	5	90	0.5	90	2.318	1204	80
5	5	90	0.5	90	1.963	1093	127
5	5	90	0.5	90	2.199	1210	62

Fuel (mol)	Oxygen (mol)	Diluent (mol)	ϕ	% Diluent	P (atm)	T (K)	τ_{ind} (μsec)
5	5	90	0.5	90	1.96	1183	70
5	5	90	0.5	90	2.298	1301	42
5	5	90	0.5	90	1.467	1252	70
5	5	90	0.5	90	1.641	1336	60
5	5	90	0.5	90	1.568	1306	50
5	5	90	0.5	90	1.414	1210	90
5	5	90	0.5	90	1.574	1290	67
5	5	90	0.5	90	1.75	1397	36
5	5	90	0.5	90	1.58	1393	34
5	5	90	0.5	90	3.065	1755	18
5	5	90	0.5	90	1.877	1280	56
5	5	90	0.5	90	1.685	1198	62
5	5	90	0.5	90	2.022	1152	90
5	5	90	0.5	90	1.591	1004	335
5	5	90	0.5	90	1.849	1014	245
5	5	90	0.5	90	2.085	1052	180

Source: Cohen (1967) **Technique: Reflected**
Mixture: $H_2/O_2/Ar$ **Equivalence Ratio (ϕ): 1.0 - 2.0**
% Diluent: 0 - 94 **Pressure (P): 0.25 - 8.3 atm**
Temperature (T): 900 - 1650 K
Induction Period (τ_{ind}) End: UV emission and pressure maximum, UV absorption

Fuel (mol)	Oxygen (mol)	Diluent (mol)	ϕ	% Diluent	P (atm)	T (K)	τ_{ind} (μsec)
							emission & pressure max
20	10	70	1	70	0.528	1583	28
20	10	70	1	70	0.493	1510	33
20	10	70	1	70	0.454	1430	47
20	10	70	1	70	0.362	1242	116
20	10	70	1	70	0.340	1197	148
20	10	70	1	70	0.251	1015	706
20	10	70	1	70	0.928	1455	18
20	10	70	1	70	0.722	1243	52
20	10	70	1	70	0.683	1202	120
20	10	70	1	70	0.646	1165	109
20	10	70	1	70	0.627	1145	166
20	10	70	1	70	0.574	1091	149
20	10	70	1	70	0.548	1064	196
20	10	70	1	70	0.499	1014	531
20	10	70	1	70	0.438	951	524
20	10	70	1	70	1.444	1094	75
20	10	70	1	70	1.303	1036	106
20	10	70	1	70	1.229	1005	133
20	10	70	1	70	1.071	941	393
8	2	90	2	90	1.168	976	878
8	2	90	2	90	0.989	901	2122
8	2	90	2	90	2.984	1111	171
8	2	90	2	90	2.395	988	491
8	2	90	2	90	2.090	924	1228
8	2	90	2	90	2.257	959	1270
8	2	90	2	90	4.571	1125	102
8	2	90	2	90	3.822	1020	393
8	2	90	2	90	3.828	1021	726
8	2	90	2	90	3.477	972	721
8	2	90	2	90	3.765	1012	1373

Fuel (mol)	Oxygen (mol)	Diluent (mol)	ϕ	% Diluent	P (atm)	T (K)	τ_{ind} (μsec)
8	2	90	2	90	5.430	1032	153
8	2	90	2	90	5.313	1020	451
8	2	90	2	90	8.320	1084	139
8	2	90	2	90	7.405	1018	957
4	2	94	1	94	2.127	1622	28
4	2	94	1	94	2.115	1615	36
4	2	94	1	94	1.705	1400	59
4	2	94	1	94	1.423	1251	181
4	2	94	1	94	0.994	1025	901
50	25	25	1	25	0.666	998	118
67	33	0	1	0	0.795	983	216
67	33	0	1	0	0.764	965	137
67	33	0	1	0	1.855	1245	5
67	33	0	1	0	1.410	1069	90
67	33	0	1	0	1.692	912	193
							absorption
8	2	90	2	90	1.168	976	647
8	2	90	2	90	0.992	902	1922
8	2	90	2	90	3.005	1116	121
8	2	90	2	90	2.386	986	394
8	2	90	2	90	2.253	958	1159
8	2	90	2	90	5.207	1213	22
8	2	90	2	90	5.102	1199	17
8	2	90	2	90	4.904	1171	52
8	2	90	2	90	4.538	1120	94
8	2	90	2	90	3.797	1016	315
8	2	90	2	90	3.843	1023	814
8	2	90	2	90	3.489	973	616
8	2	90	2	90	3.250	940	540
8	2	90	2	90	5.337	1023	533
4	2	94	1	94	2.186	1653	6
4	2	94	1	94	1.944	1525	7
4	2	94	1	94	2.169	1644	10
4	2	94	1	94	1.764	1431	15
4	2	94	1	94	2.103	1609	17

Fuel (mol)	Oxygen (mol)	Diluent (mol)	ϕ	% Diluent	P (atm)	T (K)	τ_{ind} (μsec)
4	2	94	1	94	2.137	1627	20
4	2	94	1	94	2.090	1602	23
4	2	94	1	94	2.089	1601	26
4	2	94	1	94	1.801	1450	36
4	2	94	1	94	1.708	1401	45
4	2	94	1	94	1.422	1251	126
4	2	94	1	94	0.992	1024	671
4	2	94	1	94	0.903	977	1289
4	2	94	1	94	0.820	933	2679
20	10	70	1	70	0.572	1089	98
20	10	70	1	70	0.518	1033	203
20	10	70	1	70	1.357	966	184

Source: Craig (1966) **Technique: Reflected**
Mixture: $H_2/O_2/N_2$ **Equivalence Ratio (ϕ): 1.0**
% Diluent: 55.6 **Pressure (P): 1 - 2 atm**
Temperature (T): 875 - 1000 K
Induction Period (τ_{ind}) End: OH emission onset

Fuel (mol)	Oxygen (mol)	Diluent (mol)	ϕ	% Diluent	P (atm)	T (K)	τ_{ind} (μsec)
2	1	3.76	1	55.62	1.02	875	3250
2	1	3.76	1	55.62	1.02	919	300
2	1	3.76	1	55.62	1.02	919	300
2	1	3.76	1	55.62	1.02	878	595
2	1	3.76	1	55.62	1.02	916	510
2	1	3.76	1	55.62	1.02	939	410
2	1	3.76	1	55.62	1.02	934	410
2	1	3.76	1	55.62	1.02	950	225
2	1	3.76	1	55.62	1.02	958	270
2	1	3.76	1	55.62	1.02	950	250
2	1	3.76	1	55.62	1.02	982	110
2	1	3.76	1	55.62	1.02	947	355
2	1	3.76	1	55.62	1.02	964	205
2	1	3.76	1	55.62	1.02	889	700
2	1	3.76	1	55.62	1.02	879	1850
2	1	3.76	1	55.62	1.02	884	1600
2	1	3.76	1	55.62	1.02	986	120
2	1	3.76	1	55.62	1.02	875	2400
2	1	3.76	1	55.62	1.02	906	480
2	1	3.76	1	55.62	1.02	878	1250
2	1	3.76	1	55.62	1.02	887	1500
2	1	3.76	1	55.62	1.02	886	1350
2	1	3.76	1	55.62	2.04	932	800
2	1	3.76	1	55.62	2.04	932	900
2	1	3.76	1	55.62	2.04	946	850
2	1	3.76	1	55.62	2.04	947	750
2	1	3.76	1	55.62	2.04	998	80
2	1	3.76	1	55.62	2.04	977	78
2	1	3.76	1	55.62	2.04	964	105
2	1	3.76	1	55.62	2.04	958	215

Fuel (mol)	Oxygen (mol)	Diluent (mol)	ϕ	% Diluent	P (atm)	T (K)	τ_{ind} (μsec)
2	1	3.76	1	55.62	2.04	967	140
2	1	3.76	1	55.62	2.04	938	180
2	1	3.76	1	55.62	2.04	944	245
2	1	3.76	1	55.62	2.04	956	160
2	1	3.76	1	55.62	2.04	933	520
2	1	3.76	1	55.62	2.04	940	400
2	1	3.76	1	55.62	2.04	919	2050
2	1	3.76	1	55.62	2.04	914	450
2	1	3.76	1	55.62	2.04	919	440
2	1	3.76	1	55.62	2.04	925	250
2	1	3.76	1	55.62	2.04	925	200
2	1	3.76	1	55.62	2.04	911	3400
2	1	3.76	1	55.62	2.04	918	1650
2	1	3.76	1	55.62	2.04	908	2250

Source: Fujimoto (1963) **Technique: Reflected**
Mixture: $H_2/O_2/Ar$ **Equivalence Ratio (ϕ): 1.0**
% Diluent: 70 **Pressure (P): 0.88 - 2.7 atm**
Temperature (T): 800 - 1400 K
Induction Period (τ_{ind}) End: Pressure rise and luminosity onset

Fuel (mol)	Oxygen (mol)	Diluent (mol)	ϕ	% Diluent	P (atm)	T (K)	τ_{ind} (μsec)
20	10	70	1.00	70	1.589	825	2227
20	10	70	1.00	70	0.886	870	2019
20	10	70	1.00	70	0.924	891	1525
20	10	70	1.00	70	0.966	909	1302
20	10	70	1.00	70	0.987	918	1059
20	10	70	1.00	70	1.038	945	1014
20	10	70	1.00	70	1.114	987	888
20	10	70	1.00	70	1.257	1053	543
20	10	70	1.00	70	1.413	1131	177
20	10	70	1.00	70	1.609	1215	156
20	10	70	1.00	70	1.666	1242	130
20	10	70	1.00	70	1.692	1254	143
20	10	70	1.00	70	1.733	1269	115
20	10	70	1.00	70	1.807	1308	109
20	10	70	1.00	70	1.853	1323	117
20	10	70	1.00	70	1.945	1362	84
20	10	70	1.00	70	1.863	894	1220
20	10	70	1.00	70	1.988	924	1142
20	10	70	1.00	70	2.059	942	1164
20	10	70	1.00	70	2.075	948	1120
20	10	70	1.00	70	2.129	960	1020
20	10	70	1.00	70	2.200	978	958
20	10	70	1.00	70	2.218	984	630
20	10	70	1.00	70	2.276	996	624
20	10	70	1.00	70	2.322	1008	160
20	10	70	1.00	70	2.336	1010	158
20	10	70	1.00	70	2.368	1017	190
20	10	70	1.00	70	2.392	1026	179
20	10	70	1.00	70	2.414	1029	160
20	10	70	1.00	70	2.507	1050	120

Fuel (mol)	Oxygen (mol)	Diluent (mol)	ϕ	% Diluent	P (atm)	T (K)	τ_{ind} (μsec)
20	10	70	1.00	70	2.564	1065	154
20	10	70	1.00	70	2.599	1071	126
20	10	70	1.00	70	2.608	1074	120
20	10	70	1.00	70	2.658	1086	138

Source: Jachimowski (1971) **Technique:Incident**
Mixture: $H_2/O_2/Ar$ **Equivalence Ratio (ϕ):0.063 - 2.0**
% Diluent: 91 - 95 **Pressure (P): 0.2 - 0.75 atm**
Temperature (T): 1200 - 1800 K
Induction Period (τ_{ind}) End: OH absorption at 5% of maximum

Fuel (mol)	Oxygen (mol)	Diluent (mol)	ϕ	% Diluent	P (atm)	T (K)	τ_{ind} (μsec)
4	1	95	2.00	95	0.566	1840	66
4	1	95	2.00	95	0.295	1900	120
4	1	95	2.00	95	0.293	1890	120
4	1	95	2.00	95	0.295	1900	102
4	1	95	2.00	95	0.281	1830	168
4	1	95	2.00	95	0.251	1665	268
4	1	95	2.00	95	0.248	1649	271
4	1	95	2.00	95	0.432	1469	241
4	1	95	2.00	95	0.428	1460	280
4	1	95	2.00	95	0.438	1490	251
4	1	95	2.00	95	0.716	1268	326
4	1	95	2.00	95	0.727	1310	293
4	1	95	2.00	95	0.714	1265	382
4	1	95	2.00	95	0.652	1180	621
4	1	95	2.00	95	0.628	1170	556
4	1	95	2.00	95	0.655	1185	597
4	1	95	2.00	95	0.623	1140	665
4	1	95	2.00	95	0.568	1149	705
4	1	95	2.00	95	0.625	1140	761
3	3	94	0.50	94	0.260	1705	73
3	3	94	0.50	94	0.260	1705	80
3	3	94	0.50	94	0.271	1775	77
3	3	94	0.50	94	0.275	1780	49
3	3	94	0.50	94	0.276	1790	60
3	3	94	0.50	94	0.235	1564	113
3	3	94	0.50	94	0.211	1431	212
3	3	94	0.50	94	0.211	1431	229
3	3	94	0.50	94	0.370	1289	229
3	3	94	0.50	94	0.373	1300	213
3	3	94	0.50	94	0.378	1311	217

Fuel (mol)	Oxygen (mol)	Diluent (mol)	ϕ	% Diluent	P (atm)	T (K)	τ_{ind} (μsec)
3	3	94	0.50	94	0.339	1204	337
3	3	94	0.50	94	0.344	1219	338
3	3	94	0.50	94	0.482	1155	349
3	3	94	0.50	94	0.616	1118	295
3	3	94	0.50	94	0.616	1118	343
3	3	94	0.50	94	0.621	1124	315
1	4	95	0.13	95	0.278	1802	112
1	4	95	0.13	95	0.261	1709	112
1	4	95	0.13	95	0.513	1690	86
1	4	95	0.13	95	0.500	1655	93
1	4	95	0.13	95	0.500	1655	86
1	4	95	0.13	95	0.457	1537	143
1	4	95	0.13	95	0.434	1475	168
1	4	95	0.13	95	0.210	1430	334
1	4	95	0.13	95	0.413	1415	190
1	4	95	0.13	95	0.371	1300	303
1	4	95	0.13	95	0.369	1292	308
1	4	95	0.13	95	0.658	1185	301
1	4	95	0.13	95	0.644	1165	356
1	4	95	0.13	95	0.644	1165	331
1	4	95	0.13	95	0.346	1228	405
1	4	95	0.13	95	0.350	1241	390
1	8	91	0.06	91	0.719	1230	168
1	8	91	0.06	91	0.751	1275	106
1	8	91	0.06	91	0.745	1265	133
1	8	91	0.06	91	0.739	1260	146
1	8	91	0.06	91	0.765	1295	131
1	8	91	0.06	91	0.427	1415	130
1	8	91	0.06	91	0.428	1415	151
1	8	91	0.06	91	0.424	1405	130
1	8	91	0.06	91	0.229	1495	170
1	8	91	0.06	91	0.232	1515	167
1	8	91	0.06	91	0.378	1610	96
1	8	91	0.06	91	0.267	1685	98

Fuel (mol)	Oxygen (mol)	Diluent (mol)	ϕ	% Diluent	P (atm)	T (K)	τ_{ind} (μsec)
1	8	91	0.06	91	0.269	1700	102
1	8	91	0.06	91	0.248	1590	116

Source: Just (1968) **Technique: Reflected**
Mixture: $H_2/O_2/N_2$ **Equivalence Ratio (ϕ): 0.1 - 1.0**
% Diluent: 55 - 76 **Pressure (P): 0.4 - 1.4 atm**
Temperature (T): 900 - 1250 K
Induction Period (τ_{ind}) End: Onset of light emission

Fuel (mol)	Oxygen (mol)	Diluent (mol)	ϕ	% Diluent	P (atm)	T (K)	τ_{ind} (μsec)
2	1	3.76	1	55.62	0.43	1208	30
2	1	3.76	1	55.62	0.43	1184	32
2	1	3.76	1	55.62	0.43	1087	83
2	1	3.76	1	55.62	0.43	1083	69
2	1	3.76	1	55.62	0.43	1059	102
2	1	3.76	1	55.62	0.43	1036	135
2	1	3.76	1	55.62	0.43	1003	267
2	1	3.76	1	55.62	0.43	953	1456
2	1	3.76	1	55.62	0.43	962	1832
2	1	3.76	1	55.62	1.41	1233	77
2	1	3.76	1	55.62	1.41	1201	65
2	1	3.76	1	55.62	1.41	1172	110
2	1	3.76	1	55.62	1.41	1062	210
2	1	3.76	1	55.62	1.41	1060	193
2	1	3.76	1	55.62	1.41	1043	237
2	1	3.76	1	55.62	1.41	993	336
2	1	3.76	1	55.62	1.41	996	386
2	1	3.76	1	55.62	1.41	938	655
2	1	3.76	1	55.62	1.41	929	649
2	1	3.76	1	55.62	1.41	903	878
2	1	3.76	1	55.62	1.41	900	1476
2	1	3.76	1	55.62	1.41	904	1544
2	1	3.76	1	55.62	1.41	895	2065
4	20.17	75.83	0.099	75.83	0.45	1214	96
4	20.17	75.83	0.099	75.83	0.45	1173	117
4	20.17	75.83	0.099	75.83	0.45	1145	137
4	20.17	75.83	0.099	75.83	0.45	1072	206
4	20.17	75.83	0.099	75.83	0.45	1060	245
4	20.17	75.83	0.099	75.83	0.45	1047	245
4	20.17	75.83	0.099	75.83	0.45	1017	347

Fuel (mol)	Oxygen (mol)	Diluent (mol)	ϕ	% Diluent	P (atm)	T (K)	τ_{ind} (μsec)
4	20.17	75.83	0.099	75.83	0.45	1001	388
4	20.17	75.83	0.099	75.83	0.45	984	483
4	20.17	75.83	0.099	75.83	0.45	949	815
4	20.17	75.83	0.099	75.83	0.45	924	1055
4	20.17	75.83	0.099	75.83	0.45	920	1348
4	20.17	75.83	0.099	75.83	0.45	900	2623

Source: Petersen (1996) **Technique: Reflected**
Mixture: $H_2/O_2/Ar$ **Equivalence Ratio (ϕ):1.0**
% Diluent: 97 - 99.85 **Pressure (P): 33 - 87 atm**
Temperature (T): 1100 - 1900 K
Induction Period (τ_{ind}) End: OH absorption max rate of change

Fuel (mol)	Oxygen (mol)	Diluent (mol)	ϕ	% Diluent	P (atm)	T (K)	τ_{ind} (μsec)
0.5	0.25	99.25	1	99.25	33	1802	9
0.5	0.25	99.25	1	99.25	33	1754	10
0.5	0.25	99.25	1	99.25	33	1730	11
0.5	0.25	99.25	1	99.25	33	1736	11
0.5	0.25	99.25	1	99.25	33	1709	9
0.5	0.25	99.25	1	99.25	33	1724	11
0.5	0.25	99.25	1	99.25	33	1773	10
0.5	0.25	99.25	1	99.25	33	1739	11
0.5	0.25	99.25	1	99.25	33	1715	11
0.5	0.25	99.25	1	99.25	33	1764	10
0.5	0.25	99.25	1	99.25	33	1792	9
0.5	0.25	99.25	1	99.25	33	1684	12
0.5	0.25	99.25	1	99.25	33	1709	12
0.5	0.25	99.25	1	99.25	33	1855	9
2	1	97	1	97	33	1264	29
2	1	97	1	97	33	1206	203
2	1	97	1	97	33	1189	393
2	1	97	1	97	33	1206	89
2	1	97	1	97	33	1221	133
2	1	97	1	97	33	1252	57
2	1	97	1	97	33	1289	13
2	1	97	1	97	33	1300	13
0.5	0.25	99.25	1	99.25	57	1748	7
0.5	0.25	99.25	1	99.25	57	1655	12
0.5	0.25	99.25	1	99.25	57	1678	7
0.5	0.25	99.25	1	99.25	57	1672	7
0.5	0.25	99.25	1	99.25	57	1683	13
0.5	0.25	99.25	1	99.25	57	1681	7
0.5	0.25	99.25	1	99.25	57	1714	6
0.5	0.25	99.25	1	99.25	57	1779	8

Fuel (mol)	Oxygen (mol)	Diluent (mol)	ϕ	% Diluent	P (atm)	T (K)	τ_{ind} (μsec)
0.5	0.25	99.25	1	99.25	57	1757	5
0.5	0.25	99.25	1	99.25	57	1684	6
0.5	0.25	99.25	1	99.25	57	1669	11
0.5	0.25	99.25	1	99.25	57	1685	6
0.5	0.25	99.25	1	99.25	57	1710	10
0.5	0.25	99.25	1	99.25	57	1700	6
0.5	0.25	99.25	1	99.25	57	1733	6
0.5	0.25	99.25	1	99.25	57	1713	6
0.5	0.25	99.25	1	99.25	57	1930	4
0.33	0.167	99.5	1	99.5	64	1684	12
0.33	0.167	99.5	1	99.5	64	1715	10
0.33	0.167	99.5	1	99.5	64	1779	8
0.33	0.167	99.5	1	99.5	64	1709	10
0.33	0.167	99.5	1	99.5	64	1701	9
0.33	0.167	99.5	1	99.5	64	1733	9
0.33	0.167	99.5	1	99.5	64	1712	9
0.1	0.05	99.85	1	99.85	64	1577	35
0.1	0.05	99.85	1	99.85	64	1481	53
0.1	0.05	99.85	1	99.85	64	1577	31
0.1	0.05	99.85	1	99.85	64	1616	29
0.1	0.05	99.85	1	99.85	64	1585	38
0.1	0.05	99.85	1	99.85	64	1577	42
0.1	0.05	99.85	1	99.85	64	1585	40
0.1	0.05	99.85	1	99.85	64	1575	49
0.1	0.05	99.85	1	99.85	64	1555	49
0.1	0.05	99.85	1	99.85	64	1560	47
0.1	0.05	99.85	1	99.85	64	1553	39
0.1	0.05	99.85	1	99.85	64	1524	49
0.1	0.05	99.85	1	99.85	64	1876	21
0.1	0.05	99.85	1	99.85	64	1366	202
0.1	0.05	99.85	1	99.85	64	1462	94
0.1	0.05	99.85	1	99.85	64	1361	145
0.5	0.25	99.25	1	99.25	64	1279	265
0.5	0.25	99.25	1	99.25	64	1314	152

Fuel (mol)	Oxygen (mol)	Diluent (mol)	ϕ	% Diluent	P (atm)	T (K)	τ_{ind} (μsec)
0.5	0.25	99.25	1	99.25	64	1344	69
0.5	0.25	99.25	1	99.25	87	1715	6
0.5	0.25	99.25	1	99.25	87	1704	6
0.5	0.25	99.25	1	99.25	87	1701	5
0.5	0.25	99.25	1	99.25	87	1706	6
0.5	0.25	99.25	1	99.25	87	1712	6
0.5	0.25	99.25	1	99.25	87	1715	6

Source: Schott (1958) **Technique: Incident & Reflected**
Mixture: $H_2/O_2/Ar$ **Equivalence Ratio (ϕ): 1.25 - 90**
% Diluent: 75.33 - 98.88 **Pressure (P): 0.15 - 9.53 atm**
Temperature (T): 1050 - 2650 K
Induction Period (τ_{ind}) End: OH absorption onset

Fuel (mol)	Oxygen (mol)	Diluent (mol)	ϕ	% Diluent	P (atm)	T (K)	τ_{ind} (μsec)
0.688	0.43	98.88	0.8	98.88	1.031	1437	246
0.688	0.43	98.88	0.8	98.88	0.996	1400	249
0.688	0.43	98.88	0.8	98.88	0.985	1388	292
0.688	0.43	98.88	0.8	98.88	1.076	1488	175
0.688	0.43	98.88	0.8	98.88	1.147	1570	153
0.688	0.43	98.88	0.8	98.88	1.062	1772	68
0.688	0.43	98.88	0.8	98.88	0.921	2010	52
0.688	0.43	98.88	0.8	98.88	0.936	2035	73
0.688	0.43	98.88	0.8	98.88	0.798	2528	48
0.688	0.43	98.88	0.8	98.88	1.225	1655	118
0.688	0.43	98.88	0.8	98.88	0.838	1854	98
0.688	0.43	98.88	0.8	98.88	0.859	1892	90
0.688	0.43	98.88	0.8	98.88	0.735	1660	191
0.98	0.49	98.53	1	98.53	1.023	1437	195
0.98	0.49	98.53	1	98.53	1.138	1570	148
0.98	0.49	98.53	1	98.53	1.195	1637	112
0.98	0.49	98.53	1	98.53	1.220	1663	114
0.98	0.49	98.53	1	98.53	1.315	1772	58
0.98	0.49	98.53	1	98.53	0.799	1411	308
0.98	0.49	98.53	1	98.53	0.975	1663	165
0.98	0.49	98.53	1	98.53	0.992	1687	142
0.98	0.49	98.53	1	98.53	1.101	1842	109
0.98	0.49	98.53	1	98.53	1.167	1936	78
0.98	0.49	98.53	1	98.53	0.885	1536	244
0.98	0.49	98.53	1	98.53	1.225	2015	65
0.98	0.49	98.53	1	98.53	0.947	2071	93
0.98	0.49	98.53	1	98.53	0.875	1936	97
0.98	0.49	98.53	1	98.53	0.716	1633	209
0.98	0.49	98.53	1	98.53	0.607	1428	410
0.98	0.49	98.53	1	98.53	0.627	1428	400

Fuel (mol)	Oxygen (mol)	Diluent (mol)	ϕ	% Diluent	P (atm)	T (K)	τ_{ind} (μsec)
0.98	0.49	98.53	1	98.53	0.652	1510	296
0.98	0.49	98.53	1	98.53	0.782	1705	206
0.98	0.49	98.53	1	98.53	1.073	2288	61
0.98	0.49	98.53	1	98.53	1.745	1683	87
0.98	0.49	98.53	1	98.53	1.452	1652	102
0.98	0.49	98.53	1	98.53	0.356	1624	356
0.98	0.49	98.53	1	98.53	0.367	1646	427
0.98	0.49	98.53	1	98.53	1.507	1714	82
3.781	1.99	94.23	0.95	94.23	1.102	2285	21
3.781	1.99	94.23	0.95	94.23	0.986	2080	28
3.781	1.99	94.23	0.95	94.23	0.868	1864	37
3.781	1.99	94.23	0.95	94.23	0.734	1618	63
3.781	1.99	94.23	0.95	94.23	0.763	1668	55
3.781	1.99	94.23	0.95	94.23	0.633	1435	98
3.781	1.99	94.23	0.95	94.23	0.732	1613	58
3.781	1.99	94.23	0.95	94.23	0.668	1500	84
3.781	1.99	94.23	0.95	94.23	0.604	1383	135
3.781	1.99	94.23	0.95	94.23	0.548	1283	234
3.781	1.99	94.23	0.95	94.23	1.457	1869	23
3.781	1.99	94.23	0.95	94.23	1.272	1668	34
3.781	1.99	94.23	0.95	94.23	1.159	1545	50
3.781	1.99	94.23	0.95	94.23	1.032	1414	78
3.781	1.99	94.23	0.95	94.23	0.976	1353	146
3.781	1.99	94.23	0.95	94.23	0.903	1266	168
3.781	1.99	94.23	0.95	94.23	1.545	1695	24
3.781	1.99	94.23	0.95	94.23	1.502	1641	32
3.781	1.99	94.23	0.95	94.23	1.268	1437	51
3.781	1.99	94.23	0.95	94.23	1.133	1309	102
3.781	1.99	94.23	0.95	94.23	0.986	1367	77
3.781	1.99	94.23	0.95	94.23	0.780	1342	150
3.781	1.99	94.23	0.95	94.23	0.967	1606	48
3.781	1.99	94.23	0.95	94.23	0.509	1665	73
3.781	1.99	94.23	0.95	94.23	0.477	1593	84
3.781	1.99	94.23	0.95	94.23	0.414	1414	174

Fuel (mol)	Oxygen (mol)	Diluent (mol)	ϕ	% Diluent	P (atm)	T (K)	τ_{ind} (μsec)
3.781	1.99	94.23	0.95	94.23	0.346	1407	209
2.475	0.45	97.08	2.75	97.08	0.713	1615	213
2.475	0.45	97.08	2.75	97.08	1.489	1684	94
2.475	0.45	97.08	2.75	97.08	1.509	1696	78
2.475	0.45	97.08	2.75	97.08	0.917	2004	89
2.475	0.45	97.08	2.75	97.08	0.906	1979	79
2.475	0.45	97.08	2.75	97.08	1.055	2260	59
2.475	0.45	97.08	2.75	97.08	1.097	2331	42
2.475	0.45	97.08	2.75	97.08	0.958	2444	38
2.475	0.45	97.08	2.75	97.08	0.991	2527	44
2.475	0.45	97.08	2.75	97.08	1.952	1378	158
2.475	0.45	97.08	2.75	97.08	1.383	1836	70
2.475	0.45	97.08	2.75	97.08	1.349	1800	72
1	2	97.00	0.25	97.00	0.750	1670	77
1	2	97.00	0.25	97.00	0.736	1646	78
1	2	97.00	0.25	97.00	0.928	1308	194
1	2	97.00	0.25	97.00	1.846	1304	85
1	2	97.00	0.25	97.00	1.838	1302	74
1	2	97.00	0.25	97.00	1.857	1312	94
1	2	97.00	0.25	97.00	0.913	1291	187
1	2	97.00	0.25	97.00	1.747	1086	360
1	2	97.00	0.25	97.00	1.769	1097	331
1	2	97.00	0.25	97.00	1.454	1626	45
1	2	97.00	0.25	97.00	1.445	1616	38
1	2	97.00	0.25	97.00	1.297	1180	261
1	2	97.00	0.25	97.00	1.259	1154	263
1	2	97.00	0.25	97.00	0.841	1836	43
1	2	97.00	0.25	97.00	0.834	1826	48
1	2	97.00	0.25	97.00	1.989	1200	150
1	2	97.00	0.25	97.00	0.876	1175	355
0.98	0.49	98.53	1	98.53	4.662	1740	21
0.98	0.49	98.53	1	98.53	4.716	1760	23
0.98	0.49	98.53	1	98.53	4.619	1735	23
0.98	0.49	98.53	1	98.53	9.431	1760	12

Fuel (mol)	Oxygen (mol)	Diluent (mol)	ϕ	% Diluent	P (atm)	T (K)	τ_{ind} (μsec)
0.98	0.49	98.53	1	98.53	9.528	1767	9
0.98	0.49	98.53	1	98.53	8.330	2303	5
0.98	0.49	98.53	1	98.53	8.319	2300	5
0.98	0.49	98.53	1	98.53	3.926	2212	12
0.98	0.49	98.53	1	98.53	3.981	2222	12
0.98	0.49	98.53	1	98.53	4.021	2560	6
0.98	0.49	98.53	1	98.53	4.195	2640	5
0.98	0.49	98.53	1	98.53	2.031	2586	15
0.98	0.49	98.53	1	98.53	2.014	2565	14
4.925	19.7	75.38	0.125	75.38	0.216	1742	39
4.925	19.7	75.38	0.125	75.38	0.589	1702	17
4.925	19.7	75.38	0.125	75.38	0.543	1588	22
4.925	19.7	75.38	0.125	75.38	0.315	1791	26
4.925	19.7	75.38	0.125	75.38	0.229	1847	38
4.925	19.7	75.38	0.125	75.38	0.210	1724	45
4.925	19.7	75.38	0.125	75.38	0.150	1720	64
1	4	95.00	0.125	95.00	1.291	1715	29
1	4	95.00	0.125	95.00	1.396	1834	18
1	4	95.00	0.125	95.00	1.346	1778	21
19.8	1.1	79.10	9	79.10	0.995	1933	62
19.8	1.1	79.10	9	79.10	1.329	1620	113
19.8	1.1	79.10	9	79.10	1.437	1735	64
19.8	1.1	79.10	9	79.10	1.452	1738	76
19.8	1.1	79.10	9	79.10	1.476	1767	67
19.8	1.1	79.10	9	79.10	1.042	2010	45
19.8	1.1	79.10	9	79.10	1.119	2137	36
19.8	1.1	79.10	9	79.10	1.496	1791	53

Source: Skinner (1966) **Technique:Reflected**
Mixture: $H_2/O_2/Ar$ **Equivalence Ratio (ϕ): 2.0**
% Diluent: 90 **Pressure (P): 5 atm**
Temperature (T): 900 - 1100 K
Induction Period (τ_{ind}) End: OH emission maximum

Fuel (mol)	Oxygen (mol)	Diluent (mol)	ϕ	% Diluent	P (atm)	T (K)	τ_{ind} (μsec)
8	2	90	2	90	5	964	15000
8	2	90	2	90	5	965	10000
8	2	90	2	90	5	981	4300
8	2	90	2	90	5	1004	1700
8	2	90	2	90	5	1005	2300
8	2	90	2	90	5	1024	900
8	2	90	2	90	5	1075	220

Source: Snyder (1965) **Technique:Reflected**
Mixture: $H_2/O_2/N_2$ **Equivalence Ratio (ϕ): 0.5 - 1.0**
% Diluent: 55.6 - 65.3 **Pressure (P): 1 - 9 atm**
Temperature (T): 800 - 1100 K
Induction Period (τ_{ind}) End: Pressure and UV emission onset

Fuel (mol)	Oxygen (mol)	Diluent (mol)	ϕ	% Diluent	P (atm)	T (K)	τ_{ind} (μsec)
1	1	3.76	0.50	65.28	1.020	951	550
1	1	3.76	0.50	65.28	1.020	943	600
1	1	3.76	0.50	65.28	1.020	922	2200
1	1	3.76	0.50	65.28	1.020	914	2900
1	1	3.76	0.50	65.28	1.020	912	1900
1	1	3.76	0.50	65.28	1.020	911	5800
1	1	3.76	0.50	65.28	1.020	899	8200
1	1	3.76	0.50	65.28	1.020	889	8600
1	1	3.76	0.50	65.28	2.041	1047	100
1	1	3.76	0.50	65.28	2.041	1032	140
1	1	3.76	0.50	65.28	2.041	1025	200
1	1	3.76	0.50	65.28	2.041	1014	400
1	1	3.76	0.50	65.28	2.041	991	850
1	1	3.76	0.50	65.28	2.041	989	880
1	1	3.76	0.50	65.28	2.041	983	1100
1	1	3.76	0.50	65.28	2.041	977	1300
1	1	3.76	0.50	65.28	2.041	955	4600
1	1	3.76	0.50	65.28	2.041	944	5700
1	1	3.76	0.50	65.28	2.041	922	11600
1	1	3.76	0.50	65.28	4.082	1033	240
1	1	3.76	0.50	65.28	4.082	999	520
1	1	3.76	0.50	65.28	4.082	999	760
1	1	3.76	0.50	65.28	4.082	986	6800
1	1	3.76	0.50	65.28	4.082	972	1800
1	1	3.76	0.50	65.28	4.082	967	1900
1	1	3.76	0.50	65.28	4.082	966	2900
1	1	3.76	0.50	65.28	4.082	963	1900
1	1	3.76	0.50	65.28	4.082	952	7600
1	1	3.76	0.50	65.28	4.082	950	4400
1	1	3.76	0.50	65.28	4.082	938	7000

Fuel (mol)	Oxygen (mol)	Diluent (mol)	ϕ	% Diluent	P (atm)	T (K)	τ_{ind} (μsec)
1	1	3.76	0.50	65.28	4.082	919	5600
1	1	3.76	0.50	65.28	6.803	1073	260
1	1	3.76	0.50	65.28	6.803	1051	520
1	1	3.76	0.50	65.28	6.803	1023	800
1	1	3.76	0.50	65.28	6.803	995	1300
1	1	3.76	0.50	65.28	6.803	971	1850
1	1	3.76	0.50	65.28	6.803	872	8400
1	1	3.76	0.50	65.28	6.803	871	8200
1	1	3.76	0.50	65.28	6.803	858	11400
1	1	3.76	0.50	65.28	8.844	963	260
1	1	3.76	0.50	65.28	8.844	949	600
1	1	3.76	0.50	65.28	8.844	941	960
1	1	3.76	0.50	65.28	8.844	918	1200
1	1	3.76	0.50	65.28	8.844	917	600
1	1	3.76	0.50	65.28	8.844	910	900
1	1	3.76	0.50	65.28	8.844	902	1800
1	1	3.76	0.50	65.28	8.844	898	1400
1	1	3.76	0.50	65.28	8.844	859	2400
1	1	3.76	0.50	65.28	8.844	858	5800
1	1	3.76	0.50	65.28	8.844	857	2200
1	1	3.76	0.50	65.28	8.844	837	10600
1	1	3.76	0.50	65.28	8.844	831	7600
1.5	1	3.76	0.75	60.06	1.020	969	660
1.5	1	3.76	0.75	60.06	1.020	961	420
1.5	1	3.76	0.75	60.06	1.020	959	700
1.5	1	3.76	0.75	60.06	1.020	946	1160
1.5	1	3.76	0.75	60.06	1.020	944	1180
1.5	1	3.76	0.75	60.06	1.020	935	11800
1.5	1	3.76	0.75	60.06	1.020	932	2300
1.5	1	3.76	0.75	60.06	1.020	931	7200
1.5	1	3.76	0.75	60.06	1.020	924	7400
1.5	1	3.76	0.75	60.06	1.020	918	3000
1.5	1	3.76	0.75	60.06	1.020	911	2000
1.5	1	3.76	0.75	60.06	2.041	993	600

Fuel (mol)	Oxygen (mol)	Diluent (mol)	ϕ	% Diluent	P (atm)	T (K)	τ_{ind} (μsec)
1.5	1	3.76	0.75	60.06	2.041	963	1400
1.5	1	3.76	0.75	60.06	2.041	959	1400
1.5	1	3.76	0.75	60.06	2.041	949	1300
1.5	1	3.76	0.75	60.06	2.041	945	3500
1.5	1	3.76	0.75	60.06	2.041	936	1900
1.5	1	3.76	0.75	60.06	2.041	934	4600
1.5	1	3.76	0.75	60.06	2.041	922	6400
1.5	1	3.76	0.75	60.06	2.041	918	14200
1.5	1	3.76	0.75	60.06	2.041	917	6200
1.5	1	3.76	0.75	60.06	2.041	913	2000
1.5	1	3.76	0.75	60.06	2.041	850	11400
1.5	1	3.76	0.75	60.06	4.082	1013	320
1.5	1	3.76	0.75	60.06	4.082	983	650
1.5	1	3.76	0.75	60.06	4.082	962	800
1.5	1	3.76	0.75	60.06	4.082	960	1600
1.5	1	3.76	0.75	60.06	4.082	948	1400
1.5	1	3.76	0.75	60.06	4.082	942	1400
1.5	1	3.76	0.75	60.06	4.082	924	3000
1.5	1	3.76	0.75	60.06	4.082	919	2600
1.5	1	3.76	0.75	60.06	4.082	912	4200
1.5	1	3.76	0.75	60.06	4.082	897	10400
1.5	1	3.76	0.75	60.06	4.082	894	9800
1.5	1	3.76	0.75	60.06	4.082	880	4000
1.5	1	3.76	0.75	60.06	6.803	974	370
1.5	1	3.76	0.75	60.06	6.803	957	970
1.5	1	3.76	0.75	60.06	6.803	951	1380
1.5	1	3.76	0.75	60.06	6.803	924	2500
1.5	1	3.76	0.75	60.06	6.803	903	4000
1.5	1	3.76	0.75	60.06	6.803	890	1300
1.5	1	3.76	0.75	60.06	6.803	881	1700
1.5	1	3.76	0.75	60.06	6.803	869	2100
1.5	1	3.76	0.75	60.06	6.803	855	8000
1.5	1	3.76	0.75	60.06	6.803	844	11400
2	1	3.76	1.00	55.62	1.020	967	380

Fuel (mol)	Oxygen (mol)	Diluent (mol)	ϕ	% Diluent	P (atm)	T (K)	τ_{ind} (μsec)
2	1	3.76	1.00	55.62	1.020	953	520
2	1	3.76	1.00	55.62	1.020	946	600
2	1	3.76	1.00	55.62	1.020	941	500
2	1	3.76	1.00	55.62	1.020	933	1750
2	1	3.76	1.00	55.62	1.020	924	10400
2	1	3.76	1.00	55.62	1.020	924	7000
2	1	3.76	1.00	55.62	1.020	922	3600
2	1	3.76	1.00	55.62	1.020	918	1700
2	1	3.76	1.00	55.62	1.020	918	6000
2	1	3.76	1.00	55.62	1.020	913	6200
2	1	3.76	1.00	55.62	2.041	981	550
2	1	3.76	1.00	55.62	2.041	973	1000
2	1	3.76	1.00	55.62	2.041	964	1350
2	1	3.76	1.00	55.62	2.041	959	1600
2	1	3.76	1.00	55.62	2.041	954	1900
2	1	3.76	1.00	55.62	2.041	948	2400
2	1	3.76	1.00	55.62	2.041	937	1800
2	1	3.76	1.00	55.62	2.041	932	1800
2	1	3.76	1.00	55.62	2.041	927	2400
2	1	3.76	1.00	55.62	2.041	919	1400
2	1	3.76	1.00	55.62	2.041	911	2000
2	1	3.76	1.00	55.62	2.041	887	14600
2	1	3.76	1.00	55.62	2.041	857	11000
2	1	3.76	1.00	55.62	4.082	976	1250
2	1	3.76	1.00	55.62	4.082	973	1450
2	1	3.76	1.00	55.62	4.082	972	350
2	1	3.76	1.00	55.62	4.082	972	650
2	1	3.76	1.00	55.62	4.082	964	1900
2	1	3.76	1.00	55.62	4.082	950	1350
2	1	3.76	1.00	55.62	4.082	940	1250
2	1	3.76	1.00	55.62	4.082	939	6200
2	1	3.76	1.00	55.62	4.082	937	3250
2	1	3.76	1.00	55.62	4.082	925	7200
2	1	3.76	1.00	55.62	4.082	923	8400

Fuel (mol)	Oxygen (mol)	Diluent (mol)	ϕ	% Diluent	P (atm)	T (K)	τ_{ind} (μsec)
2	1	3.76	1.00	55.62	4.082	914	1400
2	1	3.76	1.00	55.62	6.803	942	1050
2	1	3.76	1.00	55.62	6.803	941	1050
2	1	3.76	1.00	55.62	6.803	932	1050
2	1	3.76	1.00	55.62	6.803	924	1200
2	1	3.76	1.00	55.62	6.803	909	3000
2	1	3.76	1.00	55.62	6.803	909	9200
2	1	3.76	1.00	55.62	6.803	901	600
2	1	3.76	1.00	55.62	6.803	895	400
2	1	3.76	1.00	55.62	6.803	886	1000
2	1	3.76	1.00	55.62	6.803	882	5000
2	1	3.76	1.00	55.62	8.844	932	1200
2	1	3.76	1.00	55.62	8.844	917	800
2	1	3.76	1.00	55.62	8.844	916	480
2	1	3.76	1.00	55.62	8.844	908	300
2	1	3.76	1.00	55.62	8.844	892	1400
2	1	3.76	1.00	55.62	8.844	887	1400
2	1	3.76	1.00	55.62	8.844	870	1650
2	1	3.76	1.00	55.62	8.844	868	2000
2	1	3.76	1.00	55.62	8.844	844	6600
2	1	3.76	1.00	55.62	8.844	833	8400
2	1	3.76	1.00	55.62	8.844	826	8600
2	1	3.76	1.00	55.62	8.844	808	11400

Source: Steinberg (1955) **Technique: Reflected**
Mixture: H_2/O_2 **Equivalence Ratio (ϕ): 1.0**
% Diluent: 0 **Pressure (P): 4.5 - 9.0 atm**
Temperature (T): 700 - 1000 K
Induction Period (τ_{ind}) End: Luminosity onset

Fuel (mol)	Oxygen (mol)	Diluent (mol)	ϕ	% Diluent	P (atm)	T (K)	τ_{ind} (μsec)
2	1	0	1	0	6.303	918	38
2	1	0	1	0	6.307	918	117
2	1	0	1	0	5.884	885	99
2	1	0	1	0	5.591	862	25
2	1	0	1	0	5.229	833	190
2	1	0	1	0	5.131	826	260
2	1	0	1	0	4.716	793	247
2	1	0	1	0	4.551	780	178
2	1	0	1	0	8.665	884	26
2	1	0	1	0	8.172	854	44
2	1	0	1	0	7.722	826	293
2	1	0	1	0	7.395	805	292
2	1	0	1	0	6.889	774	388

Appendix B: Ethylene Shock Tube Data

Source: Baker (1972) **Technique: Reflected**
Mixture: $C_2H_4/O_2/Ar$ **Equivalence Ratio (ϕ): 0.125 - 2.0**
% Diluent: 93 - 99 **Pressure (P): 3 - 12 atm**
Temperature (T): 1000 - 1900 K
Induction Period (τ_{ind}) End: OH emission maximum

Fuel (mol)	Oxygen (mol)	Diluent (mol)	ϕ	% Diluent	P (atm)	T (K)	τ_{ind} (μsec)
1	3	96	1	96	3	1112	6210
1	3	96	1	96	3	1144	3881
1	3	96	1	96	3	1175	2488
1	3	96	1	96	3	1207	1632
1	3	96	1	96	3	1239	1094
1	3	96	1	96	3	1271	748
1	3	96	1	96	3	1302	521
1	3	96	1	96	3	1334	370
1	3	96	1	96	3	1366	266
1	3	96	1	96	3	1397	195
1	3	96	1	96	3	1429	144
1	3	96	1	96	3	1461	108
1	3	96	1	96	3	1493	82
1	3	96	1	96	3	1524	63
1	3	96	1	96	3	1556	49
0.5	3	96.5	0.5	96.5	3	1118	4127
0.5	3	96.5	0.5	96.5	3	1140	2924
0.5	3	96.5	0.5	96.5	3	1163	2099
0.5	3	96.5	0.5	96.5	3	1185	1526
0.5	3	96.5	0.5	96.5	3	1207	1123
0.5	3	96.5	0.5	96.5	3	1229	835
0.5	3	96.5	0.5	96.5	3	1252	628
0.5	3	96.5	0.5	96.5	3	1274	477
0.5	3	96.5	0.5	96.5	3	1296	365
0.5	3	96.5	0.5	96.5	3	1319	283
0.5	3	96.5	0.5	96.5	3	1341	220
0.5	3	96.5	0.5	96.5	3	1363	173
0.5	3	96.5	0.5	96.5	3	1385	137

Fuel (mol)	Oxygen (mol)	Diluent (mol)	ϕ	% Diluent	P (atm)	T (K)	τ_{ind} (μsec)
0.5	3	96.5	0.5	96.5	3	1408	110
0.5	3	96.5	0.5	96.5	3	1430	88
0.25	0.75	99	1	99	12	1176	5274
0.25	0.75	99	1	99	12	1201	3620
0.25	0.75	99	1	99	12	1227	2524
0.25	0.75	99	1	99	12	1252	1786
0.25	0.75	99	1	99	12	1277	1281
0.25	0.75	99	1	99	12	1303	931
0.25	0.75	99	1	99	12	1328	684
0.25	0.75	99	1	99	12	1353	509
0.25	0.75	99	1	99	12	1379	383
0.25	0.75	99	1	99	12	1404	291
0.25	0.75	99	1	99	12	1430	223
0.25	0.75	99	1	99	12	1455	173
0.25	0.75	99	1	99	12	1480	135
0.25	0.75	99	1	99	12	1506	106
0.25	0.75	99	1	99	12	1531	85
2	3	95	2	95	3	1117	3927
2	3	95	2	95	3	1153	2667
2	3	95	2	95	3	1188	1854
2	3	95	2	95	3	1224	1316
2	3	95	2	95	3	1260	953
2	3	95	2	95	3	1295	702
2	3	95	2	95	3	1331	526
2	3	95	2	95	3	1366	400
2	3	95	2	95	3	1402	308
2	3	95	2	95	3	1438	241
2	3	95	2	95	3	1473	190
2	3	95	2	95	3	1509	152
2	3	95	2	95	3	1545	123
2	3	95	2	95	3	1580	100
2	3	95	2	95	3	1616	82
1	1.5	97.5	2	97.5	3	1155	5046
1	1.5	97.5	2	97.5	3	1197	3327

Fuel (mol)	Oxygen (mol)	Diluent (mol)	ϕ	% Diluent	P (atm)	T (K)	τ_{ind} (μsec)
1	1.5	97.5	2	97.5	3	1240	2257
1	1.5	97.5	2	97.5	3	1282	1570
1	1.5	97.5	2	97.5	3	1324	1118
1	1.5	97.5	2	97.5	3	1366	813
1	1.5	97.5	2	97.5	3	1409	603
1	1.5	97.5	2	97.5	3	1451	455
1	1.5	97.5	2	97.5	3	1493	349
1	1.5	97.5	2	97.5	3	1536	271
1	1.5	97.5	2	97.5	3	1578	214
1	1.5	97.5	2	97.5	3	1620	171
1	1.5	97.5	2	97.5	3	1662	138
1	1.5	97.5	2	97.5	3	1705	112
1	1.5	97.5	2	97.5	3	1747	93
1	6	93	0.5	93	3	1080	4417
1	6	93	0.5	93	3	1106	2887
1	6	93	0.5	93	3	1131	1923
1	6	93	0.5	93	3	1157	1305
1	6	93	0.5	93	3	1183	900
1	6	93	0.5	93	3	1209	631
1	6	93	0.5	93	3	1234	449
1	6	93	0.5	93	3	1260	324
1	6	93	0.5	93	3	1286	237
1	6	93	0.5	93	3	1311	175
1	6	93	0.5	93	3	1337	131
1	6	93	0.5	93	3	1363	99
1	6	93	0.5	93	3	1389	76
1	6	93	0.5	93	3	1414	59
1	6	93	0.5	93	3	1440	46
0.25	6	93.75	0.125	93.75	3	1058	7387
0.25	6	93.75	0.125	93.75	3	1084	4759
0.25	6	93.75	0.125	93.75	3	1109	3129
0.25	6	93.75	0.125	93.75	3	1135	2097
0.25	6	93.75	0.125	93.75	3	1161	1430
0.25	6	93.75	0.125	93.75	3	1187	992

Fuel (mol)	Oxygen (mol)	Diluent (mol)	ϕ	% Diluent	P (atm)	T (K)	τ_{ind} (μsec)
0.25	6	93.75	0.125	93.75	3	1212	698
0.25	6	93.75	0.125	93.75	3	1238	499
0.25	6	93.75	0.125	93.75	3	1264	362
0.25	6	93.75	0.125	93.75	3	1289	265
0.25	6	93.75	0.125	93.75	3	1315	197
0.25	6	93.75	0.125	93.75	3	1341	148
0.25	6	93.75	0.125	93.75	3	1367	112
0.25	6	93.75	0.125	93.75	3	1392	86
0.25	6	93.75	0.125	93.75	3	1418	67
0.25	1.5	98.25	0.5	98.25	3	1100	5165
0.25	1.5	98.25	0.5	98.25	3	1138	3224
0.25	1.5	98.25	0.5	98.25	3	1175	2075
0.25	1.5	98.25	0.5	98.25	3	1213	1372
0.25	1.5	98.25	0.5	98.25	3	1251	930
0.25	1.5	98.25	0.5	98.25	3	1289	645
0.25	1.5	98.25	0.5	98.25	3	1326	457
0.25	1.5	98.25	0.5	98.25	3	1364	330
0.25	1.5	98.25	0.5	98.25	3	1402	242
0.25	1.5	98.25	0.5	98.25	3	1439	181
0.25	1.5	98.25	0.5	98.25	3	1477	137
0.25	1.5	98.25	0.5	98.25	3	1515	105
0.25	1.5	98.25	0.5	98.25	3	1553	82
0.25	1.5	98.25	0.5	98.25	3	1590	65
0.25	1.5	98.25	0.5	98.25	3	1628	51
0.25	1.5	98.25	0.5	98.25	3	1104	5699
0.25	1.5	98.25	0.5	98.25	3	1136	3721
0.25	1.5	98.25	0.5	98.25	3	1168	2487
0.25	1.5	98.25	0.5	98.25	3	1200	1698
0.25	1.5	98.25	0.5	98.25	3	1232	1183
0.25	1.5	98.25	0.5	98.25	3	1264	839
0.25	1.5	98.25	0.5	98.25	3	1296	605
0.25	1.5	98.25	0.5	98.25	3	1328	444
0.25	1.5	98.25	0.5	98.25	3	1359	330
0.25	1.5	98.25	0.5	98.25	3	1391	249

Fuel (mol)	Oxygen (mol)	Diluent (mol)	ϕ	% Diluent	P (atm)	T (K)	τ_{ind} (μsec)
0.25	1.5	98.25	0.5	98.25	3	1423	190
0.25	1.5	98.25	0.5	98.25	3	1455	147
0.25	1.5	98.25	0.5	98.25	3	1487	115
0.25	1.5	98.25	0.5	98.25	3	1519	90
0.25	1.5	98.25	0.5	98.25	3	1551	72
0.5	0.75	98.75	2	98.75	3	1166	8570
0.5	0.75	98.75	2	98.75	3	1217	5107
0.5	0.75	98.75	2	98.75	3	1267	3172
0.5	0.75	98.75	2	98.75	3	1318	2044
0.5	0.75	98.75	2	98.75	3	1369	1361
0.5	0.75	98.75	2	98.75	3	1420	933
0.5	0.75	98.75	2	98.75	3	1470	656
0.5	0.75	98.75	2	98.75	3	1521	472
0.5	0.75	98.75	2	98.75	3	1572	347
0.5	0.75	98.75	2	98.75	3	1622	260
0.5	0.75	98.75	2	98.75	3	1673	199
0.5	0.75	98.75	2	98.75	3	1724	154
0.5	0.75	98.75	2	98.75	3	1775	121
0.5	0.75	98.75	2	98.75	3	1825	97
0.5	0.75	98.75	2	98.75	3	1876	78

Source: Drummond (1968) **Technique: Reflected**
Mixture: $C_2H_4/O_2/Ar$ **Equivalence Ratio (ϕ): 1.0 - 2.0**
% Diluent: 84 - 95 **Pressure (P): 0.5 - 2.7 atm**
Temperature (T): 1000 - 1700 K
Induction Period (τ_{ind}) End: OH emission maximum

Fuel (mol)	Oxygen (mol)	Diluent (mol)	ϕ	% Diluent	P (atm)	T (K)	τ_{ind} (μsec)
2	6	92	1	92	1.784	1452	88
2	6	92	1	92	1.761	1441	94
2	6	92	1	92	1.704	1412	124
2	6	92	1	92	1.650	1385	132
2	6	92	1	92	1.568	1344	186
2	6	92	1	92	1.542	1331	205
2	6	92	1	92	1.499	1310	269
2	6	92	1	92	1.399	1260	458
2	6	92	1	92	1.379	1250	437
2	6	92	1	92	1.325	1223	633
2	6	92	1	92	1.269	1195	1211
2	6	92	1	92	1.192	1156	1844
2	6	92	1	92	1.088	1104	2457
2	6	92	1	92	1.068	1094	3443
4	12	84	1	84	2.062	1396	72
4	12	84	1	84	2.013	1377	84
4	12	84	1	84	1.745	1269	231
4	12	84	1	84	1.647	1230	337
4	12	84	1	84	1.508	1175	835
4	12	84	1	84	1.394	1129	1800
5	10	85	1.5	85	1.825	1289	248
5	10	85	1.5	85	1.720	1248	421
5	10	85	1.5	85	1.665	1227	451
5	10	85	1.5	85	1.524	1173	1001
5	10	85	1.5	85	1.493	1161	1394
5	10	85	1.5	85	1.472	1153	1558
5	10	85	1.5	85	1.389	1121	2222
5	10	85	1.5	85	1.327	1097	2600
2	4	94	1.5	94	2.182	1626	18
2	4	94	1.5	94	2.041	1555	29

Fuel (mol)	Oxygen (mol)	Diluent (mol)	ϕ	% Diluent	P (atm)	T (K)	τ_{ind} (μsec)
2	4	94	1.5	94	2.022	1546	33
2	4	94	1.5	94	1.889	1479	47
2	4	94	1.5	94	1.774	1422	66
2	4	94	1.5	94	1.756	1413	73
2	4	94	1.5	94	1.615	1342	193
2	4	94	1.5	94	1.564	1317	229
2	4	94	1.5	94	1.529	1300	256
2	4	94	1.5	94	1.396	1233	571
2	4	94	1.5	94	1.277	1173	906
2	3	95	2	95	1.945	1580	33
2	3	95	2	95	1.756	1480	66
2	3	95	2	95	1.740	1472	72
2	3	95	2	95	1.646	1423	101
2	3	95	2	95	1.536	1364	133
2	3	95	2	95	1.552	1373	209
2	3	95	2	95	1.431	1309	264
2	3	95	2	95	1.435	1312	332
2	3	95	2	95	1.381	1283	377
2	3	95	2	95	1.298	1239	621

Source: Gay (1967) **Technique: Incident**
Mixture: $C_2H_4/O_2/Ar$ **Equivalence Ratio (ϕ): 0.214 - 3.5**
% Diluent: 96 - 99 **Pressure (P): 0.2 - 0.4 atm**
Temperature (T): 1400 - 2300 K
Induction Period (τ_{ind}) End: CH* emission onset

Fuel (mol)	Oxygen (mol)	Diluent (mol)	ϕ	% Diluent	P (atm)	T (K)	τ_{ind} (μsec)
0.7	1.5	97.8	1.40	97.8	0.246	1953	105
0.7	1.5	97.8	1.40	97.8	0.231	1805	168
0.7	1.5	97.8	1.40	97.8	0.249	1975	108
0.7	1.5	97.8	1.40	97.8	0.198	1575	630
0.7	1.5	97.8	1.40	97.8	0.241	1915	118
0.7	1.5	97.8	1.40	97.8	0.236	1840	168
0.7	1.5	97.8	1.40	97.8	0.413	1625	199
0.4	0.9	98.7	1.33	98.7	0.226	1800	231
0.4	0.9	98.7	1.33	98.7	0.282	2240	60
0.4	0.9	98.7	1.33	98.7	0.262	2085	84
0.4	0.9	98.7	1.33	98.7	0.197	1565	1295
0.4	0.9	98.7	1.33	98.7	0.215	1710	430
0.4	0.9	98.7	1.33	98.7	0.220	1750	339
0.4	0.9	98.7	1.33	98.7	0.415	1650	312
0.4	0.9	98.7	1.33	98.7	0.371	1515	826
0.1	0.9	99	0.33	99	0.240	1910	231
0.1	0.9	99	0.33	99	0.223	1775	346
0.1	0.9	99	0.33	99	0.363	1560	440
0.1	0.9	99	0.33	99	0.262	2085	114
0.1	0.9	99	0.33	99	0.207	1650	420
0.1	0.9	99	0.33	99	0.227	1810	269
0.5	1	98.5	1.50	98.5	0.209	1690	322
0.5	1	98.5	1.50	98.5	0.244	1937	113
0.5	1	98.5	1.50	98.5	0.211	1650	333
0.5	1	98.5	1.50	98.5	0.223	1770	238
0.5	1	98.5	1.50	98.5	0.377	1500	665
0.5	1	98.5	1.50	98.5	0.405	1612	262
0.5	1	98.5	1.50	98.5	0.230	1830	130
0.5	1	98.5	1.50	98.5	0.217	1725	210
1.2	0.9	97.9	4.00	97.9	0.244	1940	147

Fuel (mol)	Oxygen (mol)	Diluent (mol)	ϕ	% Diluent	P (atm)	T (K)	τ_{ind} (μsec)
1.2	0.9	97.9	4.00	97.9	0.232	1810	245
0.3	1.9	97.8	0.47	97.8	0.234	1830	116
0.3	1.9	97.8	0.47	97.8	0.215	1710	217
0.3	1.9	97.8	0.47	97.8	0.377	1475	336
0.3	1.9	97.8	0.47	97.8	0.271	2150	22
0.3	1.9	97.8	0.47	97.8	0.387	1525	252
0.3	1.9	97.8	0.47	97.8	0.413	1627	126
0.3	1.9	97.8	0.47	97.8	0.251	1990	53
0.2	1	98.8	0.60	98.8	0.215	1710	221
0.2	1	98.8	0.60	98.8	0.382	1625	221
0.2	1	98.8	0.60	98.8	0.207	1650	357
0.1	1.4	98.5	0.21	98.5	0.223	1775	210
0.1	1.4	98.5	0.21	98.5	0.259	2060	87
0.1	1.4	98.5	0.21	98.5	0.368	1566	294
0.1	1.4	98.5	0.21	98.5	0.294	1550	430
0.1	1.4	98.5	0.21	98.5	0.231	1837	175
0.6	1.2	98.2	1.50	98.2	0.262	1766	217
0.6	1.2	98.2	1.50	98.2	0.281	1890	108
0.6	1.2	98.2	1.50	98.2	0.278	1874	115
0.6	1.2	98.2	1.50	98.2	0.266	1790	185
0.6	1.2	98.2	1.50	98.2	0.258	1740	315
0.6	1.2	98.2	1.50	98.2	0.334	1540	542
0.6	1.2	98.2	1.50	98.2	0.351	1620	305
0.6	1.2	98.2	1.50	98.2	0.401	1850	74
0.6	2.7	96.7	0.67	96.7	0.247	1680	182
0.7	0.6	98.7	3.50	98.7	0.289	1950	154
0.7	0.6	98.7	3.50	98.7	0.281	1895	203

Source: Hidaka (1974) **Technique: Reflected**
Mixture: $C_2H_4/O_2/Ar$ **Equivalence Ratio (ϕ): 1.0 - 3.0**
% Diluent: 96 - 98 **Pressure (P): 1.0 - 5.0 atm**
Temperature (T): 1400 - 2100 K
Induction Period (τ_{ind}) End: CH* emission onset

Fuel (mol)	Oxygen (mol)	Diluent (mol)	ϕ	% Diluent	P (atm)	T (K)	τ_{ind} (μsec)
1	1	98	3	98	2.422	1774	53
1	1	98	3	98	2.487	1786	44
1	1	98	3	98	2.912	1981	22
1	1	98	3	98	2.492	1786	42
1	1	98	3	98	2.683	1868	32
1	1	98	3	98	2.682	1860	28
1	1	98	3	98	2.575	1809	38
1	1	98	3	98	2.821	1929	21
1	1	98	3	98	2.528	1779	44
1	1	98	3	98	2.505	1769	41
1	1	98	3	98	2.682	1880	25
1	1	98	3	98	2.954	2007	16
1	1	98	3	98	2.904	1939	18
1	1	98	3	98	2.966	2009	18
1	1	98	3	98	2.604	1837	36
1	1	98	3	98	3.032	2077	13
1	1	98	3	98	2.554	1804	42
1	1	98	3	98	4.692	1716	34
1	1	98	3	98	4.4	1629	49
1	1	98	3	98	4.859	1751	28
1	1	98	3	98	4.896	1846	18
1	1	98	3	98	4.614	1679	50
1	1	98	3	98	4.213	1596	55
1	1	98	3	98	4.655	1694	44
1	1	98	3	98	5.004	1797	23
1	1	98	3	98	4.408	1634	62
1	2	97	1.5	97	2.655	1830	20
1	2	97	1.5	97	2.38	1733	27
1	2	97	1.5	97	2.383	1729	28
1	2	97	1.5	97	2.633	1852	15

Fuel (mol)	Oxygen (mol)	Diluent (mol)	ϕ	% Diluent	P (atm)	T (K)	τ_{ind} (μsec)
1	2	97	1.5	97	2.445	1765	31
1	2	97	1.5	97	2.33	1693	40
1	2	97	1.5	97	2.592	1804	25
1	2	97	1.5	97	2.436	1756	37
1	2	97	1.5	97	2.599	1797	22
1	2	97	1.5	97	2.372	1723	36
1	2	97	1.5	97	2.559	1827	23
1	2	97	1.5	97	2.729	1898	19
1	2	97	1.5	97	2.903	1960	15
1	2	97	1.5	97	1.857	1469	152
1	2	97	1.5	97	2.129	1588	74
1	2	97	1.5	97	2.809	1937	15
1	2	97	1.5	97	2.943	1924	14
1	2	97	1.5	97	2.38	1726	35
1	2	97	1.5	97	2.554	1799	27
1	2	97	1.5	97	1.895	1480	150
1	2	97	1.5	97	3.121	2081	8
1	2	97	1.5	97	2.043	1555	77
1	2	97	1.5	97	2.638	1847	16
1	3	96	1	96	1.824	1443	93
1	3	96	1	96	2.316	1677	30
1	3	96	1	96	2.149	1600	35
1	3	96	1	96	2.216	1645	30
1	3	96	1	96	2.213	1633	36
1	3	96	1	96	1.955	1508	68
1	3	96	1	96	1.967	1506	63
1	3	96	1	96	1.908	1474	79
1	3	96	1	96	1.959	1508	80
1	3	96	1	96	2.55	1811	14
1	3	96	1	96	2.305	1664	26
1	3	96	1	96	2.1	1582	49
1	3	96	1	96	1.997	1597	41
1	3	96	1	96	1.858	1459	108
1	3	96	1	96	2.054	1575	45

Fuel (mol)	Oxygen (mol)	Diluent (mol)	ϕ	% Diluent	P (atm)	T (K)	τ_{ind} (μsec)
1	3	96	1	96	2.036	1534	68
1	3	96	1	96	1.772	1422	108
1	3	96	1	96	2.42	1720	19
1	3	96	1	96	2.413	1735	24
1	3	96	1	96	3.124	2042	6
1	3	96	1	96	2.638	1844	10
1	3	96	1	96	2.787	1924	8
1	3	96	1	96	2.482	1766	15
1	3	96	1	96	2.562	1806	16
1	3	96	1	96	2.288	1675	22
1	3	96	1	96	2.653	1841	12
1	3	96	1	96	2.421	1716	22
1	3	96	1	96	2.789	1897	10

Source: Homer (1967) **Technique: Reflected**
Mixture: $C_2H_4/O_2/Ar$ **Equivalence Ratio (ϕ): 0.5 - 1.5**
% Diluent: 96.5 - 98.5 **Pressure (P): 0.3 - 0.8 atm**
Temperature (T): 1500 - 2300 K
Induction Period (τ_{ind}) End: CO + CO_2 emission 10% of max

Fuel (mol)	Oxygen (mol)	Diluent (mol)	ϕ	% Diluent	P (atm)	T (K)	τ_{ind} (μsec)
0.5	1	98.5	1.5	98.5	0.736	1540	157
0.5	1	98.5	1.5	98.5	0.737	1745	122
0.5	1	98.5	1.5	98.5	0.698	1850	97
0.5	1	98.5	1.5	98.5	0.558	1880	110
0.5	1	98.5	1.5	98.5	0.716	1930	85
0.5	1	98.5	1.5	98.5	0.736	2005	80
0.5	1	98.5	1.5	98.5	0.708	2045	83
0.5	1	98.5	1.5	98.5	0.647	2150	53
0.5	1	98.5	1.5	98.5	0.596	2240	48
0.5	1	98.5	1.5	98.5	0.637	2325	40
0.5	3	96.5	0.5	96.5	0.748	1505	145
0.5	3	96.5	0.5	96.5	0.431	1515	194
0.5	3	96.5	0.5	96.5	0.356	1585	193
0.5	3	96.5	0.5	96.5	0.702	1755	74
0.5	3	96.5	0.5	96.5	0.624	1905	60
0.5	3	96.5	0.5	96.5	0.621	1995	51
0.5	3	96.5	0.5	96.5	0.569	2225	34

Source: Jachimowski (1977) **Technique: Incident**
Mixture: $C_2H_4/O_2/Ar$ **Equivalence Ratio (ϕ): 0.5 - 1.5**
% Diluent: 91 - 93 **Pressure (P): 1.1 - 1.7 atm**
Temperature (T): 1800 - 2400 K
Induction Period (τ_{ind}) End: CO + CO_2 emission, [O][CO] $_{max}$

Fuel (mol)	Oxygen (mol)	Diluent (mol)	ϕ	% Diluent	P (atm)	T (K)	τ_{ind} (μsec)
1	6	93	0.5	93	1.55	2301	5
1	6	93	0.5	93	1.55	2295	5
1	6	93	0.5	93	1.52	2257	4
1	6	93	0.5	93	1.44	2160	5
1	6	93	0.5	93	1.43	2145	6
1	6	93	0.5	93	1.25	1922	12
1	6	93	0.5	93	1.22	1880	10
1	6	93	0.5	93	1.2	1865	15
1	6	93	0.5	93	1.16	1800	10
2	6	92	1	92	1.65	2339	4
2	6	92	1	92	1.61	2290	4
2	6	92	1	92	1.59	2264	5
2	6	92	1	92	1.38	2015	9
2	6	92	1	92	1.34	1963	8
2	6	92	1	92	1.3	1923	7
2	6	92	1	92	1.3	1920	8
2	6	92	1	92	1.22	1815	10
3	6	91	1.5	91	1.68	2311	3
3	6	91	1.5	91	1.66	2268	3
3	6	91	1.5	91	1.64	2248	3
3	6	91	1.5	91	1.44	2015	6
3	6	91	1.5	91	1.4	1973	5
3	6	91	1.5	91	1.37	1940	6
3	6	91	1.5	91	1.33	1895	5
3	6	91	1.5	91	1.3	1868	6

Source: Suzuki (1973) **Technique: Reflected**
Mixture: $C_2H_4/O_2/Ar$ **Equivalence Ratio (ϕ): 0.46 - 2.63**
% Diluent: 70 **Pressure (P): 1 - 3.2 atm**
Temperature (T): 800 - 1400
Induction Period (τ_{ind}) End: OH absorption max rate of change

Fuel (mol)	Oxygen (mol)	Diluent (mol)	ϕ	% Diluent	P (atm)	T (K)	τ_{ind} (μsec)
4	26	70	0.462	70	2.341	1320	31
4	26	70	0.462	70	2.140	1253	66
4	26	70	0.462	70	2.009	1209	74
4	26	70	0.462	70	1.944	1188	146
4	26	70	0.462	70	1.829	1150	155
4	26	70	0.462	70	1.846	1155	161
4	26	70	0.462	70	1.803	1141	194
4	26	70	0.462	70	1.723	1114	231
4	26	70	0.462	70	1.712	1110	322
4	26	70	0.462	70	1.673	1097	627
4	26	70	0.462	70	1.633	1084	819
4	26	70	0.462	70	1.679	1099	916
4	26	70	0.462	70	1.634	1085	1088
4	26	70	0.462	70	1.639	1086	1148
4	26	70	0.462	70	1.563	1061	1350
4	26	70	0.462	70	1.644	1088	1428
4	26	70	0.462	70	1.646	1089	1557
4	26	70	0.462	70	1.436	1018	1839
4	26	70	0.462	70	1.335	985	2163
4	26	70	0.462	70	1.307	975	2181
4	26	70	0.462	70	1.281	967	2193
4	26	70	0.462	70	1.234	951	2398
4	26	70	0.462	70	1.115	911	2751
4	26	70	0.462	70	1.090	903	2780
6	24	70	0.75	70	2.298	1241	43
6	24	70	0.75	70	2.231	1221	80
6	24	70	0.75	70	2.179	1205	106
6	24	70	0.75	70	2.127	1189	136
6	24	70	0.75	70	2.180	1205	139
6	24	70	0.75	70	2.100	1181	161

Fuel (mol)	Oxygen (mol)	Diluent (mol)	ϕ	% Diluent	P (atm)	T (K)	τ_{ind} (μsec)
6	24	70	0.75	70	2.066	1170	245
6	24	70	0.75	70	2.022	1157	255
6	24	70	0.75	70	2.087	1177	258
6	24	70	0.75	70	2.038	1162	267
6	24	70	0.75	70	2.038	1162	314
6	24	70	0.75	70	1.946	1134	344
6	24	70	0.75	70	1.985	1146	403
6	24	70	0.75	70	1.998	1150	418
6	24	70	0.75	70	1.941	1133	456
6	24	70	0.75	70	1.951	1136	521
6	24	70	0.75	70	1.947	1135	572
6	24	70	0.75	70	1.856	1107	604
6	24	70	0.75	70	1.776	1083	1050
6	24	70	0.75	70	1.773	1082	1094
6	24	70	0.75	70	1.818	1096	1152
6	24	70	0.75	70	1.772	1082	1171
6	24	70	0.75	70	1.734	1070	1178
6	24	70	0.75	70	1.815	1095	1233
6	24	70	0.75	70	1.616	1034	1416
6	24	70	0.75	70	1.516	1004	1598
6	24	70	0.75	70	1.424	976	1984
6	24	70	0.75	70	1.364	958	2130
6	24	70	0.75	70	1.247	922	2303
6	24	70	0.75	70	1.136	889	2630
8	22	70	1.091	70	2.409	1223	58
8	22	70	1.091	70	2.524	1255	59
8	22	70	1.091	70	2.279	1187	81
8	22	70	1.091	70	2.412	1224	88
8	22	70	1.091	70	2.288	1190	203
8	22	70	1.091	70	2.230	1174	219
8	22	70	1.091	70	2.284	1188	227
8	22	70	1.091	70	2.134	1147	230
8	22	70	1.091	70	2.255	1180	266
8	22	70	1.091	70	2.175	1158	274

Fuel (mol)	Oxygen (mol)	Diluent (mol)	ϕ	% Diluent	P (atm)	T (K)	τ_{ind} (μsec)
8	22	70	1.091	70	2.193	1163	284
8	22	70	1.091	70	2.285	1189	316
8	22	70	1.091	70	2.235	1175	421
8	22	70	1.091	70	2.128	1145	445
8	22	70	1.091	70	2.115	1141	470
8	22	70	1.091	70	2.021	1115	518
8	22	70	1.091	70	1.988	1106	596
8	22	70	1.091	70	2.087	1134	605
8	22	70	1.091	70	1.984	1105	671
8	22	70	1.091	70	1.908	1084	711
8	22	70	1.091	70	1.962	1099	774
8	22	70	1.091	70	1.995	1108	860
8	22	70	1.091	70	2.033	1119	912
8	22	70	1.091	70	1.959	1098	954
8	22	70	1.091	70	1.853	1069	959
8	22	70	1.091	70	1.725	1033	1006
8	22	70	1.091	70	2.000	1110	1065
8	22	70	1.091	70	1.877	1075	1147
8	22	70	1.091	70	1.775	1047	1179
8	22	70	1.091	70	1.592	996	1263
8	22	70	1.091	70	1.489	968	1421
8	22	70	1.091	70	1.586	994	1377
8	22	70	1.091	70	1.622	1005	1328
8	22	70	1.091	70	1.658	1014	1310
8	22	70	1.091	70	1.780	1048	1348
8	22	70	1.091	70	1.742	1038	1406
8	22	70	1.091	70	1.637	1009	1421
8	22	70	1.091	70	1.673	1019	1454
8	22	70	1.091	70	1.617	1003	1519
8	22	70	1.091	70	1.582	994	1563
8	22	70	1.091	70	1.457	959	1788
8	22	70	1.091	70	1.414	947	1857
8	22	70	1.091	70	1.319	920	1891
8	22	70	1.091	70	1.317	920	1986

Fuel (mol)	Oxygen (mol)	Diluent (mol)	ϕ	% Diluent	P (atm)	T (K)	τ_{ind} (μsec)
8	22	70	1.091	70	1.325	922	2047
8	22	70	1.091	70	1.450	957	2061
8	22	70	1.091	70	1.213	891	2427
8	22	70	1.091	70	1.234	897	2485
8	22	70	1.091	70	1.180	882	2929
14	16	70	2.625	70	3.168	1300	47
14	16	70	2.625	70	3.074	1278	69
14	16	70	2.625	70	2.883	1235	92
14	16	70	2.625	70	2.919	1243	104
14	16	70	2.625	70	2.849	1227	118
14	16	70	2.625	70	2.829	1223	125
14	16	70	2.625	70	2.771	1210	172
14	16	70	2.625	70	2.770	1209	179
14	16	70	2.625	70	2.589	1168	319
14	16	70	2.625	70	2.560	1162	350
14	16	70	2.625	70	2.460	1139	463
14	16	70	2.625	70	2.405	1126	573
14	16	70	2.625	70	2.311	1105	764
14	16	70	2.625	70	2.252	1091	984
14	16	70	2.625	70	2.242	1089	1042
14	16	70	2.625	70	2.173	1074	1118
14	16	70	2.625	70	2.102	1057	1186
14	16	70	2.625	70	2.035	1042	1302
14	16	70	2.625	70	1.959	1025	1325
14	16	70	2.625	70	1.892	1010	1481
14	16	70	2.625	70	1.791	987	1663
14	16	70	2.625	70	1.694	965	1888

Appendix C: Propane Shock Tube Data

Source: Burcat (1970) **Technique: Reflected**
Mixture: $C_3H_8/O_2/Ar$ **Equivalence Ratio (ϕ): 0.125 - 2.0**
% Diluent: 76 - 98 **Pressure (P): 2 - 10 atm**
Temperature (T): 1100 - 1600 K
Induction Period (τ_{ind}) End: Pressure and heat flux rise onset

Fuel (mol)	Oxygen (mol)	Diluent (mol)	ϕ	% Diluent	P (atm)	T (K)	τ_{ind} (μsec)
1.6	8	90.4	1.00	90.4	2.627	1486	89
1.6	8	90.4	1.00	90.4	2.565	1464	145
1.6	8	90.4	1.00	90.4	2.504	1443	168
1.6	8	90.4	1.00	90.4	2.500	1442	194
1.6	8	90.4	1.00	90.4	2.355	1392	254
1.6	8	90.4	1.00	90.4	2.380	1401	283
1.6	8	90.4	1.00	90.4	2.352	1391	306
1.6	8	90.4	1.00	90.4	2.341	1387	344
1.6	8	90.4	1.00	90.4	2.289	1369	421
1.6	8	90.4	1.00	90.4	2.284	1367	456
1.6	8	90.4	1.00	90.4	2.249	1355	459
1.6	8	90.4	1.00	90.4	2.229	1348	535
1.6	8	90.4	1.00	90.4	2.193	1336	558
1.6	8	90.4	1.00	90.4	2.175	1330	664
0.48	2.4	97.12	1.00	97.12	9.085	1532	83
0.48	2.4	97.12	1.00	97.12	8.931	1515	79
0.48	2.4	97.12	1.00	97.12	8.742	1495	85
0.48	2.4	97.12	1.00	97.12	8.202	1436	167
0.48	2.4	97.12	1.00	97.12	8.214	1437	212
0.48	2.4	97.12	1.00	97.12	8.095	1424	224
0.48	2.4	97.12	1.00	97.12	8.025	1417	229
0.48	2.4	97.12	1.00	97.12	7.899	1403	298
0.48	2.4	97.12	1.00	97.12	7.825	1395	322
0.48	2.4	97.12	1.00	97.12	7.626	1373	406
0.48	2.4	97.12	1.00	97.12	7.648	1376	453
0.48	2.4	97.12	1.00	97.12	7.513	1361	424
0.48	2.4	97.12	1.00	97.12	7.475	1357	418
0.48	2.4	97.12	1.00	97.12	7.396	1348	497

Fuel (mol)	Oxygen (mol)	Diluent (mol)	ϕ	% Diluent	P (atm)	T (K)	τ_{ind} (μsec)
0.48	2.4	97.12	1.00	97.12	7.230	1330	613
1.6	8	90.4	1.00	90.4	9.900	1435	79
1.6	8	90.4	1.00	90.4	9.265	1380	163
1.6	8	90.4	1.00	90.4	9.059	1362	180
1.6	8	90.4	1.00	90.4	9.079	1364	190
1.6	8	90.4	1.00	90.4	8.925	1351	182
1.6	8	90.4	1.00	90.4	8.905	1349	209
1.6	8	90.4	1.00	90.4	8.638	1326	280
1.6	8	90.4	1.00	90.4	8.442	1309	367
1.6	8	90.4	1.00	90.4	8.361	1302	383
3.85	19.23	76.92	1.00	76.92	14.016	1586	12
3.85	19.23	76.92	1.00	76.92	13.076	1521	20
3.85	19.23	76.92	1.00	76.92	10.579	1350	142
3.85	19.23	76.92	1.00	76.92	10.438	1341	139
3.85	19.23	76.92	1.00	76.92	10.422	1339	130
3.85	19.23	76.92	1.00	76.92	10.291	1330	149
3.85	19.23	76.92	1.00	76.92	9.996	1310	166
3.85	19.23	76.92	1.00	76.92	9.557	1280	253
3.85	19.23	76.92	1.00	76.92	9.349	1266	343
3.85	19.23	76.92	1.00	76.92	8.961	1239	356
3.85	19.23	76.92	1.00	76.92	8.982	1241	402
3.85	19.23	76.92	1.00	76.92	8.891	1235	420
3.85	19.23	76.92	1.00	76.92	8.368	1199	499
3.85	19.23	76.92	1.00	76.92	8.388	1200	557
3.85	19.23	76.92	1.00	76.92	8.173	1185	577
3.85	19.23	76.92	1.00	76.92	7.654	1150	732
0.8	8	91.2	0.50	91.2	8.561	1525	29
0.8	8	91.2	0.50	91.2	8.446	1513	37
0.8	8	91.2	0.50	91.2	8.237	1489	53
0.8	8	91.2	0.50	91.2	8.128	1477	59
0.8	8	91.2	0.50	91.2	8.124	1476	62
0.8	8	91.2	0.50	91.2	7.889	1450	67
0.8	8	91.2	0.50	91.2	7.754	1435	74
0.8	8	91.2	0.50	91.2	7.649	1423	70

Fuel (mol)	Oxygen (mol)	Diluent (mol)	ϕ	% Diluent	P (atm)	T (K)	τ_{ind} (μsec)
0.8	8	91.2	0.50	91.2	7.575	1415	97
0.8	8	91.2	0.50	91.2	7.372	1392	119
0.8	8	91.2	0.50	91.2	7.130	1365	155
0.8	8	91.2	0.50	91.2	7.118	1363	166
0.8	8	91.2	0.50	91.2	7.130	1365	173
0.8	8	91.2	0.50	91.2	6.999	1350	205
0.8	8	91.2	0.50	91.2	6.960	1346	256
0.8	8	91.2	0.50	91.2	6.832	1331	324
0.8	8	91.2	0.50	91.2	6.593	1304	522
0.8	8	91.2	0.50	91.2	6.473	1291	507
0.8	8	91.2	0.50	91.2	6.474	1291	429
0.84	2.1	97.06	2.00	97.06	8.281	1557	146
0.84	2.1	97.06	2.00	97.06	8.267	1556	156
0.84	2.1	97.06	2.00	97.06	8.145	1541	225
0.84	2.1	97.06	2.00	97.06	8.006	1525	179
0.84	2.1	97.06	2.00	97.06	7.852	1506	203
0.84	2.1	97.06	2.00	97.06	7.747	1494	231
0.84	2.1	97.06	2.00	97.06	7.573	1473	254
0.84	2.1	97.06	2.00	97.06	7.395	1452	304
0.84	2.1	97.06	2.00	97.06	7.395	1452	321
0.84	2.1	97.06	2.00	97.06	7.416	1454	445
0.84	2.1	97.06	2.00	97.06	7.348	1446	389
0.84	2.1	97.06	2.00	97.06	7.230	1432	384
0.84	2.1	97.06	2.00	97.06	7.288	1439	512
0.84	2.1	97.06	2.00	97.06	7.159	1424	428
0.84	2.1	97.06	2.00	97.06	7.009	1406	492
0.84	2.1	97.06	2.00	97.06	6.913	1394	565
0.84	2.1	97.06	2.00	97.06	6.850	1387	541
0.41	4.1	95.49	0.50	95.49	7.908	1535	56
0.41	4.1	95.49	0.50	95.49	7.828	1525	63
0.41	4.1	95.49	0.50	95.49	7.575	1494	78
0.41	4.1	95.49	0.50	95.49	7.448	1478	89
0.41	4.1	95.49	0.50	95.49	7.357	1467	98
0.41	4.1	95.49	0.50	95.49	7.271	1456	109

Fuel (mol)	Oxygen (mol)	Diluent (mol)	ϕ	% Diluent	P (atm)	T (K)	τ_{ind} (μsec)
0.41	4.1	95.49	0.50	95.49	7.185	1445	95
0.41	4.1	95.49	0.50	95.49	7.186	1445	109
0.41	4.1	95.49	0.50	95.49	7.002	1422	165
0.41	4.1	95.49	0.50	95.49	6.922	1412	194
0.41	4.1	95.49	0.50	95.49	6.767	1393	203
0.41	4.1	95.49	0.50	95.49	6.764	1392	228
0.41	4.1	95.49	0.50	95.49	6.671	1381	245
0.41	4.1	95.49	0.50	95.49	6.636	1376	310
0.41	4.1	95.49	0.50	95.49	6.607	1373	295
0.41	4.1	95.49	0.50	95.49	6.600	1372	308
0.41	4.1	95.49	0.50	95.49	6.374	1344	448
0.41	4.1	95.49	0.50	95.49	6.346	1340	423
0.41	4.1	95.49	0.50	95.49	6.339	1339	398
0.41	4.1	95.49	0.50	95.49	6.197	1322	485
0.41	4.1	95.49	0.50	95.49	6.160	1317	477
1.6	4	94.4	2.00	94.4	8.877	1520	126
1.6	4	94.4	2.00	94.4	8.915	1524	139
1.6	4	94.4	2.00	94.4	8.794	1511	135
1.6	4	94.4	2.00	94.4	8.641	1495	179
1.6	4	94.4	2.00	94.4	8.455	1475	208
1.6	4	94.4	2.00	94.4	8.357	1465	222
1.6	4	94.4	2.00	94.4	8.328	1462	231
1.6	4	94.4	2.00	94.4	8.187	1447	220
1.6	4	94.4	2.00	94.4	7.932	1420	380
1.6	4	94.4	2.00	94.4	7.845	1411	363
1.6	4	94.4	2.00	94.4	7.841	1411	423
1.6	4	94.4	2.00	94.4	7.778	1404	409
1.6	4	94.4	2.00	94.4	7.697	1396	407
1.6	4	94.4	2.00	94.4	7.663	1392	474
1.6	4	94.4	2.00	94.4	7.558	1381	516
1.6	4	94.4	2.00	94.4	7.450	1370	544
1.6	4	94.4	2.00	94.4	7.289	1353	569
0.41	16.4	83.19	0.13	83.19	8.916	1424	39
0.41	16.4	83.19	0.13	83.19	8.727	1406	48

Fuel (mol)	Oxygen (mol)	Diluent (mol)	ϕ	% Diluent	P (atm)	T (K)	τ_{ind} (μsec)
0.41	16.4	83.19	0.13	83.19	8.426	1376	64
0.41	16.4	83.19	0.13	83.19	8.439	1377	76
0.41	16.4	83.19	0.13	83.19	8.284	1362	78
0.41	16.4	83.19	0.13	83.19	8.150	1349	105
0.41	16.4	83.19	0.13	83.19	8.145	1349	112
0.41	16.4	83.19	0.13	83.19	7.669	1302	201
0.41	16.4	83.19	0.13	83.19	7.561	1291	223
0.41	16.4	83.19	0.13	83.19	7.515	1287	211
0.41	16.4	83.19	0.13	83.19	7.426	1278	295
0.41	16.4	83.19	0.13	83.19	7.332	1269	327
0.41	16.4	83.19	0.13	83.19	7.248	1261	332
0.8	16	83.2	0.25	83.2	9.663	1456	40
0.8	16	83.2	0.25	83.2	9.387	1430	45
0.8	16	83.2	0.25	83.2	9.296	1422	59
0.8	16	83.2	0.25	83.2	9.109	1405	62
0.8	16	83.2	0.25	83.2	9.001	1395	74
0.8	16	83.2	0.25	83.2	8.760	1372	84
0.8	16	83.2	0.25	83.2	8.712	1368	88
0.8	16	83.2	0.25	83.2	8.634	1361	108
0.8	16	83.2	0.25	83.2	8.622	1360	114
0.8	16	83.2	0.25	83.2	8.677	1365	116
0.8	16	83.2	0.25	83.2	8.411	1340	140
0.8	16	83.2	0.25	83.2	8.251	1325	177
0.8	16	83.2	0.25	83.2	8.160	1317	177
0.8	16	83.2	0.25	83.2	8.083	1310	223
0.8	16	83.2	0.25	83.2	7.438	1250	412
0.8	16	83.2	0.25	83.2	7.438	1250	432

Source: Burcat (1971) **Technique: Reflected**
Mixture: $C_3H_8/O_2/Ar$ **Equivalence Ratio (ϕ): 1.0**
% Diluent: 80.7 **Pressure (P): 8.0 - 14.2 atm**
Temperature (T): 1200 - 1700 K
Induction Period (τ_{ind}) End: Pressure and heat flux rise onset

Fuel (mol)	Oxygen (mol)	Diluent (mol)	ϕ	% Diluent	P (atm)	T (K)	τ_{ind} (μsec)
3.22	16.1	80.68	1	80.68	14.184	1701	6
3.22	16.1	80.68	1	80.68	9.737	1371	102
3.22	16.1	80.68	1	80.68	9.699	1368	126
3.22	16.1	80.68	1	80.68	9.479	1352	120
3.22	16.1	80.68	1	80.68	9.138	1327	186
3.22	16.1	80.68	1	80.68	9.055	1321	199
3.22	16.1	80.68	1	80.68	8.757	1299	267
3.22	16.1	80.68	1	80.68	8.454	1276	339
3.22	16.1	80.68	1	80.68	8.266	1262	411
3.22	16.1	80.68	1	80.68	8.182	1256	424
3.22	16.1	80.68	1	80.68	8.013	1244	499

Source: Gray (1994) **Technique: Incident**
Mixture: $C_3H_8/O_2/Ar$ **Equivalence Ratio (ϕ): 1.0**
% Diluent: 98.8 **Pressure (P): 1.4 - 1.7 atm**
Temperature (T): 1400 - 1800 K
Induction Period (τ_{ind}) End: CH* emission maximum

Fuel (mol)	Oxygen (mol)	Diluent (mol)	ϕ	% Diluent	P (atm)	T (K)	τ_{ind} (μsec)
0.2	1	98.8	1	98.8	1.652	1678	75
0.2	1	98.8	1	98.8	1.647	1673	104
0.2	1	98.8	1	98.8	1.635	1661	109
0.2	1	98.8	1	98.8	1.633	1659	99
0.2	1	98.8	1	98.8	1.626	1652	109
0.2	1	98.8	1	98.8	1.623	1649	104
0.2	1	98.8	1	98.8	1.608	1633	123
0.2	1	98.8	1	98.8	1.587	1612	138
0.2	1	98.8	1	98.8	1.586	1611	123
0.2	1	98.8	1	98.8	1.568	1593	164
0.2	1	98.8	1	98.8	1.554	1579	153
0.2	1	98.8	1	98.8	1.546	1570	154
0.2	1	98.8	1	98.8	1.547	1571	211
0.2	1	98.8	1	98.8	1.531	1555	251
0.2	1	98.8	1	98.8	1.519	1543	230
0.2	1	98.8	1	98.8	1.518	1542	302
0.2	1	98.8	1	98.8	1.494	1518	344
0.2	1	98.8	1	98.8	1.460	1483	456
0.2	1	98.8	1	98.8	1.453	1476	537
0.2	1	98.8	1	98.8	1.427	1450	534
0.2	1	98.8	1	98.8	1.417	1439	696
0.2	1	98.8	1	98.8	1.409	1431	612
0.2	1	98.8	1	98.8	1.406	1428	694

Source: Hawthorn (1966) **Technique: Incident**
Mixture: $C_3H_8/O_2/Ar$ **Equivalence Ratio (ϕ): 0.063 - 2.0**
% Diluent: 95 - 99 **Pressure (P): 0.61 - 1.7 atm**
Temperature (T): 1100 - 1500 K
Induction Period (τ_{ind}) End: Luminosity emission onset

Fuel (mol)	Oxygen (mol)	Diluent (mol)	ϕ	% Diluent	P (atm)	T (K)	τ_{ind} (μsec)
0.012	0.988	99	0.06	99	1.021	1363	255
0.012	0.988	99	0.06	99	1.021	1356	319
0.012	0.988	99	0.06	99	1.021	1332	444
0.012	0.988	99	0.06	99	1.021	1281	693
0.012	0.988	99	0.06	99	1.021	1267	802
0.012	0.988	99	0.06	99	1.021	1268	849
0.012	0.988	99	0.06	99	1.021	1249	943
0.012	0.988	99	0.06	99	1.021	1226	1252
0.012	0.988	99	0.06	99	1.021	1199	1587
0.024	0.976	99	0.12	99	1.021	1312	445
0.024	0.976	99	0.12	99	1.021	1295	572
0.024	0.976	99	0.12	99	1.021	1291	582
0.024	0.976	99	0.12	99	1.021	1289	684
0.024	0.976	99	0.12	99	1.021	1228	1331
0.024	0.976	99	0.12	99	1.021	1200	1844
0.038	0.962	99	0.20	99	1.021	1363	191
0.038	0.962	99	0.20	99	1.021	1359	248
0.038	0.962	99	0.20	99	1.021	1285	632
0.038	0.962	99	0.20	99	1.021	1276	680
0.038	0.962	99	0.20	99	1.021	1217	1331
0.038	0.962	99	0.20	99	1.021	1217	1411
0.038	0.962	99	0.20	99	1.021	1210	1470
0.038	0.962	99	0.20	99	1.021	1183	1918
0.038	0.962	99	0.20	99	1.021	1179	1811
0.038	0.962	99	0.20	99	1.021	1163	2560
0.118	0.882	99	0.67	99	1.021	1357	524
0.118	0.882	99	0.67	99	1.021	1341	768
0.118	0.882	99	0.67	99	1.021	1311	1048
0.118	0.882	99	0.67	99	1.021	1296	1235
0.118	0.882	99	0.67	99	1.021	1262	1704

Fuel (mol)	Oxygen (mol)	Diluent (mol)	ϕ	% Diluent	P (atm)	T (K)	τ_{ind} (μsec)
0.118	0.882	99	0.67	99	1.021	1253	1858
0.118	0.882	99	0.67	99	1.021	1233	2248
0.118	0.882	99	0.67	99	1.021	1181	3119
0.25	0.75	99	1.67	99	1.021	1472	459
0.25	0.75	99	1.67	99	1.021	1460	468
0.25	0.75	99	1.67	99	1.021	1454	541
0.25	0.75	99	1.67	99	1.021	1417	735
0.25	0.75	99	1.67	99	1.021	1389	1085
0.25	0.75	99	1.67	99	1.021	1348	1659
0.25	0.75	99	1.67	99	1.021	1311	1882
0.25	0.75	99	1.67	99	1.021	1277	2680
0.065	4.935	95	0.07	95	1.021	1264	389
0.065	4.935	95	0.07	95	1.021	1245	645
0.065	4.935	95	0.07	95	1.021	1244	709
0.065	4.935	95	0.07	95	1.021	1234	787
0.065	4.935	95	0.07	95	1.021	1234	833
0.065	4.935	95	0.07	95	1.021	1189	1290
0.065	4.935	95	0.07	95	1.021	1151	1897
0.065	4.935	95	0.07	95	1.021	1121	2485
0.192	4.808	95	0.20	95	1.021	1343	165
0.192	4.808	95	0.20	95	1.021	1301	326
0.192	4.808	95	0.20	95	1.021	1310	388
0.192	4.808	95	0.20	95	1.021	1284	461
0.192	4.808	95	0.20	95	1.021	1286	525
0.192	4.808	95	0.20	95	1.021	1273	567
0.192	4.808	95	0.20	95	1.021	1276	598
0.192	4.808	95	0.20	95	1.021	1264	655
0.192	4.808	95	0.20	95	1.021	1264	780
0.192	4.808	95	0.20	95	1.021	1246	840
0.192	4.808	95	0.20	95	1.021	1211	1156
0.192	4.808	95	0.20	95	1.021	1203	1346
0.192	4.808	95	0.20	95	1.021	1203	1425
0.192	4.808	95	0.20	95	1.021	1189	1430
0.192	4.808	95	0.20	95	1.021	1168	1675

Fuel (mol)	Oxygen (mol)	Diluent (mol)	ϕ	% Diluent	P (atm)	T (K)	τ_{ind} (μsec)
0.192	4.808	95	0.20	95	1.021	1168	2128
0.192	4.808	95	0.20	95	1.021	1166	2240
0.192	4.808	95	0.20	95	1.021	1151	2189
0.192	4.808	95	0.20	95	1.021	1121	2916
0.413	4.587	95	0.45	95	1.021	1378	133
0.413	4.587	95	0.45	95	1.021	1361	200
0.413	4.587	95	0.45	95	1.021	1344	261
0.413	4.587	95	0.45	95	1.021	1329	331
0.413	4.587	95	0.45	95	1.021	1285	384
0.413	4.587	95	0.45	95	1.021	1276	401
0.413	4.587	95	0.45	95	1.021	1285	428
0.413	4.587	95	0.45	95	1.021	1277	464
0.413	4.587	95	0.45	95	1.021	1269	460
0.413	4.587	95	0.45	95	1.021	1264	527
0.413	4.587	95	0.45	95	1.021	1249	591
0.413	4.587	95	0.45	95	1.021	1257	661
0.413	4.587	95	0.45	95	1.021	1246	669
0.413	4.587	95	0.45	95	1.021	1175	2368
0.413	4.587	95	0.45	95	1.021	1154	2636
0.413	4.587	95	0.45	95	1.021	1142	2678
0.413	4.587	95	0.45	95	1.021	1146	2920
0.413	4.587	95	0.45	95	1.021	1116	3172
1.429	3.571	95	2.00	95	1.021	1428	289
1.429	3.571	95	2.00	95	1.021	1365	362
1.429	3.571	95	2.00	95	1.021	1350	513
1.429	3.571	95	2.00	95	1.021	1322	769
1.429	3.571	95	2.00	95	1.021	1314	777
1.429	3.571	95	2.00	95	1.021	1320	860
1.429	3.571	95	2.00	95	1.021	1314	929
1.429	3.571	95	2.00	95	1.021	1256	2279
1.429	3.571	95	2.00	95	1.021	1240	2311
1.429	3.571	95	2.00	95	1.021	1230	2331
0.192	4.808	95	0.20	95	0.612	1353	401
0.192	4.808	95	0.20	95	0.612	1342	595

Fuel (mol)	Oxygen (mol)	Diluent (mol)	ϕ	% Diluent	P (atm)	T (K)	τ_{ind} (μsec)
0.192	4.808	95	0.20	95	0.612	1308	653
0.192	4.808	95	0.20	95	0.612	1263	1025
0.192	4.808	95	0.20	95	0.612	1265	1109
0.192	4.808	95	0.20	95	0.612	1241	1439
0.192	4.808	95	0.20	95	0.612	1233	1444
0.192	4.808	95	0.20	95	0.612	1192	1943
0.192	4.808	95	0.20	95	1.021	1344	167
0.192	4.808	95	0.20	95	1.021	1314	393
0.192	4.808	95	0.20	95	1.021	1290	522
0.192	4.808	95	0.20	95	1.021	1279	579
0.192	4.808	95	0.20	95	1.021	1266	640
0.192	4.808	95	0.20	95	1.021	1267	778
0.192	4.808	95	0.20	95	1.021	1205	1341
0.192	4.808	95	0.20	95	1.021	1205	1427
0.192	4.808	95	0.20	95	1.021	1168	2147
0.192	4.808	95	0.20	95	1.701	1282	427
0.192	4.808	95	0.20	95	1.701	1282	446
0.192	4.808	95	0.20	95	1.701	1240	669
0.192	4.808	95	0.20	95	1.701	1221	867
0.192	4.808	95	0.20	95	1.701	1227	895
0.192	4.808	95	0.20	95	1.701	1188	1235
0.192	4.808	95	0.20	95	1.701	1162	1737

Source: Myers (1969) **Technique: Incident**
Mixture: $C_3H_8/O_2/Ar$ **Equivalence Ratio (ϕ): 0.2**
% Diluent: 95 **Pressure (P): 1 atm**
Temperature (T): 1000 - 1500 K
Induction Period (τ_{ind}) End: OH emission maximum

Fuel (mol)	Oxygen (mol)	Diluent (mol)	ϕ	% Diluent	P (atm)	T (K)	τ_{ind} (μsec)
0.19	4.81	95	0.20	95	1	1463	69
0.19	4.81	95	0.20	95	1	1398	129
0.19	4.81	95	0.20	95	1	1414	152
0.19	4.81	95	0.20	95	1	1340	251
0.19	4.81	95	0.20	95	1	1334	333
0.19	4.81	95	0.20	95	1	1332	366
0.19	4.81	95	0.20	95	1	1319	453
0.19	4.81	95	0.20	95	1	1302	525
0.19	4.81	95	0.20	95	1	1282	664
0.19	4.81	95	0.20	95	1	1266	867
0.19	4.81	95	0.20	95	1	1206	1495
0.19	4.81	95	0.20	95	1	1116	2845
0.19	4.81	95	0.20	95	1	1089	3096

Source: Steinberg (1954) **Technique: Reflected**
Mixture: $C_3H_8/O_2/N_2$ **Equivalence Ratio (ϕ): 1.0**
% Diluent: 75.8 **Pressure (P): 5 - 25 atm**
Temperature (T): 1100 - 1600 K
Induction Period (τ_{ind}) End: Luminosity emission onset

Fuel (mol)	Oxygen (mol)	Diluent (mol)	ϕ	% Diluent	P (atm)	T (K)	τ_{ind} (μsec)
4	20.2	75.8	0.99	75.8	7.9	1368	14
4	20.2	75.8	0.99	75.8	7.12	1316	16
4	20.2	75.8	0.99	75.8	7.74	1244	204
4	20.2	75.8	0.99	75.8	7.24	1212	241
4	20.2	75.8	0.99	75.8	16.02	1443	11
4	20.2	75.8	0.99	75.8	15.53	1284	44
4	20.2	75.8	0.99	75.8	14.87	1261	83
4	20.2	75.8	0.99	75.8	15.53	1272	171
4	20.2	75.8	0.99	75.8	14.69	1217	233
4	20.2	75.8	0.99	75.8	14.24	1210	230
4	20.2	75.8	0.99	75.8	14.69	1215	409
4	20.2	75.8	0.99	75.8	13.63	1184	413
4	20.2	75.8	0.99	75.8	13.63	1185	277
4	20.2	75.8	0.99	75.8	13.63	1185	249
4	20.2	75.8	0.99	75.8	13.82	1155	241
4	20.2	75.8	0.99	75.8	13.82	1154	314
4	20.2	75.8	0.99	75.8	13.82	1154	439
4	20.2	75.8	0.99	75.8	13.82	1154	403
4	20.2	75.8	0.99	75.8	23.6	1334	12
4	20.2	75.8	0.99	75.8	23.3	1282	95
4	20.2	75.8	0.99	75.8	21.73	1249	101
4	20.2	75.8	0.99	75.8	21.73	1249	111
4	20.2	75.8	0.99	75.8	21.73	1232	130
4	20.2	75.8	0.99	75.8	21.2	1213	208
4	20.2	75.8	0.99	75.8	21.11	1183	255
4	20.2	75.8	0.99	75.8	20.7	1165	277
4	20.2	75.8	0.99	75.8	20.7	1164	331
4	20.2	75.8	0.99	75.8	20.35	1154	287
4	20.2	75.8	0.99	75.8	20.35	1154	418
4	20.2	75.8	0.99	75.8	20.35	1154	370

Appendix D: Analysis Results from Induction Time Comparison of Constant Volume Explosion Simulations with Shock Tube Experiments

The average deviation is defined by:

$$Deviation = \frac{1}{N}\sum_{i=1}^{N}\log\left(\frac{\tau_{s,i}}{\tau_{e,i}}\right)$$

where N is the total number of data points in the dataset or temperature range under consideration, $\tau_{s,i}$ is the i-th simulated induction time, and $\tau_{e,i}$ is the i-th experimental induction time.

Battin-Leclerc (1997) reaction mechanism

Fuel	Shock Tube Dataset	Average Error	Standard Deviation
H_2	Asaba (1965)	0.451	0.201
	Belles (1965)	0.167	0.110
	Bhaskaran (1973)	-0.126	0.148
	Cheng (1977)	0.064	0.087
	Cohen (1967)	0.222	0.435
	Craig (1966)	0.331	0.498
	Fujimoto (1963)	-0.220	0.696
	Jachimowski (1971)	0.267	0.064
	Just (1968)	-0.324	0.762
	Petersen (1996)	0.148	0.171
	Schott (1958)	0.194	0.163
	Skinner (1966)	0.301	0.168
	Snyder (1965)	0.557	1.120
	Steinberg (1955)	3.385	0.374
C_2H_4	Baker (1972)	0.394	0.453
	Drummond (1968)	0.913	0.163
	Gay (1967)	0.435	0.124
	Hidaka (1974)	0.214	0.126
	Homer (1967)	0.212	0.160
	Jachimowski (1977)	0.403	0.161
	Suzuki (1971)	1.455	0.393

Fuel	Shock Tube Dataset	Average Error	Standard Deviation
C_3H_8	Burcat (1970)	-0.700	0.480
	Burcat (1971)	-0.600	0.218
	Gray (1994)	-0.944	0.081
	Hawthorn (1966)	0.263	0.557
	Myers (1969)	0.318	0.553
	Steinberg (1954)	0.546	0.321

	H_2		C_2H_4		C_3H_8	
Temperature Range (K)	Average Error	Standard Deviation	Average Error	Standard Deviation	Average Error	Standard Deviation
775 - 900	1.731	1.214				
900 - 1000	0.228	0.957	2.091	0.291		
1000 - 1100	-0.022	0.383	1.319	0.196		
1100 - 1200	0.137	0.163	1.091	0.284	0.893	0.342
1200 - 1300	0.111	0.248	0.849	0.388	0.240	0.368
1300 - 1400	0.118	0.242	0.579	0.406	-0.448	0.428
1400 - 1500	0.234	0.129	0.319	0.373	-0.891	0.360
1500 - 1600	0.232	0.182	0.222	0.268	-1.074	0.253
1600 - 1700	0.248	0.172	0.226	0.286	-1.019	0.057
1700 - 1800	0.197	0.224	0.195	0.236		
1800 - 1900	0.315	0.222	0.304	0.226		
1900 - 2000	0.250	0.251	0.323	0.170		
2000 - 2650	0.260	0.289	0.253	0.171		

Baulch (1994) reaction mechanism

Fuel	Shock Tube Dataset	Average Error	Standard Deviation
H_2	Asaba (1965)	0.420	0.184
	Belles (1965)	0.161	0.120
	Bhaskaran (1973)	0.132	0.249
	Cheng (1977)	0.070	0.088
	Cohen (1967)	0.397	0.626
	Craig (1966)	2.215	0.622
	Fujimoto (1963)	0.265	0.990
	Jachimowski (1971)	0.254	0.062
	Just (1968)	0.441	0.890
	Petersen (1996)	0.162	0.199
	Schott (1958)	0.169	0.156
	Skinner (1966)	0.698	0.258
	Snyder (1965)	1.634	0.531
	Steinberg (1955)	3.634	0.316

	H_2	
Temperature Range (K)	Average Error	Standard Deviation
775 - 900	2.512	0.677
900 - 1000	1.458	0.819
1000 - 1100	0.289	0.472
1100 - 1200	0.152	0.155
1200 - 1300	0.124	0.255
1300 - 1400	0.123	0.241
1400 - 1500	0.229	0.121
1500 - 1600	0.229	0.173
1600 - 1700	0.232	0.169
1700 - 1800	0.172	0.211
1800 - 1900	0.286	0.227
1900 - 2000	0.230	0.262
2000 - 2650	0.218	0.255

Bowman (1995) reaction mechanism

Fuel	Shock Tube Dataset	Average Error	Standard Deviation
H_2	Asaba (1965)	0.432	0.166
	Belles (1965)	0.174	0.115
	Bhaskaran (1973)	-0.078	0.100
	Cheng (1977)	0.071	0.087
	Cohen (1967)	0.358	0.487
	Craig (1966)	1.276	0.715
	Fujimoto (1963)	0.102	0.855
	Jachimowski (1971)	0.269	0.062
	Just (1968)	-0.017	0.901
	Petersen (1996)	0.159	0.160
	Schott (1958)	0.190	0.153
	Skinner (1966)	0.451	0.156
	Snyder (1965)	0.888	0.953
	Steinberg (1955)	3.402	0.357
C_2H_4	Baker (1972)	0.604	0.618
	Drummond (1968)	1.310	0.384
	Gay (1967)	0.531	0.128
	Hidaka (1974)	0.326	0.116
	Homer (1967)	0.313	0.159
	Jachimowski (1977)	0.528	0.169
	Suzuki (1971)	2.456	0.267

	H_2		C_2H_4	
Temperature Range (K)	Average Error	Standard Deviation	Average Error	Standard Deviation
775 - 900	2.152	0.793		
900 - 1000	0.699	0.920	2.690	0.094
1000 - 1100	0.087	0.422	2.536	0.275
1100 - 1200	0.143	0.159	1.915	0.516
1200 - 1300	0.111	0.242	1.281	0.676
1300 - 1400	0.125	0.246	0.752	0.542
1400 - 1500	0.240	0.122	0.415	0.406
1500 - 1600	0.245	0.176	0.321	0.273

	H_2		C_2H_4	
Temperature Range (K)	Average Error	Standard Deviation	Average Error	Standard Deviation
1600 - 1700	0.254	0.170	0.330	0.285
1700 - 1800	0.194	0.209	0.308	0.230
1800 - 1900	0.293	0.200	0.419	0.224
1900 - 2000	0.243	0.245	0.435	0.169
2000 - 2650	0.241	0.238	0.366	0.169

Dagaut (1998) reaction mechanism

Fuel	Shock Tube Dataset	Average Error	Standard Deviation
H_2	Asaba (1965)	0.362	0.207
	Belles (1965)	0.120	0.132
	Bhaskaran (1973)	-0.071	0.061
	Cheng (1977)	0.078	0.117
	Cohen (1967)	0.488	0.594
	Craig (1966)	1.358	0.575
	Fujimoto (1963)	0.325	0.911
	Jachimowski (1971)	0.223	0.072
	Just (1968)	0.254	0.619
	Petersen (1996)	0.157	0.262
	Schott (1958)	0.107	0.176
	Skinner (1966)	0.674	0.137
	Snyder (1965)	1.011	0.715
	Steinberg (1955)	3.350	0.378
C_2H_4	Baker (1972)	-0.156	0.500
	Drummond (1968)	0.097	0.246
	Gay (1967)	0.286	0.163
	Hidaka (1974)	-0.056	0.106
	Homer (1967)	0.065	0.070
	Jachimowski (1977)	0.212	0.103
	Suzuki (1971)	1.111	0.427

Fuel	Shock Tube Dataset	Average Error	Standard Deviation
C_3H_8	Burcat (1970)	0.054	0.129
	Burcat (1971)	0.163	0.110
	Gray (1994)	-0.161	0.068
	Hawthorn (1966)	0.615	0.252
	Myers (1969)	0.431	0.380
	Steinberg (1954)	0.476	0.265

	H_2		C_2H_4		C_3H_8	
Temperature Range (K)	Average Error	Standard Deviation	Average Error	Standard Deviation	Average Error	Standard Deviation
775 - 900	2.120	0.749				
900 - 1000	0.909	0.682	1.807	0.304		
1000 - 1100	0.264	0.424	1.009	0.208		
1100 - 1200	0.163	0.164	0.601	0.486	0.728	0.340
1200 - 1300	0.111	0.283	0.183	0.643	0.471	0.230
1300 - 1400	0.102	0.274	-0.209	0.290	0.243	0.259
1400 - 1500	0.183	0.126	-0.202	0.240	0.024	0.150
1500 - 1600	0.184	0.176	-0.099	0.271	-0.140	0.083
1600 - 1700	0.172	0.171	-0.036	0.325	-0.190	0.040
1700 - 1800	0.114	0.211	-0.007	0.266		
1800 - 1900	0.216	0.228	0.119	0.227		
1900 - 2000	0.149	0.264	0.162	0.165		
2000 - 2650	0.147	0.300	0.155	0.180		

Frenklach (1994,1995) reaction mechanism

Fuel	Shock Tube Dataset	Average Error	Standard Deviation
H_2	Asaba (1965)	0.430	0.167
	Belles (1965)	0.170	0.116
	Bhaskaran (1973)	-0.084	0.100
	Cheng (1977)	0.067	0.088
	Cohen (1967)	0.335	0.553
	Craig (1966)	1.325	0.747
	Fujimoto (1963)	0.115	0.880
	Jachimowski (1971)	0.264	0.062
	Just (1968)	0.074	0.855
	Petersen (1996)	0.165	0.168
	Schott (1958)	0.186	0.154
	Skinner (1966)	0.491	0.172
	Snyder (1965)	0.920	0.967
	Steinberg (1955)	3.440	0.352
C_2H_4	Baker (1972)	0.628	0.621
	Drummond (1968)	1.323	0.387
	Gay (1967)	0.529	0.124
	Hidaka (1974)	0.334	0.117
	Homer (1967)	0.313	0.162
	Jachimowski (1977)	0.527	0.169
	Suzuki (1971)	2.469	0.264

	H_2		C_2H_4	
Temperature Range (K)	Average Error	Standard Deviation	Average Error	Standard Deviation
775 - 900	2.202	0.784		
900 - 1000	0.720	0.953	2.690	0.094
1000 - 1100	0.122	0.372	2.551	0.271
1100 - 1200	0.139	0.160	1.942	0.505
1200 - 1300	0.109	0.246	1.303	0.662
1300 - 1400	0.124	0.249	0.766	0.533
1400 - 1500	0.237	0.122	0.431	0.402
1500 - 1600	0.244	0.175	0.331	0.271

	H_2		C_2H_4	
Temperature Range (K)	Average Error	Standard Deviation	Average Error	Standard Deviation
1600 - 1700	0.250	0.170	0.336	0.280
1700 - 1800	0.191	0.209	0.310	0.225
1800 - 1900	0.290	0.201	0.419	0.222
1900 - 2000	0.239	0.245	0.433	0.168
2000 - 2650	0.238	0.239	0.366	0.168

Glassman (1996) reaction mechanism

Fuel	Shock Tube Dataset	Average Error	Standard Deviation
H_2	Asaba (1965)	0.378	0.134
	Belles (1965)	0.958	0.804
	Bhaskaran (1973)	2.004	0.221
	Cheng (1977)	2.132	0.614
	Cohen (1967)	2.159	0.938
	Craig (1966)	2.831	0.314
	Fujimoto (1963)	2.210	0.647
	Jachimowski (1971)	1.049	0.917
	Just (1968)	2.615	0.471
	Petersen (1996)	0.434	0.540
	Schott (1958)	0.393	0.695
	Skinner (1966)	1.839	0.285
	Snyder (1965)	1.979	0.398
	Steinberg (1955)	3.518	0.322
C_2H_4	Baker (1972)	0.699	0.476
	Drummond (1968)	0.962	0.199
	Gay (1967)	0.221	0.119
	Hidaka (1974)	0.142	0.224
	Homer (1967)	0.040	0.190
	Jachimowski (1977)	0.174	0.148
	Suzuki (1971)	1.331	0.439

Fuel	Shock Tube Dataset	Average Error	Standard Deviation
C_3H_8	Burcat (1970)	0.246	0.358
	Burcat (1971)	0.237	0.227
	Gray (1994)	-0.046	0.163
	Hawthorn (1966)	1.214	0.450
	Myers (1969)	1.179	0.537
	Steinberg (1954)	1.062	0.210

	H_2		C_2H_4		C_3H_8	
Temperature Range (K)	Average Error	Standard Deviation	Average Error	Standard Deviation	Average Error	Standard Deviation
775 - 900	2.540	0.646				
900 - 1000	2.307	0.570	2.047	0.395		
1000 - 1100	2.587	0.485	1.218	0.202		
1100 - 1200	2.410	0.273	1.074	0.225	1.484	0.490
1200 - 1300	1.847	0.297	1.037	0.209	1.126	0.352
1300 - 1400	1.267	0.313	0.898	0.204	0.518	0.356
1400 - 1500	0.676	0.217	0.606	0.258	0.118	0.269
1500 - 1600	0.324	0.157	0.279	0.220	-0.145	0.191
1600 - 1700	0.235	0.148	0.141	0.232	-0.207	0.076
1700 - 1800	0.161	0.194	0.034	0.202		
1800 - 1900	0.165	0.205	0.095	0.202		
1900 - 2000	0.131	0.280	0.100	0.158		
2000 - 2650	0.196	0.267	0.073	0.166		

Konnov (1998) reaction mechanism

Fuel	Shock Tube Dataset	Average Error	Standard Deviation
H_2	Asaba (1965)	0.387	0.200
	Belles (1965)	0.116	0.115
	Bhaskaran (1973)	0.021	0.154
	Cheng (1977)	0.006	0.088
	Cohen (1967)	0.240	0.439
	Craig (1966)	1.694	0.498
	Fujimoto (1963)	0.080	0.852
	Jachimowski (1971)	0.212	0.071
	Just (1968)	0.286	0.710
	Petersen (1996)	0.066	0.126
	Schott (1958)	0.127	0.161
	Skinner (1966)	0.201	0.145
	Snyder (1965)	1.187	0.532
	Steinberg (1955)	3.323	0.372
C_2H_4	Baker (1972)	-0.020	0.158
	Drummond (1968)	0.187	0.173
	Gay (1967)	0.455	0.120
	Hidaka (1974)	0.239	0.073
	Homer (1967)	0.241	0.106
	Jachimowski (1977)	0.512	0.140
	Suzuki (1971)	0.851	0.472
C_3H_8	Burcat (1970)	-0.168	0.182
	Burcat (1971)	-0.186	0.034
	Gray (1994)	-0.035	0.070
	Hawthorn (1966)	0.277	0.255
	Myers (1969)	0.055	0.200
	Steinberg (1954)	0.013	0.292

	H_2		C_2H_4		C_3H_8	
Temperature Range (K)	Average Error	Standard Deviation	Average Error	Standard Deviation	Average Error	Standard Deviation
775 - 900	2.138	0.718				
900 - 1000	1.027	0.665	1.652	0.290		

	H_2		C_2H_4		C_3H_8	
Temperature Range (K)	Average Error	Standard Deviation	Average Error	Standard Deviation	Average Error	Standard Deviation
1000 - 1100	0.116	0.332	0.782	0.254		
1100 - 1200	0.082	0.159	0.367	0.269	0.166	0.291
1200 - 1300	0.042	0.230	0.128	0.230	0.058	0.303
1300 - 1400	0.053	0.240	0.034	0.164	-0.008	0.329
1400 - 1500	0.174	0.126	0.048	0.207	-0.048	0.220
1500 - 1600	0.176	0.179	0.155	0.232	-0.096	0.096
1600 - 1700	0.185	0.174	0.239	0.259	-0.093	0.062
1700 - 1800	0.133	0.222	0.248	0.214		
1800 - 1900	0.277	0.244	0.368	0.213		
1900 - 2000	0.196	0.264	0.405	0.169		
2000 - 2650	0.183	0.266	0.357	0.168		

Lutz (1988) reaction mechanism

Fuel	Shock Tube Dataset	Average Error	Standard Deviation
H_2	Asaba (1965)	0.434	0.211
	Belles (1965)	0.137	0.105
	Bhaskaran (1973)	-0.121	0.068
	Cheng (1977)	0.010	0.088
	Cohen (1967)	0.296	0.506
	Craig (1966)	1.600	0.787
	Fujimoto (1963)	0.110	0.938
	Jachimowski (1971)	0.230	0.078
	Just (1968)	0.240	0.787
	Petersen (1996)	0.103	0.146
	Schott (1958)	0.157	0.156
	Skinner (1966)	0.362	0.172
	Snyder (1965)	1.068	0.825
	Steinberg (1955)	3.465	0.346

Fuel	Shock Tube Dataset	Average Error	Standard Deviation
C_2H_4	Baker (1972)	-0.046	0.257
	Drummond (1968)	0.523	0.255
	Gay (1967)	0.506	0.130
	Hidaka (1974)	0.212	0.069
	Homer (1967)	0.277	0.092
	Jachimowski (1977)	0.438	0.116
	Suzuki (1971)	1.519	0.468

	H_2		C_2H_4	
Temperature Range (K)	Average Error	Standard Deviation	Average Error	Standard Deviation
775 - 900	2.295	0.713		
900 - 1000	0.908	0.851	2.328	0.254
1000 - 1100	0.076	0.362	1.379	0.324
1100 - 1200	0.085	0.163	0.852	0.498
1200 - 1300	0.050	0.241	0.383	0.576
1300 - 1400	0.064	0.245	0.051	0.344
1400 - 1500	0.180	0.126	0.000	0.258
1500 - 1600	0.194	0.188	0.139	0.263
1600 - 1700	0.216	0.184	0.234	0.287
1700 - 1800	0.176	0.235	0.250	0.236
1800 - 1900	0.321	0.254	0.363	0.208
1900 - 2000	0.234	0.254	0.391	0.156
2000 - 2650	0.242	0.264	0.365	0.164

Maas (1988) reaction mechanism

Fuel	Shock Tube Dataset	Average Error	Standard Deviation
H_2	Asaba (1965)	0.462	0.158
	Belles (1965)	0.354	0.465
	Bhaskaran (1973)	1.751	0.163
	Cheng (1977)	1.392	0.615
	Cohen (1967)	1.523	0.761
	Craig (1966)	1.975	0.343
	Fujimoto (1963)	1.514	0.500
	Jachimowski (1971)	0.388	0.221
	Just (1968)	1.897	0.585
	Petersen (1996)	0.310	0.485
	Schott (1958)	0.218	0.304
	Skinner (1966)	1.021	0.405
	Snyder (1965)	1.122	0.413
	Steinberg (1955)	2.193	0.325

	H_2	
Temperature Range (K)	Average Error	Standard Deviation
775 - 900	1.438	0.635
900 - 1000	1.490	0.585
1000 - 1100	1.909	0.388
1100 - 1200	1.488	0.504
1200 - 1300	1.023	0.471
1300 - 1400	0.503	0.316
1400 - 1500	0.292	0.114
1500 - 1600	0.244	0.177
1600 - 1700	0.241	0.168
1700 - 1800	0.167	0.211
1800 - 1900	0.245	0.211
1900 - 2000	0.191	0.263
2000 - 2650	0.279	0.311

Miller (1989) reaction mechanism

Fuel	Shock Tube Dataset	Average Error	Standard Deviation
H_2	Asaba (1965)	0.435	0.213
	Belles (1965)	0.136	0.104
	Bhaskaran (1973)	-0.116	0.062
	Cheng (1977)	0.010	0.088
	Cohen (1967)	0.298	0.507
	Craig (1966)	1.628	0.783
	Fujimoto (1963)	0.117	0.941
	Jachimowski (1971)	0.229	0.079
	Just (1968)	0.247	0.794
	Petersen (1996)	0.103	0.146
	Schott (1958)	0.157	0.156
	Skinner (1966)	0.365	0.172
	Snyder (1965)	1.094	0.805
	Steinberg (1955)	3.466	0.346
C_2H_4	Baker (1972)	0.021	0.299
	Drummond (1968)	0.566	0.278
	Gay (1967)	0.462	0.123
	Hidaka (1974)	0.180	0.063
	Homer (1967)	0.223	0.108
	Jachimowski (1977)	0.382	0.126
	Suzuki (1971)	1.562	0.456

	H_2		C_2H_4	
Temperature Range (K)	Average Error	Standard Deviation	Average Error	Standard Deviation
775 - 900	2.303	0.709		
900 - 1000	0.934	0.842	2.344	0.245
1000 - 1100	0.080	0.363	1.437	0.290
1100 - 1200	0.085	0.162	0.948	0.453
1200 - 1300	0.050	0.241	0.463	0.553
1300 - 1400	0.064	0.245	0.094	0.335
1400 - 1500	0.180	0.126	0.010	0.246
1500 - 1600	0.194	0.188	0.125	0.255

	H_2		C_2H_4	
Temperature Range (K)	Average Error	Standard Deviation	Average Error	Standard Deviation
1600 - 1700	0.216	0.184	0.209	0.281
1700 - 1800	0.176	0.235	0.215	0.233
1800 - 1900	0.321	0.254	0.319	0.207
1900 - 2000	0.235	0.253	0.338	0.156
2000 - 2650	0.243	0.267	0.293	0.164

Pilling (1996a) reaction mechanism

Fuel	Shock Tube Dataset	Average Error	Standard Deviation
H_2	Asaba (1965)	0.421	0.182
	Belles (1965)	0.168	0.121
	Bhaskaran (1973)	0.141	0.260
	Cheng (1977)	0.067	0.091
	Cohen (1967)	0.407	0.578
	Craig (1966)	2.260	0.614
	Fujimoto (1963)	0.283	1.005
	Jachimowski (1971)	0.240	0.083
	Just (1968)	0.451	0.903
	Petersen (1996)	0.159	0.191
	Schott (1958)	0.169	0.160
	Skinner (1966)	0.682	0.251
	Snyder (1965)	1.703	0.540
	Steinberg (1955)	3.629	0.335
C_2H_4	Baker (1972)	1.453	0.653
	Drummond (1968)	2.124	0.322
	Gay (1967)	0.691	0.147
	Hidaka (1974)	0.681	0.340
	Homer (1967)	0.471	0.356
	Jachimowski (1977)	0.624	0.237
	Suzuki (1971)	2.799	0.161

	H_2		C_2H_4	
Temperature Range (K)	Average Error	Standard Deviation	Average Error	Standard Deviation
775 - 900	2.575	0.656		
900 - 1000	1.514	0.799	2.690	0.094
1000 - 1100	0.283	0.477	2.835	0.194
1100 - 1200	0.134	0.155	2.562	0.333
1200 - 1300	0.113	0.254	2.153	0.425
1300 - 1400	0.124	0.246	1.698	0.393
1400 - 1500	0.233	0.125	1.290	0.382
1500 - 1600	0.234	0.174	0.909	0.298
1600 - 1700	0.237	0.169	0.711	0.270
1700 - 1800	0.177	0.211	0.537	0.195
1800 - 1900	0.292	0.224	0.555	0.229
1900 - 2000	0.232	0.260	0.516	0.188
2000 - 2650	0.219	0.252	0.387	0.177

Pilling (1996b) reaction mechanism

Fuel	Shock Tube Dataset	Average Error	Standard Deviation
H_2	Asaba (1965)	0.423	0.183
	Belles (1965)	0.170	0.121
	Bhaskaran (1973)	0.142	0.259
	Cheng (1977)	0.072	0.088
	Cohen (1967)	0.393	0.564
	Craig (1966)	2.257	0.613
	Fujimoto (1963)	0.262	0.994
	Jachimowski (1971)	0.262	0.063
	Just (1968)	0.453	0.901
	Petersen (1996)	0.155	0.180
	Schott (1958)	0.178	0.159
	Skinner (1966)	0.654	0.249
	Snyder (1965)	1.700	0.539
	Steinberg (1955)	3.627	0.335

	H_2	
Temperature Range (K)	Average Error	Standard Deviation
775 - 900	2.571	0.658
900 - 1000	1.506	0.803
1000 - 1100	0.281	0.465
1100 - 1200	0.152	0.157
1200 - 1300	0.121	0.250
1300 - 1400	0.125	0.244
1400 - 1500	0.236	0.123
1500 - 1600	0.234	0.175
1600 - 1700	0.238	0.170
1700 - 1800	0.178	0.212
1800 - 1900	0.296	0.225
1900 - 2000	0.234	0.259
2000 - 2650	0.220	0.252

Pilling (1998) reaction mechanism

Fuel	Shock Tube Dataset	Average Error	Standard Deviation
H_2	Asaba (1965)	0.421	0.183
	Belles (1965)	0.168	0.120
	Bhaskaran (1973)	0.141	0.260
	Cheng (1977)	0.059	0.108
	Cohen (1967)	0.405	0.579
	Craig (1966)	2.260	0.614
	Fujimoto (1963)	0.283	1.005
	Jachimowski (1971)	0.238	0.084
	Just (1968)	0.451	0.903
	Petersen (1996)	0.157	0.189
	Schott (1958)	0.168	0.161
	Skinner (1966)	0.682	0.251
	Snyder (1965)	1.703	0.540
	Steinberg (1955)	3.629	0.335

Fuel	Shock Tube Dataset	Average Error	Standard Deviation
C_2H_4	Baker (1972)	1.453	0.653
	Drummond (1968)	2.124	0.322
	Gay (1967)	0.691	0.147
	Hidaka (1974)	0.681	0.340
	Homer (1967)	0.471	0.356
	Jachimowski (1977)	0.624	0.237
	Suzuki (1971)	2.799	0.161

	H_2		C_2H_4	
Temperature Range (K)	Average Error	Standard Deviation	Average Error	Standard Deviation
775 - 900	2.575	0.656		
900 - 1000	1.514	0.799	2.690	0.094
1000 - 1100	0.277	0.483	2.836	0.194
1100 - 1200	0.120	0.165	2.561	0.334
1200 - 1300	0.115	0.253	2.153	0.425
1300 - 1400	0.122	0.244	1.698	0.393
1400 - 1500	0.233	0.125	1.290	0.382
1500 - 1600	0.231	0.174	0.910	0.297
1600 - 1700	0.237	0.169	0.711	0.270
1700 - 1800	0.177	0.211	0.537	0.194
1800 - 1900	0.292	0.224	0.555	0.229
1900 - 2000	0.231	0.260	0.516	0.189
2000 - 2650	0.218	0.253	0.387	0.177

Tan (1994) reaction mechanism

Fuel	Shock Tube Dataset	Average Error	Standard Deviation
H_2	Asaba (1965)	0.365	0.210
	Belles (1965)	0.120	0.132
	Bhaskaran (1973)	-0.072	0.061
	Cheng (1977)	0.078	0.117
	Cohen (1967)	0.488	0.594
	Craig (1966)	1.358	0.575
	Fujimoto (1963)	0.325	0.911
	Jachimowski (1971)	0.223	0.073
	Just (1968)	0.255	0.618
	Petersen (1996)	0.157	0.262
	Schott (1958)	0.107	0.176
	Skinner (1966)	0.674	0.137
	Snyder (1965)	1.011	0.715
	Steinberg (1955)	3.350	0.378
C_2H_4	Baker (1972)	-0.178	0.432
	Drummond (1968)	0.097	0.246
	Gay (1967)	0.286	0.164
	Hidaka (1974)	-0.055	0.104
	Homer (1967)	0.065	0.070
	Jachimowski (1977)	0.212	0.103
	Suzuki (1971)	1.111	0.427
C_3H_8	Burcat (1970)	0.054	0.129
	Burcat (1971)	0.163	0.110
	Gray (1994)	-0.161	0.068
	Hawthorn (1966)	0.615	0.254
	Myers (1969)	0.431	0.380
	Steinberg (1954)	0.476	0.265

	H_2		C_2H_4		C_3H_8	
Temperature Range (K)	Average Error	Standard Deviation	Average Error	Standard Deviation	Average Error	Standard Deviation
775 - 900	2.120	0.749				
900 - 1000	0.909	0.682	1.807	0.304		

	H_2		C_2H_4		C_3H_8	
Temperature Range (K)	Average Error	Standard Deviation	Average Error	Standard Deviation	Average Error	Standard Deviation
1000 - 1100	0.264	0.424	1.009	0.208		
1100 - 1200	0.163	0.164	0.582	0.457	0.730	0.339
1200 - 1300	0.111	0.283	0.143	0.606	0.469	0.232
1300 - 1400	0.103	0.274	-0.195	0.277	0.243	0.259
1400 - 1500	0.183	0.126	-0.200	0.240	0.024	0.150
1500 - 1600	0.185	0.176	-0.097	0.267	-0.140	0.083
1600 - 1700	0.172	0.171	-0.034	0.323	-0.190	0.040
1700 - 1800	0.114	0.211	-0.007	0.267		
1800 - 1900	0.216	0.226	0.120	0.227		
1900 - 2000	0.149	0.265	0.163	0.165		
2000 - 2650	0.152	0.308	0.155	0.180		

Wang (1997) reaction mechanism

Fuel	Shock Tube Dataset	Average Error	Standard Deviation
H_2	Asaba (1965)	0.425	0.162
	Belles (1965)	0.170	0.116
	Bhaskaran (1973)	-0.084	0.100
	Cheng (1977)	0.196	0.274
	Cohen (1967)	0.754	0.792
	Craig (1966)	1.325	0.747
	Fujimoto (1963)	0.894	1.118
	Jachimowski (1971)	0.273	0.062
	Just (1968)	0.038	0.891
	Petersen (1996)	0.279	0.296
	Schott (1958)	0.197	0.161
	Skinner (1966)	1.018	0.194
	Snyder (1965)	0.920	0.967
	Steinberg (1955)	3.440	0.352

Fuel	Shock Tube Dataset	Average Error	Standard Deviation
C_2H_4	Baker (1972)	-0.075	0.408
	Drummond (1968)	0.208	0.210
	Gay (1967)	0.402	0.150
	Hidaka (1974)	0.064	0.106
	Homer (1967)	0.165	0.099
	Jachimowski (1977)	0.300	0.119
	Suzuki (1971)	1.180	0.544

	H_2		C_2H_4	
Temperature Range (K)	Average Error	Standard Deviation	Average Error	Standard Deviation
775 - 900	2.246	0.766		
900 - 1000	0.882	0.989	2.112	0.319
1000 - 1100	0.509	0.633	1.105	0.285
1100 - 1200	0.236	0.221	0.624	0.330
1200 - 1300	0.166	0.313	0.217	0.438
1300 - 1400	0.165	0.298	-0.085	0.357
1400 - 1500	0.247	0.126	-0.144	0.322
1500 - 1600	0.263	0.172	0.004	0.312
1600 - 1700	0.263	0.161	0.083	0.335
1700 - 1800	0.209	0.201	0.121	0.258
1800 - 1900	0.285	0.197	0.244	0.213
1900 - 2000	0.236	0.241	0.269	0.153
2000 - 2650	0.233	0.231	0.227	0.169

Wang (1999) reaction mechanism

Fuel	Shock Tube Dataset	Average Error	Standard Deviation
H_2	Asaba (1965)	0.433	0.153
	Belles (1965)	0.164	0.128
	Bhaskaran (1973)	0.041	0.054
	Cheng (1977)	0.108	0.107
	Cohen (1967)	0.467	0.728
	Craig (1966)	1.785	0.554
	Fujimoto (1963)	0.531	1.000
	Jachimowski (1971)	-0.247	1.411
	Just (1968)	-0.080	1.096
	Petersen (1996)	0.134	0.190
	Schott (1958)	0.099	0.491
	Skinner (1966)	0.638	0.136
	Snyder (1965)	1.206	0.553
	Steinberg (1955)	3.272	0.372
C_2H_4	Baker (1972)	0.218	0.249
	Drummond (1968)	0.438	0.135
	Gay (1967)	0.544	0.119
	Hidaka (1974)	0.411	0.089
	Homer (1967)	0.349	0.144
	Jachimowski (1977)	0.619	0.181
	Suzuki (1971)	0.947	0.439
C_3H_8	Burcat (1970)	-0.257	0.110
	Burcat (1971)	-0.228	0.103
	Gray (1994)	-0.497	0.255
	Hawthorn (1966)	0.304	0.211
	Myers (1969)	0.112	0.301
	Steinberg (1954)	0.132	0.248

	H_2		C_2H_4		C_3H_8	
Temperature Range (K)	Average Error	Standard Deviation	Average Error	Standard Deviation	Average Error	Standard Deviation
775 - 900	2.188	0.672				
900 - 1000	1.127	0.761	1.663	0.310		

	H_2		C_2H_4		C_3H_8	
Temperature Range (K)	Average Error	Standard Deviation	Average Error	Standard Deviation	Average Error	Standard Deviation
1000 - 1100	0.170	0.640	0.839	0.224		
1100 - 1200	0.068	0.391	0.556	0.281	0.361	0.305
1200 - 1300	-0.085	1.021	0.371	0.277	0.140	0.239
1300 - 1400	-0.079	1.031	0.299	0.230	-0.072	0.263
1400 - 1500	0.226	0.123	0.284	0.248	-0.245	0.162
1500 - 1600	0.219	0.175	0.345	0.236	-0.382	0.069
1600 - 1700	0.221	0.172	0.394	0.256	-0.722	0.233
1700 - 1800	0.156	0.214	0.391	0.201		
1800 - 1900	0.247	0.203	0.500	0.212		
1900 - 2000	0.193	0.251	0.510	0.170		
2000 - 2650	0.257	0.279	0.427	0.164		

Warnatz (1997) reaction mechanism

Fuel	Shock Tube Dataset	Average Error	Standard Deviation
H_2	Asaba (1965)	0.427	0.172
	Belles (1965)	0.170	0.110
	Bhaskaran (1973)	-0.018	0.030
	Cheng (1977)	0.262	0.397
	Cohen (1967)	0.879	0.865
	Craig (1966)	1.714	0.727
	Fujimoto (1963)	1.091	1.112
	Jachimowski (1971)	0.270	0.065
	Just (1968)	0.139	0.951
	Petersen (1996)	0.407	0.521
	Schott (1958)	0.194	0.166
	Skinner (1966)	1.172	0.277
	Snyder (1965)	1.178	0.694
	Steinberg (1955)	3.332	0.356

Fuel	Shock Tube Dataset	Average Error	Standard Deviation
C_2H_4	Baker (1972)	0.273	0.326
	Drummond (1968)	0.468	0.277
	Gay (1967)	0.453	0.133
	Hidaka (1974)	0.292	0.072
	Homer (1967)	0.219	0.130
	Jachimowski (1977)	0.378	0.139
	Suzuki (1971)	1.761	0.495

	H_2		C_2H_4	
Temperature Range (K)	Average Error	Standard Deviation	Average Error	Standard Deviation
775 - 900	2.249	0.674		
900 - 1000	1.199	0.836	2.552	0.123
1000 - 1100	0.724	0.771	1.754	0.299
1100 - 1200	0.296	0.320	1.102	0.506
1200 - 1300	0.223	0.457	0.526	0.463
1300 - 1400	0.207	0.410	0.251	0.230
1400 - 1500	0.243	0.127	0.247	0.171
1500 - 1600	0.263	0.172	0.257	0.177
1600 - 1700	0.261	0.158	0.316	0.209
1700 - 1800	0.215	0.197	0.302	0.191
1800 - 1900	0.292	0.205	0.359	0.176
1900 - 2000	0.248	0.248	0.346	0.138
2000 - 2650	0.231	0.244	0.279	0.165

Westbrook (1982) reaction mechanism

Fuel	Shock Tube Dataset	Average Error	Standard Deviation
H_2	Asaba (1965)	0.553	0.127
	Belles (1965)	0.250	0.117
	Bhaskaran (1973)	0.023	0.081
	Cheng (1977)	0.176	0.102
	Cohen (1967)	0.564	0.561
	Craig (1966)	1.491	0.692
	Fujimoto (1963)	0.372	0.925
	Jachimowski (1971)	0.265	0.694
	Just (1968)	0.133	0.901
	Petersen (1996)	0.199	0.209
	Schott (1958)	0.279	0.174
	Skinner (1966)	0.639	0.143
	Snyder (1965)	1.047	0.764
	Steinberg (1955)	3.374	0.353
C_2H_4	Baker (1972)	0.244	0.259
	Drummond (1968)	0.776	0.169
	Gay (1967)	0.574	0.125
	Hidaka (1974)	0.315	0.100
	Homer (1967)	0.324	0.156
	Jachimowski (1977)	0.498	0.158
	Suzuki (1971)	1.584	0.451

	H_2		C_2H_4	
Temperature Range (K)	Average Error	Standard Deviation	Average Error	Standard Deviation
775 - 900	2.209	0.698		
900 - 1000	0.920	0.823	2.357	0.240
1000 - 1100	0.299	0.428	1.458	0.282
1100 - 1200	0.244	0.165	1.013	0.396
1200 - 1300	0.142	0.611	0.643	0.453
1300 - 1400	0.197	0.254	0.380	0.310
1400 - 1500	0.315	0.129	0.295	0.276
1500 - 1600	0.306	0.189	0.330	0.253

	H_2		C_2H_4	
Temperature Range (K)	Average Error	Standard Deviation	Average Error	Standard Deviation
1600 - 1700	0.331	0.182	0.357	0.284
1700 - 1800	0.254	0.230	0.326	0.240
1800 - 1900	0.369	0.211	0.420	0.227
1900 - 2000	0.334	0.279	0.430	0.172
2000 - 2650	0.397	0.241	0.359	0.185

Westbrook (1984) reaction mechanism

Fuel	Shock Tube Dataset	Average Error	Standard Deviation
H_2	Asaba (1965)	0.558	0.131
	Belles (1965)	0.253	0.116
	Bhaskaran (1973)	0.023	0.082
	Cheng (1977)	0.177	0.102
	Cohen (1967)	0.516	0.640
	Craig (1966)	1.482	0.692
	Fujimoto (1963)	0.367	0.922
	Jachimowski (1971)	0.180	0.971
	Just (1968)	0.180	0.878
	Petersen (1996)	0.198	0.207
	Schott (1958)	0.271	0.221
	Skinner (1966)	0.634	0.142
	Snyder (1965)	1.041	0.768
	Steinberg (1955)	3.372	0.353
C_2H_4	Baker (1972)	0.398	0.370
	Drummond (1968)	1.040	0.230
	Gay (1967)	0.569	0.122
	Hidaka (1974)	0.328	0.128
	Homer (1967)	0.321	0.187
	Jachimowski (1977)	0.489	0.176
	Suzuki (1971)	1.815	0.376

Fuel	Shock Tube Dataset	Average Error	Standard Deviation
C_3H_8	Burcat (1970)	0.140	0.120
	Burcat (1971)	0.104	0.097
	Gray (1994)	-0.150	0.107
	Hawthorn (1966)	0.791	0.237
	Myers (1969)	0.644	0.339
	Steinberg (1954)	0.418	0.266

	H_2		C_2H_4		C_3H_8	
Temperature Range (K)	Average Error	Standard Deviation	Average Error	Standard Deviation	Average Error	Standard Deviation
775 - 900	2.205	0.699				
900 - 1000	0.913	0.825	2.456	0.169		
1000 - 1100	0.276	0.477	1.690	0.259		
1100 - 1200	0.228	0.240	1.292	0.405	0.808	0.420
1200 - 1300	0.084	0.821	0.912	0.519	0.587	0.296
1300 - 1400	0.198	0.253	0.574	0.399	0.344	0.278
1400 - 1500	0.316	0.128	0.392	0.324	0.142	0.148
1500 - 1600	0.307	0.189	0.369	0.263	-0.075	0.097
1600 - 1700	0.333	0.182	0.371	0.287	-0.227	0.048
1700 - 1800	0.255	0.230	0.324	0.241		
1800 - 1900	0.373	0.212	0.414	0.233		
1900 - 2000	0.334	0.277	0.418	0.175		
2000 - 2650	0.406	0.248	0.329	0.183		

Appendix E: Hydrogen Detonation Properties

Initial temperature is always 295 K, and the initial pressure is 1 bar unless otherwise stated.

Nomenclature:
0 : pre-shock condition
a : acoustic speed
CJ : Chapman-Jouguet state condition
Cp : specific heat at constant pressure
$Dil\ \%_{vol}$: percent diluent by volume
M_{CJ} : Chapman-Jouguet detonation Mach number
P : pressure
Q : heat of reaction non-dimensionalized by $R_0 T_0$
R : mixture gas constant
T : temperature
u : fluid velocity (in shock-fixed reference frame)
vN : post-shock condition
V_{CJ} : Chapman-Jouguet detonation velocity
W : molecular mass
Δ : reaction zone length
Δh^0 : heat of reaction extrapolated to zero temperature
ϕ : equivalence ratio
γ : ratio of specific heats
θ : non-dimensional effective activation energy parameter
τ: reaction zone time

Hydrogen-oxygen mixtures with varying equivalence ratio

ϕ	γ_0	a_0 (m/s)	W_0 (g/mol)	V_{CJ} (m/s)	P_{CJ} (bar)	T_{CJ} (K)	a_{CJ} (m/s)	γ_{CJ}	W_{CJ} (g/mol)	M_{CJ}	u_{vN} (m/s)	P_{vN} (bar)	T_{vN} (K)	a_{vN} (m/s)	γ_{vN}	Cp_{vN} (J/kgK)	Δh^0 (MJ/kg)	Q
0.2	1.403	383.2	23.432	1825.8	15.2	2842	1012.0	1.17	26.805	4.77	1493.6	27.1	1452	821.2	1.31	1503	4.551	43.480
0.4	1.403	429.3	18.673	2187.0	17.5	3351	1193.7	1.17	22.158	5.09	1796.6	30.9	1628	974.6	1.31	1880	6.540	49.794
0.6	1.404	469.1	15.645	2447.3	18.4	3554	1332.1	1.19	18.811	5.22	2011.1	32.4	1703	1089.9	1.31	2233	7.233	46.139
0.8	1.404	504.1	13.548	2661.4	18.8	3649	1447.4	1.21	16.351	5.28	2186.4	33.1	1745	1186.3	1.31	2567	7.643	42.216
1	1.404	535.5	12.010	2842.1	19.0	3682	1545.4	1.22	14.474	5.31	2333.4	33.5	1767	1268.7	1.32	2886	8.270	40.498
1.2	1.404	563.8	10.834	2995.2	19.1	3673	1629.4	1.22	13.002	5.31	2457.2	33.5	1776	1339.7	1.32	3187	9.185	40.574
1.4	1.405	589.7	9.906	3125.0	19.0	3635	1701.9	1.21	11.821	5.30	2561.1	33.3	1774	1401.1	1.32	3473	10.535	42.551
1.6	1.405	613.4	9.155	3235.1	18.8	3579	1764.9	1.20	10.857	5.27	2648.4	33.0	1764	1454.5	1.32	3744	11.926	44.515
1.8	1.405	635.4	8.534	3328.9	18.5	3512	1819.8	1.19	10.058	5.24	2722.0	32.5	1750	1501.0	1.32	4001	13.372	46.527
2	1.405	655.8	8.013	3409.0	18.2	3439	1868.1	1.18	9.386	5.20	2783.9	32.0	1731	1541.9	1.32	4245	14.894	48.662
2.2	1.405	674.8	7.568	3477.6	17.8	3363	1911.0	1.18	8.814	5.15	2836.2	31.4	1710	1577.9	1.33	4478	15.496	47.817
2.4	1.405	692.6	7.185	3536.7	17.5	3286	1948.8	1.18	8.322	5.11	2880.6	30.8	1688	1609.4	1.33	4705	16.020	46.929
2.6	1.405	709.2	6.852	3587.5	17.1	3209	1982.5	1.18	7.894	5.06	2918.0	30.2	1665	1637.8	1.33	4917	16.474	46.023
2.8	1.405	724.9	6.559	3631.2	16.7	3133	2012.8	1.19	7.518	5.01	2949.5	29.6	1641	1663.1	1.33	5117	15.872	42.446
3	1.405	739.7	6.299	3668.5	16.3	3059	2040.1	1.19	7.186	4.96	2975.8	29.0	1618	1685.8	1.33	5306	16.193	41.587

ϕ	Konnov (1998) Reaction Mechanism			Tan (1994) Reaction Mechanism		
	Δ (mm)	τ (μs)	θ	Δ (mm)	τ (μs)	θ
0.2	0.193	0.568	19.434	0.097	0.282	10.324
0.4	0.051	0.126	8.408	0.039	0.097	6.775
0.6	0.042	0.092	7.134	0.033	0.074	6.218
0.8	0.041	0.083	6.612	0.033	0.068	6.040
1	0.043	0.082	6.386	0.035	0.068	5.931

ϕ	**Konnov (1998) Reaction Mechanism**			**Tan (1994) Reaction Mechanism**		
	Δ ***(mm)***	τ ***(μs)***	θ	Δ ***(mm)***	τ ***(μs)***	θ
1.2	0.048	0.085	6.266	0.039	0.071	5.923
1.4	0.054	0.092	6.299	0.045	0.077	5.958
1.6	0.062	0.102	6.366	0.051	0.085	6.032
1.8	0.073	0.115	6.478	0.059	0.095	6.120
2	0.085	0.130	6.690	0.070	0.108	6.164
2.2	0.100	0.150	6.938	0.082	0.124	6.287
2.4	0.118	0.173	7.139	0.096	0.142	6.440
2.6	0.140	0.201	7.492	0.113	0.164	6.589
2.8	0.166	0.235	7.858	0.133	0.189	6.728
3	0.198	0.276	8.293	0.157	0.220	6.978

Stoichiometric hydrogen-oxygen mixtures with varying initial pressure

P_0	γ_0	a_0 (m/s)	W_0 (g/mol)	V_{CJ} (m/s)	P_{CJ} (bar)	T_{CJ} (K)	a_{CJ} (m/s)	γ_{CJ}	W_{CJ} (g/mol)	M_{CJ}	u_{vN} (m/s)	P_{vN} (bar)	T_{vN} (K)	a_{vN} (m/s)	γ_{vN}	Cp_{vN} (J/kgK)	Δh^0 (MJ/kg)	Q
0.2	1.404	535.5	12.010	2753.2	3.6	3391	1494.0	1.23	14.155	5.14	2252.7	6.3	1682	1239.2	1.32	2866	7.377	36.122
0.4	1.404	535.5	12.010	2791.4	7.4	3513	1516.0	1.22	14.286	5.21	2287.4	12.9	1719	1252.0	1.32	2872	7.979	39.072
0.6	1.404	535.5	12.010	2813.7	11.2	3586	1528.9	1.22	14.367	5.25	2307.6	19.7	1740	1259.4	1.32	2878	8.106	39.691
0.8	1.404	535.5	12.010	2829.7	15.1	3640	1538.2	1.22	14.427	5.28	2322.2	26.6	1755	1264.7	1.32	2882	8.199	40.148
1.0	1.404	535.5	12.010	2842.1	19.0	3682	1545.4	1.22	14.474	5.31	2333.4	33.5	1767	1268.7	1.32	2886	8.270	40.498
1.2	1.404	535.5	12.010	2852.1	23.0	3717	1551.2	1.22	14.514	5.33	2342.5	40.4	1777	1272.0	1.32	2888	8.329	40.787
1.4	1.404	535.5	12.010	2860.7	27.0	3746	1556.2	1.22	14.548	5.34	2350.3	47.5	1785	1274.8	1.31	2891	8.376	41.016
1.6	1.404	535.5	12.010	2868.1	31.0	3772	1560.5	1.22	14.577	5.36	2357.0	54.6	1793	1277.2	1.31	2893	8.420	41.231
1.8	1.404	535.5	12.010	2874.6	35.0	3795	1564.2	1.22	14.604	5.37	2362.9	61.7	1799	1279.3	1.31	2896	8.457	41.415
2.0	1.404	535.5	12.010	2880.4	39.0	3816	1567.6	1.22	14.628	5.38	2368.2	68.8	1805	1281.1	1.31	2900	8.492	41.586

P_0	Konnov (1998) Reaction Mechanism			Tan (1994) Reaction Mechanism		
	Δ (mm)	τ (μs)	θ	Δ (mm)	τ (μs)	θ
0.2	0.241	0.470	5.453	0.221	0.434	5.791
0.4	0.112	0.214	5.608	0.099	0.193	5.786
0.6	0.072	0.138	5.839	0.063	0.121	5.759
0.8	0.054	0.102	6.040	0.045	0.087	5.840
1	0.043	0.082	6.384	0.035	0.068	5.931
1.2	0.037	0.069	6.702	0.029	0.055	6.066
1.4	0.032	0.060	7.059	0.025	0.047	6.078
1.6	0.029	0.054	7.418	0.021	0.041	6.180
1.8	0.026	0.049	7.810	0.019	0.036	6.292
2	0.024	0.045	8.238	0.017	0.032	6.382

Hydrogen-air mixtures with varying equivalence ratio

ϕ	γ_0	a_0 (m/s)	W_0 (g/mol)	V_{CJ} (m/s)	P_{CJ} (bar)	T_{CJ} (K)	a_{CJ} (m/s)	γ_{CJ}	W_{CJ} (g/mol)	M_{CJ}	u_{vN} (m/s)	P_{vN} (bar)	T_{vN} (K)	a_{vN} (m/s)	γ_{vN}	Cp_{vN} (J/kgK)	Δh^0 (MJ/kg)	Q
0.2	1.403	358.6	26.770	1163.8	6.8	1270	704.1	1.31	27.850	3.25	888.3	12.3	858	599.6	1.35	1199	0.854	9.327
0.4	1.404	371.2	24.990	1490.9	10.5	1936	867.9	1.26	26.920	4.02	1185.3	19.0	1149	713.3	1.33	1340	1.822	18.561
0.6	1.404	383.3	23.448	1709.5	13.0	2428	973.0	1.22	26.004	4.46	1379.3	23.5	1341	793.3	1.32	1452	2.954	28.240
0.8	1.404	394.8	22.100	1865.6	14.8	2768	1044.3	1.19	25.021	4.73	1515.7	26.5	1465	852.7	1.32	1555	4.182	37.684
1	1.405	405.9	20.911	1971.4	15.8	2948	1092.2	1.17	23.904	4.86	1606.0	28.0	1531	895.6	1.32	1647	5.306	45.240
1.2	1.404	416.5	19.856	2033.6	15.9	2976	1128.9	1.18	22.699	4.88	1656.8	28.3	1545	923.9	1.32	1732	5.292	42.843
1.4	1.405	426.8	18.912	2072.8	15.6	2932	1157.4	1.19	21.538	4.86	1686.9	28.0	1536	944.3	1.32	1811	5.164	39.816
1.6	1.405	436.7	18.063	2101.8	15.3	2866	1179.8	1.20	20.474	4.81	1707.8	27.4	1517	961.0	1.32	1888	5.001	36.831
1.8	1.405	446.3	17.295	2125.5	14.9	2795	1198.7	1.21	19.510	4.76	1724.1	26.8	1495	975.7	1.32	1963	4.832	34.076
2	1.404	455.6	16.597	2146.5	14.5	2724	1215.3	1.22	18.635	4.71	1738.2	26.3	1473	989.3	1.33	2036	4.664	31.560
2.2	1.405	464.6	15.961	2165.0	14.2	2655	1230.2	1.23	17.841	4.66	1750.2	25.7	1450	1001.8	1.33	2107	4.500	29.287
2.4	1.405	473.3	15.377	2181.4	13.8	2588	1243.5	1.23	17.117	4.61	1760.4	25.1	1428	1013.4	1.33	2177	4.562	28.604
2.6	1.405	481.8	14.841	2196.2	13.5	2524	1255.8	1.24	16.454	4.56	1769.3	24.5	1406	1024.3	1.33	2246	4.395	26.594
2.8	1.405	490.1	14.345	2209.6	13.2	2463	1267.3	1.24	15.846	4.51	1777.1	24.0	1384	1034.7	1.33	2311	4.443	25.988
3	1.405	498.1	13.887	2221.8	12.9	2404	1277.8	1.25	15.286	4.46	1783.9	23.4	1363	1044.4	1.34	2377	4.274	24.198

ϕ	**Konnov (1998) Reaction Mechanism**			**Tan (1994) Reaction Mechanism**		
	Δ *(mm)*	τ *(μs)*	θ	Δ *(mm)*	τ *(μs)*	θ
0.2	171500.000	611100.000	27.519	224600.000	798000.000	27.401
0.4	91.730	298.100	22.457	83.810	271.900	25.883
0.6	2.307	6.919	25.962	0.713	2.112	18.837
0.8	0.349	0.971	14.101	0.235	0.654	9.311
1	0.215	0.571	10.122	0.164	0.438	7.975

	Konnov (1998) Reaction Mechanism			Tan (1994) Reaction Mechanism		
ϕ	Δ *(mm)*	τ *(μs)*	θ	Δ *(mm)*	τ *(μs)*	θ
1.2	0.201	0.518	9.568	0.156	0.404	7.702
1.4	0.221	0.555	9.919	0.170	0.429	7.865
1.6	0.259	0.638	10.695	0.194	0.480	8.134
1.8	0.316	0.764	11.902	0.228	0.553	8.482
2	0.395	0.941	13.510	0.271	0.646	8.927
2.2	0.510	1.199	15.646	0.325	0.761	9.531
2.4	0.684	1.590	18.159	0.393	0.909	10.217
2.6	0.951	2.187	20.494	0.481	1.097	11.074
2.8	1.356	3.089	21.955	0.596	1.343	12.211
3	1.948	4.393	22.487	0.751	1.672	13.654

Stoichiometric hydrogen-air mixtures with varying initial pressure

P_0	γ_0	a_0 (m/s)	W_0 (g/mol)	V_{CJ} (m/s)	P_{CJ} (bar)	T_{CJ} (K)	a_{CJ} (m/s)	γ_{CJ}	W_{CJ} (g/mol)	M_{CJ}	u_{vN} (m/s)	P_{vN} (bar)	T_{vN} (K)	a_{vN} (m/s)	γ_{vN}	Cp_{vN} (J/kgK)	Δh^0 (MJ/kg)	Q
0.2	1.405	405.9	20.911	1934.9	3.1	2826	1067.1	1.16	23.714	4.77	1572.7	5.4	1488	883.6	1.32	1641	5.479	46.711
0.4	1.405	405.9	20.911	1951.2	6.2	2880	1078.0	1.17	23.798	4.81	1587.6	11.0	1507	889.0	1.32	1644	5.202	44.356
0.6	1.405	405.9	20.911	1960.3	9.4	2910	1084.4	1.17	23.846	4.83	1595.9	16.6	1517	892.0	1.32	1645	5.248	44.741
0.8	1.405	405.9	20.911	1966.6	12.6	2931	1088.9	1.17	23.879	4.85	1601.7	22.3	1525	894.0	1.32	1647	5.279	45.012
1.0	1.405	405.9	20.911	1971.4	15.8	2948	1092.2	1.17	23.904	4.86	1606.0	28.0	1531	895.6	1.32	1647	5.306	45.240
1.2	1.405	405.9	20.911	1975.2	19.0	2961	1094.9	1.18	23.924	4.87	1609.5	33.7	1535	896.9	1.32	1648	4.995	42.586
1.4	1.405	405.9	20.911	1978.4	22.2	2971	1097.2	1.18	23.942	4.87	1612.4	39.5	1539	897.9	1.32	1649	5.008	42.696
1.6	1.405	405.9	20.911	1981.1	25.4	2981	1099.1	1.18	23.956	4.88	1614.9	45.2	1542	898.8	1.32	1649	5.023	42.825
1.8	1.405	405.9	20.911	1983.5	28.7	2989	1100.8	1.18	23.969	4.89	1617.1	51.0	1545	899.6	1.32	1650	5.034	42.920
2.0	1.405	405.9	20.911	1985.6	31.9	2996	1102.3	1.18	23.980	4.89	1619.0	56.8	1547	900.3	1.32	1650	5.044	43.003

P_0	**Konnov (1998) Reaction Mechanism**			**Tan (1994) Reaction Mechanism**		
	Δ (mm)	τ (μs)	θ	Δ (mm)	τ (μs)	θ
0.2	0.840	2.271	6.323	0.813	2.210	6.601
0.4	0.424	1.137	6.928	0.389	1.051	6.861
0.6	0.299	0.796	7.726	0.261	0.701	7.165
0.8	0.243	0.645	8.761	0.199	0.532	7.521
1	0.215	0.571	10.124	0.164	0.438	7.975
1.2	0.202	0.538	11.863	0.142	0.378	8.430
1.4	0.200	0.532	13.957	0.127	0.338	9.006
1.6	0.206	0.548	16.038	0.117	0.311	9.669
1.8	0.216	0.576	17.476	0.110	0.292	10.453
2	0.228	0.608	18.106	0.106	0.280	11.351

Stoichiometric hydrogen-oxygen-argon mixtures with varying argon dilution

Dil $\%_{vol}$	γ_0	a_0 *(m/s)*	W_0 *(g/mol)*	V_{CJ} *(m/s)*	P_{CJ} *(bar)*	T_{CJ} *(K)*	a_{CJ} *(m/s)*	γ_{CJ}	W_{CJ} *(g/mol)*	M_{CJ}	u_{vN} *(m/s)*	P_{vN} *(bar)*	T_{vN} *(K)*	a_{vN} *(m/s)*	γ_{vN}	Cp_{vN} *(J/kgK)*	Δh^0 *(MJ/kg)*	Q
0	1.404	535.5	12.010	2842.1	19.0	3682	1545.4	1.22	14.474	5.31	2333.4	33.5	1767	1268.7	1.32	2886	8.270	40.498
10	1.424	485.7	14.801	2566.7	19.1	3641	1399.2	1.21	17.535	5.28	2092.7	33.4	1820	1166.5	1.33	2265	7.141	43.092
20	1.441	448.1	17.597	2357.3	19.1	3594	1287.0	1.21	20.555	5.26	1906.9	33.3	1874	1092.6	1.35	1830	6.021	43.202
30	1.460	419.1	20.392	2189.7	19.0	3538	1198.8	1.20	23.478	5.23	1755.6	33.0	1928	1037.1	1.37	1513	5.490	45.645
40	1.484	396.3	23.184	2049.4	18.9	3469	1126.0	1.20	26.273	5.17	1626.5	32.5	1979	993.8	1.39	1274	4.821	45.571
50	1.509	377.5	25.977	1926.2	18.6	3382	1063.9	1.20	29.001	5.10	1510.9	31.8	2024	958.9	1.42	1083	4.264	45.164
60	1.537	361.9	28.771	1811.6	18.1	3262	1008.8	1.21	31.638	5.01	1401.5	30.8	2056	928.8	1.45	928	3.573	41.911
70	1.568	349.1	31.564	1694.3	17.1	3080	957.9	1.24	34.169	4.85	1288.9	29.1	2054	898.5	1.49	799	2.687	34.578
80	1.603	338.2	34.357	1545.4	14.8	2728	906.8	1.33	36.528	4.57	1149.5	25.9	1956	853.9	1.54	690	1.531	21.452
90	1.643	329.3	37.151	1236.0	9.4	1828	786.6	1.56	38.428	3.75	879.5	17.5	1486	730.3	1.60	595	0.478	7.235

Dil $\%_{vol}$	**Konnov (1998) Reaction Mechanism**			**Tan (1994) Reaction Mechanism**		
	Δ *(mm)*	τ *(μs)*	θ	Δ *(mm)*	τ *(μs)*	θ
0	0.043	0.082	6.386	0.035	0.068	5.931
10	0.039	0.078	5.816	0.032	0.067	5.670
20	0.036	0.076	5.343	0.030	0.066	5.550
30	0.035	0.078	5.088	0.030	0.067	5.363
40	0.036	0.084	4.861	0.031	0.072	5.270
50	0.040	0.095	4.687	0.034	0.082	5.020
60	0.049	0.116	4.550	0.042	0.101	5.039
70	0.068	0.166	4.664	0.059	0.143	5.063
80	0.136	0.338	4.794	0.120	0.299	5.276
90	1.230	3.403	6.693	1.301	3.598	7.611

Stoichiometric hydrogen-oxygen-carbon dioxide mixtures with varying carbon dioxide dilution

Dil $\%_{vol}$	γ_0	a_0 *(m/s)*	W_0 *(g/mol)*	V_{CJ} *(m/s)*	P_{CJ} *(bar)*	T_{CJ} *(K)*	a_{CJ} *(m/s)*	γ_{CJ}	W_{CJ} *(g/mol)*	M_{CJ}	u_{vN} *(m/s)*	P_{vN} *(bar)*	T_{vN} *(K)*	a_{vN} *(m/s)*	γ_{vN}	Cp_{vN} *(J/kgK)*	Δh^0 *(MJ/kg)*	Q
0	1.404	535.5	12.010	2842.1	19.0	3682	1545.4	1.22	14.474	5.31	2333.4	33.5	1767	1268.7	1.32	2886	8.270	40.498
10	1.391	473.7	15.207	2438.3	17.8	3459	1325.4	1.19	18.375	5.15	2018.5	31.5	1601	1064.2	1.29	2407	7.187	44.564
20	1.374	427.9	18.410	2136.5	16.6	3224	1161.5	1.16	22.249	4.99	1780.0	29.5	1454	915.4	1.28	2090	6.662	50.004
30	1.359	392.8	21.612	1899.5	15.5	2988	1033.6	1.15	25.992	4.84	1590.2	27.6	1327	801.9	1.26	1863	5.644	49.732
40	1.349	365.1	24.810	1703.2	14.3	2746	929.3	1.13	29.529	4.66	1430.3	25.6	1212	711.4	1.25	1697	5.324	53.859
50	1.337	342.1	28.010	1528.1	13.0	2475	838.9	1.13	32.854	4.47	1284.5	23.4	1101	635.2	1.23	1563	4.283	48.912
60	1.326	322.8	31.210	1354.7	11.4	2138	753.3	1.14	35.789	4.20	1135.4	20.6	982	566.4	1.23	1446	3.090	39.320
70	1.316	306.2	34.410	1164.7	9.3	1717	659.8	1.17	38.213	3.80	965.9	16.8	845	499.4	1.22	1333	1.814	25.452
80	1.306	291.8	37.610	957.8	6.9	1267	554.8	1.18	40.296	3.28	774.7	12.4	698	434.3	1.22	1215	1.131	17.342

Dil $\%_{vol}$	**Konnov (1998) Reaction Mechanism**			**Tan (1994) Reaction Mechanism**		
	Δ *(mm)*	τ *(μs)*	θ	Δ *(mm)*	τ *(μs)*	θ
0	0.043	0.082	6.386	0.035	0.068	5.931
10	0.094	0.215	10.994	0.060	0.139	7.208
20	0.591	1.634	20.623	0.126	0.343	10.344
30	4.117	13.190	18.946	0.606	1.928	32.954
40	25.380	91.990	19.134	13.400	48.760	26.634
50	183.500	743.000	20.262	161.600	655.800	24.233
60	2323.000	10420.000	22.439	2918.000	13100.000	24.582
70	105000.000	519900.000	26.667	156400.000	772600.000	26.592

Stoichiometric hydrogen-oxygen-helium mixtures with varying helium dilution

Dil $\%_{vol}$	γ_0	a_0 *(m/s)*	W_0 *(g/mol)*	V_{CJ} *(m/s)*	P_{CJ} *(bar)*	T_{CJ} *(K)*	a_{CJ} *(m/s)*	γ_{CJ}	W_{CJ} *(g/mol)*	M_{CJ}	u_{vN} *(m/s)*	P_{vN} *(bar)*	T_{vN} *(K)*	a_{vN} *(m/s)*	γ_{vN}	Cp_{vN} *(J/kgK)*	Δh^0 *(MJ/kg)*	Q
0	1.404	535.5	12.010	2842.1	19.0	3682	1545.4	1.22	14.474	5.31	2333.4	33.5	1767	1268.7	1.32	2886	8.270	40.498
10	1.421	557.5	11.210	2949.2	19.1	3641	1606.1	1.21	13.309	5.29	2404.5	33.4	1820	1340.0	1.33	2985	9.394	42.934
20	1.440	582.6	10.409	3065.1	19.1	3594	1673.3	1.21	12.158	5.26	2479.4	33.3	1874	1420.7	1.35	3093	10.180	43.203
30	1.462	610.9	9.608	3190.1	19.0	3538	1746.4	1.20	11.046	5.22	2557.7	33.0	1928	1510.9	1.37	3214	11.680	45.754
40	1.484	642.9	8.807	3325.0	18.9	3469	1826.9	1.20	9.981	5.17	2638.9	32.5	1979	1612.4	1.39	3354	12.690	45.567
50	1.509	680.0	8.006	3469.5	18.6	3382	1916.4	1.20	8.938	5.10	2721.5	31.8	2024	1727.2	1.42	3515	13.836	45.165
60	1.537	723.3	7.206	3619.9	18.1	3262	2015.8	1.21	7.924	5.00	2800.5	30.8	2056	1855.9	1.45	3706	14.265	41.912
70	1.568	774.9	6.405	3761.3	17.1	3080	2126.5	1.24	6.934	4.85	2861.3	29.1	2054	1994.7	1.49	3937	13.239	34.574
80	1.603	837.5	5.604	3826.4	14.8	2728	2245.2	1.33	5.958	4.57	2846.2	25.9	1956	2114.3	1.54	4229	9.389	21.454
90	1.642	915.8	4.803	3437.3	9.4	1828	2187.6	1.56	4.969	3.75	2445.9	17.5	1486	2030.9	1.60	4599	3.693	7.232

Dil $\%_{vol}$	**Konnov (1998) Reaction Mechanism**			**Tan (1994) Reaction Mechanism**		
	Δ *(mm)*	τ *(μs)*	θ	Δ *(mm)*	τ *(μs)*	θ
0	0.043	0.082	6.386	0.035	0.068	5.931
10	0.044	0.078	5.887	0.037	0.066	5.681
20	0.047	0.077	5.524	0.039	0.066	5.507
30	0.052	0.079	5.207	0.044	0.068	5.290
40	0.059	0.084	4.991	0.051	0.072	5.184
50	0.073	0.095	4.809	0.062	0.082	5.074
60	0.097	0.116	4.732	0.083	0.100	5.054
70	0.151	0.165	4.736	0.131	0.144	5.161
80	0.336	0.338	5.035	0.296	0.299	5.256
90	4.032	4.001	8.134	3.625	3.605	7.685

Stoichiometric hydrogen-oxygen-nitrogen mixtures with varying nitrogen dilution

Dil $\%_{vol}$	γ_0	a_0 *(m/s)*	W_0 *(g/mol)*	V_{CJ} *(m/s)*	P_{CJ} *(bar)*	T_{CJ} *(K)*	a_{CJ} *(m/s)*	γ_{CJ}	W_{CJ} *(g/mol)*	M_{CJ}	u_{vN} *(m/s)*	P_{vN} *(bar)*	T_{vN} *(K)*	a_{vN} *(m/s)*	γ_{vN}	Cp_{vN} *(J/kgK)*	Δh^0 *(MJ/kg)*	Q
0	1.404	535.5	12.010	2842.1	19.0	3682	1545.4	1.22	14.474	5.31	2333.4	33.5	1767	1268.7	1.32	2886	8.270	40.498
10	1.405	503.4	13.596	2644.7	18.7	3596	1438.9	1.20	16.310	5.25	2169.9	32.8	1738	1182.4	1.32	2548	7.975	44.207
20	1.405	475.9	15.211	2475.3	18.3	3503	1348.5	1.19	18.118	5.20	2029.5	32.2	1708	1108.4	1.32	2278	7.401	45.899
30	1.404	452.5	16.822	2325.1	17.8	3392	1269.4	1.18	19.866	5.14	1904.6	31.4	1674	1043.2	1.32	2061	6.934	47.559
40	1.405	432.5	18.412	2188.0	17.2	3257	1198.3	1.17	21.519	5.06	1789.9	30.4	1632	984.7	1.32	1881	6.540	49.100
50	1.405	414.9	20.012	2051.0	16.4	3078	1130.4	1.17	23.085	4.94	1674.0	29.0	1573	927.9	1.32	1725	5.749	46.909
55.621	1.405	405.9	20.911	1971.0	15.8	2948	1092.2	1.17	23.904	4.86	1605.7	28.0	1530	895.5	1.32	1647	5.307	45.246
60	1.404	399.2	21.612	1904.8	15.2	2824	1061.3	1.18	24.502	4.77	1548.7	27.0	1489	869.2	1.33	1590	4.639	40.877
70	1.404	385.1	23.212	1722.8	13.1	2434	981.0	1.22	25.683	4.47	1389.5	23.7	1350	800.3	1.32	1463	2.999	28.381
80	1.404	372.6	24.813	1469.2	10.0	1859	861.4	1.28	26.579	3.94	1162.9	18.3	1124	709.1	1.33	1337	1.608	16.266

Dil $\%_{vol}$	**Konnov (1998) Reaction Mechanism**			**Tan (1994) Reaction Mechanism**		
	Δ *(mm)*	τ *(μs)*	θ	Δ *(mm)*	τ *(μs)*	θ
0	0.043	0.082	6.386	0.035	0.068	5.931
10	0.050	0.102	6.595	0.041	0.084	6.110
20	0.060	0.129	6.844	0.049	0.106	6.218
30	0.075	0.171	7.295	0.061	0.140	6.487
40	0.099	0.241	7.793	0.080	0.196	6.820
50	0.152	0.391	8.872	0.120	0.310	7.374
55.621	0.215	0.572	10.123	0.164	0.439	7.980
60	0.312	0.852	12.033	0.226	0.619	8.744
70	2.317	6.875	25.195	0.883	2.592	16.400
80	197.500	641.200	22.252	204.000	660.400	25.276

Appendix F: Ethylene Detonation Properties

Initial temperature is always 295 K, and the initial pressure is 1 bar unless otherwise stated.

Nomenclature:
0 : pre-shock condition
a : acoustic speed
CJ : Chapman-Jouguet state condition
Cp : specific heat at constant pressure
$Dil\ \%_{vol}$: percent diluent by volume
M_{CJ} : Chapman-Jouguet detonation Mach number
P : pressure
Q : heat of reaction non-dimensionalized by R_0T_0
R : mixture gas constant
T : temperature
u : fluid velocity (in shock-fixed reference frame)
vN : post-shock condition
V_{CJ} : Chapman-Jouguet detonation velocity
W : molecular mass
Δ : reaction zone length
Δh^0 : heat of reaction extrapolated to zero temperature
ϕ : equivalence ratio
γ : ratio of specific heats
θ : non-dimensional effective activation energy parameter
τ: reaction zone time

Ethylene-oxygen mixtures with varying equivalence ratio

ϕ	γ_0	a_0 (m/s)	W_0 (g/mol)	V_{CJ} (m/s)	P_{CJ} (bar)	T_{CJ} (K)	a_{CJ} (m/s)	γ_{CJ}	W_{CJ} (g/mol)	M_{CJ}	u_{vN} (m/s)	P_{vN} (bar)	T_{vN} (K)	a_{vN} (m/s)	γ_{vN}	Cp_{vN} (J/kgK)	Δh^0 (MJ/kg)	Q
0.2	1.383	326.8	31.752	1719.1	18.1	2896	948.6	1.17	31.130	5.26	1451.5	33.3	1529	708.2	1.25	1300	4.019	52.030
0.4	1.369	326.2	31.535	1974.4	24.0	3462	1070.2	1.18	28.505	6.05	1707.3	44.3	1770	753.9	1.22	1472	4.977	63.996
0.6	1.356	325.8	31.341	2137.9	27.8	3704	1155.3	1.21	26.151	6.56	1875.5	52.2	1891	774.5	1.20	1622	4.914	62.796
0.8	1.346	325.5	31.168	2267.8	31.1	3847	1224.5	1.22	24.230	6.97	2010.2	58.9	1975	788.1	1.18	1755	5.248	66.688
1	1.338	325.3	31.013	2376.1	33.8	3937	1283.3	1.24	22.652	7.31	2123.0	64.8	2035	797.9	1.17	1878	5.226	66.076
1.2	1.330	325.1	30.872	2467.3	36.2	3989	1333.0	1.24	21.331	7.59	2218.3	69.9	2080	805.0	1.16	1989	5.633	70.903
1.4	1.324	325.0	30.744	2543.1	38.2	4008	1374.7	1.24	20.202	7.83	2297.9	74.3	2112	809.9	1.15	2090	5.985	75.023
1.6	1.318	324.9	30.627	2604.1	39.8	3993	1410.0	1.23	19.222	8.02	2362.5	77.8	2130	812.6	1.14	2181	6.576	82.111
1.8	1.312	324.8	30.519	2650.2	41.0	3945	1438.2	1.22	18.359	8.16	2412.1	80.6	2134	813.1	1.14	2263	7.147	88.938
2	1.308	324.8	30.421	2681.5	41.7	3867	1459.2	1.21	17.592	8.26	2446.9	82.4	2126	811.3	1.13	2336	7.698	95.486
2.2	1.303	324.7	30.330	2698.7	41.9	3761	1474.0	1.21	16.908	8.31	2467.5	83.4	2106	807.3	1.13	2402	7.786	96.282
2.4	1.300	324.7	30.246	2703.3	41.7	3634	1482.9	1.21	16.294	8.33	2475.5	83.5	2076	801.6	1.13	2459	7.800	96.195
2.6	1.296	324.7	30.167	2697.2	41.2	3493	1486.3	1.22	15.743	8.31	2472.8	83.0	2038	794.4	1.12	2510	7.362	90.550
2.8	1.294	324.8	30.094	2681.9	40.4	3341	1485.3	1.22	15.245	8.26	2460.8	82.0	1994	785.9	1.12	2555	7.261	89.088
3	1.291	324.8	30.026	2656.8	39.3	3183	1478.9	1.23	14.805	8.18	2438.9	80.3	1943	776.1	1.12	2594	6.767	82.842

ϕ	Konnov (1998) Reaction Mechanism			Tan (1994) Reaction Mechanism		
	Δ (mm)	τ (μs)	θ	Δ (mm)	τ (μs)	θ
0.2	0.749	2.709	11.824	0.902	3.229	19.974
0.4	0.134	0.479	9.013	0.086	0.292	11.599
0.6	0.066	0.236	8.385	0.039	0.131	9.662
0.8	0.042	0.152	8.153	0.025	0.084	8.825
1	0.031	0.112	8.020	0.019	0.063	8.369

ϕ	**Konnov (1998) Reaction Mechanism**			**Tan (1994) Reaction Mechanism**		
	Δ ***(mm)***	τ ***(μs)***	θ	Δ ***(mm)***	τ ***(μs)***	θ
1.2	0.024	0.089	7.908	0.016	0.052	8.091
1.4	0.021	0.076	7.811	0.014	0.046	7.931
1.6	0.019	0.069	7.720	0.013	0.044	7.850
1.8	0.018	0.066	7.604	0.013	0.044	7.873
2	0.018	0.066	7.501	0.014	0.046	7.977
2.2	0.018	0.069	7.388	0.015	0.051	8.162
2.4	0.019	0.075	7.241	0.017	0.059	8.444
2.6	0.021	0.083	7.087	0.020	0.070	8.803
2.8	0.023	0.094	6.922	0.024	0.086	9.263
3	0.027	0.109	6.938	0.029	0.110	9.861

Stoichiometric ethylene-oxygen mixtures with varying initial pressure

P_0	γ_0	a_0 (m/s)	W_0 (g/mol)	V_{CJ} (m/s)	P_{CJ} (bar)	T_{CJ} (K)	a_{CJ} (m/s)	γ_{CJ}	W_{CJ} (g/mol)	M_{CJ}	u_{vN} (m/s)	P_{vN} (bar)	T_{vN} (K)	a_{vN} (m/s)	γ_{vN}	Cp_{vN} (J/kgK)	Δh^0 (MJ/kg)	Q
0.2	1.338	325.3	31.013	2298.6	6.4	3611	1237.3	1.23	22.143	7.07	2049.1	12.1	1939	779.3	1.17	1861	5.129	64.861
0.4	1.338	325.3	31.013	2331.9	13.1	3747	1256.8	1.23	22.351	7.17	2080.9	25.0	1980	787.3	1.17	1868	5.279	66.749
0.6	1.338	325.3	31.013	2351.4	19.9	3829	1268.4	1.24	22.479	7.23	2099.5	38.0	2005	791.9	1.17	1873	5.117	64.705
0.8	1.338	325.3	31.013	2365.4	26.9	3890	1276.8	1.24	22.574	7.27	2112.8	51.4	2022	795.3	1.17	1876	5.180	65.496
1	1.338	325.3	31.013	2376.3	33.8	3937	1283.5	1.24	22.649	7.31	2123.2	64.8	2036	797.9	1.17	1878	5.226	66.084
1.2	1.338	325.3	31.013	2385.2	40.9	3977	1288.7	1.24	22.712	7.33	2131.7	78.3	2047	800.0	1.17	1880	5.267	66.594
1.4	1.338	325.3	31.013	2392.8	48.0	4011	1292.7	1.24	22.767	7.36	2139.0	92.0	2057	801.9	1.17	1882	5.300	67.016
1.6	1.338	325.3	31.013	2399.2	55.1	4040	1296.5	1.24	22.814	7.38	2145.1	105.7	2065	803.4	1.17	1883	5.328	67.374
1.8	1.338	325.3	31.013	2405.0	62.3	4066	1299.9	1.24	22.856	7.39	2150.6	119.5	2072	804.8	1.17	1884	5.353	67.692
2	1.338	325.3	31.013	2410.1	69.5	4090	1302.9	1.24	22.895	7.41	2155.4	133.4	2079	806.0	1.17	1885	5.377	67.990

P_0	Konnov (1998) Reaction Mechanism			Tan (1994) Reaction Mechanism		
	Δ (mm)	τ (μs)	θ	Δ (mm)	τ (μs)	θ
0.2	0.192	0.707	6.823	0.100	0.335	7.457
0.4	0.087	0.319	7.374	0.049	0.161	7.742
0.6	0.055	0.200	7.666	0.032	0.106	7.980
0.8	0.040	0.144	7.878	0.024	0.079	8.190
1	0.031	0.111	8.011	0.019	0.063	8.364
1.2	0.025	0.090	8.139	0.016	0.052	8.530
1.4	0.021	0.076	8.235	0.014	0.045	8.668
1.6	0.018	0.065	8.315	0.012	0.039	8.809
1.8	0.016	0.057	8.378	0.011	0.035	8.929
2	0.014	0.050	8.442	0.010	0.032	9.048

Ethylene-air mixtures with varying equivalence ratio

ϕ	γ_0	a_0 (m/s)	W_0 (g/mol)	V_{CJ} (m/s)	P_{CJ} (bar)	T_{CJ} (K)	a_{CJ} (m/s)	γ_{CJ}	W_{CJ} (g/mol)	M_{CJ}	u_{vN} (m/s)	P_{vN} (bar)	T_{vN} (K)	a_{vN} (m/s)	γ_{vN}	Cp_{vN} (J/kgK)	Δh^0 (MJ/kg)	Q
0.2	1.399	345.0	28.839	1119.0	6.8	1216	677.6	1.31	28.839	3.24	857.7	12.3	846	571.1	1.34	1144	0.787	9.254
0.4	1.395	344.5	28.828	1423.2	11.0	1880	828.4	1.27	28.825	4.13	1147.1	20.2	1155	658.9	1.30	1241	1.582	18.590
0.6	1.391	344.1	28.817	1622.7	14.4	2402	921.4	1.22	28.753	4.72	1337.3	26.5	1375	713.4	1.28	1308	2.656	31.206
0.8	1.387	343.7	28.807	1749.3	17.0	2748	972.6	1.18	28.463	5.09	1459.7	31.0	1514	744.5	1.27	1362	3.901	45.816
1	1.384	343.3	28.798	1824.4	18.5	2924	1005.3	1.17	27.930	5.31	1534.2	33.9	1589	759.9	1.26	1405	4.528	53.170
1.2	1.381	343.0	28.788	1867.7	19.3	2982	1031.1	1.18	27.253	5.45	1579.0	35.6	1624	765.8	1.25	1443	4.447	52.202
1.4	1.377	342.6	28.779	1886.4	19.5	2949	1050.8	1.20	26.494	5.51	1600.6	36.4	1628	764.8	1.24	1475	4.017	47.140
1.6	1.374	342.3	28.769	1886.7	19.3	2857	1061.3	1.22	25.710	5.51	1604.9	36.5	1609	758.8	1.24	1503	3.594	42.159
1.8	1.372	342.0	28.761	1876.9	18.9	2741	1063.6	1.24	24.950	5.49	1599.3	36.2	1579	750.4	1.23	1529	3.209	37.634
2	1.369	341.7	28.752	1862.2	18.5	2619	1061.0	1.25	24.234	5.45	1588.9	35.7	1545	741.0	1.23	1552	3.004	35.212
2.2	1.366	341.4	28.743	1844.0	18.0	2497	1055.4	1.27	23.566	5.40	1574.9	35.0	1508	731.1	1.23	1574	2.684	31.460
2.4	1.363	341.1	28.735	1823.2	17.6	2377	1047.8	1.28	22.943	5.34	1558.2	34.3	1470	721.0	1.22	1593	2.507	29.368
2.6	1.361	340.8	28.727	1800.0	17.1	2259	1038.5	1.28	22.363	5.28	1538.9	33.4	1431	710.6	1.22	1611	2.435	28.516
2.8	1.359	340.6	28.719	1774.6	16.5	2144	1027.6	1.29	21.821	5.21	1517.3	32.5	1391	700.0	1.22	1626	2.262	26.492
3	1.356	340.3	28.712	1747.3	16.0	2033	1015.4	1.30	21.325	5.13	1493.7	31.6	1351	689.3	1.21	1640	2.098	24.559

ϕ	Konnov (1998) Reaction Mechanism			Tan (1994) Reaction Mechanism		
	Δ (mm)	τ (μs)	θ	Δ (mm)	τ (μs)	θ
0.2	121700.000	460000.000	23.881	59120.000	226200.000	25.236
0.4	149.000	528.100	18.085	423.900	1500.000	18.087
0.6	7.271	24.480	15.449	11.940	40.570	22.051
0.8	1.799	5.871	12.427	1.584	5.127	18.923
1	0.963	3.096	10.822	0.737	2.318	14.934

	Konnov (1998) Reaction Mechanism			Tan (1994) Reaction Mechanism		
ϕ	Δ *(mm)*	τ *(μs)*	θ	Δ *(mm)*	τ *(μs)*	θ
1.2	0.724	2.314	10.082	0.557	1.733	13.633
1.4	0.665	2.131	10.035	0.549	1.710	13.636
1.6	0.703	2.274	10.552	0.645	2.035	14.431
1.8	0.809	2.652	11.412	0.840	2.715	15.560
2	0.983	3.280	12.436	1.160	3.860	16.589
2.2	1.256	4.279	13.554	1.690	5.778	17.241
2.4	1.686	5.884	14.749	2.532	8.894	17.449
2.6	2.390	8.553	15.848	3.877	13.970	17.345
2.8	3.563	13.090	16.676	6.033	22.230	17.132
3	5.533	20.880	17.101	9.498	35.700	16.862

Stoichiometric ethylene-air mixtures with varying initial pressure

P_0	γ_0	a_0 (m/s)	W_0 (g/mol)	V_{CJ} (m/s)	P_{CJ} (bar)	T_{CJ} (K)	a_{CJ} (m/s)	γ_{CJ}	W_{CJ} (g/mol)	M_{CJ}	u_{vN} (m/s)	P_{vN} (bar)	T_{vN} (K)	a_{vN} (m/s)	γ_{vN}	Cp_{vN} (J/kgK)	Δh^0 (MJ/kg)	Q
0.2	1.384	343.3	28.799	1791.9	3.6	2808	983.8	1.16	27.729	5.22	1503.9	6.5	1548	750.3	1.26	1400	4.680	54.951
0.4	1.384	343.3	28.799	1806.5	7.3	2859	993.3	1.17	27.816	5.26	1517.5	13.3	1566	754.6	1.26	1402	4.442	52.163
0.6	1.384	343.3	28.799	1814.7	11.0	2889	998.7	1.17	27.866	5.29	1525.2	20.1	1577	757.0	1.26	1404	4.483	52.639
0.8	1.384	343.3	28.799	1820.5	14.8	2909	1002.6	1.17	27.901	5.30	1530.6	27.0	1584	758.7	1.26	1405	4.509	52.943
1	1.384	343.3	28.799	1824.9	18.6	2925	1005.5	1.17	27.928	5.32	1534.7	33.9	1590	760.0	1.26	1405	4.530	53.193
1.2	1.384	343.3	28.799	1828.4	22.3	2938	1007.9	1.17	27.949	5.33	1537.9	40.8	1594	761.0	1.26	1406	4.548	53.399
1.4	1.384	343.3	28.799	1831.4	26.1	2949	1009.9	1.17	27.968	5.33	1540.7	47.8	1598	761.9	1.26	1406	4.562	53.570
1.6	1.384	343.3	28.799	1833.9	29.9	2958	1011.6	1.17	27.983	5.34	1543.1	54.8	1601	762.7	1.26	1407	4.574	53.709
1.8	1.384	343.3	28.799	1836.1	33.7	2966	1013.1	1.18	27.997	5.35	1545.1	61.7	1604	763.3	1.26	1407	4.301	50.503
2	1.384	343.3	28.799	1838.1	37.6	2973	1014.5	1.18	28.009	5.35	1547.0	68.8	1607	763.9	1.26	1408	4.310	50.603

P_0	Konnov (1998) Reaction Mechanism			Tan (1994) Reaction Mechanism		
	Δ (mm)	τ (μs)	θ	Δ (mm)	τ (μs)	θ
0.2	3.394	10.830	8.740	2.290	7.187	11.189
0.4	1.907	6.102	9.566	1.332	4.166	12.337
0.6	1.397	4.479	10.120	1.003	3.139	13.297
0.8	1.127	3.620	10.511	0.835	2.617	14.167
1	0.959	3.081	10.799	0.734	2.306	14.912
1.2	0.841	2.705	11.023	0.669	2.107	15.558
1.4	0.752	2.421	11.183	0.622	1.962	16.076
1.6	0.684	2.201	11.299	0.587	1.858	16.483
1.8	0.627	2.020	11.397	0.560	1.775	16.764
2	0.581	1.870	11.462	0.538	1.707	16.957

Stoichiometric ethylene-oxygen-argon mixtures with varying argon dilution

Dil $\%_{vol}$	γ_0	a_0 *(m/s)*	W_0 *(g/mol)*	V_{CJ} *(m/s)*	P_{CJ} *(bar)*	T_{CJ} *(K)*	a_{CJ} *(m/s)*	γ_{CJ}	W_{CJ} *(g/mol)*	M_{CJ}	u_{vN} *(m/s)*	P_{vN} *(bar)*	T_{vN} *(K)*	a_{vN} *(m/s)*	γ_{vN}	Cp_{vN} *(J/kgK)*	Δh^0 *(MJ/kg)*	Q
0	1.338	325.3	31.013	2376.1	33.8	3937	1283.3	1.24	22.652	7.31	2123.0	64.8	2035	797.9	1.17	1878	5.226	66.076
10	1.355	322.8	31.898	2296.4	32.5	3900	1242.2	1.23	23.996	7.11	2036.7	61.8	2062	796.3	1.18	1713	5.127	66.681
20	1.375	320.7	32.799	2215.9	31.1	3856	1200.7	1.22	25.457	6.91	1948.4	58.7	2092	796.0	1.19	1554	5.023	67.168
30	1.398	319.0	33.687	2136.7	29.7	3806	1160.2	1.22	26.993	6.70	1860.0	55.6	2123	797.3	1.21	1406	4.677	64.242
40	1.424	317.7	34.588	2055.7	28.2	3746	1119.3	1.21	28.659	6.47	1768.1	52.3	2157	800.3	1.24	1262	4.568	64.416
50	1.453	316.9	35.478	1974.0	26.6	3672	1078.5	1.21	30.425	6.23	1673.5	48.8	2191	805.3	1.26	1125	4.219	61.023
60	1.486	316.5	36.371	1888.1	24.9	3576	1036.4	1.21	32.326	5.97	1572.3	45.0	2222	812.4	1.30	991	3.867	57.346
70	1.524	316.7	37.264	1794.4	22.9	3440	992.1	1.21	34.363	5.67	1460.4	40.8	2241	820.9	1.35	865	3.498	53.144
80	1.570	317.6	38.158	1681.2	20.3	3218	942.4	1.23	36.535	5.29	1326.5	35.7	2221	827.4	1.41	744	2.776	43.192
90	1.622	319.2	39.051	1492.7	15.7	2687	876.0	1.33	38.719	4.68	1123.7	27.7	2020	807.0	1.51	627	1.431	22.788

Dil $\%_{vol}$	**Konnov (1998) Reaction Mechanism**			**Tan (1994) Reaction Mechanism**		
	Δ *(mm)*	τ *(μs)*	θ	Δ *(mm)*	τ *(μs)*	θ
0	0.031	0.112	8.020	0.019	0.063	8.369
10	0.033	0.115	7.957	0.020	0.063	7.915
20	0.035	0.120	7.904	0.021	0.065	7.486
30	0.038	0.126	7.857	0.022	0.068	7.122
40	0.042	0.135	7.817	0.025	0.072	6.787
50	0.048	0.148	7.693	0.028	0.079	6.495
60	0.057	0.170	7.671	0.033	0.092	6.265
70	0.076	0.215	7.661	0.043	0.115	6.087
80	0.125	0.336	7.540	0.066	0.174	6.038
90	0.460	1.205	7.264	0.220	0.571	6.322

Stoichiometric ethylene-oxygen-carbon dioxide mixtures with varying carbon dioxide dilution

Dil $\%_{vol}$	γ_0	a_0 *(m/s)*	W_0 *(g/mol)*	V_{CJ} *(m/s)*	P_{CJ} *(bar)*	T_{CJ} *(K)*	a_{CJ} *(m/s)*	γ_{CJ}	W_{CJ} *(g/mol)*	M_{CJ}	u_{vN} *(m/s)*	P_{vN} *(bar)*	T_{vN} *(K)*	a_{vN} *(m/s)*	γ_{vN}	Cp_{vN} *(J/kgK)*	Δh^0 *(MJ/kg)*	Q
0	1.338	325.3	31.013	2376.1	33.8	3937	1283.3	1.24	22.652	7.31	2123.0	64.8	2035	797.9	1.17	1878	5.226	66.076
10	1.332	318.0	32.301	2227.5	31.1	3773	1201.3	1.22	24.626	7.00	1985.8	59.3	1897	755.2	1.17	1787	5.055	66.578
20	1.326	311.1	33.612	2082.6	28.4	3598	1122.0	1.20	26.776	6.69	1851.9	53.9	1760	713.6	1.17	1704	4.908	67.263
30	1.321	304.6	34.905	1945.4	25.9	3417	1047.5	1.18	29.041	6.39	1724.9	48.8	1630	674.4	1.17	1627	4.808	68.431
40	1.315	298.5	36.215	1810.5	23.3	3223	974.8	1.16	31.489	6.07	1599.9	43.8	1502	636.0	1.17	1555	4.742	70.015
50	1.311	292.7	37.511	1678.9	20.9	3012	905.0	1.15	34.049	5.74	1477.6	38.9	1377	599.0	1.18	1486	4.376	66.930
60	1.306	287.3	38.811	1544.0	18.3	2764	834.9	1.13	36.700	5.37	1351.7	34.0	1250	561.6	1.18	1420	4.335	68.595
70	1.302	282.1	40.110	1395.2	15.5	2437	760.8	1.13	39.266	4.95	1211.9	28.7	1111	521.5	1.18	1352	3.540	57.886
80	1.297	277.2	41.410	1199.9	11.8	1929	668.4	1.15	41.321	4.33	1025.9	21.8	932	471.4	1.19	1268	2.220	37.487

Dil $\%_{vol}$	**Konnov (1998) Reaction Mechanism**			**Tan (1994) Reaction Mechanism**		
	Δ *(mm)*	τ (μs)	θ	Δ *(mm)*	τ (μs)	θ
0	0.031	0.112	8.020	0.019	0.063	8.369
10	0.052	0.200	8.241	0.036	0.128	10.100
20	0.099	0.400	9.356	0.082	0.317	13.028
30	0.223	0.953	11.376	0.247	1.036	16.595
40	0.644	2.918	13.341	1.026	4.651	18.229
50	2.355	11.280	14.732	5.071	24.390	17.662
60	11.680	59.060	15.994	30.030	152.100	17.176
70	101.700	543.100	18.033	289.400	1542.000	18.740
80	4280.000	24240.000	22.004	14920.000	84110.000	23.863

Stoichiometric ethylene-oxygen-helium mixtures with varying helium dilution

Dil $\%_{vol}$	γ_0	a_0 *(m/s)*	W_0 *(g/mol)*	V_{CJ} *(m/s)*	P_{CJ} *(bar)*	T_{CJ} *(K)*	a_{CJ} *(m/s)*	γ_{CJ}	W_{CJ} *(g/mol)*	M_{CJ}	u_{vN} *(m/s)*	P_{vN} *(bar)*	T_{vN} *(K)*	a_{vN} *(m/s)*	γ_{vN}	Cp_{vN} *(J/kgK)*	Δh^0 *(MJ/kg)*	Q
0	1.338	325.3	31.013	2376.1	33.8	3937	1283.3	1.24	22.652	7.31	2123.0	64.8	2035	797.9	1.17	1878	5.226	66.076
10	1.355	342.5	28.336	2436.5	32.5	3900	1317.9	1.23	21.317	7.11	2161.0	61.8	2062	844.8	1.18	1929	5.771	66.680
20	1.375	362.9	25.611	2507.7	31.1	3856	1358.8	1.22	19.878	6.91	2204.9	58.7	2092	900.8	1.19	1990	6.432	67.168
30	1.398	386.7	22.924	2590.2	29.7	3806	1406.5	1.22	18.369	6.70	2254.8	55.6	2123	966.5	1.21	2066	6.873	64.242
40	1.424	415.8	20.200	2690.0	28.2	3746	1464.6	1.21	16.738	6.47	2313.7	52.3	2157	1047.2	1.24	2160	7.821	64.414
50	1.453	451.1	17.508	2810.0	26.6	3672	1535.2	1.21	15.014	6.23	2382.3	48.8	2191	1146.3	1.26	2280	8.549	61.024
60	1.486	496.1	14.807	2959.3	24.9	3576	1624.3	1.21	13.160	5.96	2464.3	45.0	2222	1273.4	1.30	2435	9.499	57.346
70	1.524	555.6	12.108	3148.0	22.9	3440	1740.5	1.21	11.165	5.67	2562.0	40.8	2241	1440.2	1.35	2662	10.765	53.146
80	1.569	639.7	9.405	3386.3	20.3	3218	1898.3	1.23	9.005	5.29	2671.9	35.7	2221	1666.5	1.41	3018	11.264	43.192
90	1.623	770.5	6.704	3602.6	15.7	2687	2114.2	1.33	6.647	4.68	2712.0	27.7	2020	1947.8	1.51	3653	8.338	22.790

Dil $\%_{vol}$	**Konnov (1998) Reaction Mechanism**			**Tan (1994) Reaction Mechanism**		
	Δ *(mm)*	τ *(μs)*	θ	Δ *(mm)*	τ *(μs)*	θ
0	0.031	0.112	8.020	0.019	0.063	8.369
10	0.034	0.115	7.978	0.021	0.063	7.910
20	0.039	0.119	7.928	0.023	0.065	7.495
30	0.045	0.125	7.883	0.027	0.068	7.117
40	0.054	0.133	7.833	0.032	0.072	6.783
50	0.067	0.145	7.767	0.040	0.079	6.513
60	0.088	0.165	7.692	0.052	0.091	6.265
70	0.128	0.206	7.644	0.075	0.115	6.104
80	0.237	0.316	7.563	0.134	0.174	6.047
90	1.020	1.107	7.379	0.531	0.572	6.267

Stoichiometric ethylene-oxygen-nitrogen mixtures with varying nitrogen dilution

Dil $\%_{vol}$	γ_0	a_0 *(m/s)*	W_0 *(g/mol)*	V_{CJ} *(m/s)*	P_{CJ} *(bar)*	T_{CJ} *(K)*	a_{CJ} *(m/s)*	γ_{CJ}	W_{CJ} *(g/mol)*	M_{CJ}	u_{vN} *(m/s)*	P_{vN} *(bar)*	T_{vN} *(K)*	a_{vN} *(m/s)*	γ_{vN}	Cp_{vN} *(J/kgK)*	Δh^0 *(MJ/kg)*	Q
0	1.338	325.3	31.013	2376.1	33.8	3937	1283.3	1.24	22.652	7.31	2123.0	64.8	2035	797.9	1.17	1878	5.226	66.076
10	1.343	327.4	30.715	2317.0	31.9	3862	1251.2	1.22	23.325	7.08	2059.0	60.7	1995	796.6	1.18	1818	5.476	68.582
20	1.349	329.8	30.413	2258.6	30.1	3784	1220.5	1.21	24.005	6.85	1995.2	56.9	1957	795.9	1.18	1757	5.482	67.975
30	1.355	332.2	30.114	2198.2	28.2	3696	1189.1	1.20	24.704	6.62	1929.3	53.1	1915	794.7	1.19	1696	5.483	67.317
40	1.361	334.7	29.812	2132.3	26.3	3590	1155.1	1.19	25.442	6.37	1857.8	49.2	1867	792.3	1.21	1635	5.462	66.396
50	1.368	337.2	29.513	2060.3	24.3	3461	1118.6	1.18	26.195	6.11	1780.3	45.1	1810	788.2	1.22	1571	5.418	65.194
60	1.375	339.7	29.213	1977.2	22.2	3291	1077.2	1.17	26.957	5.82	1692.0	40.8	1738	781.2	1.23	1503	5.317	63.327
70	1.381	342.3	28.913	1874.1	19.7	3051	1028.1	1.17	27.681	5.47	1584.8	36.0	1640	768.1	1.25	1433	4.779	56.343
73.821	1.385	343.4	28.798	1824.4	18.5	2924	1005.3	1.17	27.930	5.31	1534.2	33.9	1589	759.9	1.26	1405	4.529	53.175
80	1.388	345.0	28.613	1722.7	16.3	2649	961.4	1.19	28.246	4.99	1432.6	29.8	1480	739.8	1.27	1355	3.557	41.499

Dil $\%_{vol}$	**Konnov (1998) Reaction Mechanism**			**Tan (1994) Reaction Mechanism**		
	Δ *(mm)*	τ *(μs)*	θ	Δ *(mm)*	τ *(μs)*	θ
0	0.031	0.112	8.020	0.019	0.063	8.369
10	0.041	0.145	7.950	0.025	0.082	8.602
20	0.054	0.191	7.867	0.033	0.107	8.830
30	0.075	0.257	7.784	0.046	0.145	9.117
40	0.107	0.363	7.739	0.066	0.208	9.507
50	0.164	0.545	7.819	0.103	0.323	10.116
60	0.282	0.919	8.292	0.185	0.577	11.151
70	0.617	1.988	9.778	0.445	1.390	13.323
73.821	0.963	3.096	10.822	0.737	2.318	14.934
80	2.853	9.216	13.304	2.681	8.629	19.709

Appendix G: Propane Detonation Properties

Initial temperature is always 295 K, and the initial pressure is 1 bar unless otherwise stated.

Nomenclature:
0 : pre-shock condition
a : acoustic speed
CJ : Chapman-Jouguet state condition
Cp : specific heat at constant pressure
$Dil\ \%_{vol}$: percent diluent by volume
M_{CJ} : Chapman-Jouguet detonation Mach number
P : pressure
Q : heat of reaction non-dimensionalized by R_0T_0
R : mixture gas constant
T : temperature
u : fluid velocity (in shock-fixed reference frame)
vN : post-shock condition
V_{CJ} : Chapman-Jouguet detonation velocity
W : molecular mass
Δ : reaction zone length
Δh^0 : heat of reaction extrapolated to zero temperature
ϕ : equivalence ratio
γ : ratio of specific heats
θ : non-dimensional effective activation energy parameter
τ: reaction zone time

Propane-oxygen mixtures with varying equivalence ratio

ϕ	γ_0	a_0 (m/s)	W_0 (g/mol)	V_{CJ} (m/s)	P_{CJ} (bar)	T_{CJ} (K)	a_{CJ} (m/s)	γ_{CJ}	W_{CJ} (g/mol)	M_{CJ}	u_{vN} (m/s)	P_{vN} (bar)	T_{vN} (K)	a_{vN} (m/s)	γ_{vN}	Cp_{vN} (J/kgK)	Δh^0 (MJ/kg)	Q
0.2	1.369	321.6	32.464	1692.4	17.9	2780	937.3	1.18	30.829	5.26	1436.7	33.2	1479	685.2	1.24	1327	3.645	48.242
0.4	1.344	316.5	32.895	1957.5	24.6	3368	1060.5	1.17	28.235	6.18	1710.3	45.9	1710	719.3	1.20	1535	5.198	69.720
0.6	1.323	312.2	33.295	2123.2	29.2	3611	1145.4	1.19	25.886	6.80	1887.2	55.4	1816	728.5	1.17	1718	5.398	73.280
0.8	1.306	308.4	33.668	2253.3	33.2	3749	1213.8	1.21	23.957	7.31	2027.5	63.7	1884	731.7	1.15	1882	5.434	74.590
1	1.291	305.1	34.015	2360.6	36.7	3829	1271.0	1.22	22.362	7.74	2143.7	71.2	1930	732.3	1.14	2030	5.657	78.454
1.2	1.279	302.2	34.340	2449.0	39.8	3864	1318.8	1.22	21.013	8.10	2239.9	77.8	1960	730.9	1.13	2165	6.085	85.191
1.4	1.269	299.7	34.645	2519.5	42.3	3856	1358.0	1.21	19.844	8.41	2317.4	83.5	1975	727.7	1.12	2288	6.778	95.738
1.6	1.259	297.3	34.932	2571.0	44.3	3801	1388.5	1.20	18.811	8.65	2375.3	88.0	1975	722.5	1.11	2399	7.441	105.982
1.8	1.251	295.2	35.201	2602.1	45.5	3697	1410.5	1.19	17.884	8.81	2412.4	91.1	1959	714.9	1.10	2496	8.054	115.594
2	1.244	293.3	35.455	2612.3	45.9	3547	1423.4	1.19	17.049	8.91	2428.3	92.7	1927	704.9	1.10	2581	8.098	117.058
2.2	1.237	291.5	35.695	2603.0	45.5	3362	1427.6	1.20	16.294	8.93	2424.3	92.8	1880	692.8	1.10	2653	7.576	110.253
2.4	1.231	290.0	35.923	2575.7	44.5	3151	1423.2	1.22	15.611	8.88	2402.2	91.6	1821	678.8	1.09	2712	6.649	97.390
2.6	1.226	288.5	36.138	2531.5	42.8	2918	1410.9	1.23	14.988	8.78	2362.9	89.1	1751	663.0	1.09	2758	6.079	89.576
2.8	1.221	287.1	36.342	2470.7	40.6	2671	1389.4	1.26	14.420	8.61	2306.8	85.5	1672	645.6	1.09	2790	5.008	74.213
3	1.217	285.8	36.536	2394.4	38.0	2417	1358.2	1.28	13.904	8.38	2235.0	80.7	1585	626.6	1.09	2807	4.288	63.883

ϕ	Konnov (1998) Reaction Mechanism			Tan (1994) Reaction Mechanism		
	Δ (mm)	τ (μs)	θ	Δ (mm)	τ (μs)	θ
0.2	0.542	1.945	13.552	1.094	3.930	15.882
0.4	0.091	0.328	10.523	0.143	0.516	12.754
0.6	0.050	0.187	9.803	0.075	0.277	11.707
0.8	0.037	0.139	9.576	0.055	0.204	11.205
1	0.030	0.117	9.540	0.045	0.172	10.933

ϕ	**Konnov (1998) Reaction Mechanism**			**Tan (1994) Reaction Mechanism**		
	Δ ***(mm)***	τ ***(μs)***	θ	Δ ***(mm)***	τ ***(μs)***	θ
1.2	0.027	0.107	9.577	0.042	0.159	10.801
1.4	0.026	0.104	9.685	0.041	0.158	10.775
1.6	0.026	0.109	9.818	0.044	0.171	10.825
1.8	0.029	0.124	9.960	0.051	0.202	10.955
2	0.036	0.154	10.143	0.064	0.261	11.126
2.2	0.047	0.209	10.223	0.088	0.367	11.314
2.4	0.067	0.304	10.265	0.129	0.557	11.472
2.6	0.103	0.475	10.199	0.202	0.910	11.599
2.8	0.167	0.793	9.985	0.345	1.617	11.657
3	0.285	1.391	9.613	0.636	3.099	11.571

Stoichiometric propane-oxygen mixtures with varying initial pressure

P_0	γ_0	a_0 (m/s)	W_0 (g/mol)	V_{CJ} (m/s)	P_{CJ} (bar)	T_{CJ} (K)	a_{CJ} (m/s)	γ_{CJ}	W_{CJ} (g/mol)	M_{CJ}	u_{vN} (m/s)	P_{vN} (bar)	T_{vN} (K)	a_{vN} (m/s)	γ_{vN}	Cp_{vN} (J/kgK)	Δh^0 (MJ/kg)	Q
0.2	1.291	305.1	34.015	2287.9	6.9	3526	1228.1	1.22	21.876	7.50	2073.5	13.3	1846	716.7	1.14	2012	5.312	73.667
0.4	1.291	305.1	34.015	2319.1	14.2	3653	1246.6	1.22	22.076	7.60	2103.6	27.5	1882	723.4	1.14	2020	5.460	75.717
0.6	1.291	305.1	34.015	2337.4	21.6	3730	1257.3	1.22	22.199	7.66	2121.3	41.8	1903	727.3	1.14	2024	5.548	76.937
0.8	1.291	305.1	34.015	2350.5	29.1	3785	1265.0	1.22	22.290	7.70	2133.9	56.5	1918	730.1	1.14	2027	5.608	77.776
1	1.291	305.1	34.015	2360.6	36.7	3829	1271.0	1.22	22.362	7.74	2143.7	71.2	1930	732.3	1.14	2030	5.657	78.454
1.2	1.291	305.1	34.015	2368.8	44.3	3865	1275.9	1.22	22.422	7.76	2151.6	86.0	1939	734.0	1.14	2032	5.696	79.000
1.4	1.291	305.1	34.015	2375.8	52.0	3896	1280.1	1.22	22.473	7.79	2158.3	101.0	1947	735.5	1.14	2033	5.730	79.471
1.6	1.291	305.1	34.015	2381.9	59.6	3923	1283.9	1.22	22.519	7.81	2164.2	116.0	1954	736.8	1.14	2035	5.759	79.869
1.8	1.291	305.1	34.015	2387.2	67.3	3948	1287.1	1.22	22.559	7.82	2169.3	131.0	1960	737.9	1.14	2036	5.787	80.261
2	1.291	305.1	34.015	2392.0	75.1	3969	1289.9	1.22	22.596	7.84	2174.0	146.0	1966	739.0	1.14	2037	5.809	80.559

P_0	**Konnov (1998) Reaction Mechanism**			**Tan (1994) Reaction Mechanism**		
	Δ *(mm)*	τ (μs)	θ	Δ *(mm)*	τ (μs)	θ
0.2	0.166	0.647	10.520	0.226	0.865	11.966
0.4	0.080	0.311	10.128	0.113	0.432	11.530
0.6	0.052	0.203	9.869	0.076	0.287	11.272
0.8	0.038	0.149	9.677	0.057	0.215	11.079
1	0.030	0.117	9.539	0.045	0.172	10.933
1.2	0.025	0.096	9.417	0.038	0.143	10.820
1.4	0.021	0.082	9.322	0.032	0.122	10.724
1.6	0.018	0.071	9.237	0.028	0.107	10.640
1.8	0.016	0.062	9.168	0.025	0.095	10.571
2	0.014	0.056	9.120	0.023	0.086	10.509

Propane-air mixtures with varying equivalence ratio

ϕ	γ_0	a_0 (m/s)	W_0 (g/mol)	V_{CJ} (m/s)	P_{CJ} (bar)	T_{CJ} (K)	a_{CJ} (m/s)	γ_{CJ}	W_{CJ} (g/mol)	M_{CJ}	u_{vN} (m/s)	P_{vN} (bar)	T_{vN} (K)	a_{vN} (m/s)	γ_{vN}	Cp_{vN} (J/kgK)	Δh^0 (MJ/kg)	Q
0.2	1.396	343.7	28.978	1091.4	6.5	1159	663.6	1.31	28.738	3.18	833.5	11.7	819	560.2	1.34	1142	0.742	8.772
0.4	1.389	342.1	29.103	1388.4	10.5	1782	810.9	1.27	28.628	4.06	1119.0	19.4	1112	642.3	1.30	1244	1.498	17.776
0.6	1.382	340.5	29.226	1587.5	13.9	2280	905.7	1.23	28.488	4.66	1311.5	25.8	1324	692.7	1.27	1321	2.404	28.645
0.8	1.375	339.0	29.346	1721.7	16.7	2638	961.5	1.19	28.201	5.08	1443.5	30.7	1465	722.4	1.26	1386	3.545	42.420
1	1.370	337.7	29.465	1801.0	18.5	2822	994.3	1.17	27.670	5.33	1524.1	34.0	1541	735.5	1.24	1438	4.402	52.878
1.2	1.364	336.3	29.582	1835.9	19.1	2845	1018.7	1.19	26.931	5.46	1563.0	35.6	1561	735.9	1.23	1482	4.027	48.576
1.4	1.358	334.9	29.698	1834.0	18.8	2741	1031.7	1.22	26.067	5.48	1566.9	35.8	1538	726.7	1.23	1516	3.386	41.002
1.6	1.353	333.6	29.811	1813.2	18.3	2587	1029.5	1.24	25.195	5.44	1552.5	35.2	1494	713.0	1.22	1545	2.980	36.227
1.8	1.348	332.4	29.923	1784.8	17.7	2425	1019.6	1.26	24.374	5.37	1530.4	34.3	1443	698.0	1.22	1569	2.619	31.958
2	1.343	331.2	30.033	1751.9	17.0	2265	1005.7	1.27	23.613	5.29	1503.6	33.3	1390	682.7	1.21	1590	2.403	29.431
2.2	1.338	330.0	30.141	1715.5	16.3	2109	989.1	1.28	22.910	5.20	1473.0	32.1	1337	667.1	1.21	1608	2.195	26.979
2.4	1.333	328.8	30.247	1675.6	15.6	1958	970.2	1.29	22.259	5.10	1438.6	30.7	1282	651.4	1.20	1623	1.997	24.626
2.6	1.329	327.7	30.352	1632.5	14.8	1812	949.2	1.30	21.656	4.98	1400.7	29.3	1227	635.4	1.20	1634	1.808	22.373
2.8	1.326	326.7	30.456	1586.0	14.0	1670	926.2	1.30	21.097	4.85	1359.2	27.8	1171	619.2	1.20	1643	1.694	21.038
3	1.321	325.7	30.557	1535.6	13.1	1531	901.4	1.31	20.576	4.72	1313.6	26.1	1114	602.7	1.20	1646	1.510	18.816

ϕ	Konnov (1998) Reaction Mechanism			Tan (1994) Reaction Mechanism		
	Δ (mm)	τ (μs)	θ	Δ (mm)	τ (μs)	θ
0.2	134900.000	515400.000	26.505	208800.000	780200.000	24.029
0.4	173.000	604.800	15.697	540.100	1883.000	14.056
0.6	13.340	45.040	13.689	36.120	124.200	15.989
0.8	3.637	12.080	13.059	7.269	24.620	16.239
1	2.072	6.847	12.671	3.547	11.940	15.587

	Konnov (1998) Reaction Mechanism			Tan (1994) Reaction Mechanism		
ϕ	Δ *(mm)*	τ *(μs)*	θ	Δ *(mm)*	τ *(μs)*	θ
1.2	1.889	6.283	12.515	3.126	10.580	15.176
1.4	2.427	8.196	12.415	4.181	14.360	14.974
1.6	3.629	12.520	12.226	6.716	23.550	14.752
1.8	5.674	20.010	11.895	11.340	40.590	14.380
2	8.958	32.260	11.390	19.270	70.440	13.755
2.2	14.080	51.650	10.712	32.280	120.500	12.737
2.4	21.800	81.400	9.927	52.600	199.800	11.248
2.6	32.920	125.300	9.266	81.500	314.200	9.503
2.8	49.450	191.100	9.099	120.800	470.900	8.404
3	76.020	298.800	9.928	179.000	705.300	8.986

Stoichiometric propane-air mixtures with varying initial pressure

P_0	γ_0	a_0 (m/s)	W_0 (g/mol)	V_{CJ} (m/s)	P_{CJ} (bar)	T_{CJ} (K)	a_{CJ} (m/s)	γ_{CJ}	W_{CJ} (g/mol)	M_{CJ}	u_{vN} (m/s)	P_{vN} (bar)	T_{vN} (K)	a_{vN} (m/s)	γ_{vN}	Cp_{vN} (J/kgK)	Δh^0 (MJ/kg)	Q
0.2	1.370	337.7	29.465	1771.6	3.6	2721	974.3	1.16	27.499	5.25	1496.6	6.6	1505	727.1	1.25	1432	4.564	54.827
0.4	1.370	337.7	29.465	1784.7	7.3	2766	983.2	1.17	27.574	5.29	1508.8	13.3	1521	730.8	1.24	1435	4.327	51.980
0.6	1.370	337.7	29.465	1792.0	11.0	2791	988.2	1.17	27.617	5.31	1515.7	20.2	1530	732.9	1.24	1437	4.360	52.381
0.8	1.370	337.7	29.465	1797.1	14.7	2809	991.6	1.17	27.647	5.32	1520.5	27.1	1536	734.3	1.24	1438	4.385	52.675
1	1.370	337.7	29.465	1801.0	18.5	2822	994.3	1.17	27.670	5.33	1524.1	34.0	1541	735.5	1.24	1438	4.402	52.878
1.2	1.370	337.7	29.465	1804.1	22.2	2833	996.4	1.18	27.688	5.34	1527.0	40.9	1545	736.3	1.24	1439	4.143	49.770
1.4	1.370	337.7	29.465	1806.7	26.0	2842	998.3	1.18	27.703	5.35	1529.5	47.9	1548	737.1	1.24	1440	4.154	49.905
1.6	1.370	337.7	29.465	1808.9	29.7	2850	999.8	1.18	27.716	5.36	1531.5	54.8	1551	737.7	1.24	1440	4.164	50.029
1.8	1.370	337.7	29.465	1810.9	33.5	2857	1001.2	1.18	27.728	5.36	1533.4	61.8	1553	738.3	1.24	1440	4.173	50.134
2	1.370	337.7	29.465	1812.6	37.3	2863	1002.4	1.18	27.738	5.37	1535.0	68.9	1555	738.7	1.24	1441	4.181	50.225

P_0	Konnov (1998) Reaction Mechanism			Tan (1994) Reaction Mechanism		
	Δ (mm)	τ (μs)	θ	Δ (mm)	τ (μs)	θ
0.2	9.009	30.300	14.159	13.040	44.670	17.422
0.4	4.823	16.130	13.616	7.453	25.370	16.693
0.6	3.332	11.090	13.216	5.379	18.230	16.229
0.8	2.551	8.460	12.917	4.256	14.370	15.872
1	2.071	6.845	12.674	3.547	11.940	15.587
1.2	1.745	5.751	12.466	3.058	10.260	15.346
1.4	1.507	4.956	12.300	2.694	9.020	15.142
1.6	1.328	4.357	12.153	2.415	8.068	14.965
1.8	1.186	3.883	12.028	2.192	7.306	14.804
2	1.072	3.505	11.923	2.010	6.687	14.662

Stoichiometric propane-oxygen-argon mixtures with varying argon dilution

Dil $\%_{vol}$	γ_0	a_0 *(m/s)*	W_0 *(g/mol)*	V_{CJ} *(m/s)*	P_{CJ} *(bar)*	T_{CJ} *(K)*	a_{CJ} *(m/s)*	γ_{CJ}	W_{CJ} *(g/mol)*	M_{CJ}	u_{vN} *(m/s)*	P_{vN} *(bar)*	T_{vN} *(K)*	a_{vN} *(m/s)*	γ_{vN}	Cp_{vN} *(J/kgK)*	Δh^0 *(MJ/kg)*	Q
0	1.291	305.1	34.015	2360.6	36.7	3829	1271.0	1.22	22.362	7.74	2143.7	71.2	1930	732.3	1.14	2030	5.657	78.454
10	1.310	304.6	34.611	2285.6	35.0	3795	1232.6	1.22	23.612	7.50	2061.2	67.5	1954	734.2	1.15	1859	5.313	74.983
20	1.329	304.3	35.201	2210.6	33.2	3756	1194.3	1.21	24.951	7.26	1977.7	63.7	1981	737.4	1.16	1696	5.244	75.261
30	1.353	304.4	35.793	2134.3	31.5	3710	1155.6	1.21	26.408	7.01	1891.4	59.9	2011	741.9	1.18	1536	4.896	71.453
40	1.379	304.8	36.387	2056.0	29.7	3655	1116.3	1.20	27.996	6.74	1801.3	55.9	2045	748.2	1.20	1381	4.805	71.284
50	1.409	305.7	36.980	1974.9	27.8	3588	1076.0	1.20	29.729	6.46	1706.1	51.8	2080	756.6	1.22	1229	4.444	67.006
60	1.445	307.1	37.572	1889.2	25.7	3500	1034.2	1.20	31.628	6.15	1603.3	47.4	2116	767.3	1.26	1082	4.076	62.436
70	1.489	309.3	38.165	1794.8	23.5	3375	989.8	1.20	33.712	5.80	1487.9	42.6	2146	780.5	1.30	937	3.687	57.372
80	1.540	312.2	38.758	1680.9	20.7	3168	940.0	1.22	35.993	5.38	1348.7	36.8	2147	794.2	1.37	795	2.911	46.005
90	1.605	316.3	39.351	1493.5	15.8	2668	874.3	1.33	38.382	4.72	1138.0	28.3	1985	787.7	1.48	652	1.433	22.991

Dil $\%_{vol}$	**Konnov (1998) Reaction Mechanism**			**Tan (1994) Reaction Mechanism**		
	Δ *(mm)*	τ *(μs)*	θ	Δ *(mm)*	τ *(μs)*	θ
0	0.030	0.117	9.540	0.045	0.172	10.933
10	0.031	0.119	9.512	0.046	0.168	10.722
20	0.033	0.120	9.476	0.046	0.165	10.469
30	0.034	0.121	9.412	0.047	0.162	10.164
40	0.036	0.123	9.334	0.048	0.160	9.790
50	0.038	0.126	9.212	0.051	0.161	9.375
60	0.042	0.134	9.043	0.055	0.167	8.913
70	0.050	0.151	8.924	0.064	0.186	8.481
80	0.074	0.209	8.879	0.090	0.247	8.216
90	0.299	0.795	10.345	0.294	0.781	9.637

Stoichiometric propane-oxygen-carbon dioxide mixtures with varying carbon dioxide dilution

Dil $\%_{vol}$	γ_0	a_0 *(m/s)*	W_0 *(g/mol)*	V_{CJ} *(m/s)*	P_{CJ} *(bar)*	T_{CJ} *(K)*	a_{CJ} *(m/s)*	γ_{CJ}	W_{CJ} *(g/mol)*	M_{CJ}	u_{vN} *(m/s)*	P_{vN} *(bar)*	T_{vN} *(K)*	a_{vN} *(m/s)*	γ_{vN}	Cp_{vN} *(J/kgK)*	Δh^0 *(MJ/kg)*	Q
0	1.291	305.1	34.015	2360.6	36.7	3829	1271.0	1.22	22.362	7.74	2143.7	71.2	1930	732.3	1.14	2030	5.657	78.454
10	1.291	300.7	35.019	2224.4	33.6	3684	1196.8	1.20	24.164	7.40	2013.1	64.9	1820	702.0	1.14	1924	5.581	79.684
20	1.291	296.5	36.014	2092.1	30.7	3530	1124.9	1.19	26.101	7.06	1886.3	59.0	1710	672.3	1.14	1824	5.221	76.661
30	1.291	292.4	37.012	1961.3	27.8	3366	1054.3	1.17	28.213	6.71	1761.1	53.1	1600	642.6	1.15	1729	5.189	78.310
40	1.290	288.5	38.013	1831.4	25.0	3187	984.8	1.16	30.513	6.35	1636.8	47.5	1488	612.8	1.15	1639	4.835	74.939
50	1.290	284.8	39.013	1700.7	22.2	2987	915.7	1.14	32.995	5.97	1511.7	41.9	1374	582.5	1.16	1553	4.832	76.862
60	1.289	281.1	40.012	1564.8	19.4	2748	845.4	1.13	35.629	5.57	1381.5	36.3	1253	550.7	1.16	1470	4.439	72.413
70	1.289	277.7	41.012	1413.3	16.2	2430	770.0	1.13	38.280	5.09	1236.1	30.2	1117	515.1	1.17	1386	3.620	60.539
80	1.289	274.3	42.011	1215.3	12.2	1937	676.1	1.15	40.566	4.43	1045.0	22.8	940	468.9	1.18	1290	2.273	38.930

Dil $\%_{vol}$	**Konnov (1998) Reaction Mechanism**			**Tan (1994) Reaction Mechanism**		
	Δ ***(mm)***	τ (μ***s)***	θ	Δ ***(mm)***	τ (μ***s)***	θ
0	0.030	0.117	9.540	0.045	0.172	10.933
10	0.056	0.227	10.047	0.091	0.366	11.978
20	0.113	0.477	10.535	0.207	0.874	12.947
30	0.253	1.112	11.001	0.542	2.403	13.694
40	0.643	2.942	11.448	1.644	7.644	14.005
50	1.922	9.166	11.933	5.815	28.180	13.515
60	7.353	36.550	12.624	24.180	121.400	12.219
70	44.340	231.300	14.193	137.100	712.100	12.399
80	1106.000	6230.000	21.139	2717.000	15010.000	18.596

Stoichiometric propane-oxygen-helium mixtures with varying helium dilution

Dil $\%_{vol}$	γ_0	a_0 *(m/s)*	W_0 *(g/mol)*	V_{CJ} *(m/s)*	P_{CJ} *(bar)*	T_{CJ} *(K)*	a_{CJ} *(m/s)*	γ_{CJ}	W_{CJ} *(g/mol)*	M_{CJ}	u_{vN} *(m/s)*	P_{vN} *(bar)*	T_{vN} *(K)*	a_{vN} *(m/s)*	γ_{vN}	Cp_{vN} *(J/kgK)*	Δh^0 *(MJ/kg)*	Q
0	1.291	305.1	34.015	2360.6	36.7	3829	1271.0	1.22	22.362	7.74	2143.7	71.2	1930	732.3	1.14	2030	5.657	78.454
10	1.309	321.8	31.000	2415.0	35.0	3795	1302.4	1.22	21.149	7.51	2177.9	67.5	1954	775.8	1.15	2076	5.932	74.974
20	1.329	341.1	28.013	2478.1	33.2	3756	1338.8	1.21	19.856	7.26	2217.0	63.8	1981	826.6	1.16	2131	6.589	75.258
30	1.352	364.1	25.015	2553.0	31.5	3710	1382.4	1.21	18.456	7.01	2262.4	59.9	2011	887.5	1.18	2198	7.006	71.451
40	1.378	391.9	22.010	2643.5	29.7	3655	1435.3	1.20	16.935	6.75	2316.0	55.9	2045	962.0	1.20	2282	7.943	71.279
50	1.409	426.4	19.009	2754.6	27.8	3588	1500.7	1.20	15.282	6.46	2379.6	51.8	2080	1055.3	1.22	2391	8.645	67.003
60	1.445	470.5	16.008	2894.3	25.7	3500	1584.4	1.20	13.475	6.15	2456.2	47.4	2116	1175.5	1.26	2540	9.567	62.440
70	1.488	529.7	13.006	3074.5	23.5	3375	1695.5	1.20	11.489	5.80	2548.8	42.6	2146	1337.0	1.30	2751	10.818	57.367
80	1.540	614.5	10.005	3308.3	20.7	3168	1850.0	1.22	9.291	5.38	2654.6	36.8	2147	1563.0	1.37	3080	11.279	46.009
90	1.605	749.8	7.004	3540.1	15.8	2668	2072.3	1.33	6.831	4.72	2697.4	28.3	1985	1867.0	1.48	3664	8.052	22.994

Dil $\%_{vol}$	**Konnov (1998) Reaction Mechanism**			**Tan (1994) Reaction Mechanism**		
	Δ *(mm)*	τ *(μs)*	θ	Δ *(mm)*	τ *(μs)*	θ
0	0.030	0.117	9.540	0.045	0.172	10.933
10	0.033	0.119	9.498	0.048	0.168	10.722
20	0.036	0.120	9.437	0.052	0.165	10.464
30	0.040	0.121	9.388	0.056	0.162	10.164
40	0.046	0.123	9.283	0.062	0.160	9.795
50	0.053	0.126	9.201	0.071	0.161	9.380
60	0.065	0.133	9.026	0.085	0.167	8.922
70	0.086	0.151	8.812	0.109	0.185	8.476
80	0.145	0.208	8.876	0.175	0.246	8.230
90	0.709	0.794	10.384	0.701	0.786	9.662

Stoichiometric propane-oxygen-nitrogen mixtures with varying nitrogen dilution

Dil $\%_{vol}$	γ_0	a_0 *(m/s)*	W_0 *(g/mol)*	V_{CJ} *(m/s)*	P_{CJ} *(bar)*	T_{CJ} *(K)*	a_{CJ} *(m/s)*	γ_{CJ}	W_{CJ} *(g/mol)*	M_{CJ}	u_{vN} *(m/s)*	P_{vN} *(bar)*	T_{vN} *(K)*	a_{vN} *(m/s)*	γ_{vN}	Cp_{vN} *(J/kgK)*	Δh^0 *(MJ/kg)*	Q
0	1.291	305.1	34.015	2360.6	36.7	3829	1271.0	1.22	22.362	7.74	2143.7	71.2	1930	732.3	1.14	2030	5.657	78.454
10	1.300	308.9	33.412	2305.9	34.4	3760	1241.9	1.21	22.974	7.47	2082.3	66.4	1900	735.9	1.15	1961	5.687	77.468
20	1.309	312.8	32.815	2252.2	32.3	3691	1214.0	1.20	23.592	7.20	2021.3	61.9	1872	740.1	1.15	1892	5.732	76.689
30	1.318	316.7	32.215	2194.9	30.1	3611	1184.5	1.19	24.251	6.93	1956.3	57.4	1841	744.1	1.17	1819	5.766	75.730
40	1.328	321.0	31.614	2132.2	27.9	3515	1152.6	1.18	24.956	6.64	1885.3	52.8	1804	747.4	1.18	1744	5.780	74.508
50	1.339	325.4	31.014	2062.2	25.6	3396	1117.4	1.17	25.703	6.34	1806.7	48.1	1758	749.6	1.19	1664	5.764	72.884
60	1.350	329.9	30.414	1980.7	23.2	3239	1077.3	1.17	26.482	6.00	1716.4	43.2	1699	749.4	1.21	1581	5.321	65.978
70	1.362	334.8	29.814	1878.6	20.4	3014	1029.1	1.17	27.257	5.61	1605.8	37.7	1614	743.9	1.23	1493	4.791	58.241
75.806	1.370	337.7	29.465	1801.0	18.5	2822	994.3	1.17	27.670	5.33	1524.1	34.0	1541	735.5	1.24	1438	4.402	52.878
80	1.375	339.7	29.214	1728.4	16.8	2632	963.4	1.19	27.919	5.09	1449.6	30.8	1468	724.4	1.26	1395	3.574	42.567

Dil $\%_{vol}$	**Konnov (1998) Reaction Mechanism**			**Tan (1994) Reaction Mechanism**		
	Δ *(mm)*	τ *(μs)*	θ	Δ *(mm)*	τ *(μs)*	θ
0	0.030	0.117	9.540	0.045	0.172	10.933
10	0.040	0.153	9.747	0.061	0.226	11.247
20	0.054	0.202	9.976	0.082	0.298	11.560
30	0.076	0.278	10.238	0.115	0.412	11.923
40	0.114	0.405	10.564	0.171	0.605	12.373
50	0.187	0.649	10.974	0.282	0.979	12.952
60	0.358	1.214	11.484	0.546	1.867	13.714
70	0.916	3.046	12.175	1.464	4.943	14.783
75.806	2.072	6.847	12.671	3.547	11.940	15.587
80	4.809	15.900	13.045	9.068	30.570	16.158